LOAD-CARRYING CHARACTERISTICS OF DRILLED SHAFTS CONSTRUCTED WITH THE AID OF DRILLING FLUIDS

by

Walter R. Barker
Lymon C. Reese

Research Report Number 89-9

Soil Properties as Related to Load Transfer Characteristics of Drilled Shafts

Research Project 3-5-65-89

conducted for

The Texas Highway Department

in cooperation with the
U. S. Department of Transportation
Federal Highway Administration

by the

CENTER FOR HIGHWAY RESEARCH
THE UNIVERSITY OF TEXAS AT AUSTIN

August 1970

The opinions, findings, and conclusions expressed in this publication are those of the authors and not necessarily those of the Federal Highway Administration.

PREFACE

This report is the ninth in a series of reports from Research Study 3-5-65-89 of the Cooperative Highway Research Program between the Center for Highway Research, the Texas Highway Department, and the U.S. Department of Transportation. It describes the construction, instrumentation, and testing of a drilled shaft which had been constructed utilizing drilling mud. Suggestions are made for avoiding the dangers of construction employing drilling mud. The observed test data were analyzed and the factors affecting the load transfer were discussed. The results of an analytical procedure for the predicting of shaft behavior were compared with the observed results of the test.

This report is the product of the combined efforts of many people. Special thanks for technical contributions are given to Michael W. O'Neill, Harold H. Dalrymple, Frederick E. Koch and James N. Anagnos. Others concerned with and making contributions to the report were Olen Hudson, Mark Koch, Mark Toth, Travis Bowen, and Breck Graves. Editing of the manuscript was done by Eddie B. Hudepohl, with the typing being done by Kathleen L. Loveless and Mary Elizabeth Kern.

The Texas Highway Department Contact Representative, Mr. Horace Hoy, along with the personnel from District 12 and the Houston Urban Office have been helpful and cooperative in the development of the work. Mr. Gaston P. Berthelot and his office personnel earned special thanks for their numerous contributions and efforts exerted in the interest of the project.

LIST OF REPORTS

Report No. 89-1, "Field Testing of Drilled Shafts to Develop Design Methods," by Lymon C. Reese and W. Ronald Hudson, describes the overall approach to the design of drilled shafts based on a series of field and laboratory investigations.

Report No. 89-2, "Measurements of Lateral Earth Pressure in Drilled Shafts," by Lymon C. Reese, J. Crozier Brown, and H. H. Dalrymple, describes the development and evaluation of pressure gages to measure lateral-earth pressures on the drilled shaft.

Report 89-3, "Studies of Shearing Resistance Between Cement Mortar and Soil," by John W. Chuang and Lymon C. Reese, describes the overall approach to the design of drilled shafts based on field and laboratory investigations.

Report No. 89-4, "The Nuclear Method of Soil-Moisture Determination at Depth," by Clarence J. Ehlers, Lymon C. Reese, and James N. Anagnos, describes the use of nuclear equipment for measuring the variations of moisture content at the drilled shaft test sites.

Report No. 89-5, "Load Distribution for a Drilled Shaft in Clay Shale," by Vasant N. Vijayvergiya, W. Ronald Hudson, and Lymon C. Reese, describes the development of instrumentation capable of measuring axial load distribution along a drilled shaft, the development, with the aid of full-scale load testing, of a technique of analysis of observed data, and the correlation of observed data with the Texas Highway Department cone penetration test.

Report No. 89-6, "Instrumentation for Measurement of Axial Load in Drilled Shafts," by Walter R. Barker and Lymon C. Reese, describes the development and performance of various instrumentation systems used to measure the axial load distribution in field tests of full-scale drilled shafts.

Report No. 89-7, "The Determination of Soil Properties In Situ," by David B. Campbell and W. Ronald Hudson, describes the use of the Menard Pressuremeter, the Texas Highway Department cone penetrometer, and The University of Texas in situ device in estimating soil properties in situ and estimating load transfer values obtained from drilled shaft tests.

Report No. 89-8, "Behavior of Axially Loaded Drilled Shafts in Beaumont Clay," by Michael W. O'Neill and Lymon C. Reese, describes the results of axial load tests of instrumented drilled shafts having varying geometry and differing methods of installation and presents a tentative design procedure for drilled shafts in Beaumont Clay.

Report No. 89-9, "Load Carrying Characteristics of Drilled Shafts Constructed with the Aid of Drilling Fluids," by Walter R. Barker and Lymon C. Reese, describes the construction, instrumentation, and testing of a drilled shaft constructed with the use of drilling mud.

ABSTRACT

In modern day construction it is frequently advantageous to use drilled shafts as a foundation element. In the last few years research has opened the way for the design of drilled shafts based on the shearing resistance developed along the side of the shaft. When such a shaft is constructed utilizing drilling mud in the construction process, serious doubt may arise as to the adequacy of the design. The skepticism is justified, because little has been published on the effects of the drilling mud on the performance of drilled shafts.

The research being conducted by The University of Texas at Austin included field load tests of two straight test shafts, constructed by employing drilling mud. Both shafts were instrumented for the measurement of axial load utilizing a strain transducer designed and constructed at The University of Texas. The shafts were tested several times under axial loads and the load distributions in the shafts were measured. Just prior to conducting the last test, the upper portion of the soil around each shaft was excavated providing an opportunity for a visual examination of the shafts.

The study presented is concerned mainly with the construction, instrumentation and testing of one of the two shafts. This test shaft was 36 inches in diameter with the base located 60 feet below the ground surface. The shaft was tested a total of seven times utilizing various testing procedures. The maximum applied load was 832 tons. The soil at the test site consisted of a layered system of sand, silt, and clay.

The test results from this shaft provide a basis for a discussion of soil-shaft interaction, interaction between soil layers; and the effects of drilling mud, reloading, end conditions and soil properties on the load transfer which was developed. Constant monitoring of the instrumentation gave data on the stability and reliability of the instrumentation system and on the action of the concrete during the curing process.

The examination of both test shafts illustrated the contrasting results of the construction utilizing drilling mud. The procedure for shaft construction and the dangers involved in the construction are discussed. Suggested methods to avoid the dangers of construction are given.

An analysis of the test shaft was made using empirical load transfer data developed from basic soil properties. The analysis demonstrates that basic soil properties can be used in predicting the behavior of drilled shafts.

SUMMARY

Two shafts of the Cooperative Research Program 3-5-65-89 have been constructed utilizing drilling mud to prevent caving of the walls of the boreholes prior to placing concrete. The study is concerned mainly with the construction, instrumentation, and testing of one of the two shafts. This test shaft, 36 inches in diameter with the base located 60 feet below the ground surface, was instrumented for the measurement of axial loads along the shaft length. The soil at the test site was a multilayered system of sand, silt and clay. The shaft was tested a total of seven times from July 3, 1969 to April 6, 1970. Just prior to the final test, the soil from around the upper portion of the shaft was excavated and this portion of the shaft was examined.

From the study it was found that: (1) If proper construction procedures are used, drilling mud employed in the construction process will not affect the shear stress developed along the side of the shaft. (2) To avoid trapping drilling mud along the side of the shaft, the concrete should be as fluid as practical. (3) For the stiff Beaumont clay the shear stress developed (in the center portion of the shaft) will be approximately 0.6 times the undrained shear strength of the clay. (4) The shear stress developed along the side of the shaft will be greatly reduced in the vicinity of the ground surface and shaft tip.

IMPLEMENTATION STATEMENT

For heavily loaded foundations it has been shown that straight drilled shafts, designed for side friction, are much more economical than comparable driven pile foundations. The demonstration that such shafts can be successfully constructed in caving soils greatly increases the number of possible applications for the straight drilled shaft. Immediate tangible benefits were realized by the employment of straight drilled shafts for the foundation of the HB&T overpass.

The information presented in the study will aid in establishing design and construction procedures for drilled shafts. The identification of the pitfalls involved in the construction of drilled shafts in caving soils will be especially useful in reducing the risk for these shafts.

TABLE OF CONTENTS

NOMENCLATURE

Symbol	Typical Units	Definition
A_c	sq. in.	Effective cross-sectional area of shaft
$AVRD_n$		Gage reading at gage level n
c	lbs./sq. in.	Apparent cohesion of soil
D	inches	Average diameter of a shaft
D_1, D_2,...	inches	Diameter of a shaft at gage level 1, 2,...
E	microinches	Circuit strain
E_c	lbs./sq. in.	Young's modulus of elasticity of concrete
E_o	microvolts	Gage reading
F(RD)		Function relating gage reading to load in the shaft
G(z)		Function representing load-distribution curve
K		Gage factor
k		Ratio pressure on a horizontal plane to pressure on a vertical plane
$\bar{k}$		Ratio of soil pressure on a drilled shaft to the computed overburden pressure
L	inches	Length of the shaft from the ground surface to the base
N		Ratio of maximum developed stress on the shaft base to the <u>in situ</u> shear strength of the soil beneath the base
Q_B	lbs.	Load at the base of a shaft
Q_N	lbs.	Load in a shaft at gage level N

Symbol	Typical Units	Definition
Q_T	lbs.	Load applied to the top of a shaft
Q_z	lbs.	Load in a shaft at a depth z below the ground surface
R	lbs.	Total load supported by shear resistance along the side of a shaft
R_z	lbs.	Total load supported by shear resistance along the side of a shaft from the ground surface to a depth z
RD		Mustran gage reading
S	lbs./sq. in.	Shear resistance developed along the side of a shaft
$S_{0.2}$	lbs./sq. in.	Shear resistance developed at 0.2 of an inch shaft movement
S_{ult}	lbs./sq. in.	Ultimate shear resistance developed along the side of a shaft
SL	microinches/lb.	Slope of the Mustran gage response curves
W_T	inches	Total movement of a shaft at the location of the settlement gages
W_z	inches	Total movement of a shaft at a depth z
V	volts	Voltage applied to Mustran cells
z	inches	Depth below ground surface
α		Ratio of ultimate shear resistance developed along the side of a shaft to the <u>in situ</u> shear strength of the soil
γ	lbs./cu. ft.	Unit weight of soil
Δ	inches	Total deformation of the shaft between the top of the shaft and a point at a depth z
ϵ_z	inches/inch	Strain in a shaft at a depth z

Symbol	Typical Units	Definition
θ	radians	Angular distance around a shaft
ϕ	degrees	Angle of internal friction of a soil

CHAPTER I

INTRODUCTION

A foundation is defined by Tomlinson (1969) as that part of the structure in direct contact with the ground which transmits the load of the structure to the ground. In a pile foundation, the pile is the principal element of the foundation. The driven pile, in one form or another, has been used since prehistoric times but only in modern-day construction has the drilled shaft evolved as a major foundation element. The history of the drilled shaft is given by O'Neill and Reese (1970).

A drilled shaft may be defined as a deep foundation constructed by drilling a hole and filling it with concrete. For axial loads, the shaft thus becomes a concrete column supported vertically by both bottom bearing and side friction. The capacity of the shaft may be increased by enlarging the base to form a bell.

The advantages and disadvantages of drilled shafts versus driven piles are well presented by other authors (Glossop and Greeves, 1946; Tomlinson, 1969; Greer, 1969; O'Neill and Reese, 1970). The above authors have demonstrated that in soils where holes may be drilled without the use of special drilling techniques, there is a potential economic advantage in the use of drilled shafts as opposed to the use of driven piles for the support of very large loads. These soils, referred to as well-behaved soils, are mostly stiff clay, shale or cemented sand. There are other soils, not so well behaved, such as sands, silts, and soft clays which require special techniques in the drilling of the hole

and construction of the shaft. In such soils, the economic advantage of the drilled shaft over driven piles diminishes rather drastically.

As the construction of modern superhighways and high-rise structures continues at an unprecedented rate, the trend is toward an increased use of drilled shafts even in soils which are not well-behaved. Five basic procedures are utilized in the construction of drilled shafts in unstable soils. Although there are many variations, the basic procedures are as follows:

1. Drilling the hole rapidly so that a casing may be set before caving occurs. This procedure is used most often in small, shallow shafts where the consequence of a construction failure is not great. In any case, the driller must be prepared to deal with caving should it occur.
2. Driving or vibrating a casing to the desired depth and excavating from within the casing. This method is most effective in loose sands where a vibrator may be used to place the casing.
3. Excavating the hole and placing the casing simultaneously. Special equipment, such as Benoto rigs (Palmer and Holland, 1966), has been designed specifically for this purpose. This method is usually slow and costly, but it is a reliable method of getting a good hole.
4. Stabilizing the soil by lowering the water table. In special cases where a large number of shafts are to be

constructed in a small area, it may be economical to put down wells and stabilize the soil by dewatering. The application of this procedure is limited and would require a comprehensive study prior to its utilization.

5. Stabilizing the wall of the hole by the use of drilling fluid. This method has rapidly gained acceptance and is widely used. The procedure appears to offer an economical method that is reasonably reliable for construction of drilled shafts in troublesome soils. The basic technique is to fill the hole with a drilling fluid during the drilling process and to maintain the fluid level as the hole is advanced to the desired depth.

In the last decade, the technique of using drilling fluid has been adopted for providing a feasible method of drilling in difficult soils. Although the procedure has been widely used throughout the world, very little information has been published concerning the behavior of shafts constructed by this method. To be presented herein are the results of tests of two drilled shafts located in layered-soil systems which necessitated the use of drilling mud and casing in the construction process. The principal concern of the studies is the effect of the drilling fluid on the load transfer along the sides of the shaft. Also, some aspects of the interaction of a shaft with a layered-soil system are investigated.

Drilling Fluids

Drilling fluids have been used since ancient times as an aid to rock softening and cutting removal. Modern day drilling-fluid technology has

developed along with the oil well drilling industry. A drilling fluid, which was prepared by driving cattle through a shallow water pit, was used to prevent the caving of stratum of loose sand in the drilling of the famous Spindletop oil well. The clay-water mixture lined the borehole, and the well was successfully completed (Gatlin, 1960).

In modern oil well drilling, fluids perform five essential functions in the drilling operation. These functions as given by Gatlin (p. 74) are:

1. To cool and lubricate the bit and drill string,
2. To remove and transport cuttings from the bottom of the hole to the surface,
3. To suspend cuttings during times when circulation is stopped,
4. To control encountered subsurface pressures, and
5. To wall the hole with an impermeable mud cake.

As the use of drilled shafts increased, it was natural that the same people who were in the oil well industry would be associated with drilled-shaft construction. Thus, when caving conditions were encountered with drilled shafts, the same techniques were adopted as were used previously in the drilling of oil wells. While drilling fluid has several purposes in the drilling of oil wells, the primary, and many times the only, purpose of the drilling fluid in the construction of drilled shafts is to prevent the caving of unstable soil.

There is a three-fold action of drilling fluid to stabilize the walls of a borehole. First, the hydrostatic head of the fluid will counter the head of any water-bearing stratum and prevent the flow of water into the

hole. Secondly, the drilling fluid penetrates permeable soils and holds the soil particles in suspension. Thirdly, a relatively impermeable mud cake is formed along the wall of the hole. The mud cake is supported by the hydrostatic head of the drilling fluid. The more viscous the fluid, the thicker will be the mud cake formed and, consequently, the greater will be the support to the wall of the hole. But increasing the viscosity of the drilling mud will increase the effort required in rotating the auger through the drilling mud.

Drilling fluid is usually made by mixing bentonite clay with water. The particular bentonite best suited for use in drilling fluid is Wyoming bentonite. The Wyoming bentonite, in which the positive sodium ion is the dominant ion, absorbs more water, and yields higher viscosity at lower clay content than do other clay minerals. The viscosity relationship for Wyoming bentonite in fresh water is given in Fig. 1.1.

In salt water, the salt concentrations neutralize the electric charge on the dispersed bentonite particles and allow flocculation. The gelling characteristic of the bentonite is, therefore, greatly reduced. However, the clay mineral, attapulgite, will hydrate and form a stable suspension in salt water. Although attapulgite clay lacks the water-holding qualities of bentonite, it has gained general acceptance in areas where bentonite is not effective.

Construction Procedure for Drilled Shafts

In contrast with the oil well industry, the use of drilling fluids in the construction of drilled shafts is not a science but an art based on experience. Although the basic procedure is pretty well established, the techniques employed vary with soil conditions and with the individual

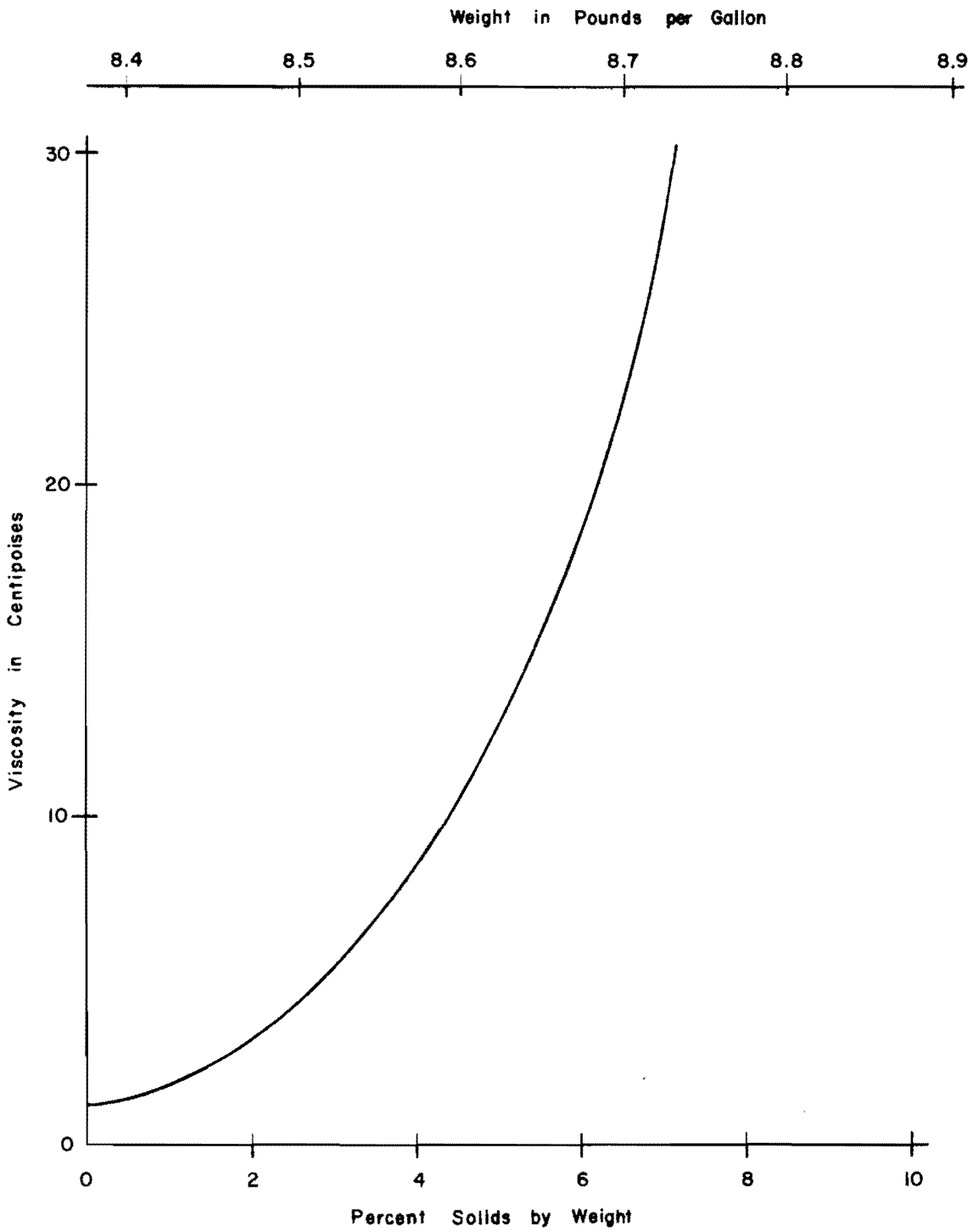

Fig. 1.1. Relationship between fluid viscosity and Percent of bentonite (After Gatlin)

experience of the driller. The success or failure of the basic procedure is dependant upon the skill that the driller displays in the use of the individual techniques.

The hole is drilled slightly over-sized until the unstable soil conditions are encountered. At the first indication of caving, the hole is filled with water and bentonite is added. The hole is advanced beneath the slurry by alternately rotating and lifting the auger. The churning action mixes the cuttings with the bentonite slurry. Much of the excavated material is held in suspension and later is removed from the hole along with the drilling fluid. The larger cuttings are removed on the auger.

Probably the most critical part of drilling in unstable soils is immediately taking appropriate action when such soils are encountered. One case of a hole being lost is known to the author because an inadequate amount of processing water was available at the site. A simple check prior to starting the hole would have disclosed the lack of processing water. The most useful aid in preparation for drilling will be to study soil information from borings at the site. Adequate soil information allows the driller to predetermine the needed amount of slurry, the proper length of casing, and the techniques to be used in the drilling. The exact location of any artesian stratum is very important as it is necessary to add the drilling fluid prior to penetration of this type of stratum.

The amount of bentonite needed in the preparation is dictated by the soil conditions. The recommendation has been made by McKinney and Gray (1963) that one 100-pound sack of good grade commercial bentonite

for every 4-5 cubic yards of material to be processed is enough to assure good results. Approximately 30 pounds of bentonite for each cubic yard of material to be excavated was recommended by Palmer and Holland (1966). In very troublesome soil conditions in India, a seven per cent bentonite slurry was reported as being used successfully in the stabilization of the boreholes (Pandey, 1967). In any case, the per cent of bentonite in the processing fluid is very small and is mainly determined by the driller at the site. The introduction of clay spoils previously excavated from the hole may reduce or in some cases may completely eliminate the need for prepared bentonite. The amount of bentonite needed is estimated by the driller from the rate of fluid loss from the hole. As the wall of the hole is coated with a mud cake, the rate of flow is reduced. Should caving occur, the rate of loss will show a sudden increase. Should the slurry become too thick, the effort required in drilling increases and the auger may become stuck in the hole. With a thick slurry, there is also the danger of collapsing the wall of the hole as the auger is being withdrawn.

The primary purpose of casing, if used in conjunction with drilling mud, is to allow removal of the drilling mud without the wall caving. The manner in which the casing is used is dictated by soil conditions and by techniques favored by the driller. For the case in which as impermeable soil is beneath the unstable soil, it is possible to seal the bottom of the casing in the impermeable soil, bail the hole dry and continue drilling in the dry.[1] The casing may be removed or may remain

[1]"Drilling in the dry" means that water is not being used in the borehole to aid in drilling.

in the hole. If the casing is to be removed, care should be taken so that the drilling fluid level in the annular space between the casing and hole wall remains high in order to maintain a hydrostatic head on the wall of the unstable soil.

It is common that after casing the unstable soil zones, the hole is advanced into a stable zone and the bottom is belled. Whenever conditions permit, the bottom of the hole is cleaned by a workman lowered into the hole. After the hole has been prepared, reinforcing steel is set and concreting is begun. The concrete may be placed in the hole by a tremie, a bucket or a pump. If the casing is to be removed, concrete is placed in the casing to the maximum level which would still permit extraction of the casing. The exact level to which the concrete is placed is normally determined by the construction supervisor. The minimum height of concrete in the casing should be that height such that the hydrostatic head of the concrete at the bottom of the casing is greater than the hydrostatic head of the drilling fluid. This minimum level should be maintained in order to attain proper displacement of the drilling fluid in the annular space outside of the casing. After concrete has been placed to a sufficient level in the casing, the bottom seal is broken and the casing is slowly extracted. During extraction, the concrete in the casing should be maintained above the minimum level. The greater the height of concrete maintained in the casing the more positive will be the displacement of the drilling fluid along the length of the borehole. The problems associated with the displacement of the drilling fluid are major aspects of this study and will be discussed in more detail in the following sections.

When it is not possible to terminate the casing in impervious soil, other procedures for placing the concrete must be employed. One method which was used early in the development of drilled shafts was to pressurize the casing, expelling the drilling fluid. Concrete was placed through a specially designed fitting to a level where the pressure could be removed from the casing. The concreting could then be completed in the normal manner.

Another method widely used in practice is to place a concrete plug under the mud by the use of a tremie. After this plug has set sufficiently to hold the bottom, the drilling fluid is removed and concreting begun. As soon as the level of concrete has reached sufficient height to hold down the plug, the plug is broken loose from the casing by the simultaneous rotating and lifting of the casing. With the casing broken loose, the concreting proceeds as before.

A method becoming more popular, but which involves a considerable risk, is concreting through the drilling fluid. When this is done, it is possible in many cases to eliminate the casing completely (Pandey, 1967). The concrete may be placed under the mud either by the use of a tremie, a concrete pump, or a bottom-opening concrete bucket. The tremie method is the most widely used and has proven successful when the proper technique is used. The essentials of this concreting operation are listed by Palmer and Holland (1966, p. 117) as follows:

(a) The concrete should be rich in cement, preferably 1: 1 1/2: 3, and of high slump, say 6 inches. Economies on this specification do not pay.

(b) In unstable ground the concreting should be carried out with a temporary casing to the full depth of the borehole so that fragments of ground cannot drop from the sides of the hole into the concrete as it is placed.

(c) The hopper and tremie pipe must be a closed system embedded in the placed concrete, through which water cannot pass.

(d) The tremie pipe must be large enough, having regard to the size of aggregate, a minimum of 8 inches diameter being preferable. The use of 3/4 inches down aggregates is preferable to larger sizes.

(e) The first charge of concrete should push the "rabbit"[2] ahead of it down the tube to prevent mixing of concrete and water.

(f) The tremie pipe should always penetrate well into the concrete with an adequate margin of safety against accidental withdrawal as the pipe is surged to discharge the concrete.

(g) It is preferable to concrete wholly by tremie and not change the method of deposition half-way up the pile. In this way laitance is carried up the pile on the top of the concrete.

(h) All tremie tubes should be scrupulously cleaned after use.

(i) The supervision must be competent, constant, and vigilant.

The use of a concrete pump is similar to that of a tremie, and the same precautions should be taken in its use as are taken with a tremie. A bottom-opening bucket, even with a skilled operator, is risky and is not recommended. The three principal methods of placing concrete in a processed hole[3] are illustrated in Fig. 1.2.

Even though concreting under mud has been employed successfully (Komornik and Wiseman, 1967; Pandey, 1967), the procedure of placing concrete utilizing casing offers several advantages.

---

[2]The term "rabbit" refers to a plug placed in the tremie to separate the concrete from the water. Normally a plug made of plastic is used as a rabbit.

[3]A "processed hole" is a hole drilled utilizing a drilling fluid.

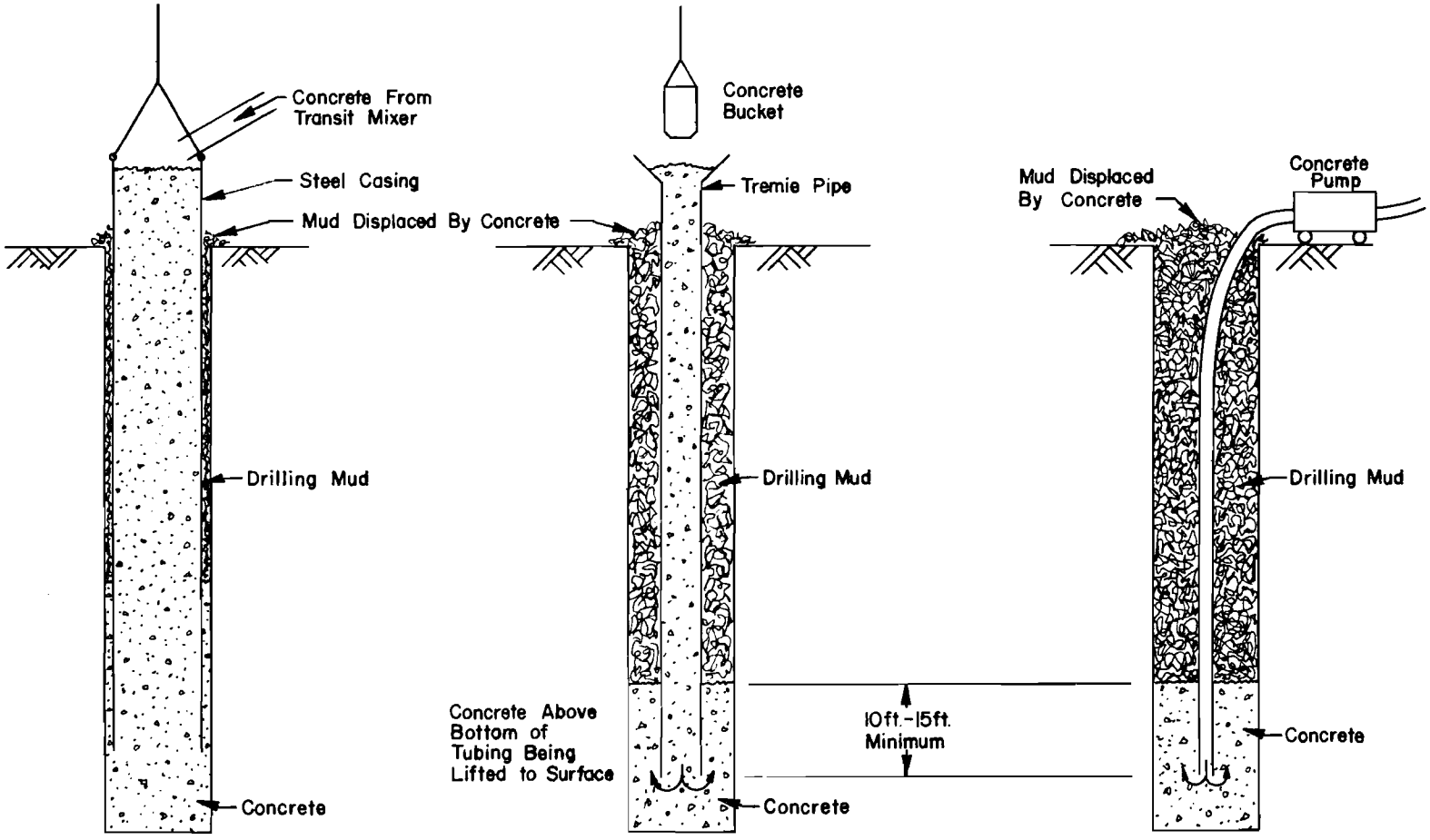

Fig. 1.2. Three procedures for placing concrete in a processed hole

1. The bottom of the hole may be inspected and cleaned if necessary prior to concreting.
2. The concrete is placed in the dry with visual observation possible and less danger of concrete contamination.
3. The reinforcing steel remains dry.
4. Delays would not as likely result in the loss of a shaft.

For shafts designed on the basis of bottom bearing, the advantages are well-founded and every effort should be made to construct these shafts utilizing casing.

For shafts designed on the basis of side friction, the use of casing presents two disadvantages that warrant further studies. These two disadvantages are:

1. A vigorous scouring of the wall of the hole does not occur as does when the concrete is placed under the mud with a tremie, and
2. There is a danger, especially for low-slump concrete, that the concrete will become stuck in the casing, causing intrusions of drilling mud into the shaft.

Although drilling mud has been widely used in the construction of drilled shafts, little is known concerning the effect of the mud on the load-carrying characteristics of the shaft. As more shafts are designed relying on the development of shear along the side of the shaft, the effect of the drilling mud becomes more critical.

CHAPTER II

MECHANICS OF SHAFT-SOIL INTERACTION

Although the load-carrying characteristics of a drilled shaft are complicated functions of many parameters, the two basic parameters are soil properties and shaft dimensions. Other factors which may affect the load transfer capabilities of the shaft are: (1) construction procedure, (2) concrete properties, (3) rate and method of loading, (4) environmental conditions, and (5) time.

Recent tests in London clay by Whitaker and Cooke (1966) and in Beaumont clay by O'Neill and Reese (1970) have advanced the understanding of the relationship between soil properties and load transfer of a shaft in a uniform clay soil. Very little information has been published concerning shaft-soil interaction in a layered-soil system. In addition to shaft-soil interaction, there is an interaction among the soil layers themselves. An added complication of a layered system is that a shaft in this type of soil is often constructed by utilizing drilling fluid. The bottom and sides of the shaft are likely to be coated with the drilling mud, and this coating may have considerable effect on the load-transfer characteristics of the shaft.

Theory

A typical drilled shaft in a layered-soil system is shown in Fig. 2.1a. The applied load is transferred to the soil, partly by the friction along the side of the shaft and partly by bearing support at the

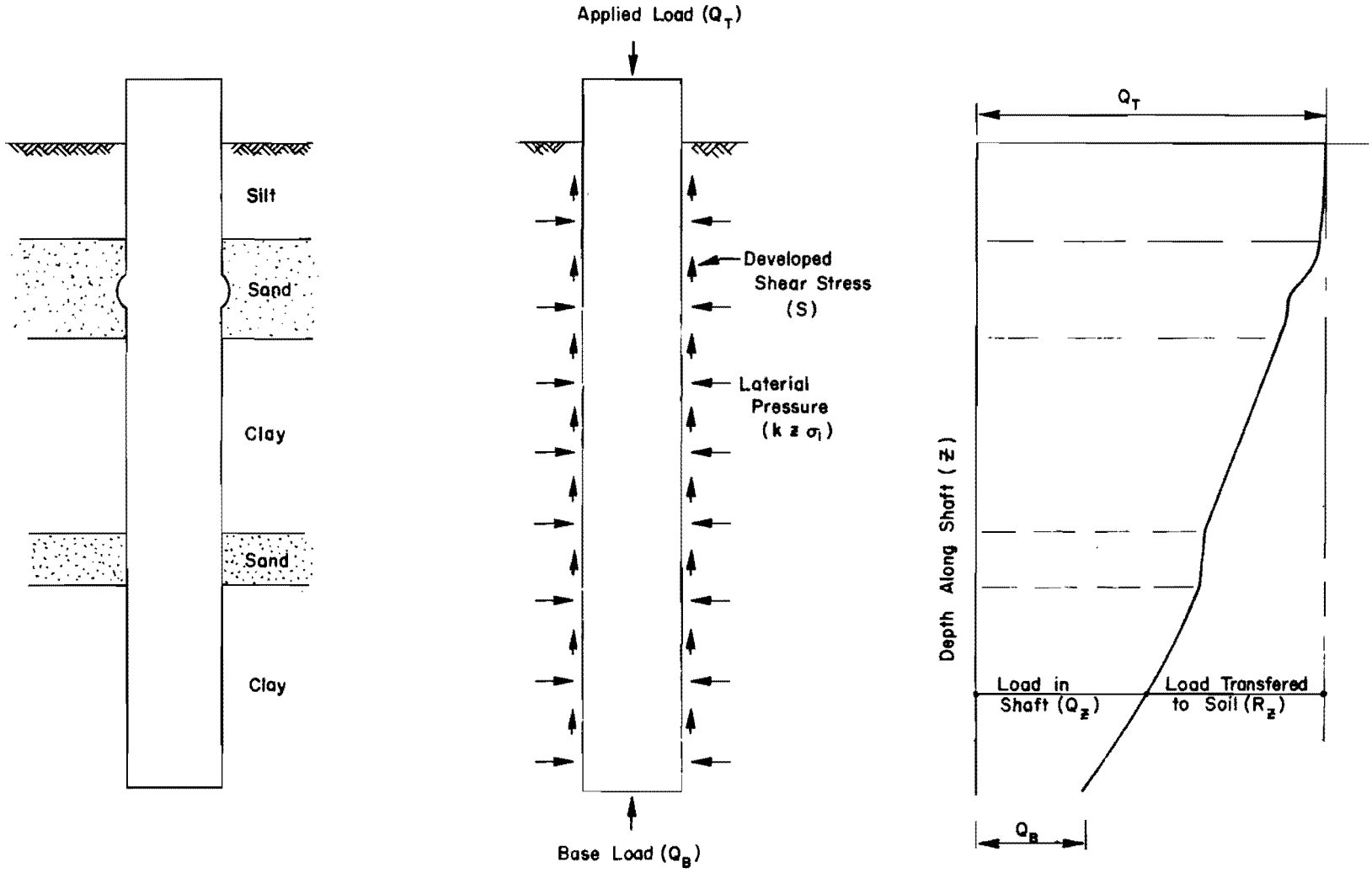

Fig. 2.1. Typical Drilled Shaft in a Layered-Soil System

bottom of the shaft. Thus, the load carried by the shaft may be defined by the equation:

$$Q_T = Q_B + \int_0^L \int_0^{2\pi} s\ (d\theta)(dz) \quad \ldots\ldots\ldots\ldots\ldots\ldots\ldots (2.1)$$

where

Q_T = the total load at the top of the shaft,

s = the shearing stress developed at a depth z ,

Q_B = the bearing support at the bottom of the shaft,

L = the length of the shaft,

$d\theta$ = an incremental distance around the circumference of the shaft, and

dz = an incremental distance along the depth of the shaft.

The term $\int_0^L \int_0^{2\pi} s\ (d\theta)(dz)$ represents the total load supported by the side friction. If the shearing stress is considered to be constant around the circumference of the shaft, and a single-valued function of the depth, then the total side friction may be expressed by:

$$R = \int_0^L s\ (\pi D)(dz) \quad \ldots\ldots\ldots\ldots\ldots\ldots\ldots\ldots\ldots (2.2)$$

where

R = the total side friction, and

D = the diameter of the shaft.

A plot of the load carried by the shaft as a function of depth is called the load-distribution curve and may be defined by the equation:

$$Q_z = Q_T - \int_0^z s\,(\pi D)(dz) \quad \ldots\ldots\ldots\ldots\ldots\ldots (2.3)$$

or

$$Q_z = Q_T - R_z \quad \ldots\ldots\ldots\ldots\ldots\ldots\ldots\ldots (2.4)$$

where

Q_z = the total load in the shaft at a depth of z, and

R_z = the total load transferred to the soil by friction from the ground surface to a depth z.

The load-distribution curves from a pile load test can be used to compute shaft movement and load transfer, parameters relating the shaft behavior to the soil properties. A typical load distribution along a drilled shaft is shown in Fig. 2.1c. The load transferred, per unit length of the shaft, at any point is represented by the slope of the load-distribution curve. Calculating the movement at a point along the length of the shaft involves the movement of the top of the shaft and the deformation of the shaft between the top and the point in question. The top movement can be measured directly for each applied load by the use of dial gages.

Assuming elastic behavior of the concrete, the strain of the shaft at any point is obtained by dividing the indicated load at the point

by the effective shaft area and concrete modulus of elasticity. This relationship can be expressed in equation form as:

$$\epsilon_z = \frac{Q_z}{A_c \cdot E_c} \quad \ldots\ldots\ldots\ldots\ldots\ldots\ldots\ldots\ldots\ldots (2.5)$$

where

A_c = the effective area of the concrete which includes the transformed area of steel, and

E_c = the modulus of elasticity of the concrete.

The deformation of the shaft between the top and any point may then be calculated by integrating the strain function from the top of the shaft to the point z .

$$\Delta = \int_0^z \epsilon_z dz = \frac{1}{A_c \cdot E_c} \int_0^z Q_z dz \quad \ldots\ldots\ldots\ldots\ldots\ldots (2.6)$$

The net movement of the shaft at the point may be computed by subtracting the computed shaft deformation from the movement measured at the top of the shaft. In equation form the net movement can be expressed as:

$$W_z = W_T - \frac{1}{A_c \cdot E_c} \int_0^z Q_z dz \quad \ldots\ldots\ldots\ldots\ldots\ldots\ldots (2.7)$$

where

W_z = the movement of a point at a depth z , and

W_T = the downward movement of the top of the shaft.

For each applied load, a value of load transfer and shaft movement may be determined for any point along the shaft. By applying the load in small increments, a curve of load transfer versus shaft movement may be developed for any particular point along the shaft. This type of curve, called a load-transfer curve, was first presented for driven piles by Seed and Reese (1955) and was set forth for drilled shafts by O'Neill and Reese (1970). The way in which these load-transfer curves are used in conjunction with the bottom-load settlement curve to predict the behavior of a driven pile is given by Coyle and Reese (1966), and for a drilled shaft by O'Neill and Reese (1970).

Factors Affecting Load Transfer in a Layered-Soil System

The factors affecting load transfer of a drilled shaft in a clay soil have been adequately discussed by others (Whitaker and Cooke, 1966; Vijayvergiya, et al.,1968; O'Neill and Reese, 1970). It has been stressed by each of the authors that the most important factors influencing the behavior of a given shaft are the soil properties, the most important of which is the shear strength of the soil. Skempton (1959) presented the following equation which relates the ultimate side friction to the undrained shear strength of a clay soil.

$$R = (\pi \cdot D \cdot L)(\alpha \cdot c) \quad \ldots\ldots\ldots\ldots\ldots\ldots\ldots (2.8)$$

where

R = the total side friction developed along the length of the shaft,

c = the undrained shear strength of the clay, and

α = the ratio of ultimate shearing stress developed to the in situ shear strength of the soil.

The ultimate shearing resistance which may be developed, then, is

$$s_{ult} = \alpha \cdot c \quad \ldots\ldots\ldots\ldots\ldots\ldots\ldots\ldots\ldots\ldots \quad (2.9)$$

From the results of load tests of drilled shafts in saturated clay, α is computed by dividing the maximum shearing stress developed along the side of the shaft by the undrained shear strength of the clay. Skempton (1959) in a study of the test results of drilled shafts in London Clay found values of α ranging between 0.3 and 0.6. In that study it was suggested that fractional α factors are the result of a reduction in the shear strength of the soil adjacent to the shaft. A theory is described by Skempton which indicates that the migration of moisture from the unset concrete is the principal cause of the reduction in the soil shear strength. O'Neill and Reese (1970) found that such a migration of moisture did occur and support the theory advanced by Skempton. In the tests by O'Neill and Reese it was also observed that lower α factors were obtained in the vicinity of the ground surface and the shaft tip than were obtained in the center portion of the shaft. For the design of drilled shafts in Beaumont Clay, O'Neill and Reese (1970) suggest an α factor of 0.5 for the center portion of the shaft and an α factor of 0.0 for that portion of the shaft within two shaft diameters of the ground surface and two shaft diameters of the shaft tip.

In a cohesionless soil the shearing strength of the soil is a function of the normal force on the shearing plane and the angle of internal friction of the soil. If this normal force could be measured, the α factor for cohesionless soils could be computed by defining the shear strength of the soil as the product of the normal force and the tangent of ϕ. Assuming the cohesion of the soil to be zero, α may be computed by the equation:

$$\alpha = \frac{s_{ult}}{\sigma_2 \cdot \tan \phi} \quad \ldots\ldots\ldots\ldots\ldots\ldots\ldots\ldots \quad (2.10)$$

where

s_{ult} = the measured shearing stress developed along the side of the shaft,

σ_2 = the normal pressure on the shearing surface, and

ϕ = the angle of internal friction for the soil.

In tests of drilled shafts the attempts to measure the normal forces on the shafts have been unsuccessful. With σ_2 of equation 2.10 unknown, the computation of α is impossible. Another factor, say $\bar{k}$, can be introduced relating the normal force on a shaft to the overburden pressure of the soil as follows:

$$\sigma_2 = \bar{k} \cdot z \cdot \gamma \quad \ldots\ldots\ldots\ldots\ldots\ldots\ldots\ldots \quad (2.11)$$

where

$\bar{k}$ = the ratio of the normal stress on the side of a drilled shaft to the computed overburden pressure,

z = the depth below the ground surface at which the product of α and $\bar{k}$ is being computed, and

γ = the average unit weight of the soil above the point at which the computations are being made.

Using Eqs. 2.10 and 2.11 the product of α and $\bar{k}$ may be computed.

$$\alpha \cdot \bar{k} = \frac{s}{z \cdot \gamma \cdot \tan \phi} \quad \ldots\ldots\ldots\ldots\ldots\ldots\ldots (2.12)$$

In a cohesionless soil it is quite possible, due to penetration of the soil by the wet concrete, to have an α factor greater than unity. Any reduction in the shear developed along the side of a drilled shaft in a cohesionless soil would then be the result of fractional values of $\bar{k}$ rather than fractional values of α .

Drilling Mud. When drilling mud is used in the drilling operation, a mud cake is formed along the wall of the shaft. The formation of a bentonite cake along the sides of trenches is demonstrated in experiments performed by the ICOS Construction Company (ICOS, 1969). In these tests, it was shown that the thickness of the cake could be increased by an electrical current passing between the bentonite mud and the moist cohesionless material. The fact that the bentonite penetrates into permeable materials was shown by McKinney and Gray (1963) and by ICOS (1969).

The published data on field tests indicate that there are no detrimental effects on the load carrying characteristics of the shaft due to the use of drilling mud. In fact, it appears that in cohesionless soil, the effect may be beneficial. In pull-out tests of two shafts in Spain (Fernandez-Renau, 1966), one installed with the use of a bentonite mud

and one without bentonite mud, the shaft installed with the bentonite carried a considerably higher load than was expected; whereas, the other shaft failed at a load considerably lower than was anticipated. In the test by Komornik and Wiseman (1967), drilled shafts were constructed in sand by using a bentonite mud to keep the hole open during the drilling. The concrete was then placed below the mud by use of a tremie. The results of the test gave no indication of any reduction in the capacity of the shaft due to the use of drilling mud.

The beneficial action of the bentonite mud in cohesionless soil is not fully understood. Perhaps the bentonite penetrating the walls gives the soil some cohesion and, therefore, some added shear strength. Dr. Fleming (1970) of McKinney Foundations advances the theory that in the placing of the concrete by tremie, the walls of the hole are scoured by the lifting concrete. Dr. Fleming (1970) states that, for concrete with a slump of 6-8 inches, it is possible, by keeping the bottom of the tremie pipe below the surface of the concrete, to lift 15-30 feet of concrete in a body from the bottom of the shaft to the top. In the construction reported by Komornik and Wiseman (1967), the bottom of the tremie was kept approximately 15 feet below the level of the concrete, lifting the first concrete placed from the bottom of the hole to the top. With the lifting of this amount of concrete from the bottom, a vigorous scouring would certainly have taken place, as contended by Dr. Fleming.

While it would seem, due to the coating action of the bentonite, that in a clay the bentonite would prove detrimental to the load transfer properties of the soil, such may not be the case. The only test known

to have been conducted involving clay and bentonite was the test of two concrete-wall elements in London clay (Burland, 1963). In these tests, two wall elements were installed about 40 feet into the London clay. One element was installed with the aid of a special liner that sealed off the overlying gravel, and the other employing the normal ICOS system using bentonite. After three weeks, each element was tested. For all practical purposes the performance of both sections was identical. The ultimate load of both sections was about 15 per cent higher than the theoretical load calculated using an α factor of 0.45. Some months after the test, moisture contents were taken around each test element. From the results of these tests, it was concluded that the change in the moisture content due to the placing of both elements was approximately the same.

Based on the few tests reported to date, it would seem that the effect of drilling mud on load transfer characteristics of shafts constructed in cohesionless soil is beneficial. For a shaft constructed in a clay soil, it is indicated that a bentonite cake created during drilling operation has no effect on the load carrying characteristics of the shaft. It could very well be that the construction technique which is used may be a major factor in nullifying the effect of the drilling fluid.

CHAPTER III

PROJECT REVIEW

In view of the increasing use of drilled shafts in highway construction, The Center for Highway Research at The University of Texas at Austin initiated a cooperative study of the behavior of drilled shafts with the Texas Highway Department in 1965. The decision was made at the outset of the project that it would be necessary to conduct experiments using full-scale drilled shafts. The specific objectives of the project were:

1. To identify the various factors influencing the behavior of drilled shafts,
2. To design, construct, and/or test equipment and instrumentation for use in studying the behavior of drilled shafts,
3. To conduct field tests of full-scale drilled shafts for the purpose of studying the influence of the various parameters on the behavior of drilled shafts; and, from the data collected,
4. To develop design procedures and appropriate design aids for use by the design engineer.

The project began in September 1965 and it is not expected to be completed until September, 1971. It is expected that at its completion, ten full-scale drilled shafts will have been constructed and loaded. In addition to the field testing, five supporting studies will have been completed and reported.

Supporting Studies

Several investigations were made in support of the load testing of full-scale drilled shafts. Reports of these studies made to assist in the determination of the soil-shaft interaction are briefly described as follows:

1. Measurements of Lateral Earth Pressure in Drilled Shafts by Lymon C. Reese, J. Crozier Brown, and H. H. Dalrymple. This report describes the development and evaluation of pressure cells to measure lateral-earth pressures on the drilled shafts. Two types of cells, one commercial and one constructed at The University of Texas, were installed in the first two drilled shafts. The effort to measure the lateral pressures was largely unsuccessful, and no lateral pressure cells were installed in succeeding shafts.
2. Studies of Shearing Resistance Between Cement Mortar and Soil by John W. Chuang and Lymon C. Reese (1968). This report presents the laboratory investigation of factors influencing the shearing resistance between cement mortar and soil. In this study, a series of tests were performed on remolded samples and undisturbed samples of soil to study the migration of water or cement from the fresh mortar into the soil. Factors considered were water-cement ratio, grain-size distribution, pressure-head on unset cement mortar, type of cement, time, void ratio, and initial moisture content of the soil. Some of the conclusions from the study were:

a. After the cement mortar is poured, water moving from the mortar causes local softening and a decrease in the shearing strength of the soil. For a given soil the value of α depends mainly on the original moisture content of the soil and on the water-cement ratio of the cement mortar. In the tests conducted, the value of α was found to lie between 0.40 and 0.68.

b. At the same void ratio, moisture content, and water-cement ratio, more water will migrate into clay than into sandy clay.

c. The weakest zone of the soils tested is located approximately one-fourth inch from the cement mortar. When the intended shear plane is located at the interface of the mortar and soil, the actual failure plane occurs at least one-eighth inch from the interface.

d. For sandy clay and sandy-clay loam, one-eighth inch of soil cement will be formed near the interface of the mortar and soil.

3. The Nuclear Method of Soil-Moisture Determination at Depth by Clarence J. Ehlers, Lymon C. Reese, and James N. Anagnos. This report describes the use of nuclear equipment for measuring the variations of moisture content within a soil media. Measurements utilizing the nuclear equipment were made at two of the drilled-shaft test sites. From the investigation which was conducted, it was found that nuclear equipment could be used

successfully to measure the variation in moisture content of the undisturbed soil.

4. Instrumentation for Measurement of Axial Load in Drilled Shafts by Walter R. Barker and Lymon C. Reese (1969). This report presents the development and performance of various instrumentation systems which were used to measure the distribution of axial load in the field testing of four drilled shafts. Primary emphasis was placed on a strain-measuring transducer, the Mustran cell, which was designed and constructed at The University of Texas and which was adopted for the instrumentation of the remaining shafts to be axially loaded.
5. The Determination of Soil Properties In Situ by David B. Campbell and W. Ronald Hudson. This report reviews several methods for determining the in situ shear strength of the soil. The Menard Pressuremeter, the THD cone penetrometer, developed by the Texas Highway Department, and an in situ device designed by The University of Texas were studied in detail. Specific test results for the THD cone penetrometer, and the in situ device are given for one of the test sites.

Field Tests

To date, seven shafts located at four separate sites have been instrumented and tested. These sites, all located in the south-central and southeastern part of Texas, are designated as the Austin Montopolis site, the San Antonio site, the Houston SH 225 site and the Houston HB&T site. The location of these different sites are shown in Fig. 3.1 as Sites I, II, III, and IV, respectively. Shown also, is the proposed location of

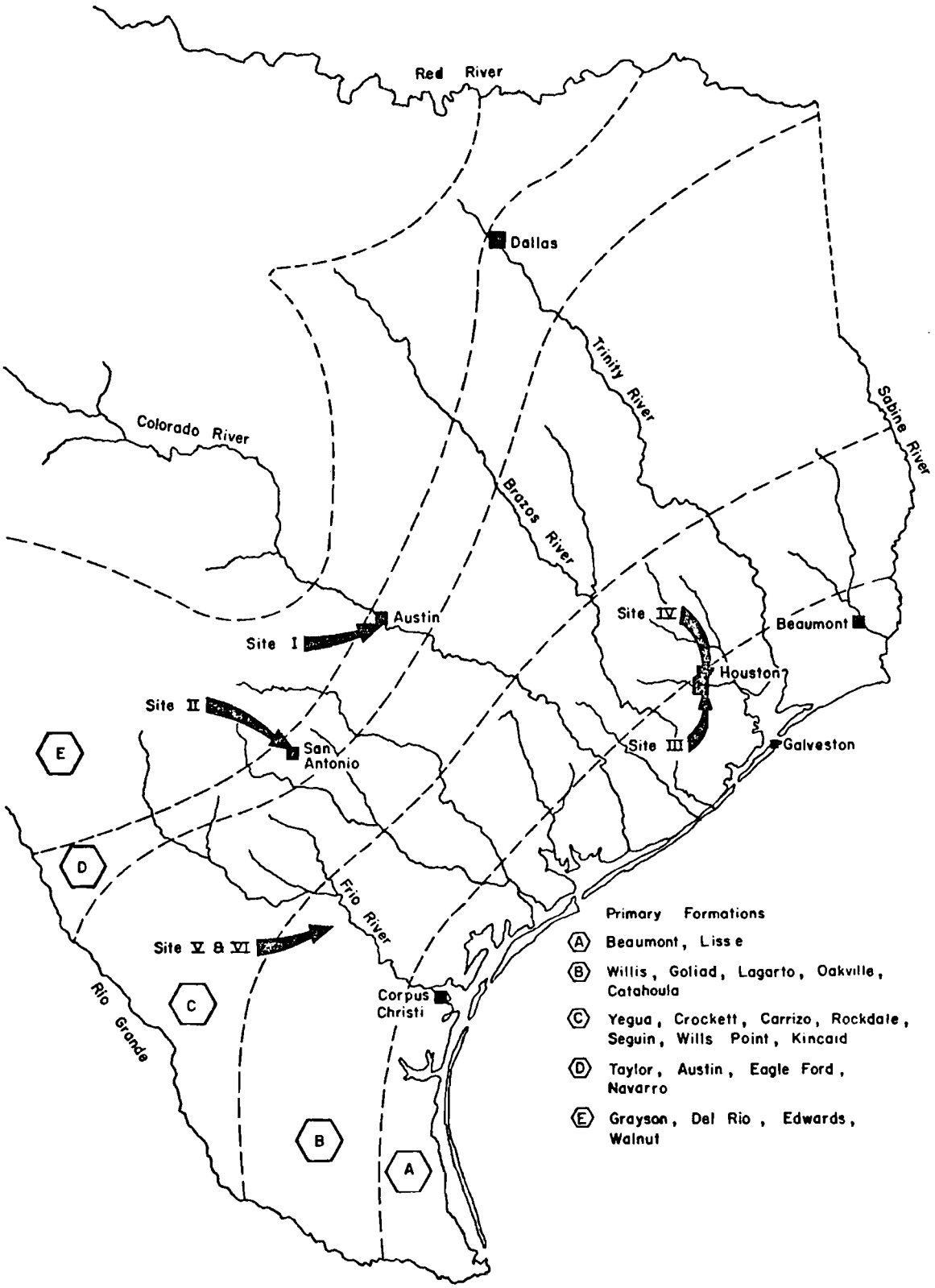

Fig. 3.1. Location of the Different Test Sites

Sites V and VI, each of which will be the site of one test shaft. In the figure, primary geological formations in the testing areas are identified by name. One additional shaft to be tested by loading laterally is to be constructed at the Houston SH 225 test site.

Austin Montopolis Site. It was felt that a preparatory test shaft should be installed to develop instrumentation, loading equipment, and testing technique for the more complex tests to follow. For its convenience to The University of Texas, a site just south of Austin in the small community of Montopolis was chosen. Since the prime purpose of the shaft was in preparation of succeeding tests, the soil conditions at the site were not a major consideration.

A single test shaft, 24 inches in diameter and 13 feet 4 inches long, was installed on August 18, 1966. A total of eight tests were conducted during the period from October 5, 1966, to March 22, 1967. The results of the tests are given by Reese and Hudson (1968).

San Antonio. This test site was located in the southwest portion of San Antonio in the Navarro soil formation. The soil at this site was basically a very stiff clay graduating to a clay shale at the bottom of the shaft. The test shaft was 30 inches in diameter and was 28 feet 6 inches long with 26 feet 8.5 inches below the ground surface. The shaft was loaded a total of five times during the period of June 21, 1967, to May 14, 1968. The results of these tests and a procedure developed for the prediction of the load-settlement curve are presented by Vijayvergiya, et al., (1968).

Houston SH 225. This test site, located in the southeastern part of Houston at the proposed interchange of Loop 610 and State Highway 225,

is in the Beaumont soil formation. The formation at the side consisted of three distinct layers. From 0-29 feet was fissured clay with a shear strength of approximately one ton per square foot; from 29-32 feet was a waterbearing clayey-silt; and from 32-50 feet was a very heavily fissured clay with a shear strength of about 2 tons per square foot. The water table at the site was approximately 17 feet below the ground surface.

Four shafts, each 30 inches in diameter but with variations in the tip configuration, were instrumented and tested. The description of the different shafts and the test results are given in Table 3.1.

Complete laboratory studies were conducted on undisturbed soil samples from the site. These not only included unconfined, triaxial, direct shear, transmatic and pocket penetrometer shear strength tests, but also a moisture migration study similar to the one conducted by Chuang and Reese (1969). In addition to the study of the undisturbed samples, the THD cone penetration tests were conducted and moisture variations with depth obtained by the use of a nuclear method of moisture determination. For Shafts 1 and 4, moisture profiles, with a base line of distance from the shafts, were obtained at various depths. The complete results of the laboratory and field studies are presented by O'Neill and Reese (1970).

TABLE 3.1. SUMMARY OF SH 225 TEST RESULTS

Shaft No.	Depth to Base (Feet Inches)	Ultimate Capacity (Tons)	Peak Side Shear (Tons)	Ultimate Side Shear (Tons)	Base Load (Tons)	Average α Factors (Peak)	Remarks
1	23 0	140	97	88	52	0.44	Straight shaft
2	23 0	537	92	90	447	0.53	Belled shaft with bell diameter of 7'6"
3	23 0	64	121	64	0	0.54	Bottom support of shaft eliminated
4	45 0	320	194	179	142	0.38	Drilled by using drilling mud and casing to keep hole open

CHAPTER IV

SITE CONDITION

Site Location

At approximately the same time that tests were being conducted on Shafts 1 and 2 at the Houston SH 225 Test Site, the Texas State Highway Department was in the process of designing the foundations for the Interstate Highway 610 - HB&T Railroad overpass structure. The location of the structure, shown in Fig. 4.1, is in the northern part of Houston near the location of the North Loop 137 - HB&T underpass. In addition to the HB&T Railroad, the structure is to carry IH 610 over Gold, Elysian, and Hardy Streets, and the east-bound lane of Loop 137.

The overall length of the structure is to be 1,358 feet with span lengths of up to 76 1/2 feet. In the structure, there will be 44 individual interior bents, each supported by an average of 4 columns. The standard design for column foundations was either driven piles or belled drilled shafts. The drilling of test bells indicated that in the center portion of the structure the bells would not remain open. Thus, the preliminary design called for belled shafts on either end of the structure with driven piles in the center. A total of 79 columns were to be supported by driven piles, while the remaining 97 columns were to be supported by drilled shafts with bells. A pile cap was to be constructed to provide connection between the bridge column and the driven piles.

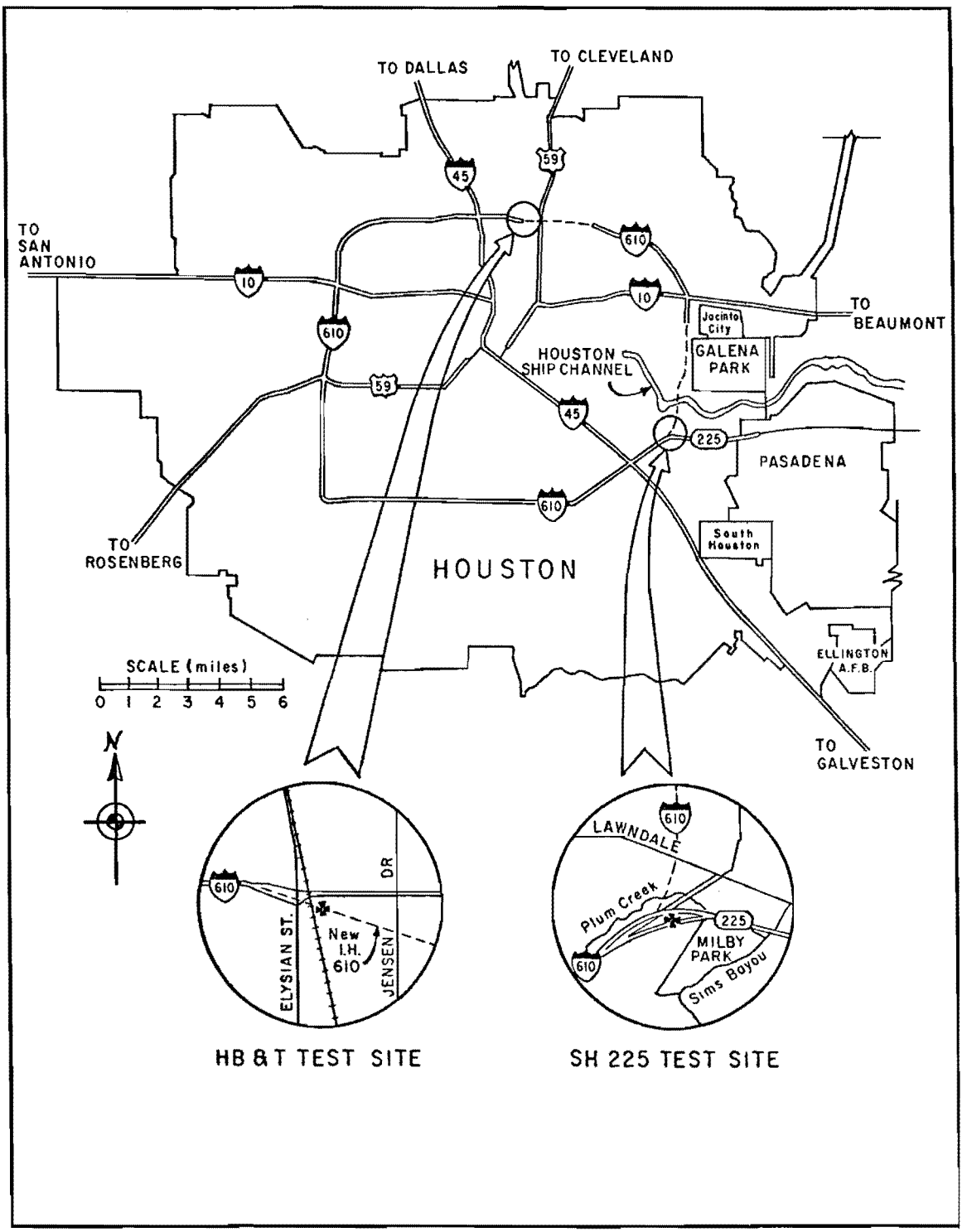

Fig. 4.1. Location of the Houston Test Sites
(After O'Neill and Reese, 1970)

The drilled shafts were to be 36 inches in diameter with either an 8- or an 8.5-foot bell at the base. The design of these drilled shafts was based on bottom bearing with no allowance being made for support gained from shear along the sides of shafts.

The tests of Shafts 1 and 2 at the SH 225 Test Site indicated the development of considerable side resistance along drilled shafts. Therefore, personnel of the Texas Highway Department decided to consider, as an alternate design for the HB&T foundations, drilled shafts with no bells. It was decided to conduct a load test on a full-scale drilled shaft at the construction site. The site selected for the test shaft was in Bent 13 near the east end of the bridge. The test was designed so that the reaction shafts could be used as column foundations in the completed structure; thus, the test shaft was located midway between two columns. The general area and location of the test shaft, reaction shafts, and test borings are shown in Fig. 4.2.

In Bent 13 of the structure the preliminary design for each foundation was six 14-inch square concrete piles driven to a depth of 40 feet. The alternate design called for a 36-inch diameter straight shaft with the base 60 feet below ground surface. For use in the estimate, it was assumed that had belled shafts been used in the bent they would have been belled at the 60-foot depth. The economics of using the straight shafts versus the driven piles is demonstrated in the following cost estimate. The values used are based on average costs of driven piles and drilled shafts in the Houston area as of January, 1970, according to data obtained from the Texas Highway Department.

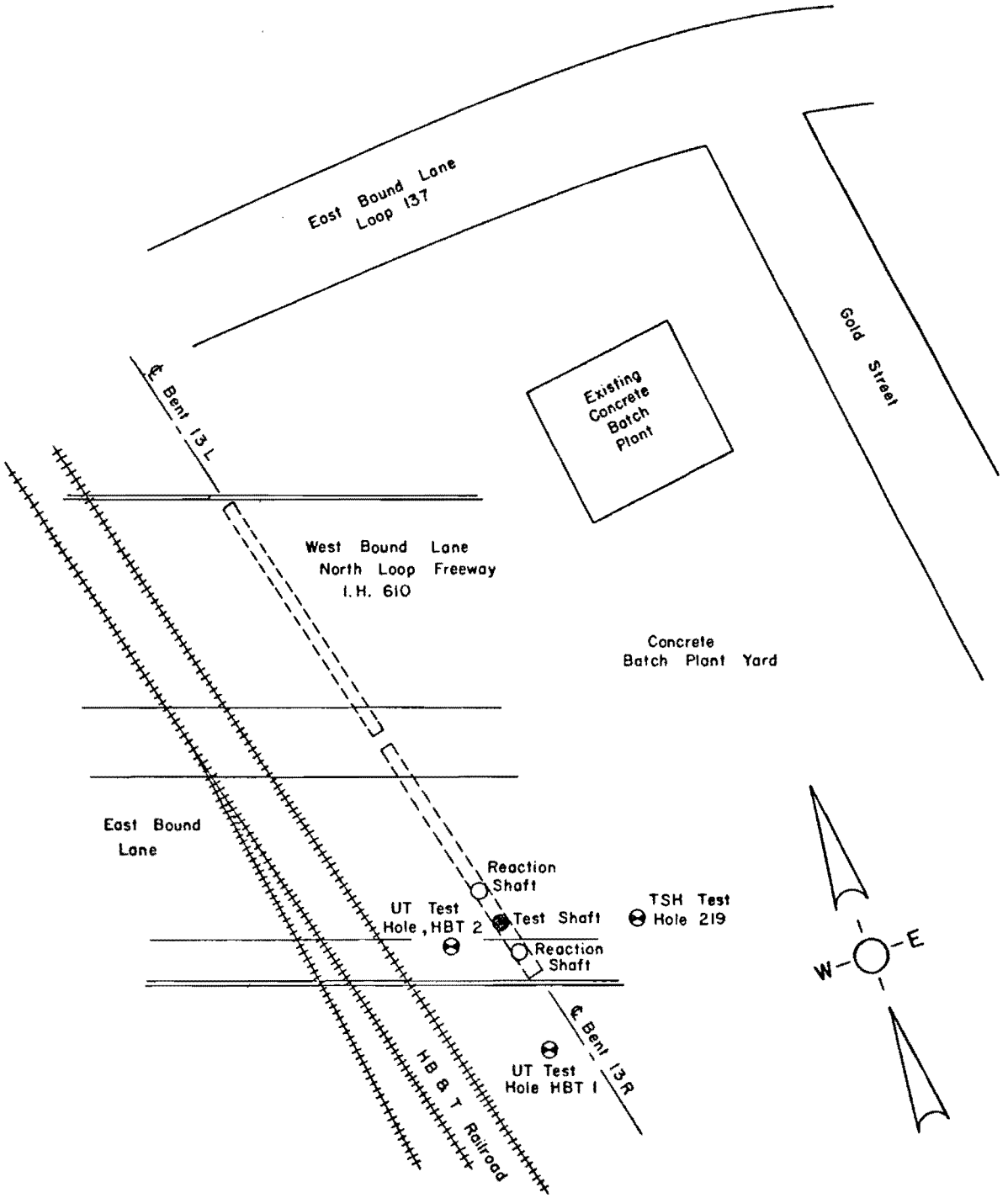

Fig. 4.2. Site Plan for the HB&T Test Site

A. Cost of driven pile foundation

Six 14-inch square concrete piles, 40 feet long, at $9.76 per foot	$2,342
Concrete pile cap	400
Total	$2,742

B. Cost of belled shaft assumed to be belled at 60 feet, straight shaft at $18.43 per foot

	$1,106
Bell at $44.67 per cubic yard	165
Total	$1,271

C. Cost for 60-foot straight shaft at $18.43 per foot

	$1,106
Total	$1,106

D. Saving realized per foundation by using straight drilled shafts

1. Straight shaft versus driven piles	$1,636
2. Straight shaft versus belled shaft	165

Geological Description

The test site is located in the northern edge of the Beaumont clay formation. This formation, described by O'Neill and Reese (1970), is typically a layered formation consisting of fissured overconsolidated clays, silts, and fine sands. The area was formed by delteric depositions of the old Brazos River. Several small bayous still cross the area. Just to the north of the site is the Lissie Sand formation. Between the Lissie Sand and the Beaumont Clay is a secondary formation, locally named the Second Terrace. The divisions of the different formations in this area are almost indistinguishable and the formations tend to blend together.

Soil Profile

The site at which the test shaft was to be located was completely covered with a concrete slab of varying thickness. The elevation of the top of the slab at the location of the test shaft was +66 feet with the elevation of the water table at +52 feet.

The soil profile and undisturbed soil samples were taken from three borings located in the vicinity of the test site. The first boring, sampled and logged by personnel of the Texas Highway Department, was located some 40 feet to the east of the shaft site. The boring, designated as boring THD 219, was made with the soil survey for design of the bridge foundation. The design of the test shaft was based on this boring. For the other two borings, the logging was done by personnel from The University of Texas. These two borings, designated as HBT-1 and HBT-2, were located approximately 40 feet south of the test site and approximately 10 feet west of the test site, respectively.

The boring was accomplished with a truck-mounted boring rig capable of boring and sampling to depths in excess of 100 feet. The undisturbed samples were obtained using the standard Texas Highway Department thin-walled sample tube. From a sample tube, three soil samples, each approximately 6 inches long and 2 7/8 inches in diameter, were obtained. The samples to be returned to The University of Texas were extruded at the site, identified, and sealed using parafin wax. Each sample was stored in a moist room until testing of the sample could be performed. In addition to taking undisturbed samples, the soil was evaluated by use of the THD cone penetrometer. The THD cone penetrometer and operating procedure is described by Vijayvergiya and Reese (1968). The logs of

all three borings are contained in Appendix A. From these logs, a profile for the THD cone penetrometer values was constructed (Fig. 4.3). The profile indicates the variance of the soil at the test site and is the basis for a determination of the shear strength for the different soil zones.

The composite profile shown in Fig. 4.4 was constructed from the three borings. Unlike the Houston SH 225 site, the profile could not be divided into a reasonable number of zones of uniform soil. For analysis and discussion purposes, the profile was divided into the seven zones shown in the profile. The zones were based not only on soil properties but also on the location of the instrumentation. The density of the instrumentation was such that no finer resolution of the load distribution curves could be obtained. Within several of the zones, the soil properties varied considerably; but, due to the limited instrumentation, division of the profile into additional zones would serve no purpose.

Laboratory Tests

Laboratory tests were conducted by personnel from both the Texas Highway Department and The University of Texas. Samples from borings THD 219 were tested by personnel from the Texas Highway Department using the transmatic-triaxial testing procedure, while the samples from borings HBT-1 and HBT-2 were tested by personnel from The University of Texas. The tests conducted on the latter samples included Atterberg limits, hydrometer, triaxial, and direct shear.

Atterberg Limits and Hydrometer Tests. The determination of the Atterberg limits was performed in accordance with standard laboratory

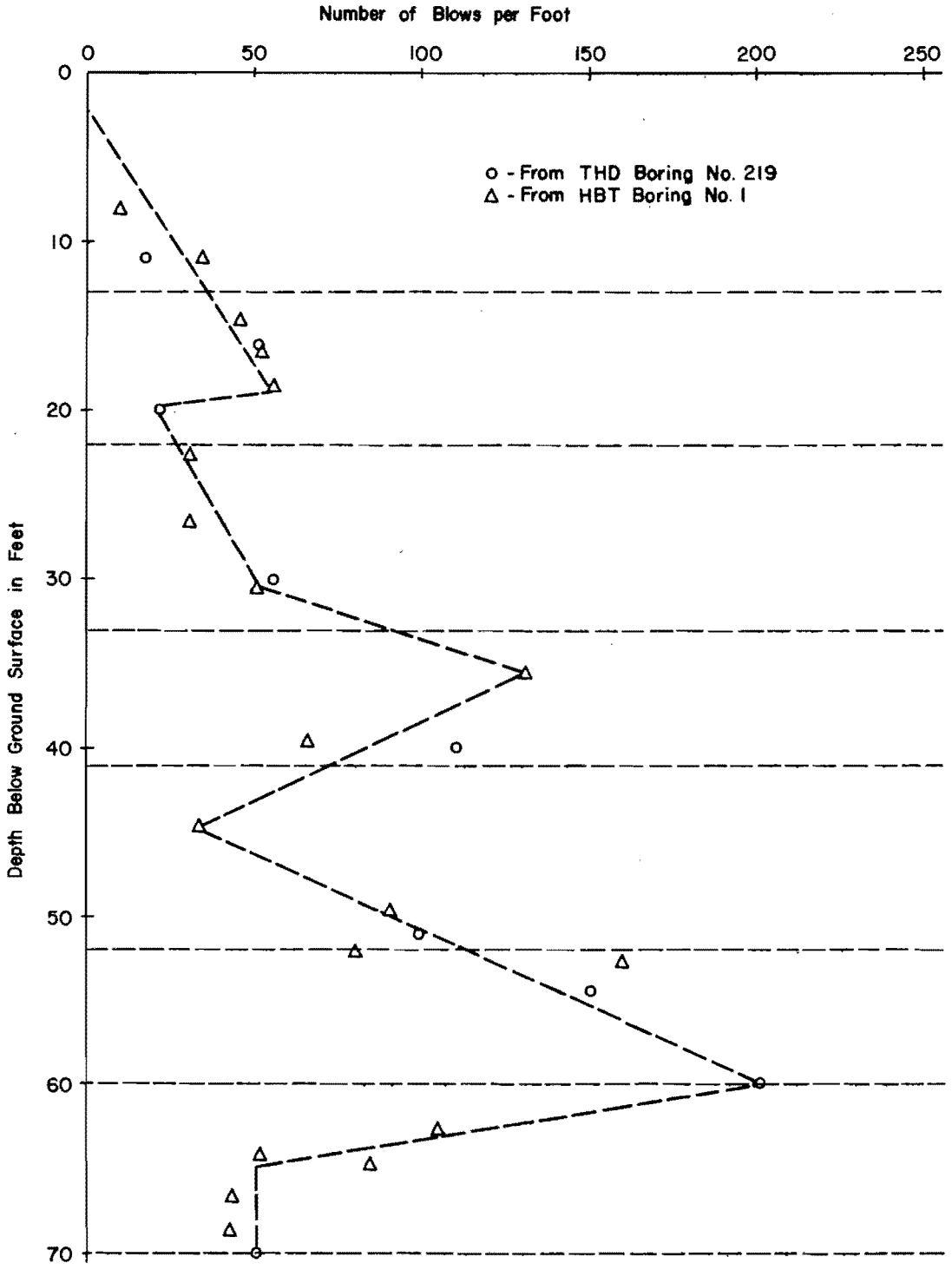

Fig. 4.3. Profile of THD Cone Penetrometer Readings

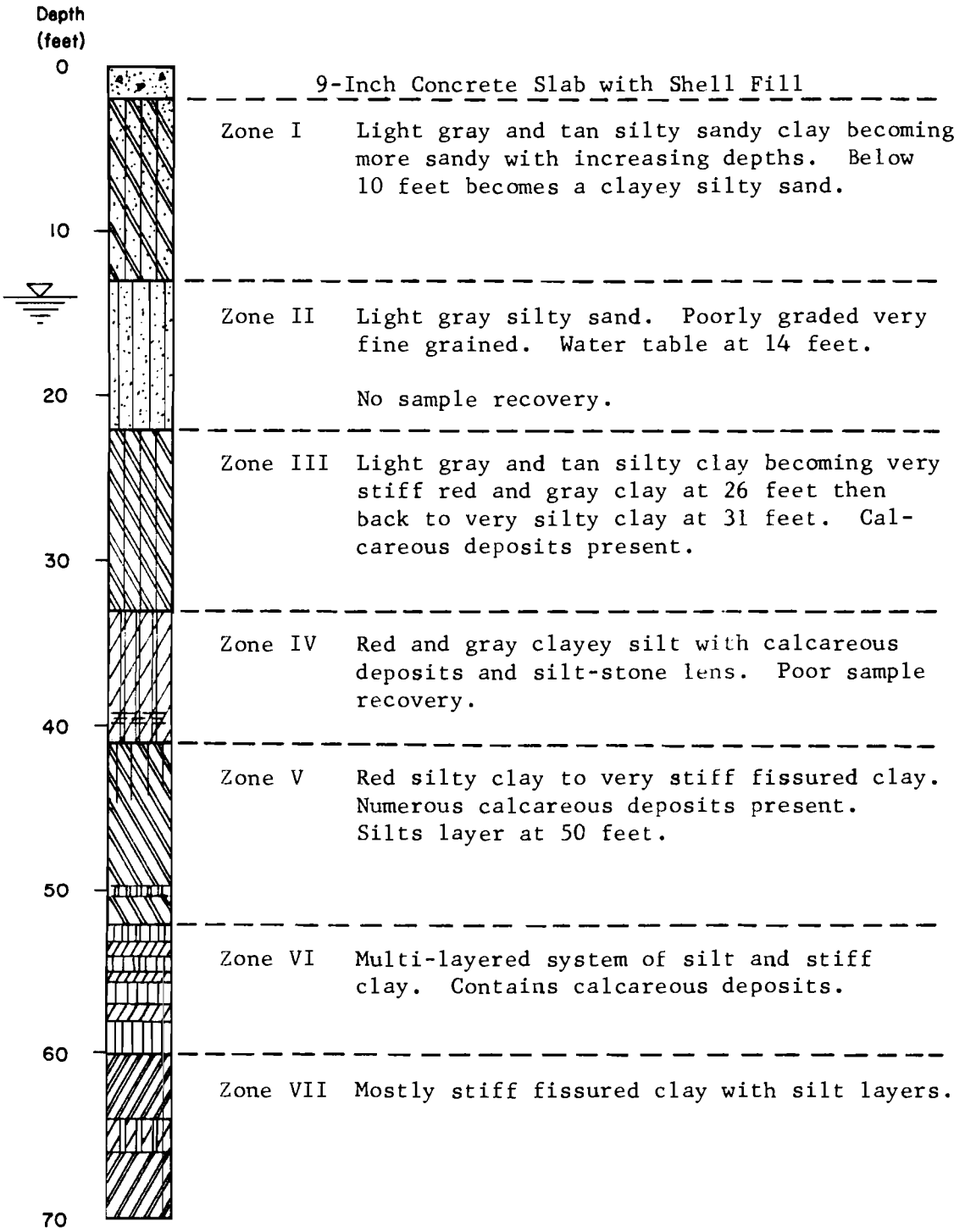

Fig. 4.4. Composite Soil Profile

procedures. The hydrometer tests were conducted according to test procedure D422-62, given by the American Society for Testing Materials. The results of these tests are presented in Fig. 4.5 through 4.8 and in Tables 4.1, 4.2, and 4.3.

As previously noted, the soil varies considerably between zones. The variance of the soil is reflected in the results of the Atterberg limits of the soil. Using nomenclature of the unified classification system, the soils in Zones I, III, and IV were mostly of the CL type; soil in Zones V and VII were of the CH type; and the soil in Zone II was the SM type. The soil of Zone VI was a multilayered zone of silt and clay.

Triaxial Tests. Triaxial tests using the transmatic device were conducted by personnel of the Texas Highway Department on the samples from boring TSH 219. The results of these tests are shown in Table 4.4.

Personnel from The University of Texas conducted controlled-rate-of-strain triaxial tests of unconsolidated and undrained samples from borings HBT-1 and HBT-2. In the first tests, an effort was made to obtain two test specimens from each sample by cutting the sample in half along the longitudinal axis. Each half could then be trimmed to a 1.4-inch diameter test specimen. This method of testing was successfully employed for the SH 225 test samples, but proved almost impossible for the samples from the HB&T Test Site. The samples were either so badly fissured, contained so many calcareous deposits, or were so silty that extensive trimming usually resulted in a ruined sample.

As a result of the difficulty encountered in the trimming operation, it was decided to test specimens of 2.8-inch diameter. Since the

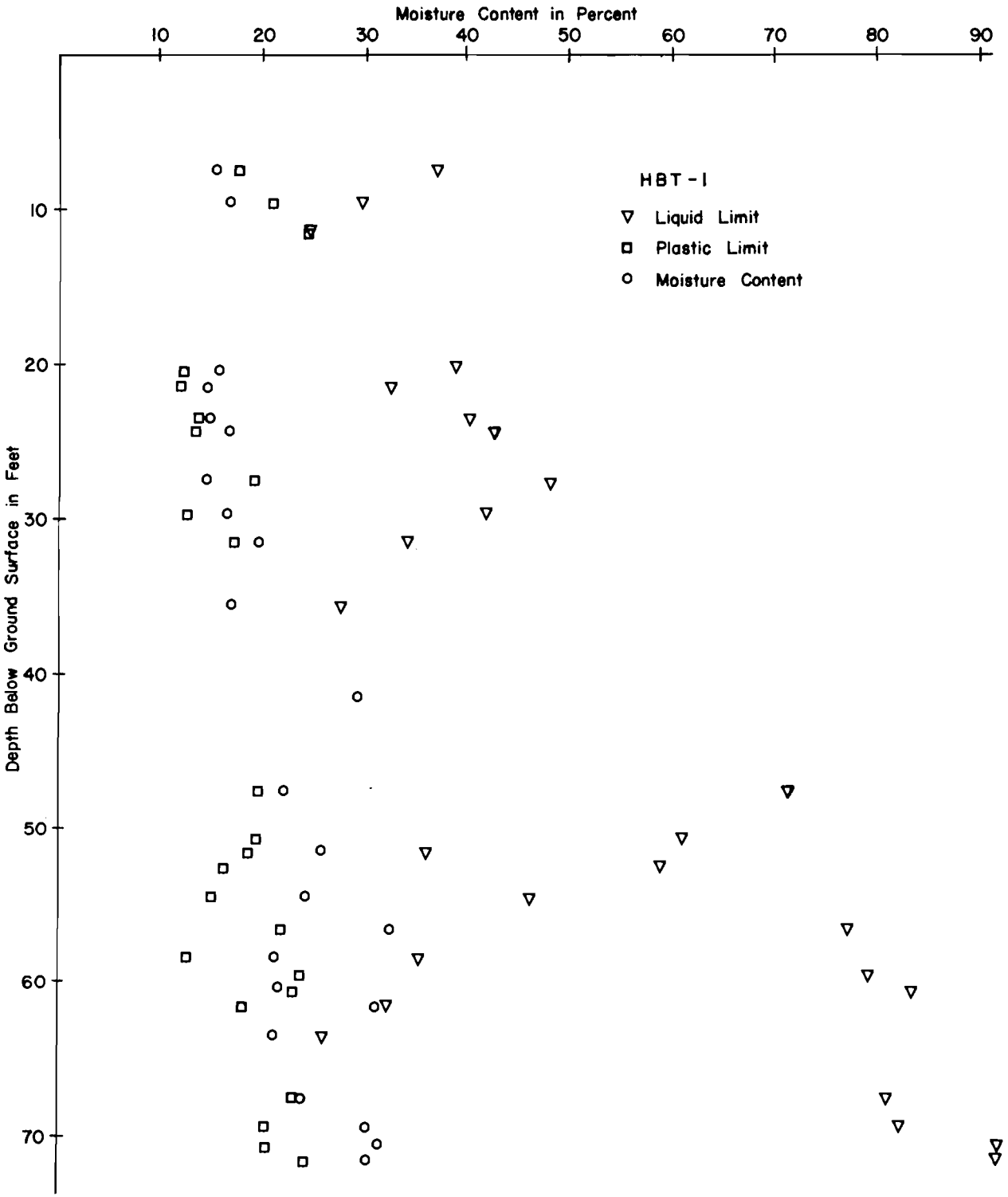

Fig. 4.5. Profile of Liquid Limit, Plastic Limit, and Moisture Content from Boring HBT-1

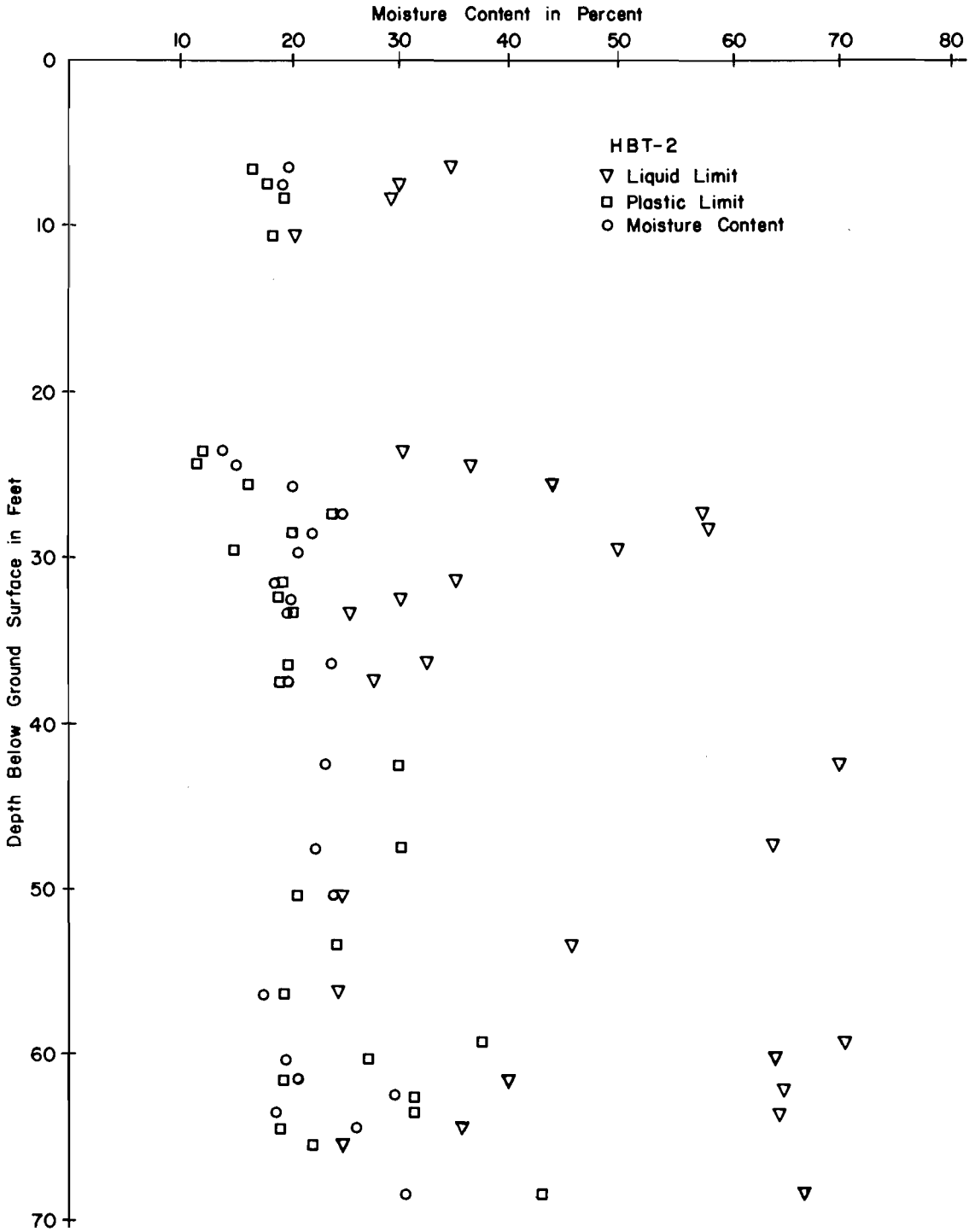

Fig. 4.6. Profile of Liquid Limit, Plastic Limit, and Moisture Content from Boring HBT-2

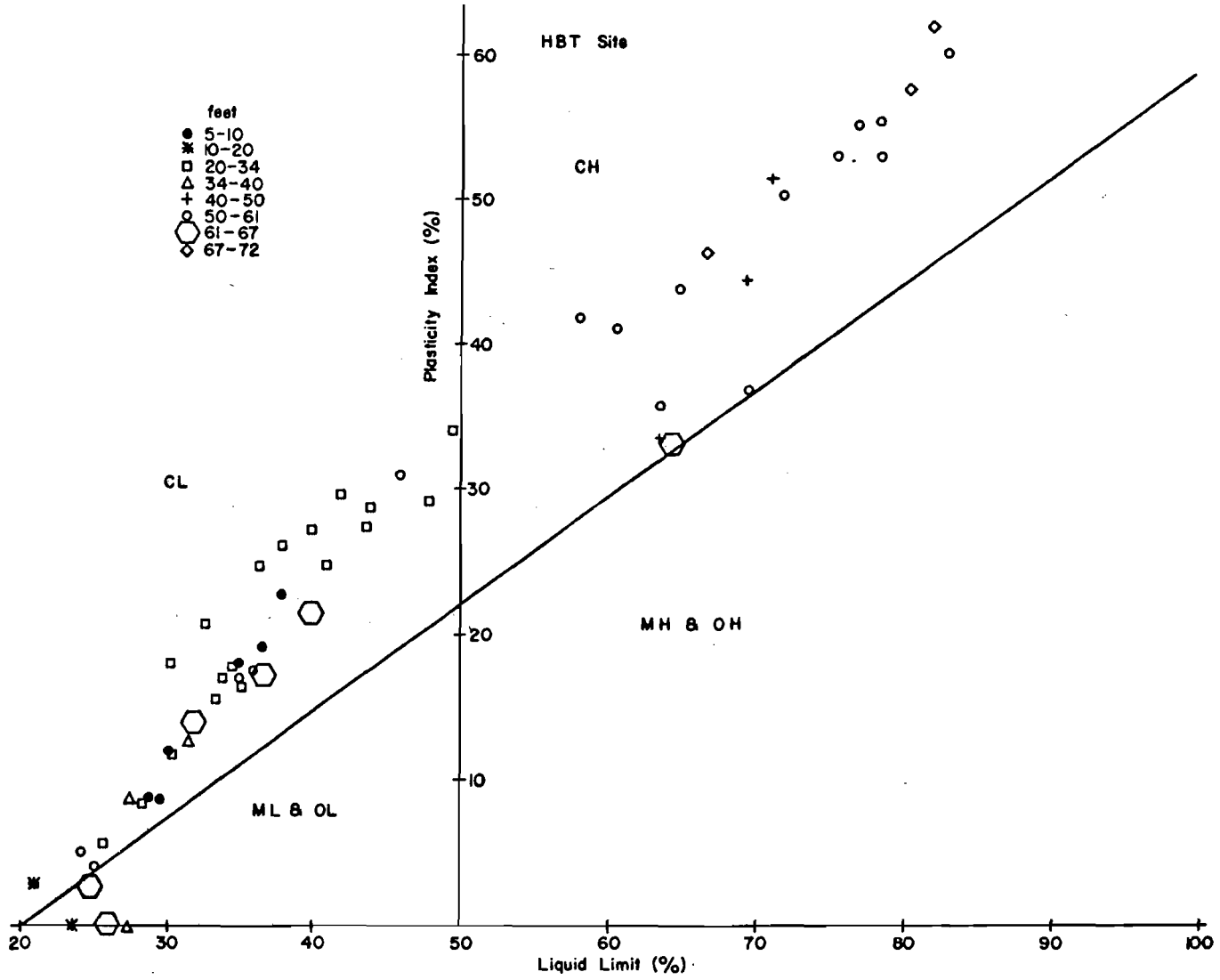

Fig. 4.7. Plasticity Chart for the HB&T Test Site

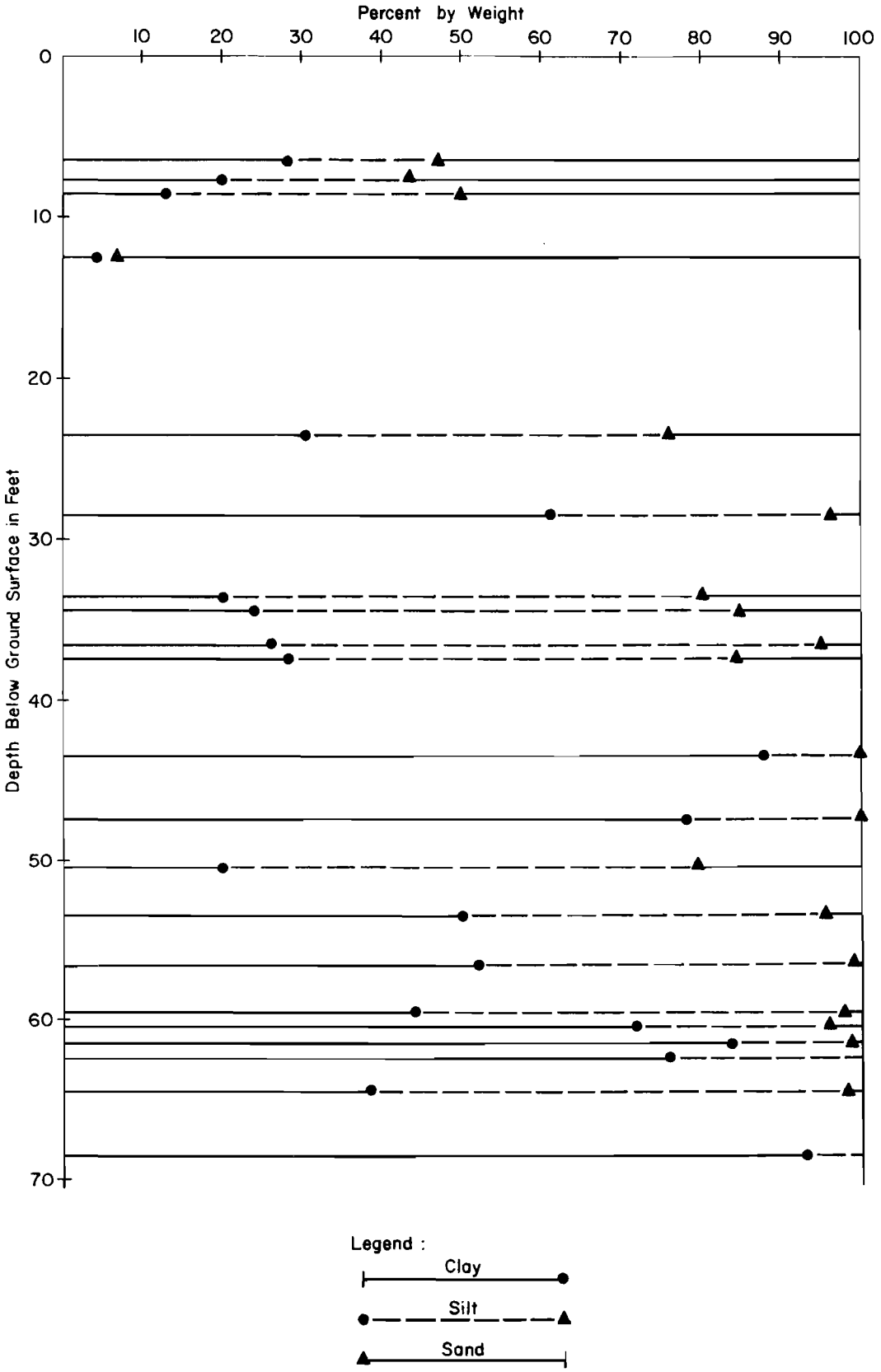

Fig. 4.8. Profile of Grain-Size Distribution

TABLE 4.1 UNIFIED SOIL CLASSIFICATION DESCRIPTION

HBT BORING NO. 1

Sample	Depth in feet	Description	Unified Classification
2	7.5	clayey sand	SC-CL
3	9.5	clayey sand	SC-CL
4	11.5	silty sand	SM
5	20.5	silty clay	CL
6	21.5	silty clay	CL
7	23.5	silty clay	CL
8	24.5	silty clay	CL
10	27.5	silty clay	CL
12	29.5	silty clay	CL
13	31.5	silty clay	CL
17	35.5	clayey silt	ML
21	46.5	clay	CH
24	50.5	clay	CH
25	51.5	silty clay	CL
26	52.5	clay	CH
27	54.5	silty clay	CL
28	56.5	clay	CH
29	58.5	silty clay	CL
30	59.5	clay	CH
31	60.5	clay	CH
32	61.5	silty clay	CL
33	63.5	clayey silt	ML
34	67.5	clay	CH
35	69.5	clay	CH
36	70.0	clay	CH
37	70.5	clay	CH

TABLE 4.2 UNIFIED SOIL CLASSIFICATION DESCRIPTION

HBT BORING NO. 2

Sample	Depth in feet	Description	Unified Classification
2	6.5	clayey sand	SC
3	7.5	clayey sand	SC
4	8.5	clayey sand	SC
6	10.5	silty sand	SM
9	13.5	silty sand	SM
11	23.5	silty clay	CL
12	24.5	silty clay	CL
13	25.5	silty clay	CL
17	29.5	silty clay	CL
19	31.5	silty clay	CL
20	32.5	silty clay	CL
21	33.5	silty clay	CL
22	36.5	silty clay	CL
23	37.5	silty clay	CL
25	43.5	clay	CH
30	47.5	clay	CH
33	50.5	silty clay	CL
39	56.5	silty clay	CL
41	59.5	clay	CH
42	60.5	clay	CH
43	61.5	silty clay	CL
44	62.5	clay	CH
45	64.5	clay	CH
46	65.5	clayey silt	ML
48	68.5	clay	CH

TABLE 4.3 RESULTS OF HYDROMETER TESTS

HBT BORING NO. 2

Clay size <.005mm Sand size >.074mm

Sample and Description	%Clay	%Silt	%Sand
HBT 2-2			
Lt tn & Gr sandy clay w/calc	28	19	53
HBT 2-3			
Lt tn & Gr sandy clay w/calc	20	23.6	56.4
HBT 2-4			
Lt tn & Gr clayey sandy silt	13	37	50
HBT 2-9			
Lt tn sand	4	3	93
HBT 2-11			
Yellow & tn silty clay	30.4	45.6	24
HBT 2-13			
Rd, yellow & tn silty clay	40.8	37.4	21.8
HBT 2-16			
V stiff Rd & Gr silty clay	61	35	4
HBT 2-20			
Rd & Gr V silty clay	22.1	54.5	22.1
HBT 2-21			
Rd & Gr V silty clay	24.0	60.6	15.4
HBT 2-22			
Rd & Gr silty clay w/calc	26	68.8	5.2
HBT 2-23			
Rd & Gr silty clay w/calc	28.4	56.0	15.6
HBT 2-26			
Rd silty clay w/calc	88	12	0
HBT 2-30			
Stiff Rd silty clay w/calc	78	22	0
HBT 2-33			
Rd clayey silt w/calc	20	59.4	20.6
HBT 2-36			
Rd Clayey silt	50	45.7	4.3
HBT 2-39			
Rd clayey silt	52	47	1
HBT 2-41			
Rd silty clay w/calc	44	53.7	2.3
HBT 2-42			
Stiff Rd silty clay w/calc	72	24	4
HBT 2-43			
Stiff Rd silty clay w/calc	82	17	1
HBT 2-44			
Stiff Rd silty clay w/gr silt lens	76	24	0
HBT 2-45			
Rd clayey silt	38.8	59.6	1.6
HBT 2-48			
Rd silty clay w/calc	93	7	0

TABLE 4.4 RESULTS OF THE TRANSMATIC-TRIAXIAL TESTS CONDUCTED BY PERSONNEL OF THE TEXAS HIGHWAY DEPARTMENT

Depth (Feet)	Angle of Internal Friction (Degrees)	Cohesion (Psi)	Overburden (Psi)	Shear Strength (Psi)
0-14	21	0	12.81	4.92
14-22	No Sample	-	-	-
22-27	15	9	19.17	14.14
27-35	9	14	23.11	17.66
35-42	No Sample	-	-	-
42-47	3	14	28.41	15.48
47-54	8	15	31.69	19.46
54-55	No Sample	-	-	-
55-58	5	17	33.46	19.92
58-62	No Sample	-	-	-
62-63	11	5	35.65	11.92
63-68	No Sample	-	-	-
68-75	12	11	40.67	10.20

diameter of the samples obtained with the thin-walled sampler was approximately 2 7/8 inches, little trimming was required.

The results of the triaxial tests were very erratic due mainly to the slickensides and silt lenses. One sample which failed along a slickenside is shown in Fig. 4.9. Due to the erratic results obtained, the results from some tests were deleted for determining a strength profile.

The stress-strain curves obtained from the triaxial tests are presented in Appendix A. From each of these curves, a peak shear strength for the sample was determined. The peak shear strengths are given in profile form in Fig. 4.10. It is noted in the profile that the soil from Zones I, IV, and VI had lower indicated shear strength than did the soil from Zones III, V, and VII. Due to the lack of samples, very little information is available for Zone II.

Direct Shear Tests. The direct shear tests were conducted to obtain an indication of the possible effect of a bentonite slurry on the shear strength developed between soil and concrete. From tests presented by Chuang and Reese (1969), it was concluded that for mortar cast against sandy loam and sandy clay, the shearing resistance at the interface is slightly increased above the undisturbed strength. For clay, this strength was found to be slightly less than the undisturbed strength. O'Neill and Reese (1970) varified these results by direct shear tests of samples from the Houston SH 225 Test Site. Both of these studies indicated that the weakest zone was from one-fourth to three-eighths of an inch from the interface.

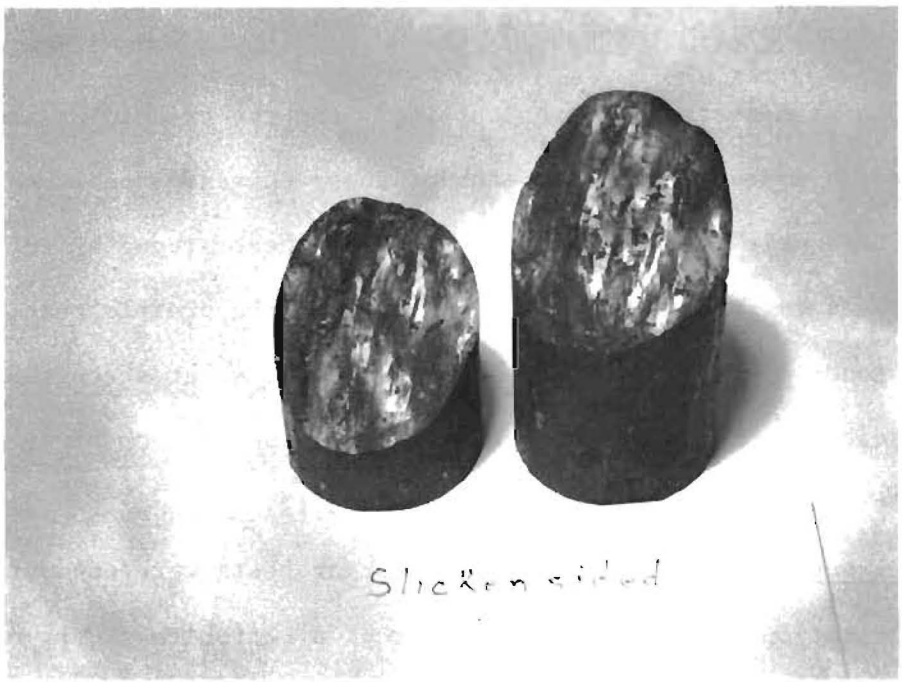

Fig. 4.9. Example of Slickensided Soil Sample

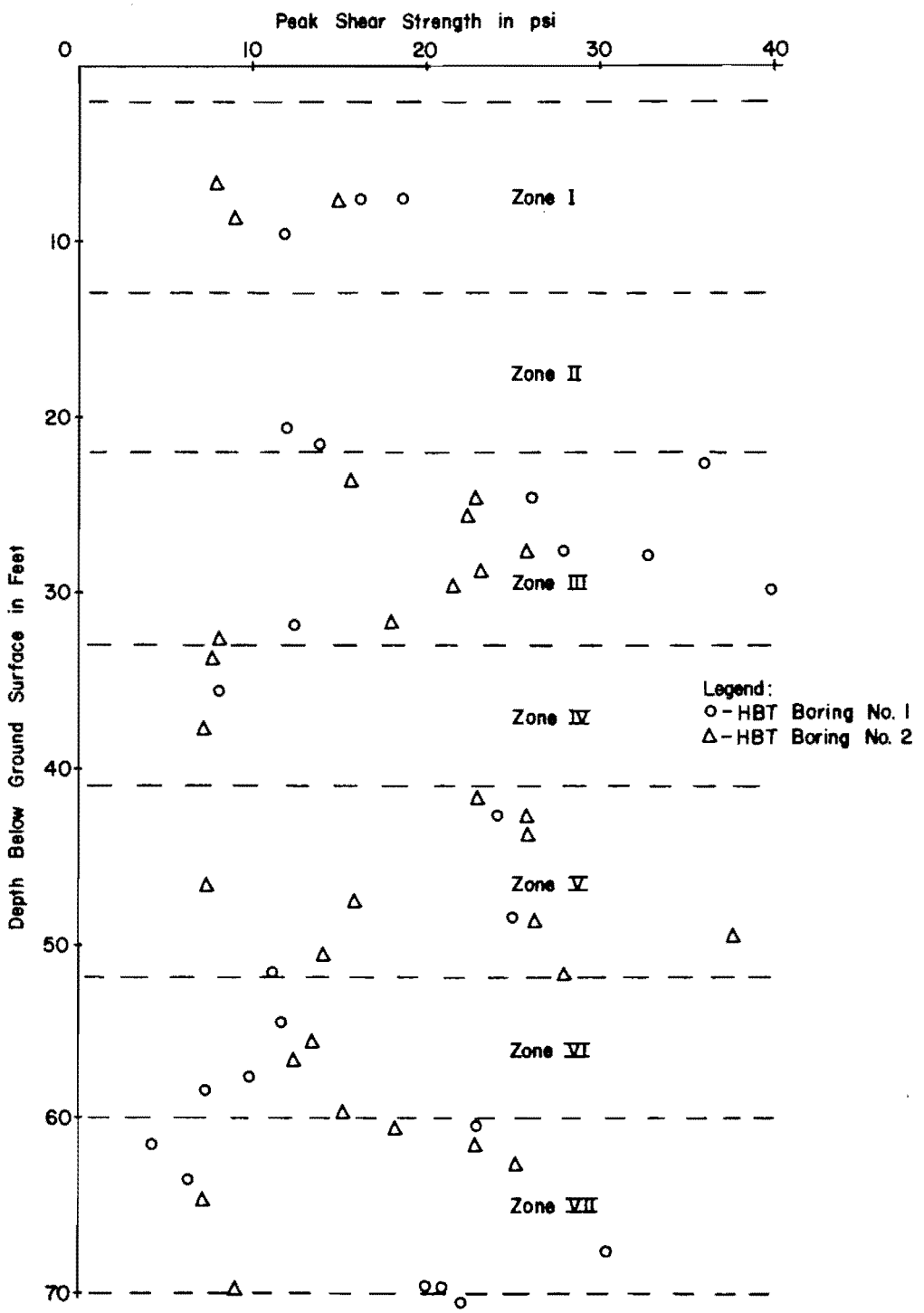

Fig. 4.10. Profile of Peak Shear Strength from Triaxial Tests

If a bentonite slurry is introduced between the soil and the mortar, it may be assumed that the shear strength at the interface would be most affected. For this reason, all of the direct shear tests were conducted at the interface of the soil and mortar. A shear box similar to that described by O'Neill and Reese (1970) was used in these tests. The box was changed by lining the upper section with a teflon insert to reduce the friction between the sides of the box and the mortar. Control tests on Colorado River sand indicated that the experimental system was working satisfactorily.

For each full-sized sample three tests were conducted. By cutting perpendicular to the longitudinal axis, the sample was first subdivided into three separate specimens. The first of the specimens was tested immediately in the direct shear apparatus as shown in Fig. 4.11a.

The other two specimens were placed in the direct shear apparatus and concrete mortar was cast against the soil. In one case, a layer of bentonite slurry approximately one-eighth-inch-thick was placed against the soil before the mortar was cast (Fig. 4.11c); in the other case the mortar was cast without the bentonite slurry (Fig. 4.11b).

The mortar was mixed using Type I cement and Colorado River sand. The water-cement ratio was 0.6. The slurry was a 7-per-cent solution of pure Wyoming bentonite. Each specimen was cured for one week under a confining pressure of 20 psi. No attempt was made to keep the specimens wet during the curing period. After the curing period, each specimen was tested using the same confining pressure as was used for the curing. In each test, the intended shearing plane was at the interface of the soil and mortar. The results of the tests are presented in

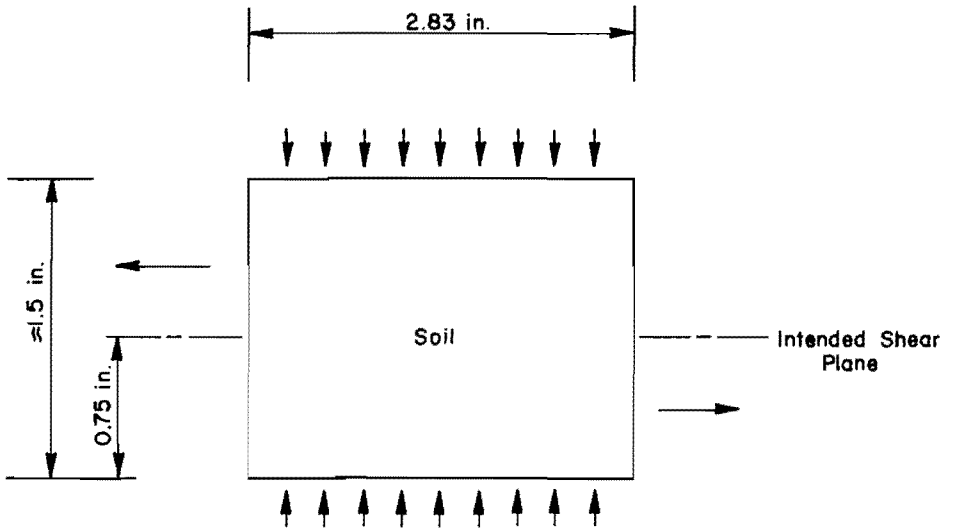

a. Plain Sample

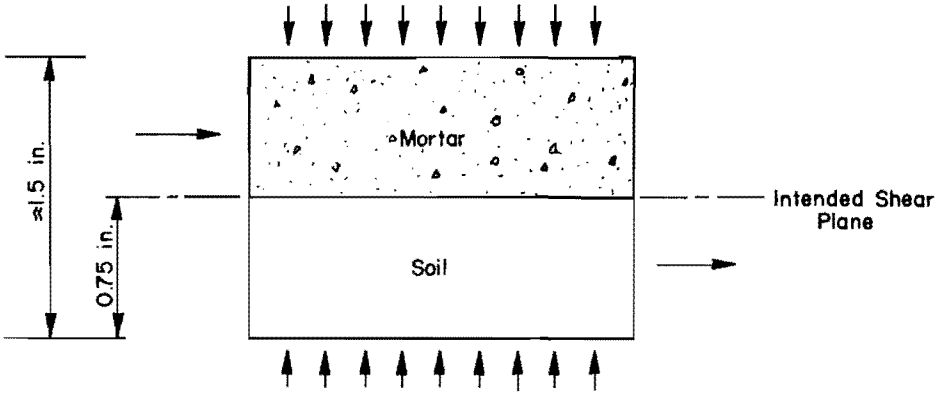

b. Sample without Bentonite

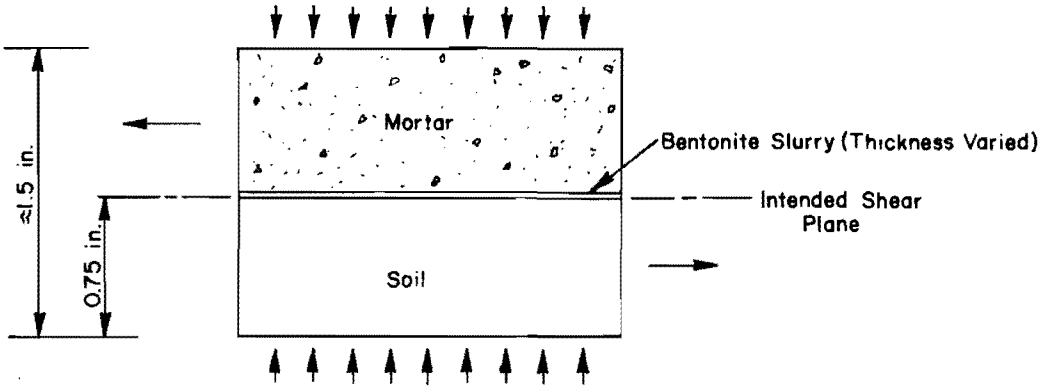

c. Sample with Bentonite

Fig. 4.11. Illustration of Direct Shear Tests

Table 4.5. After each test, moisture contents were measured at varying distances from the interface.

From the tests, it was concluded that for sandy and silty soil, the bentonite slurry had very little affect on the interface shear strength. In the tests of these samples, the failure occurred from one-eighth to one-fourth of an inch away from the interface and indicated a slightly higher shear strength than the undisturbed soil. The failure plane for both tests of a silty sample is shown in Fig. 4.12. In this particular sample, the specimen cast with bentonite showed a greater dishing effect than did the sample cast without bentonite. For other sandy or silty samples, hardly any difference could be detected.

For the clay samples, the interface strength was greatly reduced by introduction of the bentonite slurry. When the mortar was cast against the soil, a dishing effect was noted but not to as great an extent as had been observed in the sand and silt. For the specimens cast with the bentonite slurry between the mortar and soil, the failure plane occurred along the interface with no blending of the mortar and soil.

The moisture profiles failed to show any variation between the specimens cast with bentonite and those cast without bentonite.

The results of the test infer that for drilled shafts in sand or silt there will be no effect of the drilling mud. For shafts in clay, however, the shear strength developed along the sides of the shaft may be seriously reduced.

Soil Strength Profile. The shear strength and the stress-strain characteristics of the soil are felt to be the major soil parameters

TABLE 4.5 RESULTS OF DIRECT SHEAR TESTS - HOUSTON BORING NO. 2

Sample No.	Depth In Feet	Type	PL	LL	Plain	Mortar Without Bentonite	Mortar With Bentonite	Normal Pressure
1	3.5	dark brown clayey silt	----	----	8.80	12.40	12.90	5
5	9.5	tan & gray sandy silt	----	----	14.70	16.20	16.50	10
6	10.5	light gray & tan clayey sand	17.9	21.0	13.20	-----	-----	10
7	11.5	light tan & gray sandy clay	----	----	10.65	-----	-----	10
8	12.5	tan & gray silty sand	----	----	9.84	16.00	12.60	10
9	13.5	wet gray silty sand	----	----	6.60	8.60	4.85	5
					7.16	9.85	12.00	10
					12.60	15.65	14.70	15
10	22.5	yellow & tan silty clay	----	----	18.10	31.70	24.60	20
14	26.5	very stiff red & gray silty clay	----	----	18.70	26.00	16.40	20
18	30.5	very stiff red & gray silty clay	----	----	17.10	28.70	12.60	20
27	44.5	stiff red clay slickensided	----	----	17.10	26.20	10.80	25-20-20
28	45.5	stiff red clay slickensided	----	----	18.70	30.50	17.40	25
35	52.5	stiff red clay with silt lens	----	----	20.80	31.60	10.80	20
36	53.5	stiff red clay with hard silt lens	23.6	45.5	19.50	17.90	16.90	20
37	54.5	stiff red clay with hard silt lens	----	----	18.20	24.20	19.40	20
40	57.5	highly saturated clayey silt	----	----	16.40	-----	16.80	20

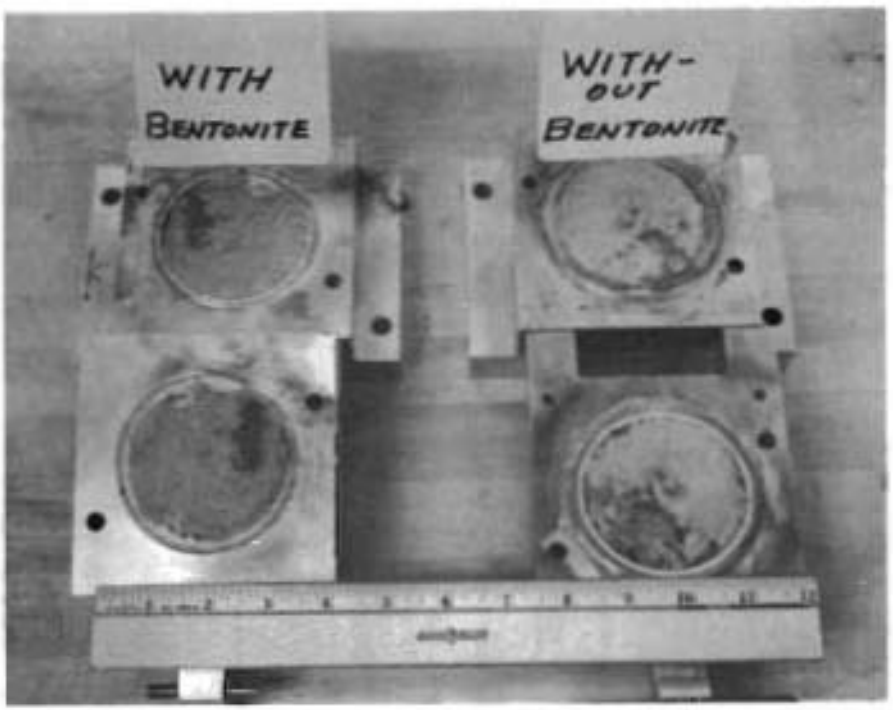

Fig. 4.12. Comparison of Failure Surfaces for Direct Shear Tests of Silty-Soil Samples

influencing the shearing resistance that could be developed along a drilled shaft. For this reason much effort was exerted in developing a soil strength profile and the stress-strain relationships that best represent the in situ properties of the soil. The soil in the vicinity of a drilled shaft, however, may be greatly changed from the in situ conditions, particularly for sands and silts in which the confining pressure has a major effect on the shear strength.

At the HB&T Test Site the determination of the soil properties was especially difficult. It was not possible with the equipment available to sample the sandy soil of Zone II; therefore, the angle of internal friction ϕ was estimated from the THD cone utilizing the following three-step procedure.

1. The average reading from the THD cone penetrometer was converted to penetration of the standard split spoon. The correlation for the conversion was furnished by the Texas Highway Department (1970).
2. Using Fig. 7 presented by Gibbs and Holts (1957) the sand was classified as being dense with a relative density of approximately 80 per cent. This placed the sand in the upper end of the dense classification.
3. In the chart given on page 222 of the textbook by Peck, Hanson and Thornburn (1953), it is noted that a sand with a ϕ value of 40 degrees falls at the upper end of the dense classification. Thus, a value of 40 degrees was chosen as being a good estimate of the angle of internal friction for Zone II.

The best estimate of the stress-strain relationship for each zone was obtained from the average of the stress-strain curves of The University of Texas triaxial tests (Fig. 4.13). As discussed earlier, due to the numerous slickensides, calcareous deposits and silt-stone lens, these curves must be considered as only an estimate of the true stress-strain relationships.

The shear strengths obtained from the three different procedures are presented in comparison form in Fig. 4.14. The shear strengths shown for The University of Texas triaxial tests were taken from the average stress-strain curves presented in Fig. 4.13. The values for the transmatic triaxial test were taken from Table 4.4. Due to difficulty in sampling, there were no transmatic triaxial tests conducted on any soil from Zone IV. Conversion of the THD cone penetrometer reading was accomplished by use of the correlation curve presented in the Foundation Design Manual of the Texas Highway Department (1964).

The comparison of The University of Texas triaxial tests and the transmatic triaxial tests show that, in general, The University of Texas triaxial tests gave higher values of shear strengths than did the transmatic triaxial tests. This comparison would be consistant with the finding presented by O'Neill and Reese (1970) for the SH 225 Test Site.

For the shear strengths of soil Zones IV and VI the THD cone penetrometer gave values more than twice as large as those obtained in The University of Texas triaxial tests. The soils in these two zones were mostly silts. For the clay soils, the THD cone penetrometer gave results which compared favorably with the triaxial results. O'Neill

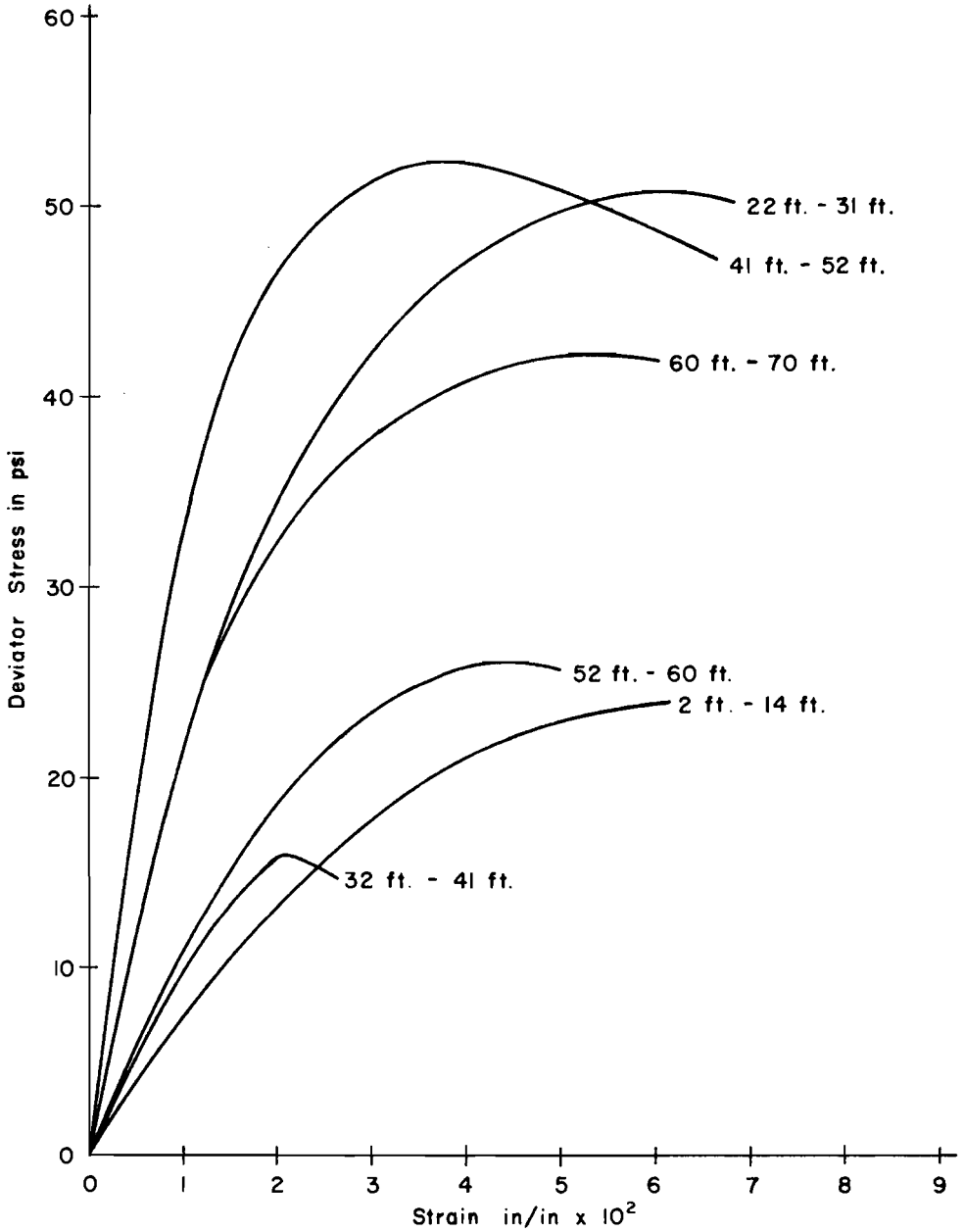

Fig. 4.13. Average Stress-Strain Curves from Triaxial Tests

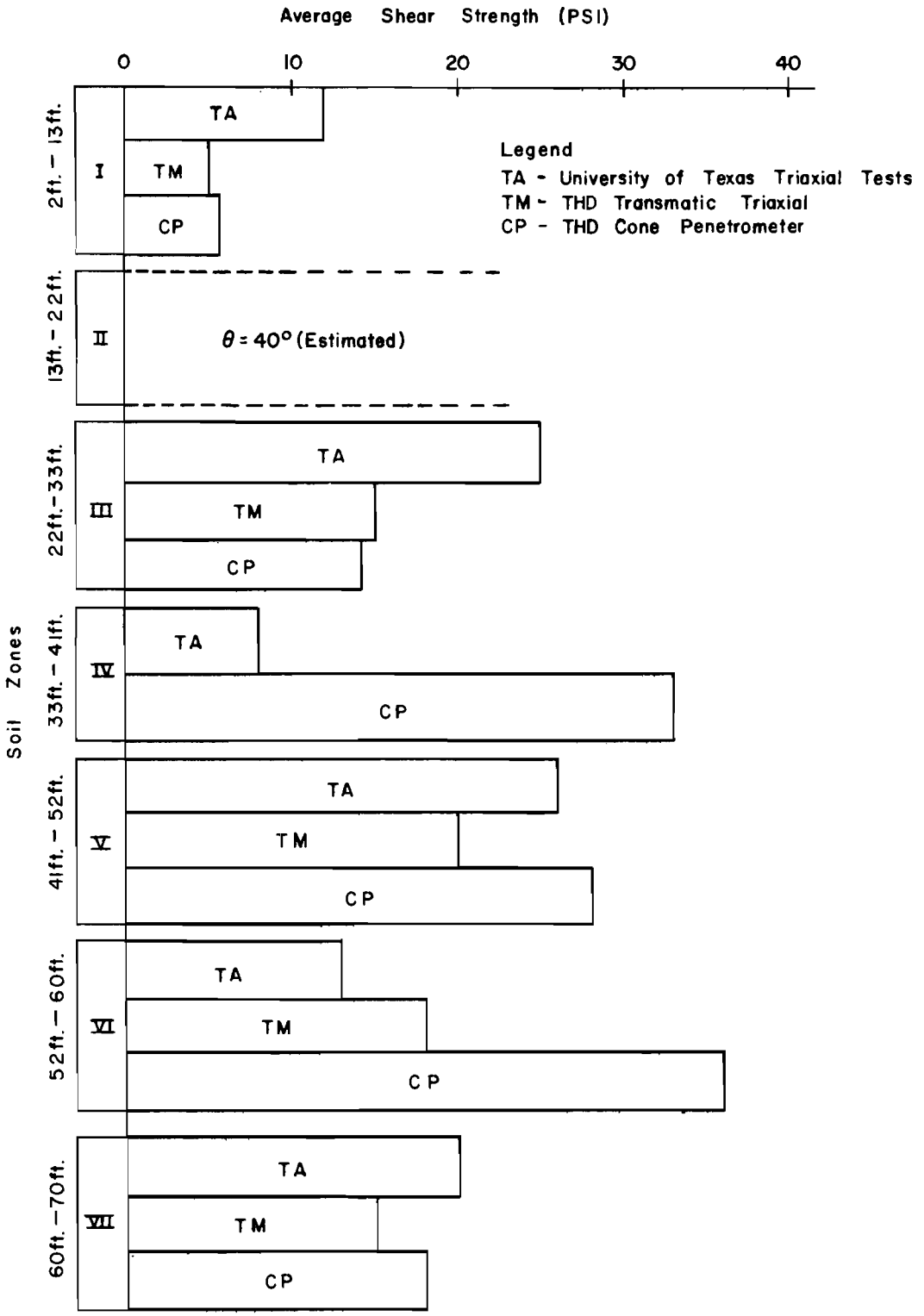

Fig. 4.14. Comparison of Soil Strength as Obtained by Different Methods

and Reese (1970) indicated that, in the Beaumont clay at the SH 225 site, the penetrometer gave conservative values for shear strengths. For the HB&T Test Site, except for Zone V, this appeared to be true. Zone V was heavily fissured and slickensided. Because of the secondary structure of this clay, the in situ shear strength is thought to be considerably higher than the values obtained from the triaxial tests. Although many investigators doubt the usefulness of a dynamic penetrometer test for determining the shear strength of clay, it is believed that the strengths obtained from the penetrometer readings represent fairly well the true strength of the soil in Zone V.

Based on the data available, the soil strength profile in Fig. 4.15 is presented as being the best possible estimate of the soil shear strength. The difficulties encountered at the HB&T Test Site in obtaining a good soil profile of the soil strength may be considered typical for locations where drilled shafts are to be constructed with the aid of drilling mud. These difficulties certainly underscore the importance of further study of the in situ testing of soils.

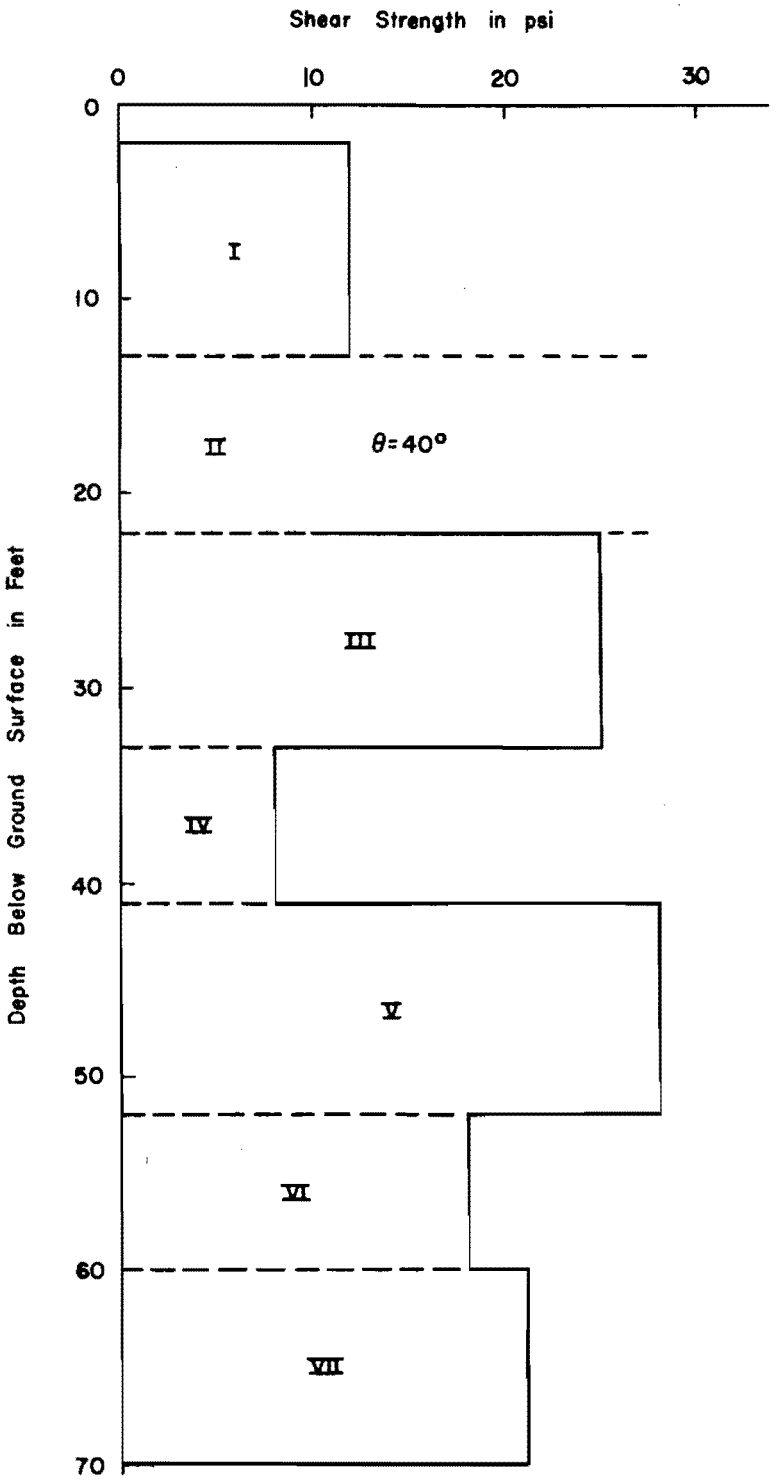

Fig. 4.15. Composite Soil Strength Profile

CHAPTER V

TEST SYSTEM

Test Shaft

As described earlier, the test shaft was designed by the Texas Highway Department as the proof design to permit a more economical foundation for the North Loop overpass structure. The original plan called for a combination of drilled shafts belled at 90 feet where belling was possible, and driven concrete piles elsewhere. As a direct result of the SH 225 tests, the personnel at the Texas Highway Department felt that straight drilled shafts could be incorporated into the structure foundation, allowing a considerable financial saving. Since this was to be a pilot design based on untried research, a field test was considered to be essential.

The design load for the test shaft was to be 206 tons, using a safety factor of 2. Correlation of the soil properties and shaft behavior was obtained by using design procedures outlined in the Foundation Exploration and Design Manual of the Texas Highway Department (1964). The design was based on both the expected side shear and the bottom bearing.

The final design called for a shaft 3 feet in diameter extending 60 feet below the ground surface. The shaft was founded in a soil system alternating between layers of water-bearing silt and highly fissured clay. The shaft, along with the shaft instrumentation, is shown diagramatically in Fig. 5.1. The designation used in identifying

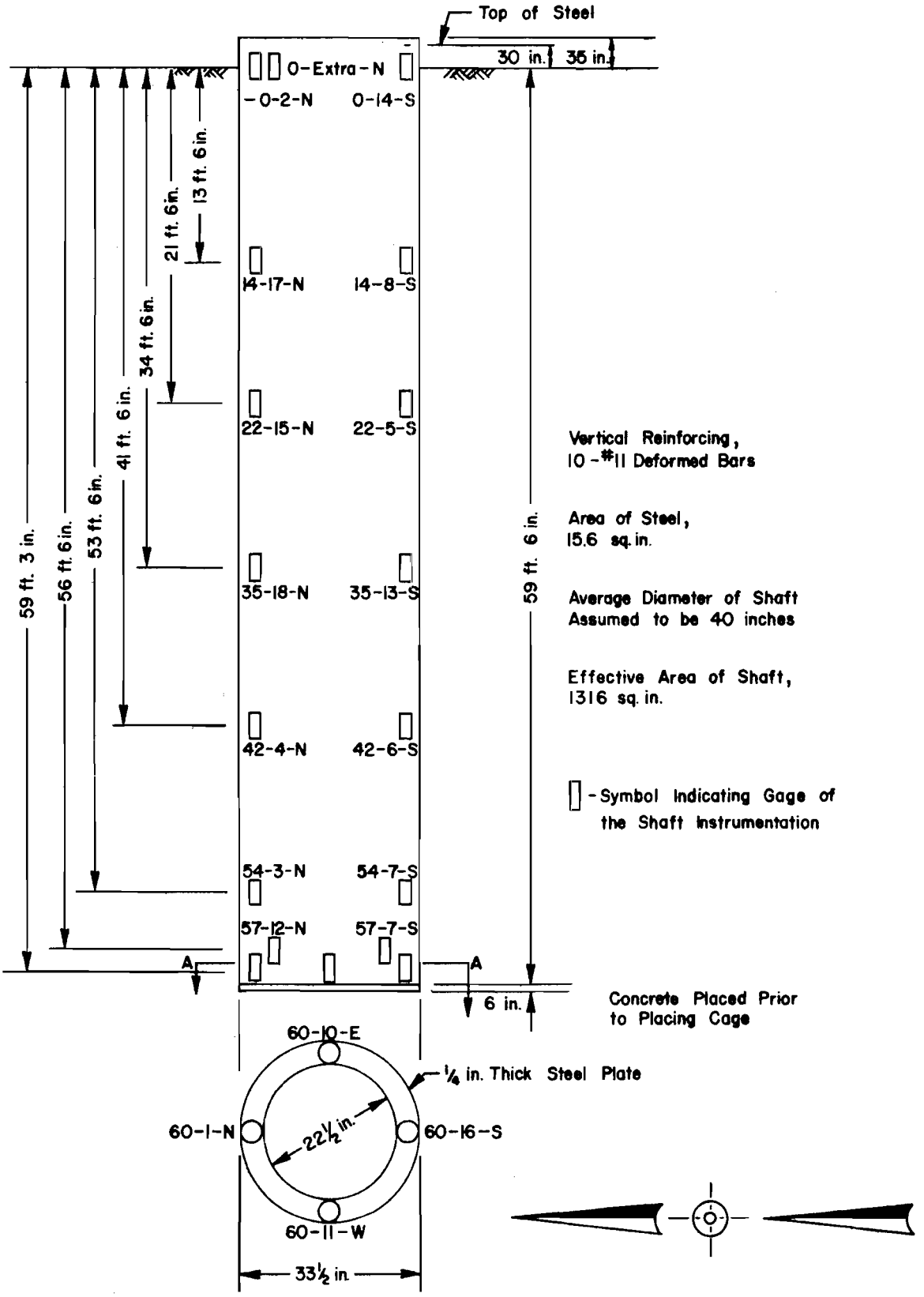

Fig. 5.1. HB&T Test Shaft

individual gages of the shaft instrumentation will be explained later in the text.

The longitudinal reinforcement consisted of ten No. 11 steel bars. The reinforcement was delivered in standard 60-foot lengths that required splicing the vertical bars. These splices were made at the ground surface of the shaft. Tied spiral reinforcement was intermittently welded to the axial reinforcement for lateral reinforcing.

A one-fourth-inch-thick steel ring, 33 1/2 inches in outside diameter and 22 1/2 inches in inside diameter was welded at the bottom of the shaft, to the vertical reinforcement, as shown in Fig. 5.2. The purpose of the ring was to provide firm anchorage for the bottom level of instrumentation. In addition, the ring acted to stiffen the reinforcement and to aid in the handling of the cage. The bottom plate, being hollow, did permit concrete to be in contact with the bottom of the hole.

Reaction System

The reaction system for the test was similar to the systems used in the San Antonio test and the tests at the SH 225 site. The superstructure was identical to that employed in the tests of Shafts 2 and 4 at the SH 225 site and is described in detail by O'Neill and Reese (1970).

The reaction shafts of this test were to serve as foundation shafts for the overpass structure, and therefore, each was constructed as required by the original foundation design. Each shaft was 3 feet in diameter and 96 feet long, with the bottom belled to a 9-foot diameter. The center to center distance between the reaction shafts was 20 feet.

Fig. 5.2. Steel Plate Welded to Bottom of Reinforcing

Fig. 5.3. Drilling Rig Working at the HB&T Test Site

The construction procedure for the reaction shafts was similar to that employed for the test shaft. The hole was first drilled to within a few feet of the top of the bell utilizing drilling mud. The casing was then set, sealed at the bottom, and the hole bailed dry. The hole was completed by drilling and belling beneath the casing.

The casing was left in the hole with no attempt being made to extract it. The reinforcement extended above the reaction shaft to tie into the proposed structure. The reaction beam was supported by two 14 WF 142 beams embedded in the reaction shafts. These beams had an embedment length of 15 feet. Concrete bond was assumed adequate to provide load transfer between the vertical supports and the reaction shafts.

Construction of Test Shaft

Construction of the test shaft began at 8 a.m. on June 12, 1969, with the removal of a portion of the concrete slab. The drilling rig to be used was a large truck-mounted rig capable of drilling and handling casing (Fig. 5.3). Actual drilling began at 9 a.m. and continued in the dry for several feet. At 13 feet, a water-bearing silty-sand, requiring the use of a drilling fluid, was encountered. Processing was accomplished by filling the hole with water to within a few feet of the top, then introducing two 100-pound sacks of Wyoming bentonite while simultaneously mixing and stirring with the auger. In this manner, the hole was advanced through the sand to a depth of 22 feet. Continued augering under the mud required introducing spoils and one additional sack of bentonite to the drilling fluid. At a depth of 54 feet the casing was set and sealed. The hole was then bailed dry using a

bailing bucket handled by the drilling rig (Fig. 5.4). From 54 to 60 feet, the drilling proceeded in the dry below the casing. The casing was advanced along with the drilling by the simultaneous rotating and pushing of the casing with the kelly bar (Fig. 5.5).

At the desired 60-foot depth, a water-bearing silt seam was penetrated, causing a minor blow-out at the bottom of the hole. The bottom was quickly plugged by placing a 6-inch-thick layer of concrete at the bottom of the hole. The layer of concrete also served as a seating pad for the instrumentation ring attached to the reinforcing cage.

The reinforcing cage was set quickly; and at 1:30 p.m. concreting was begun. An 8-inch steel pipe was employed as a tremie for concreting (Fig. 5.6). The pipe had windows cut at intervals along its length allowing the concrete to be poured directly into the tremie from the ready-mix trucks. Concrete was first placed about one-fourth of the way up the casing, at which time the casing was lifted a few feet to break the seal and to keep the casing free. As concreting continued, the casing was slowly lifted until the top of the casing was approximately 10 feet above the ground surface (Fig. 5.7). By using a concrete bucket, the casing was completely filled with concrete so that as the casing was removed, the hole was filled. As the casing was raised, the drilling mud between the casing and the wall of the hole was displaced and flowed out of the top of the hole.

After the hole had been completely filled with concrete, a section of Sonotube form was pushed into the wet concrete for a distance of 25 inches, leaving approximately 35 inches of the form above the ground

Fig. 5.4. Bailing Bucket for Removal of Drilling Mud

Fig. 5.5. Setting of Casing for the HB&T Test Site

Fig. 5.6. Placing Tremie Pipe

Fig. 5.7. Filling Casing with Concrete

surface. The Sonotube form was filled with concrete and leveled. The concreting was completed at 3:35 p.m.

Concrete

The concrete was purchased from a ready-mix plant in the Houston area. It was a 6-sack-per-cubic-yard mix with a 5 1/2 to 6-inch slump. The concrete was delivered to the site in two separate transit mix trucks. As the concrete was being placed, a total of 12 standard concrete test cylinders were taken. A local test laboratory conducted modulus and strength tests on each of the test cylinders. The average value of the concrete modulus for the 12 cylinders was 5.2 by 10^6 psi, and the average value for the compressive strength was approximately 5,000 psi.

Instrumentation

The only instrumentation for the shaft consisted of Mustran cells of Type 1. The Mustran cell shown in Fig. 5.8 was developed at The University of Texas specifically for use in drilled shafts. The development of this cell was reported by Barker and Reese (1969). Since previous tests had indicated that the use of a drying agent in the cell increased the cell stability, the interior of the cell was filled with eight-mesh anhydrous calcium chloride. Each cell was pressurized at 20 psi and submerged under water as a check against leaks in the fittings. As in the previous systems, a field pressure system was provided as additional protection against the leakage of moisture into the gages. This pressure system, shown schematically in Fig. 5.9, was identical to the system employed in Shafts 3 and 4 at the SH 225 site.

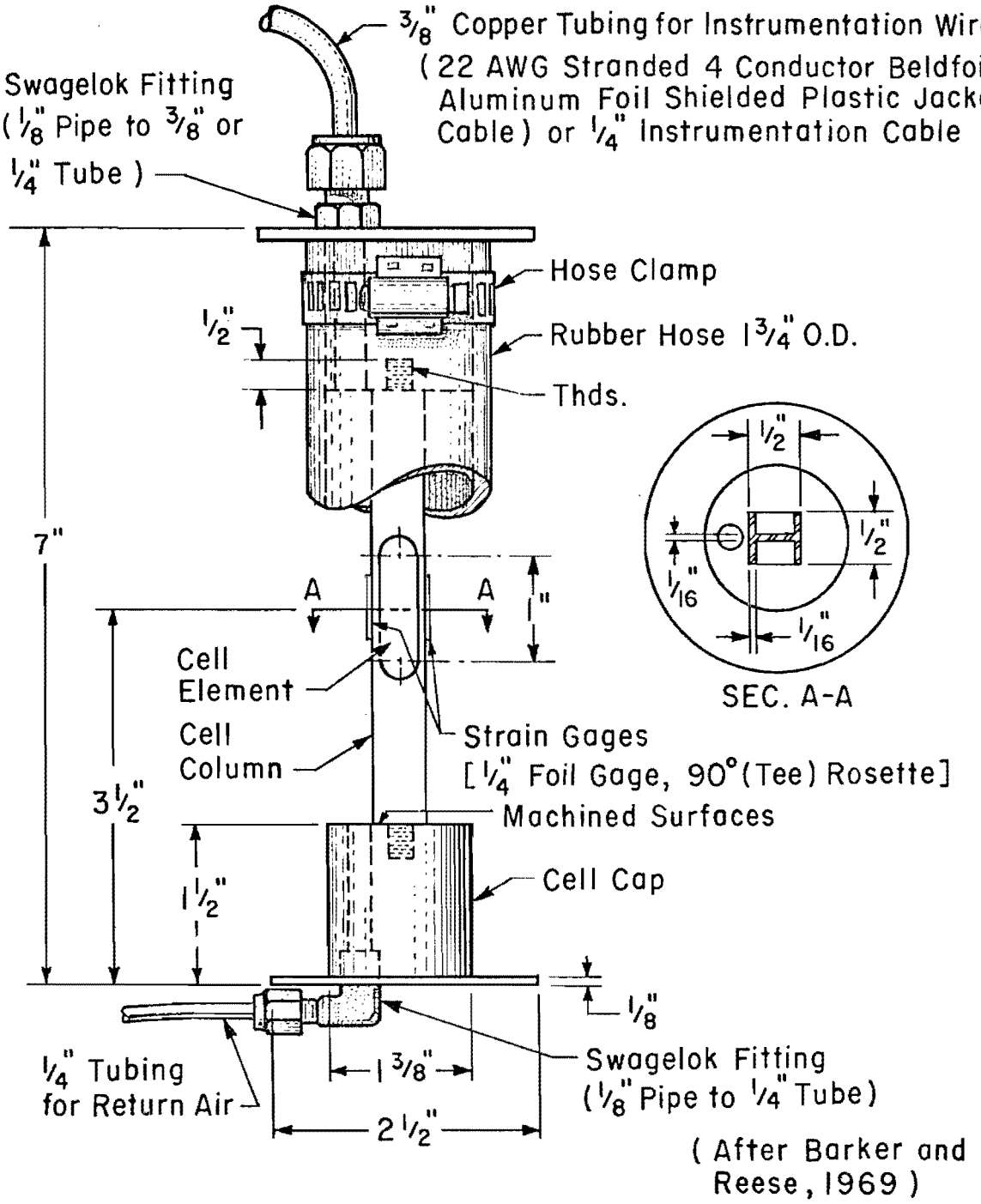

Fig. 5.8. Schematic of Mustran Cell

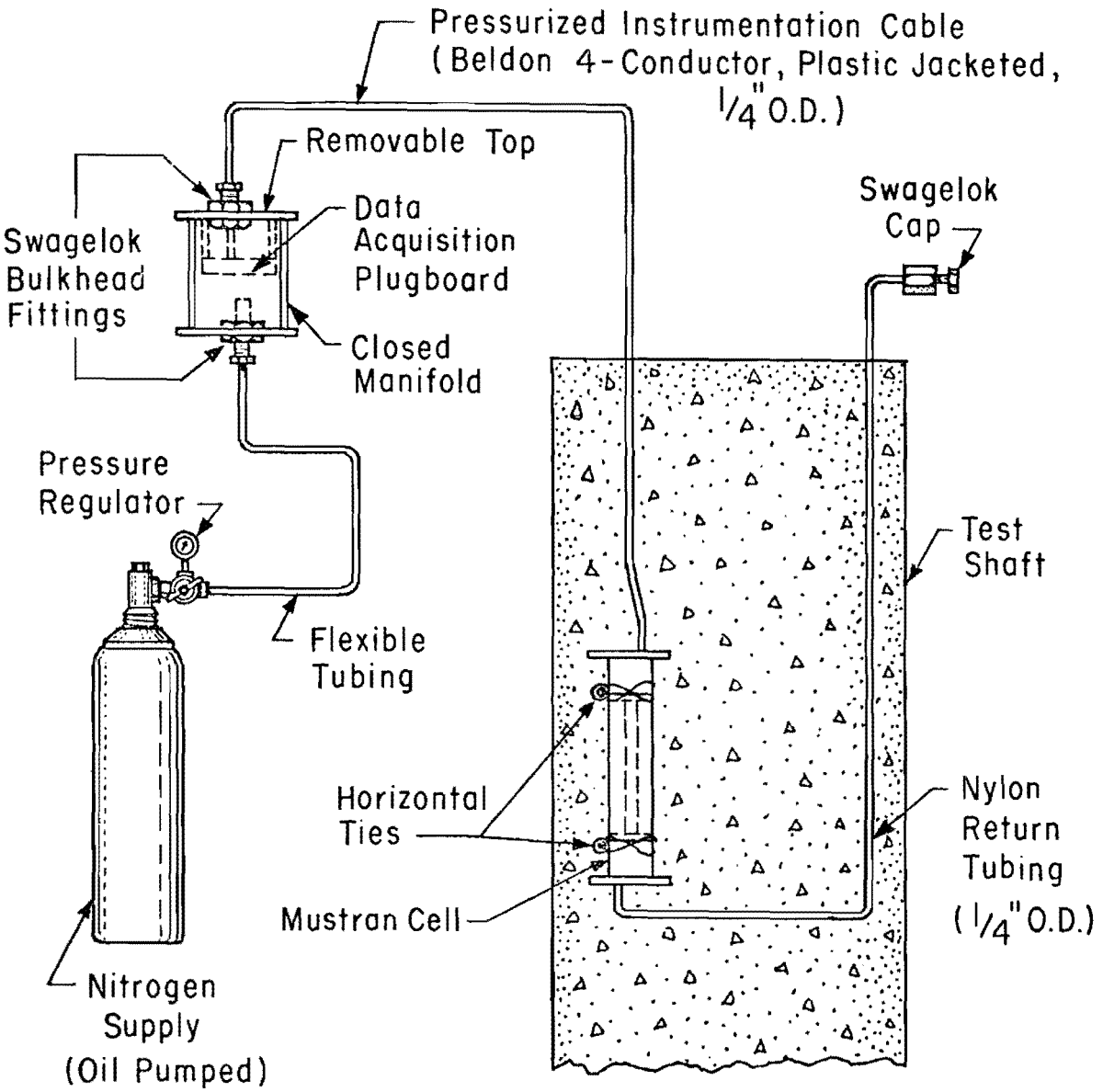

Fig. 5.9. Schematic of Instrumentation Pressure System

The cage was instrumented at the site one day prior to shaft installation. Eighteen gages were placed in eight instrumentation levels. There were two gages per level with the exception of the bottom level which contained four gages. The gages at each level were placed on opposite sides of the shaft as a check on any bending which might occur during the loading of the shaft. If bending does occur, averaging the readings at a gage level should eliminate the effect of the bending. The gages in the upper seven levels were installed by using soft wire to tie the gages to the horizontal bars as shown in Fig. 5.10. Each of the bottom gages was bolted to the bottom steel ring by placing four small bolts through the flange of the bottom end cap (Fig. 5.11). To facilitate this type of installation, the return tube for the pressure system was omitted. The complete cage is shown being lifted in Fig. 5.12.

Each gage was designated by the depth of the instrumentation level, the gage number, and the side of the shaft on which the gage is located. Thus, a gage designation of 35-18-N would indicate Gage No. 18 which is located at a depth of 35 feet and on the north side of the shaft. This system is used in designating the gages shown in Fig. 5.1.

During the lifting of the instrumented cage, two gage-mounting bars, one for Gage 0-2-N and one for Gage 14-5-S, were torn loose from the vertical reinforcement. The damage was caused by the relative movement of the vertical bars. It appeared that both the alignment and integrity of these two gages had been affected. Thus, the cage was stopped temporarily during the lowering process allowing each gage to be repaired. To insure that there would be two good calibration gages, an extra gage (0-Extra-N) was placed beside Gage 0-2-N.

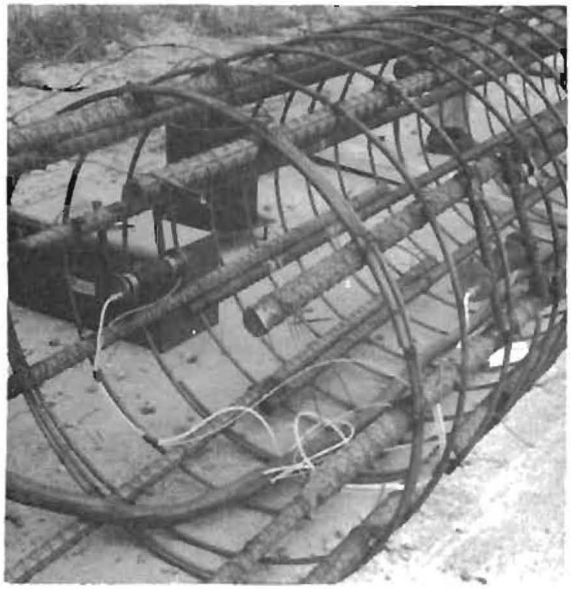

Fig. 5.10. Top Level of Mustran Cells

Fig. 5.11. Bottom Level of Mustran Cells

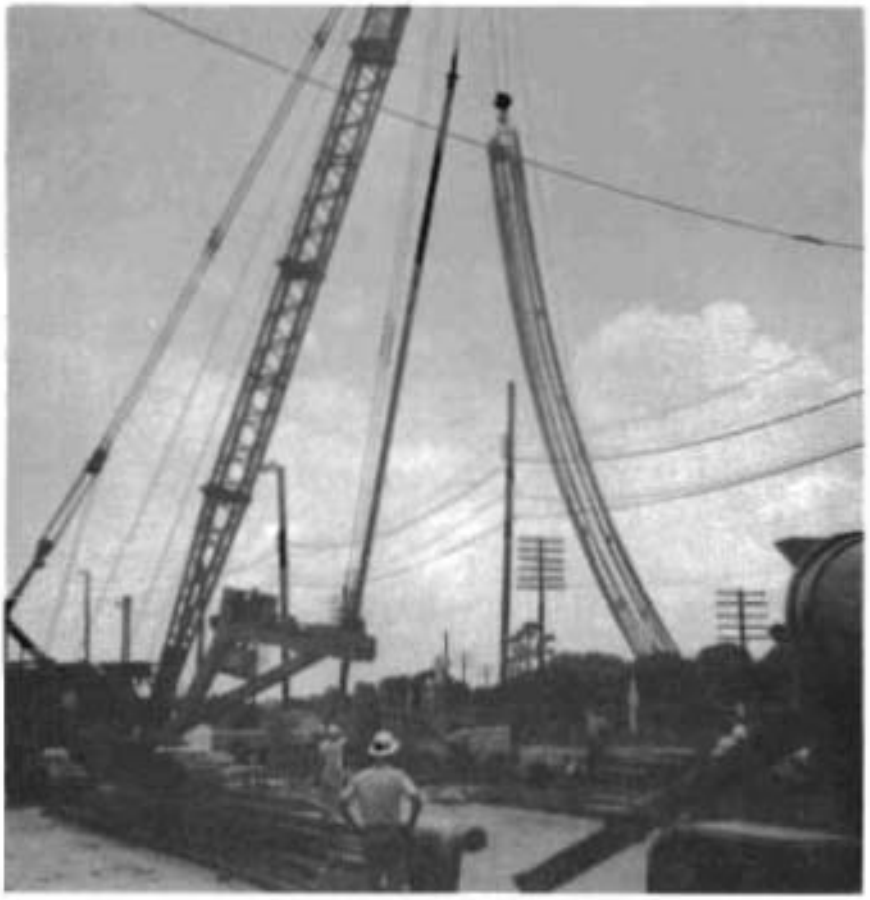

Fig. 5.12. Lifting of the Instrumented Reinforcing Cage

After the concrete had been placed, the nitrogen system was pressurized to 30 psi overnight. The following morning the pressure was reduced to 10 psi, where it was maintained for approximately two months.

Readout Systems

Two systems were used for reading the gages; the first was a system employing a Budd Model P-350 Portable Strain Indicator for monitoring and for Tests 3 through 7; and the second was the Honeywell Model 620 Data Logging System used for Tests 1 and 2.

When the strain indicator was used to monitor the gages, a standard Wheatstone bridge served to zero the instrument. The standard bridge consisted of four temperature-compensated foil gages mounted on a square piece of steel. It was assumed that this standard gage remained stable. A short length of instrumentation cable provided a connection between the strain indicator and the plug board (Fig. 5.13). The first readings were taken with a specified hook-up of the gage wiring to the strain indicator. The power leads were reversed and the gages were read again. It was believed that in this manner errors in readings could be detected and compensations made. A complete set of readings could be taken by two men in approximately fifteen minutes.

When the Budd strain indicator was employed in the readout of gage data during a test, two switch and balance units were utilized to provide a means of balancing the gages to zero at the start of the test and of switching rapidly from one gage to another during the test. In this case, a longer instrumentation cable (approximately 25 feet) was provided for each gage to connect between the plug board and the switch

Fig. 5.13. Reading Mustran Cells for Monitoring Data Utilizing a Strain Indicator

Fig. 5.14. Taking Mustran Cell Test Data Utilizing Strain Indicator in Conjunction with Two Switch and Balance Units

and balance unit. Using this arrangement, the 18 gages could be read and recorded by 2 people in slightly less than 2 minutes (Fig. 5.14).

The readings obtained utilizing the strain indicator were in microinches of circuit strain. The conversion of circuit strain into concrete strain required a gage multiplication factor, which was obtained from the results of the top level of gages during a load test. The calculation of this factor involved the modulus of elasticity of the concrete, which varies with the stress level. Using a modulus value of 5.2 by 10^6 and the results from Test 2, a factor of 7.3 was computed to convert circuit strain into concrete strain. This factor was not employed in obtaining load distribution curves (this will be discussed later), but was used for converting gage readings to concrete strains during curing, discussed in this chapter.

The Honeywell System (Fig. 5.15) employed in Tests 1 and 2 was the same system described by Barker and Reese (1969) and O'Neill and Reese (1970). The system performed satisfactorily only during the monitoring period for the first test, after which the printer began to malfunction and readings had to be recorded by hand. Because of the difficulties experienced with the system during Tests 1 and 2, the strain indicator was used for the remaining tests.

Since only two tests were conducted utilizing the Honeywell System, it was found convenient for the analyses described later to convert the readings in microvolts to readings in microinches. To make this conversion the readings were multiplied by 0.319. The factor was obtained from the equation:

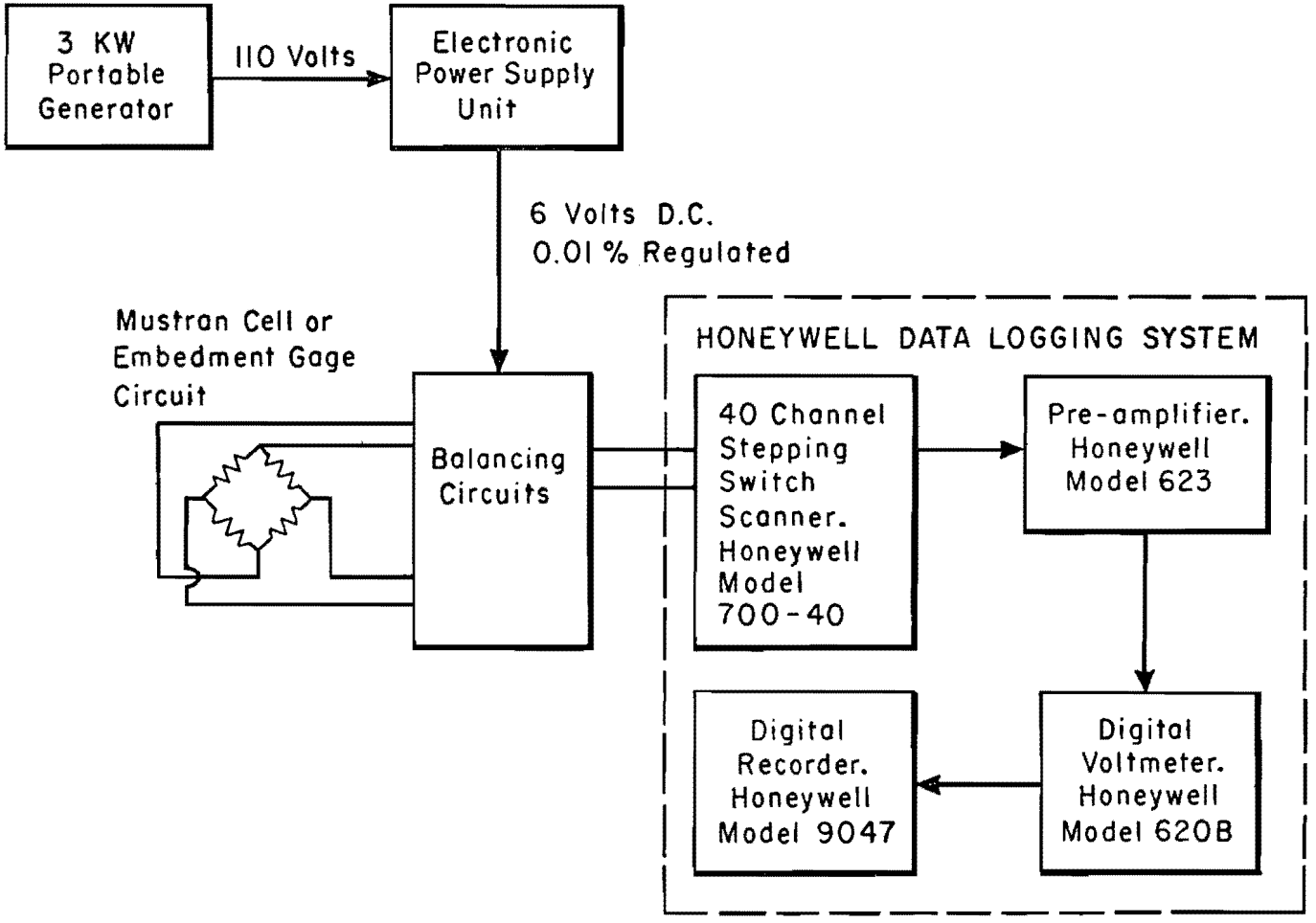

Fig. 5.15. Data Logging System

$$\frac{E}{4} = \frac{E_o}{KV} \quad \ldots\ldots\ldots\ldots\ldots\ldots\ldots\ldots\ldots\ldots\ldots\ldots (5.1)$$

where

E_o = the reading in microvolts,

K = the gage factor,

V = the applied voltage in volts, and

E = the circuit strain in microinches.

For the system used, K was 2.09 and V was 6.00. Thus, using Eq. 5.1, E/E_o was computed to be 0.319.

Gage Stability

Prior to the installation of the gages in the shaft, the gages were monitored for approximately a month while located inside a climate-controlled building. During this time the maximum change in gage readings was six microinches. The resistance to ground for all gages remained above 5 by 10^9 ohms.

After casting the shaft, the gages were read at various times during the period June 12, 1969, to April 10, 1970. The gage stability data are given in graph form in Appendix B (Fig. B.18-B.25).

After the initial set of the concrete was completed, the changes in gage readings were relatively small, with the exception of the changes due to testing. The trend was what may be expected from the continued curing of the concrete.

The greatest changes that occurred were in the readings of the top level of gages. To understand the changes in the readings of the top

instrumentation level, it is helpful to look at the variation of gage readings over a 24-hour period (Appendix B). It is noted in the plots that for the top level, a relatively large change of approximately 80 microinches occurred in the gage readings. The changes which diminish with increases in the depth of the gages appear to be following the changes in temperature. O'Neill and Reese (1970) indicate that the gages themselves are essentially temperature compensated, thus the major portion of the changes due to temperature variations may be assumed to be changes occurring in the concrete. Over the 24-hour period, a small constant change was noted in the lower level gages. Since at these depths no changes in temperature would be expected, the variations are probably due to some other cause. Since all of the gages experienced the same change, gage drift would not seem to be a factor. The most probable cause would be drift in the readout system.

As a result of the monitoring of the gages, electrical drift was found to be nil and it was concluded that the gage readings would be a true indication of the concrete action.

Concrete Curing

The gages were read from time to time, primarily as a check on the stability of the gages, but in the process some interesting information was obtained on the curing action of the concrete. When the shaft was first cast, all the gages except those at the top level went into compression, indicating that the shaft was shrinking. By the fifth day the trend had reversed for all the gages, except the bottom level. These trends with depth at different monitoring times are shown in

Fig. 5.15. The gages at the top and bottom levels indicated compression of the concrete, while the gages at the center levels indicated an elongation of the concrete. The trends of the individual gages with time are shown in Fig. B.1 through B.8 of Appendix B.

Just prior to the first test, it is seen that the plot (Fig. 5.16) of the readings formed a curve which was approximately parabolic with respect to the vertical axis of the shaft. The readings at that time reached a maximum tension of approximately 400 microinches circuit strain at a depth of 35 feet. The top level showed a compression of approximately 290 microinches and the bottom level a compression of 50 microinches. Using a multiplication factor of 7.3, a maximum elongation of 54 microinches per inch is obtained for the shaft. Neville (1963) gives a value of swell of 100 to 150 microinches per inch for concrete with a cement content of 500 pounds per cubic yard when cured under water. The swell in the shaft started just above the water table and ended just above the base. The shrinkage above the water table and the swell below the water table can be attributed to the effect of the water. What is not understood is the decreasing in swell below the 35-foot level. It would appear that concrete below this level would have just as much tendency to swell as the concrete at the 35-foot level.

The effects of the concrete swelling or shrinking on the behavior of the shaft is not known. The absolute movements are small and certainly not sufficient to develop significant axial forces along the side or the bottom of the shaft. In granular soil it may be possible that the lateral movements change the lateral confining pressure sufficiently to affect the shear resistance along the side of the shaft.

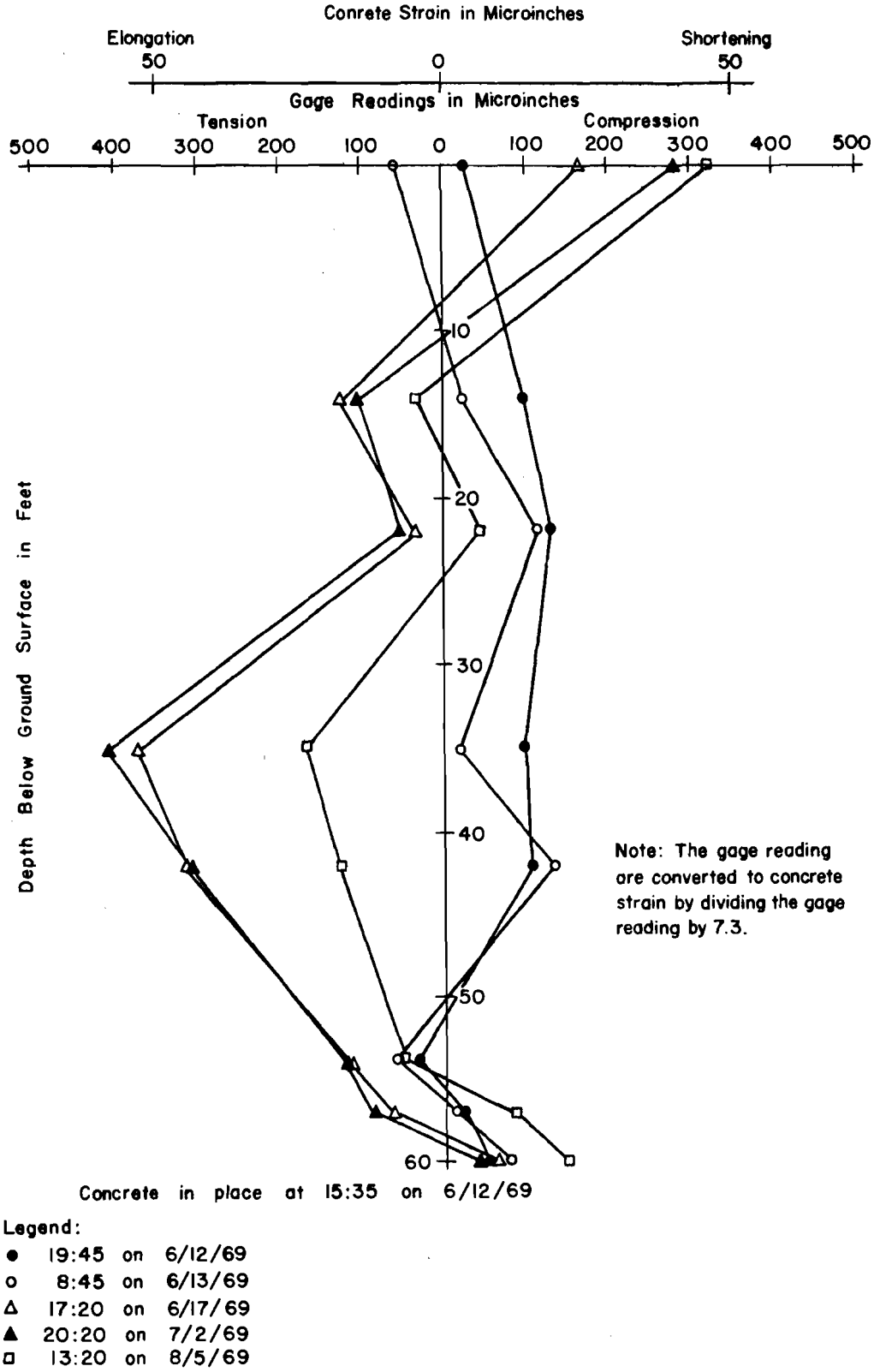

Fig. 5.16. Changes in Gage Reading with Zero Load as a Function of Depth

Loading System

The loading system shown schematically in Fig. 5.17 is the same system employed for the tests of the shafts at the SH 225 site. The load measurement was obtained by measuring the pressure of the hydraulic fluid going to the jack. The measurement of the pressure was accomplished by both a Bourdon tube pressure gage and an electrical pressure transducer. In Tests 1 and 2 the transducer and the Mustran cells were read with the Honeywell Logging System. In the remaining tests, a separate Budd strain indicator was used to read the pressure transducer. It was advantageous to adjust the gage factor on the indicator so that the load reading would be obtained in tons. The resolution of this system was to the nearest tenth of a ton. It was observed that the load could be held to ±2 tons.

The accuracy of measuring the applied load by measuring the jack pressure has been questioned by some investigators. It has been reported that friction in the piston may cause considerable error. If it is assumed that when the direction of travel of the jack head is reversed, the direction of the friction force will be reversed; then at the time when unloading of the shaft begins, the friction present will cause a shift in the plot of the calibration gages. Fig. C.1 in Appendix C is a plot of the gage readings for the calibration level versus the applied load. In the plot, if the unloading curve is projected back to the beginning of the unloading, it is noted that a shift of approximately 50 tons does occur. If it is also assumed that the friction in unloading is equal to the friction in loading, then the error in the applied load would be approximately 25 tons. Based on these assumptions, there

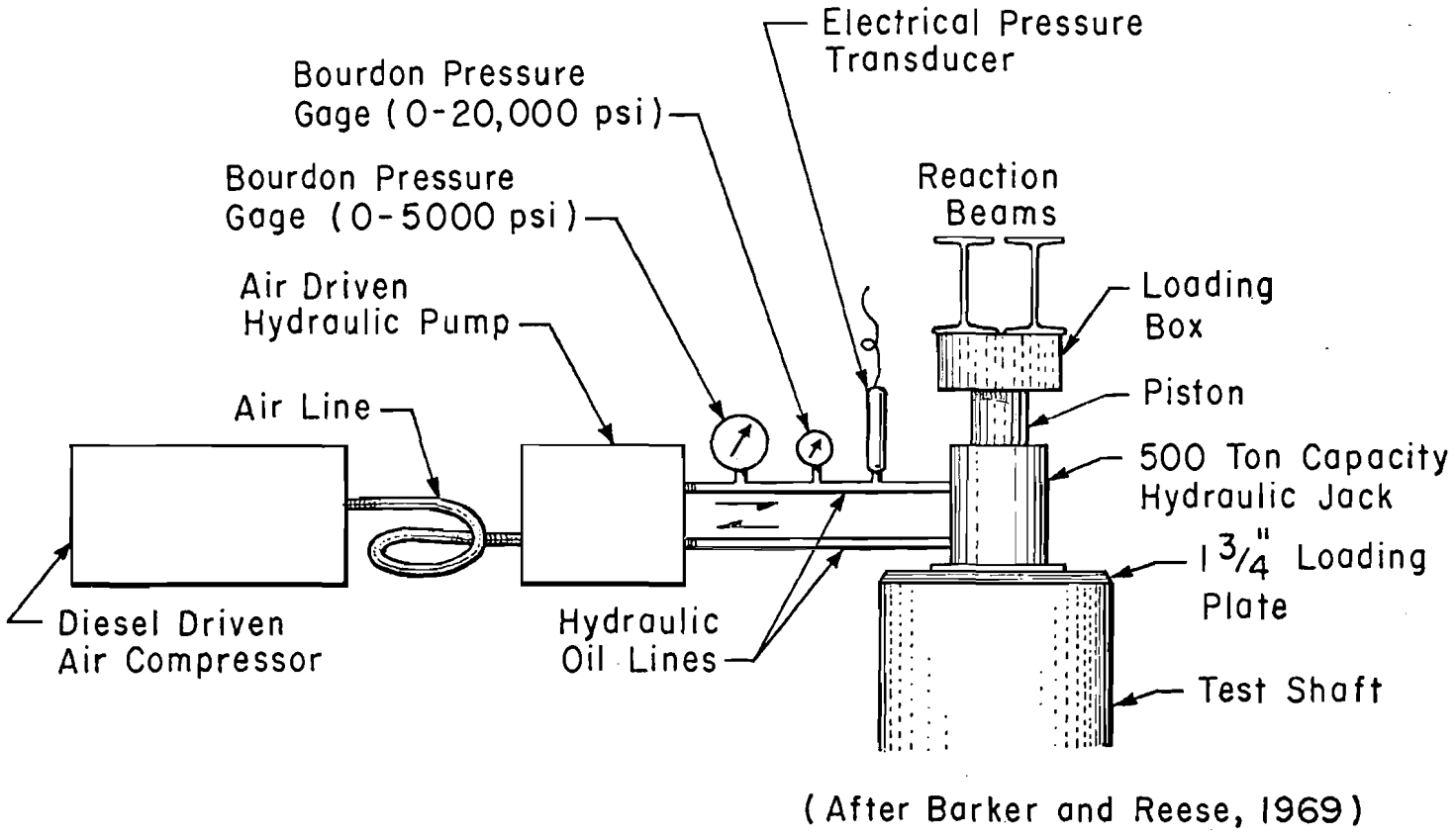

Fig. 5.17. Schematic of Loading System

would be a 3.2 per cent error in the applied load at ultimate load. How this error varies with the applied load is not known, but it is felt that an estimate of 5 per cent error at any time would be conservative.

Subsequent to the tests on the HB&T Test Shaft, one test was conducted at the SH 225 Test Site utilizing an independent load cell between the loading ram and the reaction beam. The load measured by the load cell was compared with the load obtained by measuring the jack pressure (O'Neill and Reese, 1970). The error computed, assuming the load cell to be correct, was approximately the same as the error obtained for the HB&T test. For the tests being conducted, the indicated error is acceptable and it is felt that additional instrumentation to measure the applied load is unnecessary.

CHAPTER VI

LOAD TEST

Test Description

Seven load tests were conducted on the test shaft. The testing period began on July 3, 1969, twenty-one days after casting, and ended on April 8, 1970. The tests were conducted utilizing three basic procedures. The first was the quick load procedure. The applied load was increased in increments, with each increment being held for 2 1/2 minutes while readings were taken. In the second test, a predetermined load was applied using the quick-load test procedure and maintained for a specified period of time. The third procedure was a cyclic test in which the applied load was increased in increments but was dropped back to no load before each new increment of load was applied.

Of the seven tests, four were conducted by personnel from The University of Texas, and three were conducted by personnel from the Texas Highway Department. A summary of information about the tests is contained in Table 6.1.

Test 1

Test 1 was conducted as a proof test for the design load of 206 tons. If the shaft could sustain an applied load of 1 1/2 times the design load for three hours, the shaft design would be considered by the Texas Highway Department personnel as being adequate. The maximum allowable residual settlement for the test was 0.25 inches. It was desired that the curing time for the test shaft be approximately the same as the minimum time

TABLE 6.1 SUMMARY OF LOAD TESTS - HB&T TEST SHAFT

Test Number	Date Conducted	Type Test	Maximum Applied Load Tons	Maximum Settlement Inches	Remarks
1	July 3, 1969	Quick Load	300	0.070	Test was conducted as proof test. The maximum applied load was 1 1/2 times the design load and was maintained for 3 hours.
2	July 17, 1969	Quick Load	824	1.224	Shaft was loaded to failure.
3	August 5, 1969	Sustained Load	650	0.540	Load was maintained for 64 hours. Mustran cells were monitored for 43 hours.
4	September 3, 1969	Quick Load	832	1.216	Shaft was loaded to failure. Test conducted by personnel from Texas Highway Department.
5	September 4, 1969	Cyclic Load	793	1.054	Test conducted by personnel from Texas Highway Department.
6	September 29, 1969	Sustained Load	668	0.402	Maximum load was maintained for 70 hours. Test conducted by personnel from Texas Highway Department.
7	April 6, 1970	Quick Load	727	1.110	Test conducted to recalibrate Mustran cells. Top 14 feet of soil had been excavated from around the shaft.

that the shafts in the structure would be allowed to cure. Thus, the test was to be conducted approximately three weeks after casting. An additional incentive for early testing was to allow time for changing and finalizing the foundation design in case the straight shaft proved adequate.

The test was planned for July 3, 1969, twenty-one days after casting. The loading system previously described and the Honeywell Data Logging System were used in the test. The automatic printout section of the data-logging system did not work, requiring that the data be recorded by hand. Recording by hand increased the time to take a set of Mustran cell readings from approximately 20 seconds to approximately 2 minutes. Settlement was measured using two 1/1,000-inch and four 1/10,000-inch Ames dials. On July 2, the gage readout system was connected and the gages monitored from 5:33 p.m. until 10:10 p.m. During this time, the maximum changes occurred in the top level of gages, Gage 0-2-N changing 101 microvolts and Gage 0-14-S changing 26 microvolts. Below the top level, the average change for all of the gages was 8 microvolts, with a maximum change of 21 microvolts.

On the morning of July 3rd, the gages were again monitored for approximately three hours prior to loading. The trend in the gage readings was very similar to those taken the evening before. The data taken during these monitoring periods showed that the drift in the gages was minor and would not pose a problem during the test. Data taken later (presented in Appendix B) during a 24-hour monitoring period, indicated that the changes in gage readings were caused by temperature changes and differential heating of the shaft.

Loading of the shaft began at 9:40 a.m., with incremental loads of 10 tons being applied and held for 2 1/2 minutes. Thirty seconds after attainment of the load, a set of settlement gage readings were taken and reading of the Mustran gages was started. At two minutes after attainment of the load, another set of settlement gage readings was taken. Since the Mustran cells could be read and recorded in a little under two minutes an additional load increment could be applied after the load had been held for 2 1/2 minutes.

The desired load of 300 tons was reached at 11:00 a.m. and maintained until 2:00 p.m. Unloading of the shaft was accomplished in a similar manner as loading, using 25-ton load increments. The shaft was completely unloaded at 2:29 p.m.

Plots of the settlement gage data and Mustran cell data versus applied load are shown in Figs. 6.1 and 6.2, respectively. As can be noted in Fig. 6.1, the settlement gages indicated that the shaft rose approximately .012 of an inch during the time the load was being carried. When unloaded, the settlement gages indicated that the shaft had actually risen 0.004 of an inch. Later, maintained load tests showed the settlement readings to be cyclic with temperature as were the Mustran cell readings. An increase in temperature produced an apparent rising of the shaft. Since the test was conducted during a period of time when the temperature was increasing, it was felt that a correction to the rebound curve was justified. After the correction has been made, a net settlement of 0.008 of an inch was indicated at unloading.

For the reason previously stated, the readings obtained for each applied load were averaged by gage levels. The plots of these averages

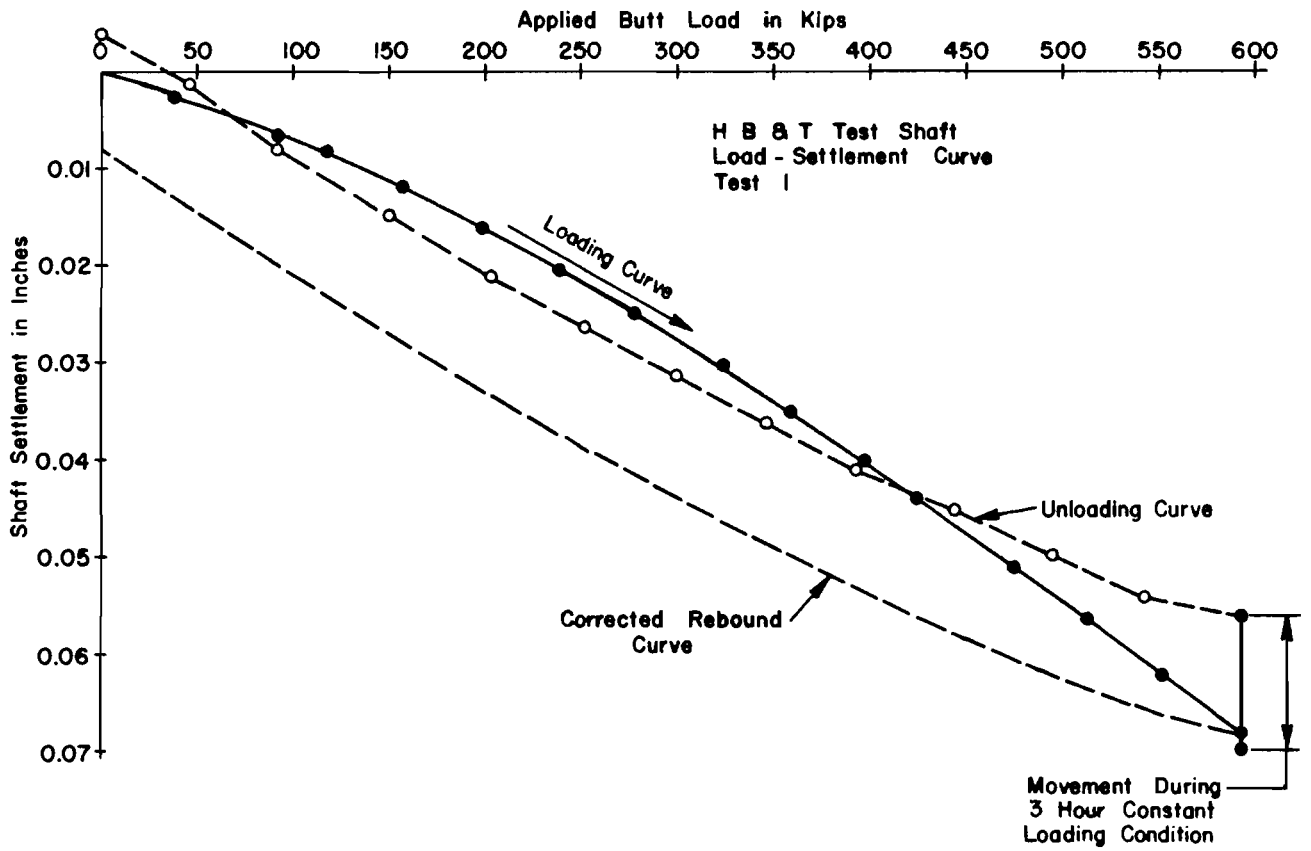

Fig. 6.1. Load-Settlement Curve for Test 1

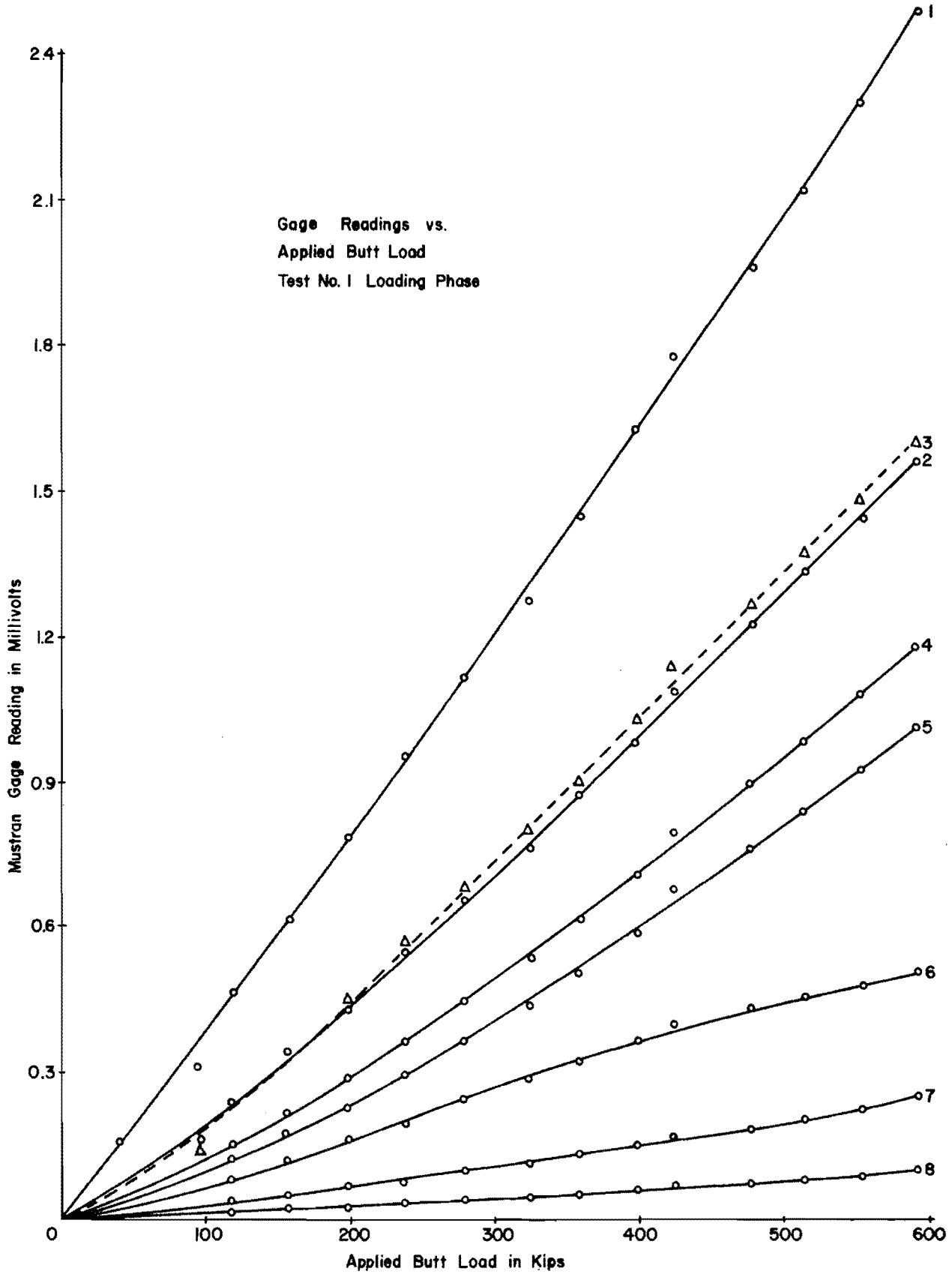

Fig. 6.2. Gage Response Curves for Test 1

as a function of the applied load, presented in Fig. 6.2, are called gage response curves. When studying the response curves, two inconsistencies are apparent. The first one is that Gage Level 3 registered higher readings than Gage Level 2, and the second inconsistency is that there are large differences between the response of Level 1 and the response of Levels 2 and 3. In the top portion of the shaft, it would be expected that very little load would have been taken out, yet the gages indicated the opposite. Examination of the lack of scatter in the plotted points in Fig. 6.2, and studies of other aspects of Mustran gage behavior indicated that almost certainly the Mustran gages were correctly indicating strain. Therefore, the probable cause of the two inconsistencies noted would be the differences in the size of the shaft at the different levels. Since drilling fluid was used to aid in drilling, the hole was not inspected along its length prior to concreting. It would seem reasonable that in the drilling process the upper portion of the hole would be larger than the nominal diameter of the shaft, whereas the portion of the shaft cast inside of the Sonotube form would be very close to the nominal shaft diameter. In later load tests, the same two inconsistencies noted above were observed. Thus, in obtaining the internal load in the shaft it was necessary to obtain actual shaft diameters, over the upper portion of the shaft.

The personnel of the Texas Highway Department believed that the shaft more than adequately met the design requirements and that bridge foundations could be constructed utilizing straight shafts. Thus, as a direct result of the research program, the proposed design of the foundation was changed, effecting a savings in both time and money.

From a research point of view, it was still desirable to determine the ultimate capacity of the shaft and to analyze the interactions of the shaft and soil. In order to accomplish the expanded objectives, additional tests were planned, the next test being a quick test to failure.

Test 2

Test 2 was to be the test to determine the capacity of the shaft at failure. Failure in this case is defined as being the load at which continuous pumping is required to maintain the applied load. Expressing it in another way, failure may be said to be the load at which plunging of the shaft occurs. A discussion is given later of the effect of a previous loading on the behavior of the shaft.

The test was conducted on July 23, 1969, using the same procedure in applying the load as was used in Test 1. The settlement in this test was obtained from two 1/1,000-inch Ames dials. The Mustran cells were read using the Honeywell System, but the data were recorded manually, as was done in Test 1. Monitoring time for the gages was limited to a 15-minute period just prior to the start of the test. It was believed that this was adequate time for the gage to stabilize after powering. The data previously obtained on gage stability eliminated the need for a long period of monitoring prior to testing.

Loading of the shaft began at 10:43 a.m. with the loads being applied in 50-ton load increments. Each load increment was held for 2 1/2 minutes before applying the next increment. After obtaining an applied load of 500 tons, the size of the load increment was reduced to 20 tons. Plunging of the shaft occurred at approximately 820 tons, giving a gross

settlement of 1.18 inches before the load was dropped back to 700 tons. The shaft was then unloaded in 100-ton increments. The residual settlement was 1.04 inches.

The information for this test is incorporated as sample data for a computer program. The program, Program DARES, is presented in Chapter VII. The load-settlement curve for the test, along with load-settlement curves for Tests 4 and 7, is shown in Fig. 6.3. The response curves are presented in Figs. C.1 and C.8, in Appendix C. The same inconsistencies noted for Test 1, were observed in Test 2. Again, the load transfer indicated between Gage Level 1 (the calibration gages) and Gage Level 2 is very large. In this test, Gage Level 2 did show a greater response than Gage Level 3, but the difference was very small.

Two levels, Levels 4 and 6, gave very strange results. In the plot of Gage Level 4 (Fig. C.4), it is seen that the readings appear reliable up to an applied load of 1,350 kips. With the application of an additional load increment, the readings of both gages of the level suddenly dropped approximately 150 microvolts. The two gages tracked each other almost perfectly, both in the loading and unloading phases of the test. The type of curve obtained would tend to indicate a discontinuity in the shaft and not a gage malfunction. The cause offered, is that there may have been a collar or ring of concrete in the vicinity of the gages. It is suspected that the collar sheared causing a change in load distribution and the sudden drop in the gage readings.

Gage Level 6 gave strange readings from the start of the test. As the shaft was first loaded, one gage gave high readings and the other gave low readings. The trend continued up to approximately 1,000 kips,

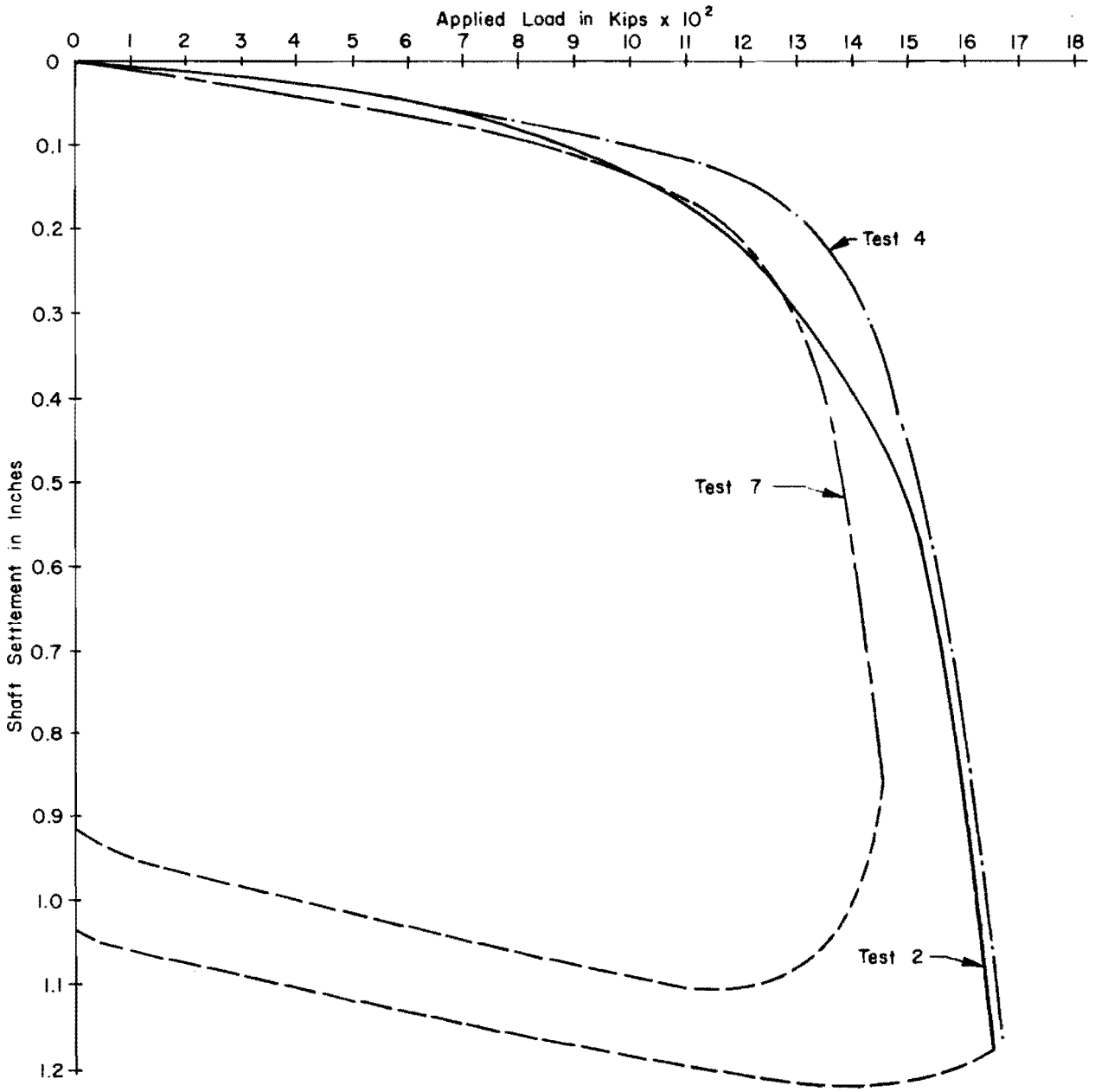

Fig. 6.3. Load-Settlement Curves for Tests 2, 4 and 7

at which point the trend reversed. In the last load increments, the readings from Gage 54-3-N dropped. This gage level acted differently from Level 4, but the cause is believed to be very similar. In the case of Level 6, the unusual behavior would seem to be caused by a projection from one side of the shaft producing uneven stress distributions in the shaft. This level, as was Level 4, was located near a silt seam which could have caved during the drilling process.

With the exception of the two levels discussed, the data appear to be very good. By examining gage response curves in Appendix C, confidence is gained in the gages. In each level, including Level 4, the gages tracked the applied load in both the loading and unloading phase of the tests. For the lower loads, the readings of the gages for an individual level fell very close to each other. As the load increased, particularly above 950 kips, the bending in the shaft became noticeable in the first two levels and the last level of gages. Bending in the center of the shaft did not develop until just before failure.

The gage response of Test 2 appeared to be affected by differences in the shaft size as was indicated in Test 1. It appeared that at Gage Levels 2 and 3, the shaft may have been considerably larger than the nominal size. To determine the calibration constant for the levels required a critical look at the data and the test shaft itself. To assist in the determination, a final test was planned at the end of the testing period. The soil was to be excavated from around the shaft to a depth of 14 feet. The 14-foot depth gages would then be uncovered and could serve as an additional calibration level. This would also allow a visual examination of the top 14-foot section of the shaft.

Test 3

The purpose of Test 3 was to acquaint University personnel with mechanics and problems of sustained load tests. Additional information was hoped to be obtained which would give some insight into the failure mechanism of a drilled shaft. The idea was to attain a load at which a very slow rate of settlement occurred. At this load, the settlement gages and Mustran cells would be monitored to detect signs of any progressive failure of the shaft.

Since the Honeywell Logging System had been malfunctioning, the Budd Strain Indicator was used for the readout of the gages. By use of the Budd Strain Indicator, the dependence on a portable generator was eliminated. For the loading system, the requirement for an air compressor to power the air-driven hydraulic pump still remained.

Reading of the gages began at 2:00 p.m. of August 5, 1969. With no load on the shaft, the gages were monitored until 4:52 p.m. during which time the maximum change for any gage reading was 14 microinches. Below the top level of gages, the maximum change was three microinches with no change at all occurring below the 35-foot level.

On the basis of Test 2, a load of 650 tons was chosen as the load at which the shaft was to be tested. The loading was begun at 4:52 p.m. and loads were increased in 50-ton increments until the desired load of 650 tons was attained. This load was reached at 5:57 p.m., approximately one hour after the start of the loading. The immediate settlement of the shaft for the applied load was 0.18 of an inch.

During the night, difficulty was experienced in the maintenance of the air compressor causing minor fluctuations in the applied load.

Settlement of the shaft continued during this time as indicated in Fig. C.17 in Appendix C. The readings of the upper levels in the gages increased considerably with the largest change occurring during the first hour of load maintenance. In the lower three levels, the gages appeared to stabilize completely after the first two hours of loading.

The following morning, condensation collected in the airline between the compressor and the hydraulic pump. At 8:30 a.m. a sudden surge of the collected water plugged the pump, causing a loss of load to approximately 200 tons. The clearing of the pump and the restoring of the load required 20 to 30 minutes. The effect of the reloading was reflected in all of the gage readings, Figs. C.18-C.20 in Appendix C. For the very bottom gages, this increase in readings is the major increase indicated during the time the load was maintained.

The settlement gages and the top two levels of gages reflected a cyclic trend that appears to follow changes in temperature. The south settlement gage, which in the afternoons indicated the shaft to be rising, was more affected by the temperature change than was the north gage. Where the change takes place is not fully understood. The Mustran cells did not indicate the concrete in the shaft to be expanding and contracting sufficiently with changes in temperature to cause the magnitude of deflections reflected by the settlement gages. Most likely, the cyclic trend is caused by temperature effects in the dial-gage supporting system. This same temperature effect is believed to have caused the apparent rising of the shaft in Test 1.

Tests 4, 5, and 6

Tests 4, 5, and 6, were all conducted by personnel from the Texas Highway Department so that they could become familiar with the testing equipment, shaft instrumentation, and testing procedure. The three tests were conducted using a different procedure for each test.

Test 4 was conducted on September 3, 1969, as a quick test, following the same procedures as were used in Test 2. Test 5 was run immediately following Test 4. The procedure for Test 5 used a load and an unload technique to determine at what load a residual net settlement of one-quarter of an inch is obtained. The load increments were the same as those used in Tests 2 and 4. An increment of load was first applied and the gage readings taken. The shaft was then unloaded in one step back to zero load and readings taken. The last previous load was reapplied in a one-step loading and readings were again taken for this loading. After the reading of the gages, the load was increased by another load increment. The procedure for releasing the load, reloading, and adding load increments was repeated until failure of the shaft occurred.

The procedure for Test 6 was almost identical to that of Test 3, except that there were differences in the amount of load maintained and the length of time the load was sustained. A load of 620 tons was obtained at 6:00 p.m. on September 29, 1969, and was maintained until 4:00 p.m. on October 2, about 70 hours.

In order to reduce the number of channels of instrumentation, not all of the Mustran gages were read. The gages selected for reading were the gages of Levels 1, 3, 5, 7, and two gages from Level 8. This gave a

total of ten channels which could be handled by one switch and balance unit, thus simplifying the reading of the gages. The plotted results of these tests are in Appendix C.

Test 7

Test 7 was designed to reconcile the inconsistencies in the Mustran gage readings from the previous tests. The soil was first excavated to the 13-foot level, which was the top of the silty-sand layer. This uncovered Gage Level 2 and provided an opportunity to examine the upper portion of the shaft. The excavation was accomplished on December 9, 1969 by personnel from the Texas Highway Department using a small truck-mounted drilling rig. As suspected, from just below the ground surface to approximately five feet, the shaft was enlarged considerably. The shape of the shaft is shown in the sketch in Fig. 6.4. At the bottom of the Sonotube form, the concrete in the collar had cracked and separated from the concrete below. A portion of the bulge formed when this upper section of concrete was removed as shown in Fig. 6.5. The circumference of the shaft just below the ledge was 12.2 feet, giving a shaft diameter of just over 46 inches. Below the 7-foot depth to the 13-foot level, the shaft was relatively smooth and straight (Fig. 6.6) with a diameter of approximately 41 inches. Below the 13-foot level, the silty-sand starts; therefore, the excavation could be carried no further. By probing along beside the shaft with a spade, ears could be felt projecting for a distance of about 5 inches from the shaft.

The soil clinging to the shaft was examined very closely by shaving at angles to the shaft. The natural soil in this section was a light

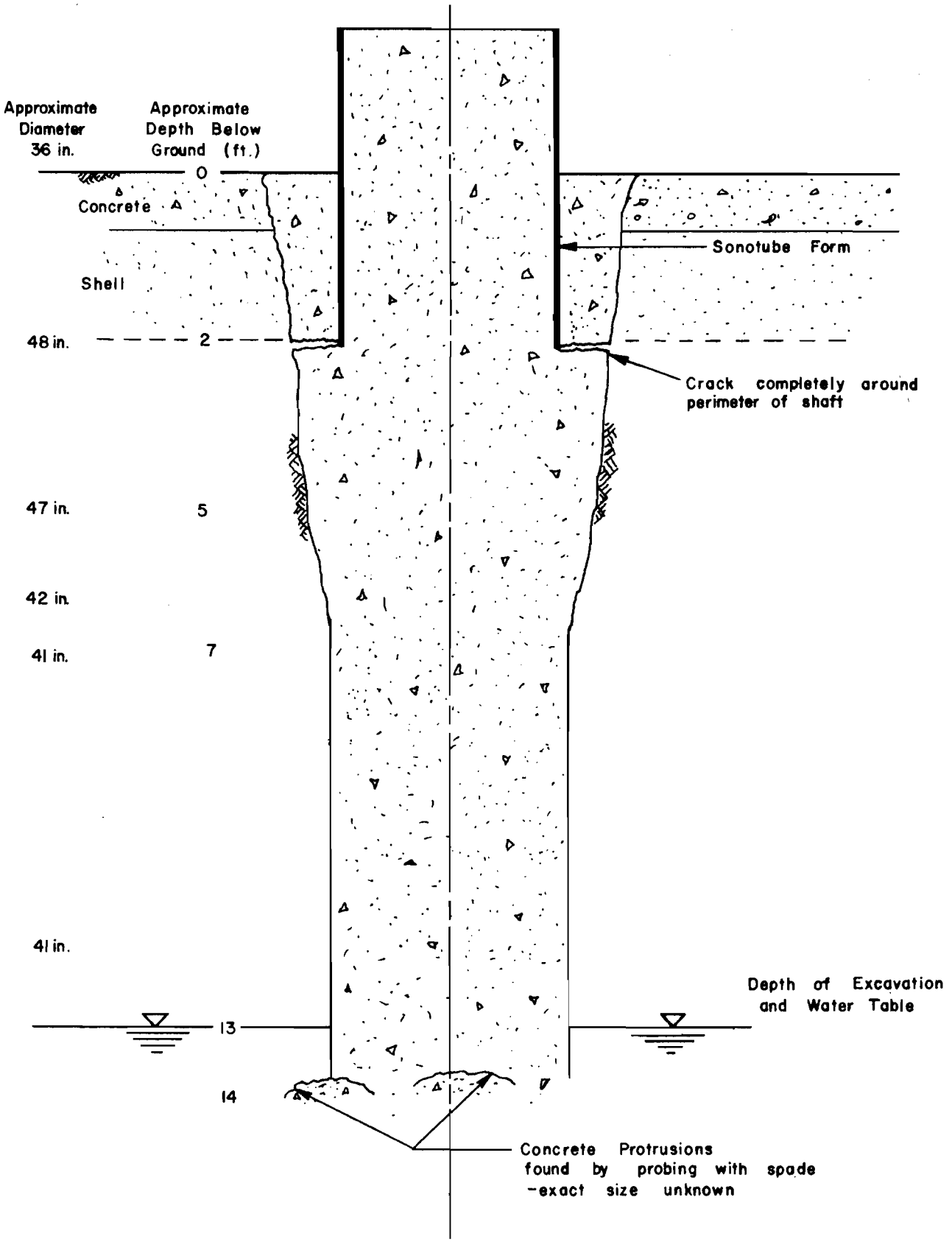

Fig. 6.4. Observed Shape of HB&T Test Shaft

Fig. 6.5. Shaft Enlargement in Upper Section

Fig. 6.6. View of the Test Shaft from Ground Surface to Approximately the 13 Foot Level

gray silty clay. Next to the shaft a layer of reddish-brown clay approximately one-thirty-second of an inch thick was found. The layer was quite distinct from the natural soil and was undoubtedly deposited there from the drilling mud. This layer extended uniformly along the length of the uncovered section of the shaft.

Test 7 was conducted on April 8, 1970, as a quick test using 50-ton load increments. The air-driven hydraulic pump was used for loading, and a Budd Indicator with two switch-and-balance units was used for reading the gages. The plots of the results of the test are given in Appendix C.

The data obtained in the excavation and the test provide a basis for making computations of internal load in the shaft at the different levels.

CHAPTER VII

ANALYSIS OF DATA

Program DARES

To aid in reduction and analysis of the data from the tests, a computer program (Program DARES) was developed for in data processing. The object in developing the program was threefold.

1. To compute and list the differences and averages of both the settlement gage and the Mustran gage readings;
2. To correlate the Mustran gage readings at each level with the applied load providing an easy check for erratic readings in the data; and
3. To compute and list the load distribution along the length of the pile, the load-transfer curve at selected points along the pile length, and the bottom load-settlement curve.

The program was written with the aim of becoming a production-type program to be used by both The University of Texas and the Texas Highway Department in the analysis of data for future instrumented shaft tests. An attempt was made to keep the data input to a minimum and as simple as possible, and at the same time to obtain maximum utilization of the computer. The input formats, described in Appendix E, are based on a series of input tables. Each table contains a different type of information that is printed immediately after reading. One provision for reprinting the Mustran data is to provide a scale factor by which the gage reading may be presented in any desired units. Likewise, the

applied load is input in any desirable units and is converted to load in pounds. To aid in plotting, load-settlement data is reprinted at even increments of load by linear interpolation between applied loads.

After reprinting the test data, only the average readings at a gage level and the average settlement gage readings are stored in the computer for computing the load distribution and load transfer. For each level, the average readings are adjusted inversely, proportioned to the ratio of the square of the shaft diameter at the gage level to the square of the shaft diameter at the calibration level. This procedure adjusts for the differences in shaft diameter at the various levels. From the readings of the calibration gages a function relating the adjusted gage readings to the load in the shaft is determined. The function, a polynomial of chosen order, is computed by a technique of curve fitting by least squares. The adjusted readings at each gage level are converted to a shaft load, in pounds, by the application of the calibration function as follows:

$$Q_N = AVRD_N \cdot F(RD) \quad \ldots\ldots\ldots\ldots\ldots\ldots\ldots\ldots (7.1)$$

where

Q_N = the measured load in pounds, at level number N,

AVRD = the average gage reading at level number L, and

F(RD) = the function relating gage reading, RD, to the load in the shaft.

For a given applied load, a load-distribution function is computed which relates load in the shaft to distance along the shaft. The

function is computed in a manner similar to computation for the calibration function, that is, a least squares polynomial of chosen order is placed through the data points. At the ground surface a restriction is imposed on the load-distribution function, such that the curve is forced through the applied load. With a minor program modification another restriction may be imposed. The slope of the curve at the ground surface may be set.

The load-distribution function then becomes the basis for computing the data for the load-transfer curves. The slope of the load-distribution curve at a point represents the load being transferred from the shaft to the soil at that point. Thus, a function relating load transfer to distance along the shaft is obtained by differentiating the load-distribution polynomial.

$$f(z) = d\left[G(z)\right] \quad \ldots\ldots\ldots\ldots\ldots\ldots\ldots\ldots\ldots\ldots (7.2)$$

where

$f(z)$ = the function for the load transfer at distances of z along the shaft, and

$d\left[G(z)\right]$ = the derivative of load-distribution function $G(z)$.

The load transfer per unit surface area of shaft would be the total load transfer per unit length of shaft, as expressed by the function $f(z)$, divided by the circumference of the shaft.

The shaft movement is determined by subtracting the compression of the shaft, from the top to the point in question, from the measured shaft settlement.

$$W_z = W_T - \frac{1}{A_c \cdot E_c}\left(Q_T \cdot W_s + \int_0^z G(z)\right) \quad \ldots\ldots\ldots (7.3)$$

where

W_z = the shaft movement at a point z distance below the ground surface,

W_T = the measured shaft settlement,

A_c = the effective cross-sectional area of the shaft,

E_c = the modulus of elasticity of the concrete,

W_s = the distance the settlement gages are located above the ground surface,

z = the distance below the ground surface, and

$G(z)$ = the load distribution function.

Using Eqs. 7.1, 7.2, and 7.3, for each applied load, computations are made; and values are printed for load distribution, load transfer, and shaft movement for preselected increments of distance along the length of the shaft. The values of load transfer and shaft movement are stored and may be reprinted later as load-transfer curves. An example of the output for the load-distribution and load-transfer curves is contained in Appendix V.

A method is provided for checking the input data and for the computation of the load-distribution curves for any value of applied load. The method involves fitting a polynomial through the data from each level of instrumentation. From these best-fit polynomials, the process of checking for erratic readings is relatively easy. For each selected

applied load, readings for each gage level are computed using the best-fit polynomial. The program is then routed back to the section of the program where the load-distribution curves are calculated. Using the selected loads as the applied loads and the computed gage readings as data points, the load-distribution and load-transfer curves are computed in the same manner as were the curves for the actual applied loads.

An efficient procedure for the analysis of a set of data involves running the program, skipping the calculations for the load-distribution and load-transfer curves, and fitting the gage data with a best-fit polynomial. The data can then be checked for consistency and correctness. The applicability of the in-shaft calibration may also be evaluated by examining the plots of the gage data versus applied load (Fig. 7.1) and also the plots of the slope of the best-fit polynomial versus applied load (Figs. 7.2 and 7.3). After ascertaining the correctness of the data and applicability of the gage calibration, the program is run for complete analysis of the data.

Calibration of the Gages

The purpose of the top level of Mustran gages was to establish a gage response curve relating load in the shaft to gage readings. If there were uniformity in the properties of the shaft at the gage levels, then the top level of gages would furnish a direct means of converting gage readings to load in the shaft. Therefore, the top level of gages has been referred to as the calibration gages and the response curve of these gages has been referred to as the gage calibration curve. The conversion would not only be independent of the shaft properties but

would also be independent of the Mustran gage factor computed earlier in Chapter V.

As mentioned previously, a rather large load transfer was indicated between the ground surface and the 14-foot gage level. Since very little load transfer was expected in the upper portion of the shaft, the procedure of directly applying the gage response of the top level of gages to the response of the other levels of gages was suspected as being erroneous. It was observed during the construction process that the top portion of the borehole was considerably larger than the nominal shaft diameter. The shaft diameter at the top level of gages was determined by the inside diameter of the Sonotube form which was 36 inches, whereas, the shaft diameters at the other gage levels were determined by the diameter of the borehole. Due to the use of drilling mud in the construction process, direct measurement of borehole diameter was not possible. Since the gage response is inversely proportional to the area of the shaft, a small error in the shaft diameter could cause relatively large errors in the conversion of the gage readings to load in the shaft.

Another suspiciously large load transfer was indicated between Gage Levels 7 and 8 (the 51-foot and 60-foot gage levels). Because of the blowout during construction, it was thought that a large difference could exist between the shaft diameters at the two levels.

If an estimate could be obtained of the shaft diameters at the different gage levels, the response curve of the top level of gages could be modified inversely proportional to the square of the diameters. These modified response curves could then be applied to the gage readings to

attain the load in the shaft at the various gage levels. The application of these response curves would still involve the assumption that the concrete properties are uniform over the length of the shaft.

The results of excavating from around the shaft have been discussed earlier in the text. The diameter of the shaft just above Gage Level 2 was measured to be approximately 41 inches. It was not possible to measure the shaft exactly at the gage level, but an estimate of approximately 41 inches for the shaft diameter at the gage level seemed reasonable. The direct application of the top-level gage response curve to the gage readings of Gage Level 2 would have introduced an error in the indicated load of approximately 33 per cent. Since such errors were possible, estimates of the shaft diameter at the other gage levels were necessary for the proper analysis of the data.

Prior to running Test 7, an attempt was made to reconcile the inconsistencies by examining the slope of the gage response curves of Test 2. The gage response curves for the test are presented in Fig. 7.1. The slope of the curves were obtained by taking the derivative of the best fit polynomial representing the response curve for each level. The plot of the slopes versus applied load is given in Fig. 7.2. These slopes are functions of the shaft properties and load transfer characteristics of the shaft. If the shaft were uniform along its length, the slopes of the gage response curve would approach a constant value as an unchanging load transfer is attained. From the previous tests conducted at the SH 225 Test Site, it has been observed that with large shaft deformations the load transfer does tend to reach a constant value. Thus, it would be expected that the plots of the slopes

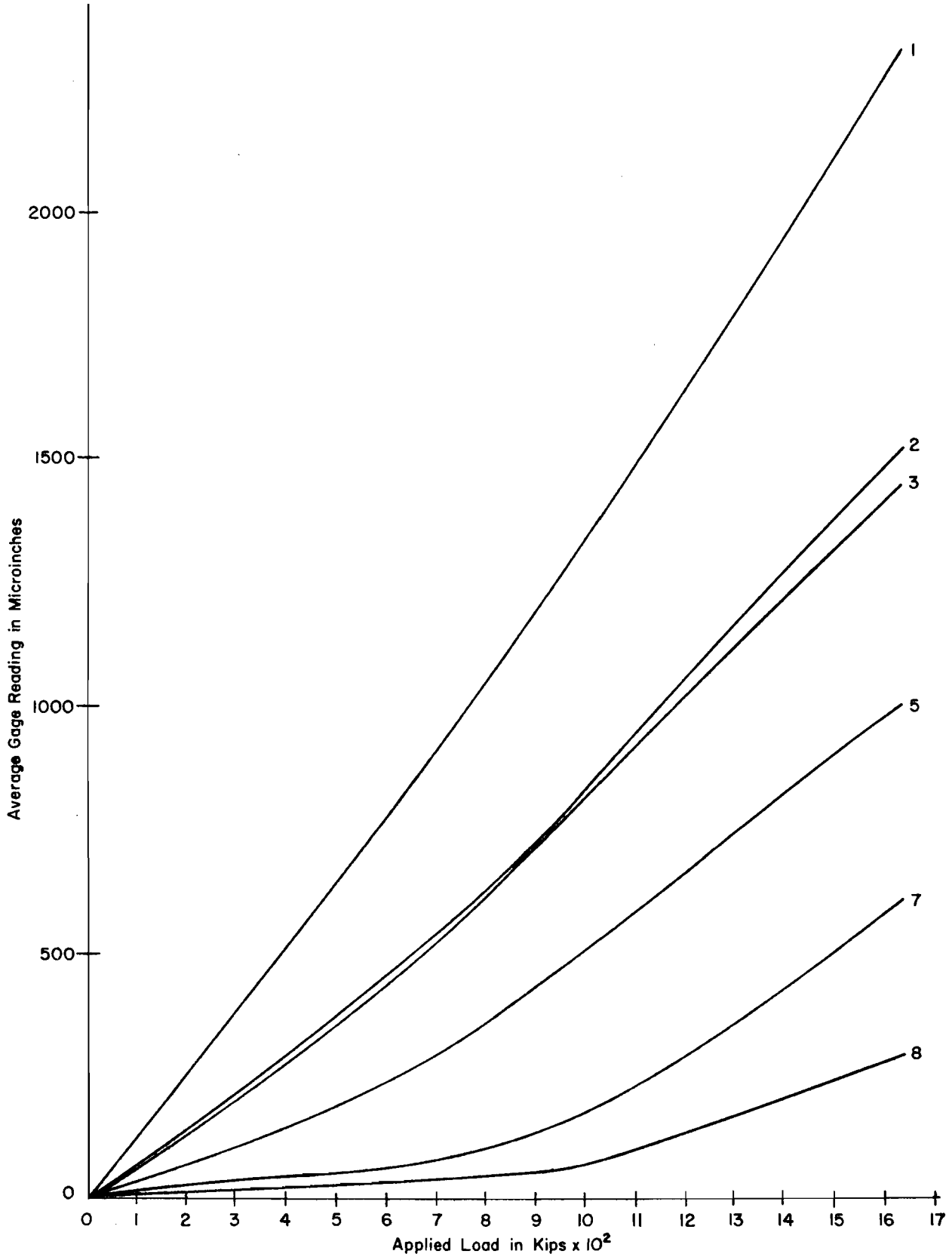

Fig. 7.1. Gage Response Curves for Test 2

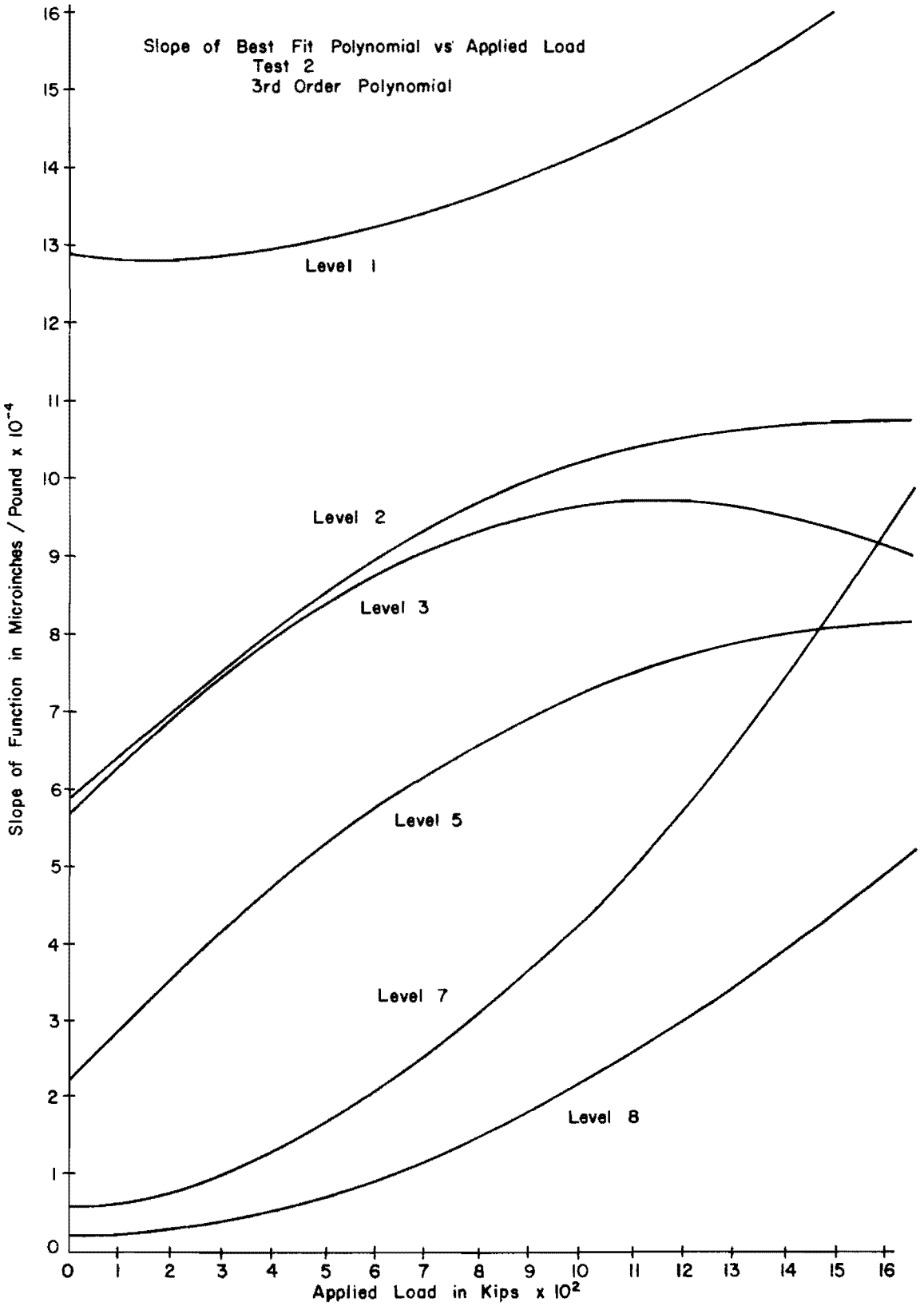

Fig. 7.2. Slopes of the Functions Representing the Gage Responses for Test 2

presented in Fig. 7.2 should converge with impending failure of the shaft.

For Gage Level 2, a trend is indicated in Fig. 7.2 which could lead to an estimate of the shaft diameter at the gage level. At a load of approximately 500 tons, the curve representing the slope of the response curve for Gage Level 2 begins to level out, indicating that there is no additional load being transferred out of the shaft above this level. If the assumption that no additonal load is being transferred out of the shaft above this level is correct, then the difference in slope of the calibration gage level and Gage Level 2 must be related to the difference in the diameter of the shaft at the gage levels. Using the fact that the slope should be inversely proportional to the shaft areas, the diameter of the shaft at Gage Level 2 may be estimated. Take for example, the applied load of 750 tons. The gage reading for Gage Level 2 is approximately 1,320 microinches. For Level 1 the same gage reading is obtained at 500 tons. The comparison is made at the same gage readings because of the nonlinearity of the concrete. The slope of the calibration curve at 1,320 microinches (500 tons applied load) is approximately 14.2 by 10^{-4} microinches per pound of applied load, and the slope of Level 2 at 1,320 microinches (750 tons applied load) is approximately 10.7 by 10^{-4} microinches per pound of applied load. The diameter at Level 2 is estimated by the relationship:

$$(D_2)^2 \approx (D_1)^2 \cdot \left(\frac{SL_1}{SL_2}\right) \quad \ldots\ldots\ldots\ldots\ldots\ldots\ldots\ldots (7.4)$$

where

D_1 = the shaft diameter at Level 1,

D_2 = the shaft diameter at Level 2,

SL_1 = the slope at Level 1, and

SL_2 = the slope at Level 2.

Thus, the diameter was estimated as

$$(D_2)^2 \approx (36)^2 \cdot \left(\frac{10.7 \times 10^{-4}}{14.2 \times 10^{-4}}\right) \quad \ldots\ldots\ldots\ldots\ldots\ldots (7.5)$$

$$D_2 \approx 41.5 \text{ inches}$$

The plot of Level 3 follows Level 2 to an applied load of about 450 tons, however, after 550 tons the slope actually begins to decrease. This would indicate that the load transfer between the two levels is increasing with higher applied loads. Such action would most likely be caused by projections of the shaft that would tend to increase the load transfer as the deflection becomes greater. It would seem quite reasonable that projections would exist in the sand layer between the two levels.

The slopes of Levels 7 and 8 differ by an almost constant ratio. Again, the most logical explanation of this would be differences in the shaft diameter. Supporting this would be the fact that during construction, a minor caving occurred at the bottom of the hole where a small bell could have formed. Assuming the diameter at Level 7 to equal the

outside diameter of the casing, the diameter at the bottom was estimated as being approximately 50 inches.

Thus, by using the plot of the gage data, rational estimates of the shaft diameter at the various gage levels were made.

Using the data from Test 7 (Fig .7.3) in a similar manner, a shaft diameter at Gage level 2 of 41.8 inches is obtained. The measured diameter just above the level of gages was approximately 41 inches. It is felt that the difference between the calculated and measured values are due to the fact that additional caving occurred in the sand layer where the gage level was located. Protrusions projecting from the shaft could be felt by probing down into the sand layer. The extent of these protrusions could not be determined, but it is felt that these caused the reduction in slope noted in Test 2 for Level 3. By removing the overburden, the load transfer appeared to have been reduced between Gage Levels 2 and 3. Thus, Level 3 seemed to have a sensitivity of about the same as that of Level 2. In looking at the plot of the data (Fig. 6.2) from Test 1, it is seen that the readings obtained from Level 3 were slightly higher than those from Level 2. The only way this could occur would be for the shaft to be larger at Level 2 than at Level 3. Thus, the evidence indicated the diameter was slightly less at Level 3. An approximation would be 40.5 inches, which was the measured diameter in the exposed section.

In Test 7, the ratio of Level 7 to Level 8 was again computed to be 1.9, confirming the computations from Test 2.

At Level 5, about all that can be done is to estimate the diameter based on observations. It would be reasonable to expect that at a

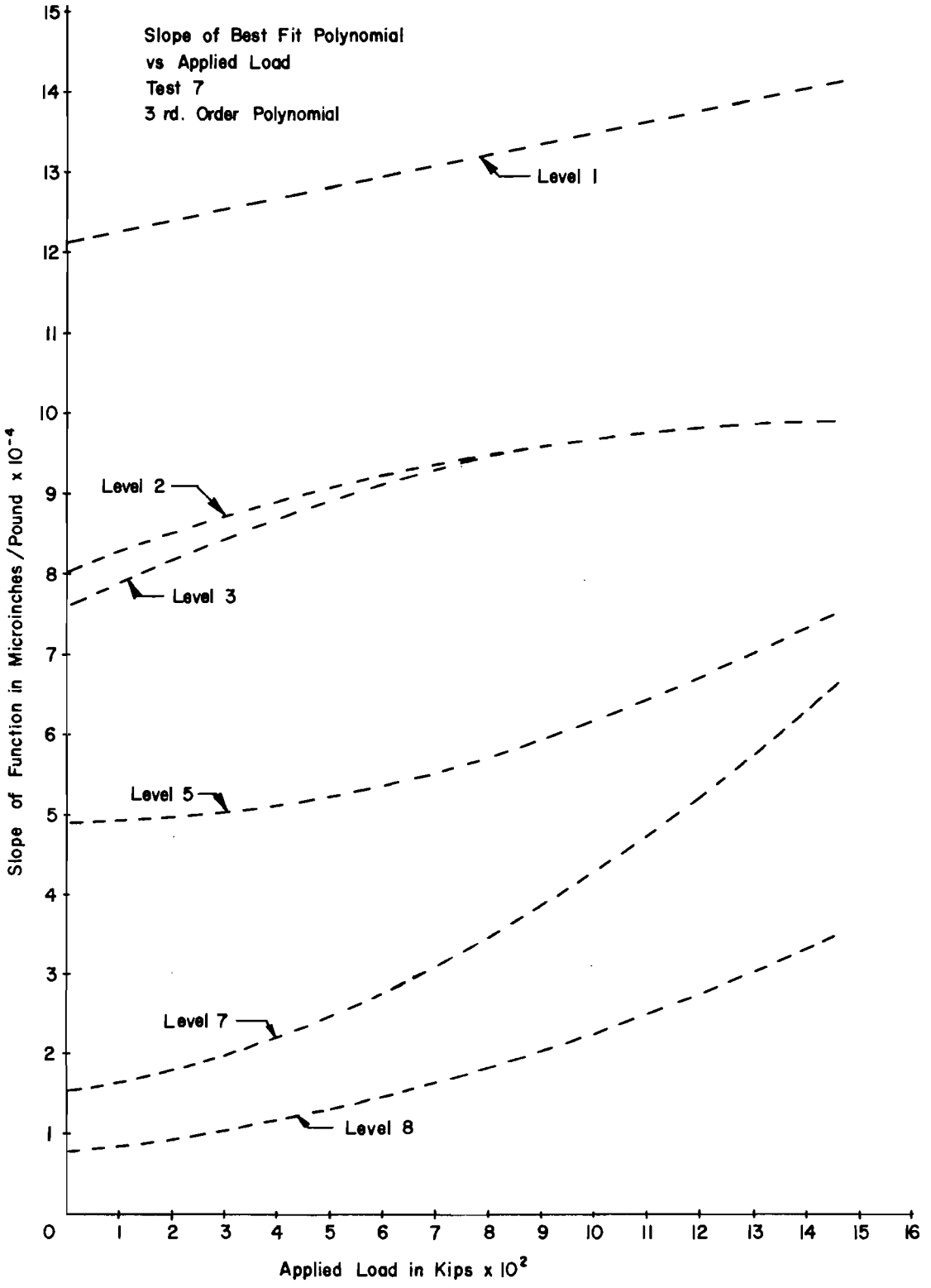

Fig. 7.3. Slope of the Functions Representing the Gage Responses for Test 7

depth of 42 feet the hole would not be oversized by more than 2 inches. So, a diameter of 38 inches was the accepted estimate.

Since Gage Levels 4 and 6 were not used in the analysis of the data, no attempt was made to estimate the shaft diameter at these locations.

In summary, at the gage levels the diameters that are to be used in determining the load distribution are estimated as follows:

Level 1 - 36 inches

Level 2 - 41.8 inches

Level 3 - 40.5 inches

Level 5 - 38 inches

Level 7 - 37 inches

Level 8 - 50 inches

Load-Distribution Curves

The load distribution in the shaft for applied and selected loads was approximated using the least squares curve fitting technique of Program DARES 6. The data points for the load-distribution curves for Tests 1, 2, 3, and 7 were obtained from the measured applied load and Gage Levels 2, 3, 5, 7, and 8. The data from Gage Levels 4 and 6, although plotted on load-distribution curves, were not given any weight in the curve fit, and thus did not influence the curve. The reasons for eliminating these gage levels were explained previously in Chapter VI. In Tests 4, 5, and 6, only Gage Levels 1, 3, 5, 7, and 8 were read eliminating Level 2 as a data point for the load-distribution curves of these tests.

For the tests with six data points, a fifth order polynomial would be the maximum order to fit the data. In fact, a fifth degree curve

would become nothing more than an interpolating polynomial. As a comparison, a third-degree curve and a fifth-degree curve were plotted for the data from Test 2. These curves are given in Figs. 7.4 and D.2, respectively. Although the set of third-degree curves greatly resemble idealized load-distribution curves, they do not adequately fit the observed data of Test 2. For Test 2, it appears the fifth-degree curve which actually forces the curve through the data points, provides the best representation of the measured loads. For the remaining tests, having six data points, only the fifth-degree curves are given. In the analysis of the tests having only five data points, the third-degree curve provided adequate representation of the data.

In order to compare the load-distribution curves for the different tests, it would be better to have the load-distribution curves for the same shaft butt loads. Program DARES 6 provides a means of estimating the load distribution for any selected butt load. In comparing the load-distribution curves for the applied loads with the load-distribution curves for the selected butt loads the differences were found to be of no consequence in the data analysis. Thus, for simplicity and comparison, all of the load-distribution curves are presented for selected applied loads.

A phase of tests 1, 3, and 6, involved maintaining the load for a period of time. For these tests several load-distribution curves are presented for the maintained load.

These load-distribution curves (Fig. D.1, D.4, and D.7) give some indication of the effect of maintaining a very high load on a drilled shaft.

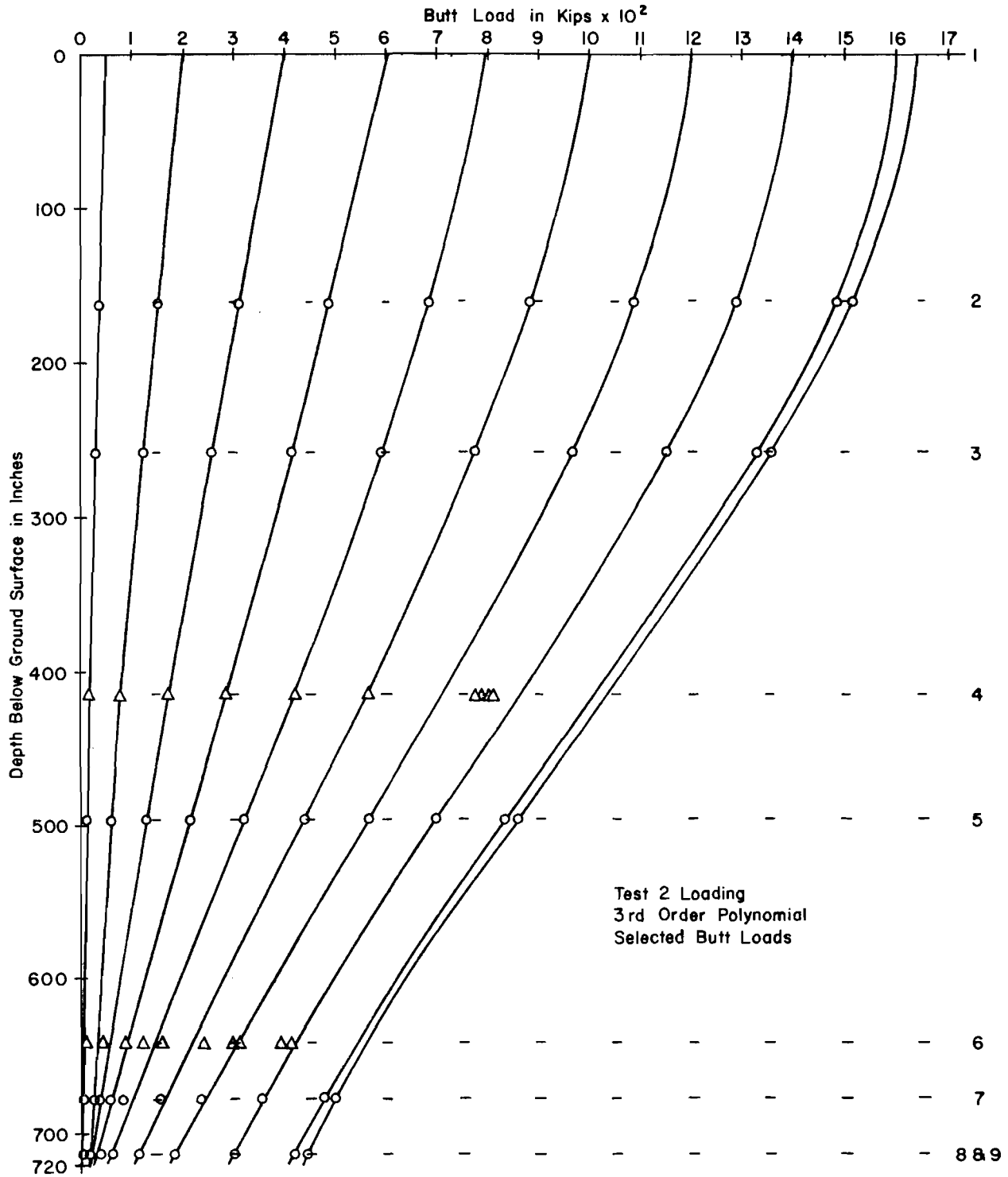

Fig. 7.4. Load Distributions for Test 2 Represented by Third-Order Polynomial

Load-Transfer Curves

Load-transfer curves are presented along with the load-distribution curves in Appendix D. The data for the curves were obtained by the utilization of Program DARES as previously explained. Load-transfer curves were computed at the five-foot stations along the length of the shaft. For Test 2, three sets of load-transfer curves are given as a comparison of the different sets of load-transfer curves obtained from the different load-distribution curves. The first set of curves, shown in Fig. 7.5, was obtained using a third-order polynomial for the load-distribution function. The other two sets were obtained from fifth-order functions of load distribution. The set shown in Fig. D.17 was computed from the load-distribution functions for the applied loads, and the set shown in Fig. 7.6 was computed from the load-distribution functions for the selected butt loads. The load-transfer curves for the third-order polynomial tended more toward an average load-transfer curve. It is felt that the two sets of load-transfer curves obtained from the fifth-order polynomial more closely represent the true load transfer. It seems that by using the selected butt loads in place of the applied loads, a smoothing of the load-transfer curves is obtained. The difference is minor and is not enough to justify plotting both sets of load-transfer curves. The load-transfer curves given are based on load-distribution functions for the actual applied loads.

Load transfer as a function of time was also obtained in Tests 1, 3, and 6. These plots are presented along with the other load-transfer curves in Appendix D. These results will be discussed later.

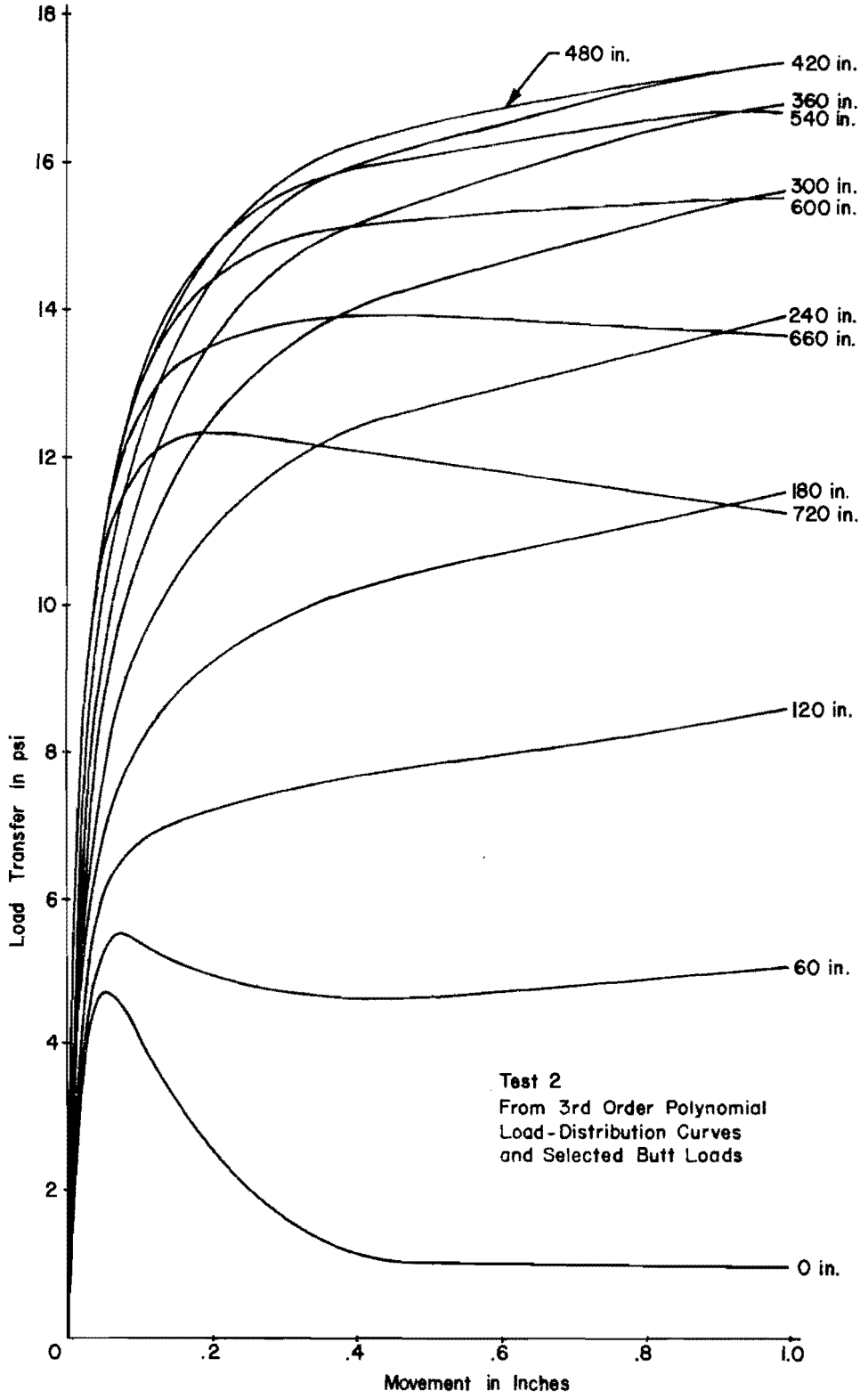

Fig. 7.5. Load-Transfer Curves for Test 2 which were obtained from Third Order Polynomial Load-Distribution Curves at Selected Butt Loads

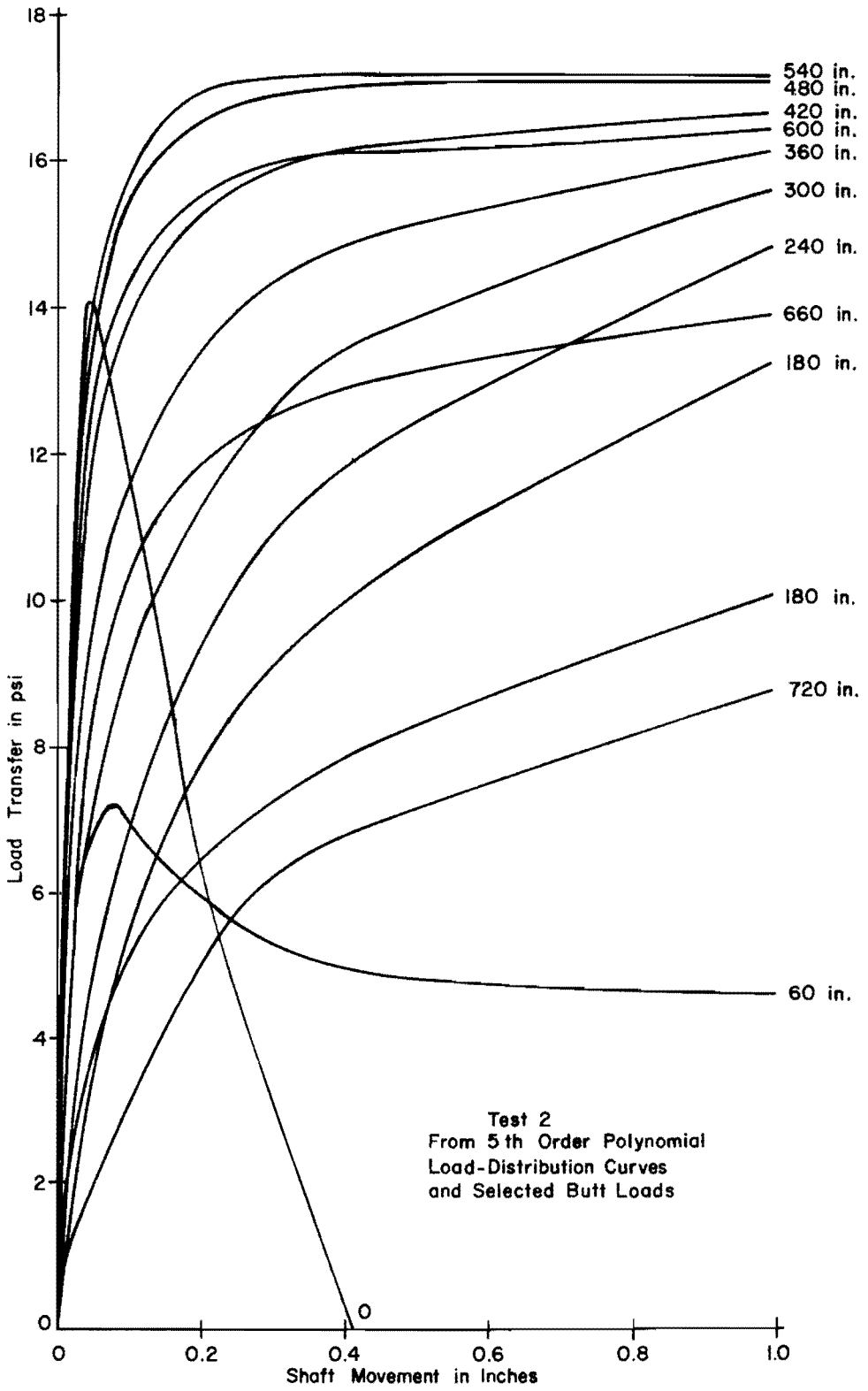

Fig. 7.6. Load-Transfer Curves for Test 2 which were obtained from Fifth Order Polynomial Load-Distribution Curves at Selected Butt Loads

In Test 5, load-transfer curves were available on the first loading and the recycle loading for each load increment. Thus, for each station two load-transfer curves were computed. The comparison of the two curves for a few of the stations is shown in Fig. D.15.

Discussion of Test Results

Unlike the SH 225 Test Site, which was chosen based on its "ideal" soil properties, the site for the HB&T shaft was dictated by the location of the HB&T Railroad Overpass. As such, the variation in soil properties at the test site represent the typical variation which may be expected at a construction site for drilled shafts. The dimensions of the shaft and the expected shaft capacity fit into the research program being conducted by The University of Texas. The largest shaft previously planned in the research program was a shaft 30 inches in diameter and 45 feet long. The failure load anticipated for the HB&T shaft was sufficient to give excellent gage readout, yet it did not exceed the capacity of the loading system. The soil consisted of sands, silts, and clays. All of the tests previously conducted had been associated with clay soils, but additional tests were planned for the Summer of 1970 in a sandy soil. Thus, the testing of the HB&T shaft not only provided additional information on the interaction in clay soils, but it also gave an indication of the load transfer characteristics of a drilled shaft in a layered soil system.

Construction of a test shaft employing a drilling fluid was also new to the research program. Drilling mud was later used in the construction of one test shaft at the SH 225 Test Site, and it may be used in the construction of one of the shafts to be tested in sand.

Unfortunately, three factors lead to uncertainties in the test results. First, the soil conditions were such that good soil data were difficult, if not impossible, to obtain. Second, funds were not available for an adequate number of instrumentation levels; and third, due to inexperience in the instrumentation of drilled shafts in sand or silt, some of the instrumentation levels were placed in the shaft at the location of silt or sand seams. The caving of these soils caused the loss of two instrumentation levels. The loss of these two gage levels were particularly detrimental to the analysis of the test data.

Construction Procedures. In addition to excavating the soil from around the HB&T Test Shaft, the soil was removed from around Shaft 4 at the SH 225 Test Site. The tests of the shaft for the SH 225 site indicated the same type of discontinuities found for the HB&T shaft. The excavation was made for each in order to recalibrate the top gages and to examine the top portion of the shaft.

The excavating of the SH 225 shaft provided an opportunity to compare two shafts constructed with processed holes. The basic construction procedure for both shafts was the same. The major differences of the shaft were shaft dimensions and soil conditions. The SH 225 shaft was 30 inches in diameter and 45 feet long. The soil was primarily a stiff clay with a silty layer from 29 feet to 32 feet. It was the presence of this silty layer that made necessary the use of the drilling mud in the construction process.

The excavation of the SH 225 shaft was accomplished on April 7, 1970, approximately nine months after installation of the shaft. A procedure

similar to that used in excavating the HB&T shaft was employed for SH 225 excavation. The depth of excavation was 24 feet, placing the bottom of excavation below the area of the shaft suspected of being irregular in shape.

The examination of the HB&T shaft disclosed no serious irregularities due to the use of drilling mud. The upper five foot section of this shaft was greatly enlarged and quite irregular, but the portion of the shaft on down to the top of the sand layer was almost a perfect cylinder. As could be expected for any shaft, the diameters of all the upper part of the shaft were greater than the normal shaft diameter. By probing into the sand layer below the bottom of the excavation, protrusions from the shaft could be felt. There were no indications of any reduction in the shaft diameter anywhere along its length.

The thin layer of drilling mud, previously discussed, did exist but there was no evidence of the existence of any large pockets of trapped mud. The effect, if any, of this layer on the load carrying ability of the shaft was thought to be minor. Nothing else detrimental was found in the examination of the HB&T shaft. Actually, the enlarged upper section of the shaft and the protrusions in the sand layer served to give a shaft capacity greater than that of a perfect shaft. The fact that load was actually being transferred at the top of the shaft is evidenced by the cracking of the concrete as shown in Fig. 6.4. The load being carried at the time this upper segment of shaft cracked is estimated to be 50 tons. This estimate is verified by the load-distribution curves of Test 2 (Fig D.2). It appears from the load

distribution that the concrete cracked at a load just above 300 tons. In the tests following Test 2, very little load was transferred out of the shaft in the section above the second gage level.

The examination of the SH 225 shaft revealed results contrasting to those found at the HB&T site. As suspected from the test data, it was found that the shaft was not regular. The upper six feet of the shaft were oversized by an amount that would be expected due to drilling. From the 6-foot depth to the 18-foot depth the shaft was approximately of nominal size with a pocket of drilling mud existing between the wall of the hole and the concrete. The maximum thickness of the pocket of drilling mud was measured to be six inches at about the 9-foot depth. The drilling mud for this shaft was light gray in color making it easy to distinguish from the dark red clay. The color of mud undoubtedly came from the deeper silt layer which was also a very light grey. Below and around the pocket of drilling mud, the clay was very wet and soft. Below the 18-foot level the shaft was again oversized by 2 to 3 inches with all signs of the drilling mud having disappeared.

In the excavating process, chunks of concrete were broken from the shaft at about the 20-foot level. The chunks broke along cleavage planes, leaving a perfect cylindrical shaft the approximate size of the casing. For the chunks to break in such a fashion would indicate that the concrete had become contaminated along the surface of the casing.

One explanation for the pocket of drilling mud and for the contaminated concrete is offered. When the pulling of the casing was first begun the concrete was forced up along the outside of the casing. This

action cleaned the drilling mud from the sides of the hole and the casing. As the casing was pulled, the pressure on the concrete was greatly reduced. At the 20-foot level the concrete head was reduced so much that the concrete on the outside of the casing stopped rising. With further pulling of the casing, concrete was deposited with the greatest amount of contamination occurring along the outside of the casing. Although the concrete never became stuck in the casing, the drilling mud was not displaced. When the bottom of the casing neared the six-foot level, the friction between the casing and the concrete had decreased so that the concrete again displaced the drilling mud and completely filled the hole. The action at this level was such that the drilling mud below was trapped.

The explanation is substantiated by observations of the shaft construction. It was reported that, although the level of concrete in the casing never rose with the casing, the drilling mud did stop flowing out of the hole while the casing was being pulled through the section where the drilling mud was trapped. As the bottom of the casing neared the ground surface, there was a sudden gush of drilling mud from the hole and a steady flow thereafter.

Four principal factors could contribute to the formation of pockets of drilling mud such as was found at the SH 225 site. These factors are: (1) the wet concrete stiffness, (2) the rate at which the casing is pulled, (3) the casing diameter, and (4) the clearance between the casing and wall of the borehole. There was no detectable difference in the concrete slump nor in the rate at which the casing was pulled for the two shafts. The primary known differences were for Item 3,

the casing diameter, and Item 4, the clearance between the casing and the wall of the borehole. The ratio of the casing area to perimeter for the HB&T site was 9.0 as compared to 7.5 for the SH 225 site. The clearance between the casing and the wall for the upper portion of the HB&T shaft was approximately three inches, while for the SH 225 site this clearance was only about one-half as much. The combination of the two factors of a smaller shaft diameter and a smaller clearance is felt to have been the major contributing factor to the formation of the pocket of drilling mud.

The key to success in placing concrete under drilling mud by the use of casing appears to be the attainment of a vigorous scouring of the wall of the borehole by the rising of the concrete along the outside of the casing. An ideal procedure would be to employ some method by which the concrete could be forced out of the bottom and up the outside of the casing to the ground surface prior to pulling the casing. One method of accomplishing this is by pressurizing the casing. The system for pressurizing the casing to expell water from boreholes has been used, and such a system is also practical for expelling concrete from the casing.

It may be that for friction shafts, placing the concrete under the drilling mud with a tremie or concrete pump is less risky than using a casing. If the rules listed by Palmer and Holland (1966) are strictly followed, little chance exists that drilling mud will be trapped. A better scouring of the hole, particularly in the upper portions, will occur when the concrete is placed by either the tremie or the pump

method. This scouring is very beneficial, and it is believed that a better shaft will be obtained than if the concrete is placed in the casing.

The HB&T shaft did demonstrate that drilled shafts could be constructed utilizing drilling mud and casing with no evidence of detrimental effects. There are certain precautions which are considered absolutely necessary when this method is employed. Of major importance is the concrete slump which should be no less than six inches. The concrete mix should contain a retardant to prevent setting and premature stiffening. The head of the concrete in the casing should be maintained as high as practicable even though it would mean wasting concrete at the end of the concreting operation. Also, the pulling of the casing must be at a very slow rate with constant observation of both the concrete level and the fluid flow from the borehole. It is likely that the first indication of trouble would be the erratic flow of the drilling mud. Should this trouble develop, the pulling should be stopped, and either the concrete freed or the head of the concrete in the casing increased. As a routine practice, an accurate record of the amount of concrete used should be maintained and the volume of concrete used checked against the computed volume of the borehole. If less concrete were used than was expected, the possibility of voids should be checked by whatever means possible.

It may be said that the elimination of the risk in the construction of a drilled shaft in unstable soils, utilizing a drilling mud is by constant, competent, and vigilant supervision. The fact that few failures have been reported in the use of drilled shafts should be no reason

for complacency. For drilled shafts designed on the basis of side friction, relaxation of proper supervision and inspection for even one shaft could mean the loss of a major structure.

Effects of Reloading on Shaft Behavior. The several tests conducted on the HB&T Test Shaft offered an opportunity for observing the effects of reloading on the shaft behavior.

The principal comparison of the behavior of the shaft in the different tests was obtained by the examination of the resulting load-settlement curves (Fig. 7.7). The load-settlemen curves are good indicators of any differences in the soil-shaft interaction.

For the same loading, the settlement observed in Test 2 was almost identical to the settlement observed in Test 1. The effects caused by the relatively light loading of Test 1 were indicated to be very minor, as expected. The small shaft settlement produced by the light loading would not be sufficient to strain the soil past its "elastic" range. The load-transfer curves for Test 1 (Fig. D.10) differ from the load-transfer curves for Test 2 (Fig. D.11) in that Test 1 did not develop the maximum value of load transfer indicated in Test 2. The comparison of the load developed on the shaft base is obtained from the response curves (Fig. C.16, Appendix C) of the bottom gages. For Tests 1 and 2, the response curves for these gages are shown as one line. Thus, for all practical purposes the base behavior in Test 2 was the same as the base behavior in Test 1.

After Test 2, exclusive of Test 7, the shaft exhibited a stiffer behavior. Between the loads of 300 tons and 600 tons, the load-settlement curve for Test 2 shows more settlement of the shaft than

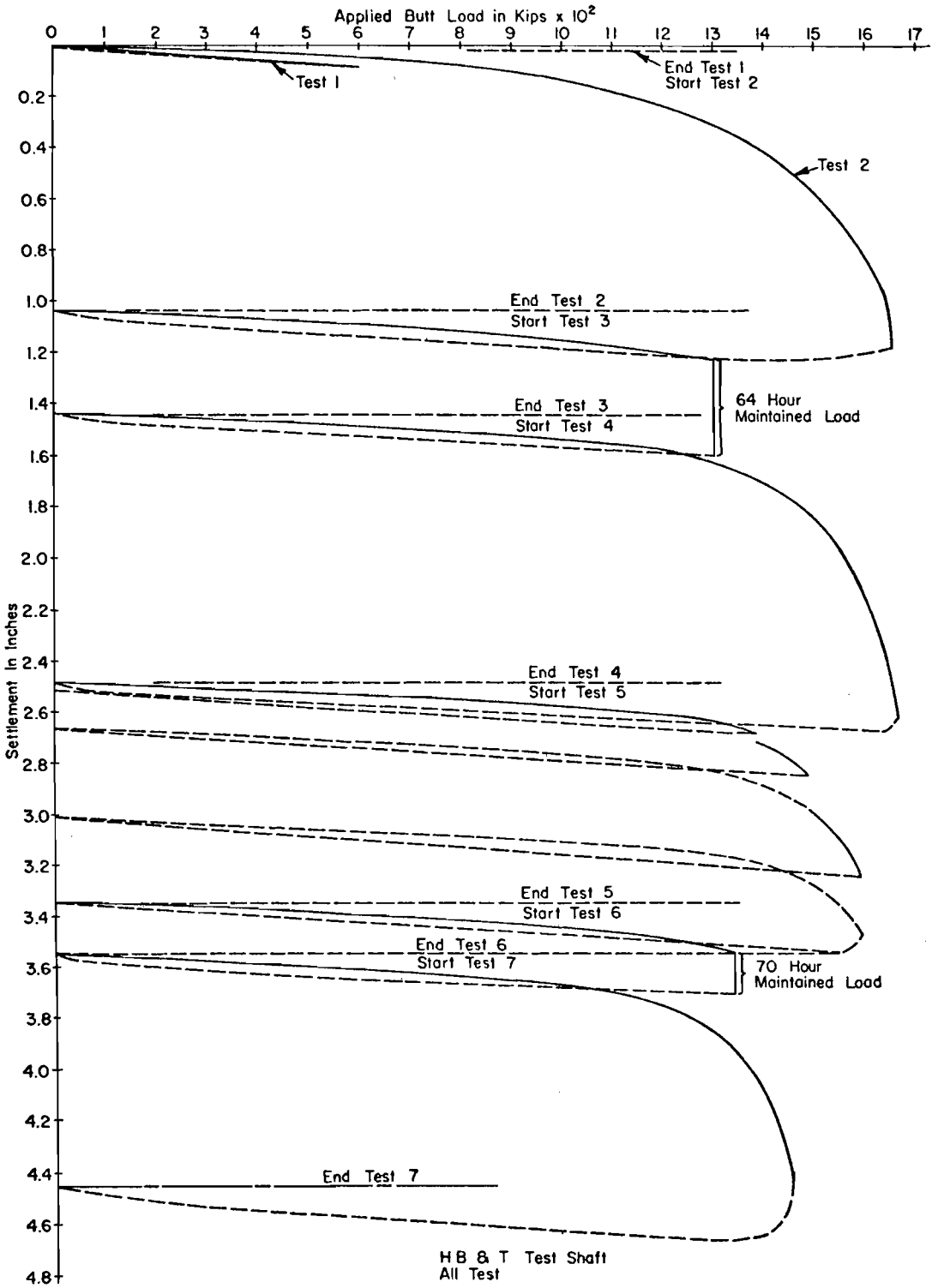

Fig. 7.7. Gross Settlement of the Test Shaft by Tests

did the curves from Tests 4 and 7. For the tests taken to failure, Test 4 indicated approximately the same ultimate load as Test 2; Test 5 indicated an ultimate load of about 40 tons less than Test 2; and Test 7 indicated an ultimate load of about 120 tons less than Test 2. It must be recalled from Chapter 6 that only Tests 2 and 4 were conducted as identical tests. In Test 5, the testing procedure was changed and prior to Test 7 the top 13 feet of soil had been excavated from around the test shaft.

The differences in top load-settlement curves can be attributed more to the change in the load-settlement characteristics of the base than to changes in characteristics of the load transferred by side resistance. The effect of the reloading on the base load is reflected by the response curves of the bottom level of gages (Fig. C.16, Appendix C). Below 600 tons applied butt load, the response of the gages indicates a stiffer action by the base. This stiffer action by the base would be the cause of the changes observed in the load-settlement curves of the later tests. The ultimate capacity of the base in Tests 4 (188 tons) and 5 (182 tons) was not as great as the ultimate capacity in Test 2 (217 tons). The stiffer base action and reduced ultimate capacity are consistent with the findings of other researchers and are the expected effects of reloading. For Test 7 the developed base load was approximately the same as the base load developed in Test 2 (Figs. 7.10 and 7.11). Perhaps the time allowed between testing was a factor in that the soil had sufficiently healed prior to Test 7.

The effects of immediate reloading side friction were observed in Test 5. The testing procedure, described earlier, involved immediate

reloading. Using the data from the test, two sets of load-transfer curves were constructed (Fig. D.15, Appendix D). With reloading of the shaft, the indication is that there is a slight reduction in side resistance. Because the base capacities of Tests 4 and 5 were approximately the same, it is this decrease in side resistance which caused the reduction in shaft capacity for Test 5 from Test 4.

From the examination of the load-transfer curves obtained in Tests 2, 4, and 7, it is noted that when the soil was allowed to heal, there was no reduction in load transfer in the center portion of the shaft. In fact a higher side resistance was indicated in the tests following Test 2, exclusive of that portion of the shaft within a few feet of the ground surface and of the shaft base. The increase of side resistance in the sandy and silty soils of Zones 2 and 3 is felt to be due to increasing confinement pressures caused by the downward movement of the shaft. The effect of shaft movement is to be discussed later in the text. The additional support gained in the sandy and silty soils appears to have been offset, at least in part, by a decrease in the side resistance developed near the ground surface and near the base of the shaft. The loss of support at the ground surface was caused by the cracking of the concrete surrounding the shaft as was illustrated in Fig. 6.4. During the first test and the beginning of the second test, it is believed that the concrete slab and the compacted shale fill were the major factors contributing to the load transfer developed at the ground surface. After the concrete cracked the load transfer in this area was practically eliminated.

On reloading there was a marked reduction in the load transferred by side resistance in the vicinity of the shaft base. In Fig. 7.8, it is seen that the ultimate side shear developed at the base was approximately 8 psi, 4 psi, and 1 psi for Tests 2, 4, and 7, respectively. This noted decrease is believed to be due to the downward movement of the shaft base. The effect of the base action on the side resistance will be discussed later.

Effects of Drilling Mud on Load Transfer. There are several facets of load transfer which merit additional discussion. Probably of foremost interest, is the effect of drilling mud on the load-transfer characteristics of drilled shafts. For the HB&T shaft, no effect of the drilling mud on the load-transfer characteristics in any of the soils could be detected in the seven tests. As may be expected for the SH 225 shaft, which was constructed with a processed hole, very little load was transferred out of the shaft along the pocket of the trapped drilling mud. Below the 20-foot level, normal load transfer developed, indicating no effect due to the presence of the drilling mud, O'Neill and Reese (1970).

Development of Side Resistance at the Ground Surface and at the Shaft Base. The results of the tests conducted at the SH 225 Test Site indicated a marked reduction in the side resistance developed along a drilled shaft near the ground surface and the base (O'Neill and Reese, 1970). The maximum side resistance developed along the HB&T Test Shaft in Tests 2, 4, and 7 is presented in Fig. 7.8 as a function of depth. It is apparent from the data presented in the figure that this side resistance is affected by the discontinuities existing at the ends of the shaft.

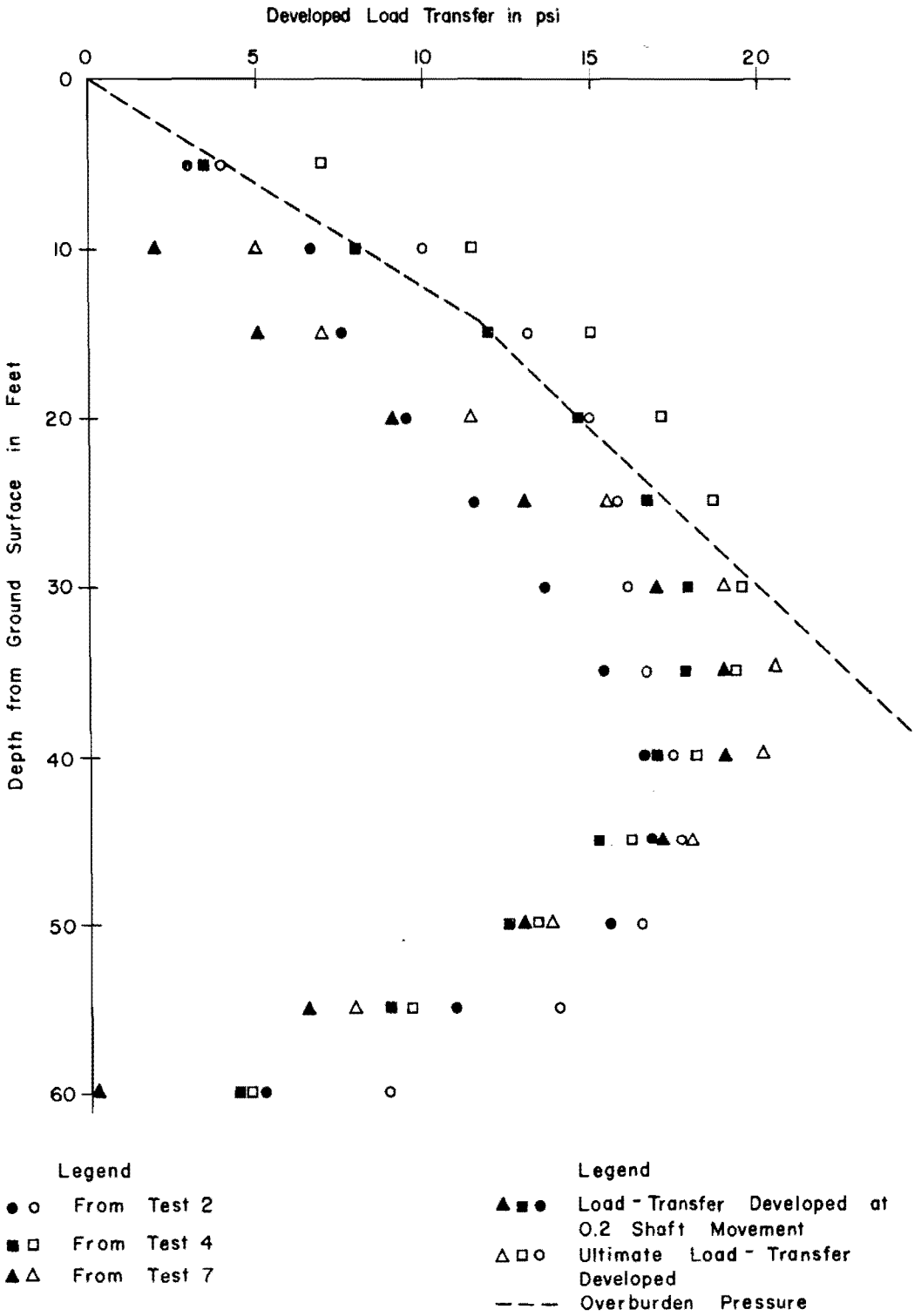

Fig. 7.8. Load Transfer Developed in Tests 2, 4, and 7 at a Shaft Movement of 0.2 of an inch and at Shaft Failure

The load transfer near the surface is mainly affected by the lack of overburden pressure on the soil. Even in the clay soil at the SH 225 Test Site, it was felt that a lack of overburden pressure was the primary cause of the reduced load transfer near the ground surface. For a sandy or silty soil, it would be expected that the surface effects are even more marked than the surface effects observed at the SH 225 Test Site. In sandy and silty soils the shear strength is dependent on the confining pressure, and thus the surface effect is compounded more than for clay.

Although at the HB&T Test Site the surface effects may have been partly masked by the action of the concrete slab and the taper of the top portion of the shaft, it is felt the data obtained in the testing sustained the findings of O'Neill and Reese (1970).

At lower loads in Test 2, the concrete slab and the enlarged upper section of the shaft contributed greatly to the ground-level load transfer. From the load-distribution curve of Test 2, Fig. D.1, it is estimated that at an applied load of 300 tons, the load being taken out at the surface was approximately 50 tons. At this applied load, the concrete slab began to crack as shown in Fig. 6.4 resulting in a decrease in top load transfer. At the ultimate load of Test 2 very little load transfer was being indicated in the top 8 to 9 feet of the shaft. For Test 3 considerably less load transfer was manifested at the ground surface than was indicated in Test 2. As shown by the load-distribution curves, Fig. D.4, whatever load transfer that was developed at the ground surface dissipated after the load had been maintained for the 43 hours. The load being supported by the top portion of the shaft was

transferred to the base of the shaft. A similar loss in the support of the top section during load maintenance of Tests 1 and 6 was observed. The loss occurred during Test 1 even though the load for this test was relatively low and was maintained for only three hours.

As discussed in Chapter V, during the shaft construction the bottom of the borehole is believed to have caved forming a small bell. The maximum load transfer just above the base was developed during Test 2. During Test 1, insufficient movement was produced at the bottom to develop the load transfer. In the tests following Test 2, very little load transfer was developed in the five to six feet above the base. It appears that little load transfer in this area existed after large movements of the base.

The greatest load transfer is indicated as occurring in a section below the top one-third and above the bottom one-sixth of the shaft. This also happens to be the area of the greatest soil strength, but the increase in shear strength developed is not proportional to the increase in soil strength.

Effects of Soil Properties on Load Transfer. One of the basic aims of the study being conducted by The University of Texas is to correlate soil properties to the load transfer of drilled shafts. The results of the direct shear test (Table 4.5) strongly indicate that the full shear strengths of silty and sandy soils may be developed along the sides of drilled shafts. For clay soils, a reduction in shear strength due to increases in moisture content at the interface is just as strongly indicated.

For the computations of the α factors (ratio between developed shear stress and shear strength of a clay) at the HB&T Test Shaft the values of soil shear strengths for the silts and clays were obtained from the soil shear strength profile (Fig. 4.15). The shear strength shown for the clay represents the undrained shear strength of the clay (which assumes the angle of internal friction of the soil to be zero). The shear strength of the silt and silty-clay was obtained from triaxial strength tests. The tests were conducted on soil samples at confining pressures equal to the computed overburden pressure at the depth from which the soil samples were taken. Values of α were computed for both the shear stress developed at a shaft movement of 0.2 of an inch and the ultimate shear stress developed.

A plot of the average α factors for the HB&T site is contained in Fig. 7.9. The α factors of soil Zones I and VI are very low and appear to be influenced more by discontinuities at the ground surface and base tip than by soil properties. The concrete slab and the shaft being tapered at the top may have had considerable effect on the α factor of Zone I.

For the stiff clay, Zone V, an average α factor of 0.6 was measured agreeing closely with the average value of α observed from the tests at the SH 225 site. The following equation was used in the computation for the α factor of the clay.

$$\alpha = \frac{S_{0.2} \text{ or } S_{ult}}{c} \quad \ldots\ldots\ldots\ldots\ldots\ldots\ldots\ldots\ldots (7.1)$$

where

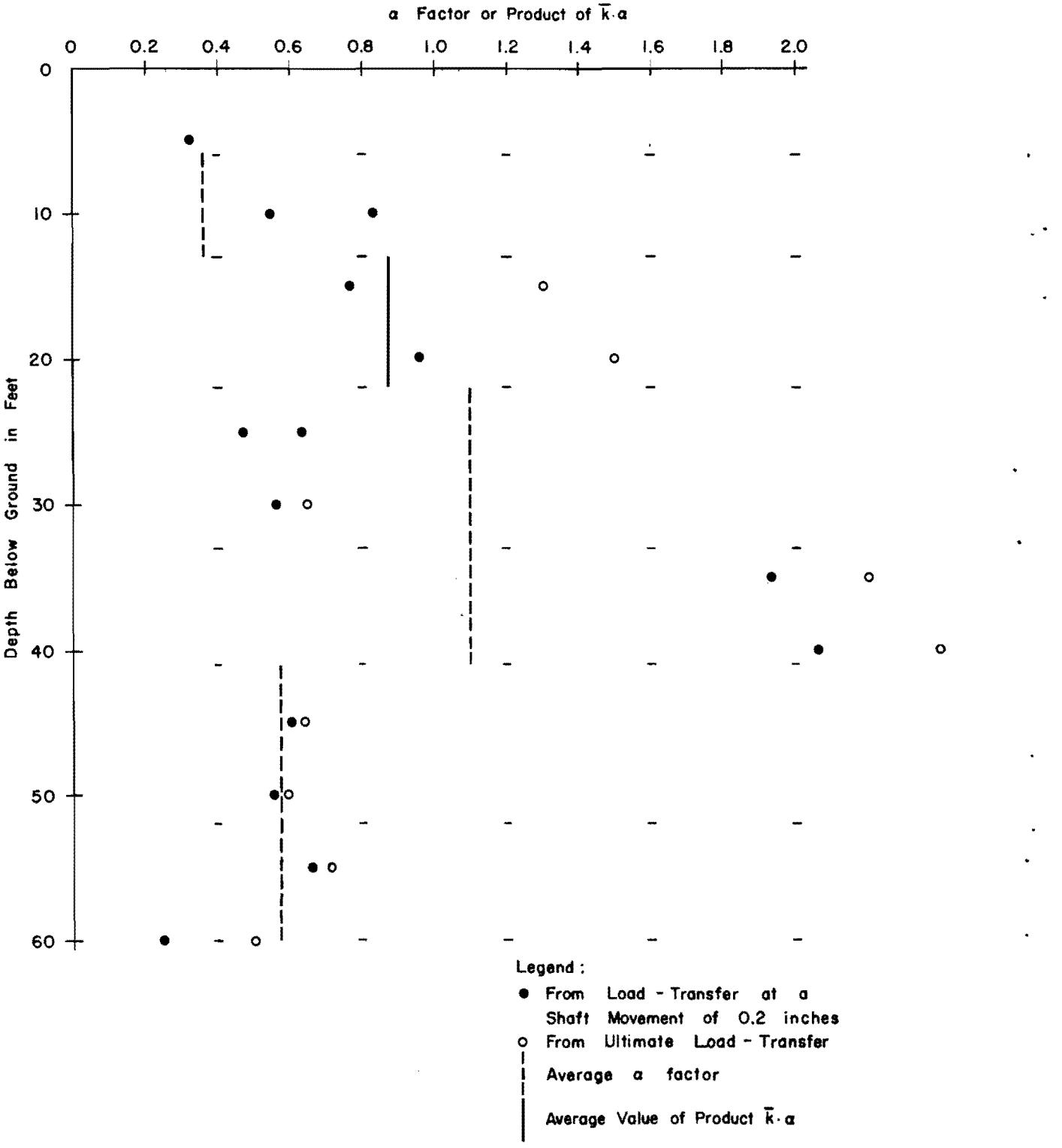

Fig. 7.9. Average α Factors obtained for each Soil Zone

c = the undrained shear strength of clay,

$S_{0.2}$ = the shear stress developed at a shaft movement of 0.2 of an inch, and

S_{ult} = ultimate shear stress developed.

The load transfer developed in the sand layer, Zone II, varied with the different testing conditions. In Test 1 and the early part of Test 2, very little load transfer was developed in this zone. During Test 2 as the shaft movement increased, the load transfer continued to develop. Even though Test 2 resulted in a large settlement of the shaft, a maximum load transfer was not reached. In Tests 3, 4, 5, and 6, the load transfer continued to increase. The measured load transfer in Test 7, which was conducted after the excavation of the overburden was much lower and did not show the tendency to increase with additional shaft movements. The indication is that the confining pressure was increasing with the settlement of the shaft. As discussed previously, the load transfer in granular soils is greatly affected by the lateral pressure between the shaft and the soil. There was no instrumentation to measure the lateral pressure at the side of the shaft; thus, there was no way to obtain a true soil strength at any instant during the tests. Therefore, the product of α and $\bar{k}$ was computed by the following equation:

$$\alpha \cdot \bar{k} = \frac{S_{0.2} \text{ or } S_{ult}}{z \cdot \gamma \cdot \tan \phi} \quad \ldots\ldots\ldots\ldots\ldots\ldots \quad (7.2)$$

The cause of the apparent increase in the confinement pressure of the sand with shaft movement is not known for certain. It is suspected that the combined effect of the concrete slab and shaft taper was the most likely cause.

For such action to have developed would have required a large shaft movement and would have accounted for the low load transfer observed for Zone II in Test 1. The results of Test 7 sustain the belief that the increase in the lateral pressure was caused by increases in the stress of soil in Zone I. After the excavation of the soil of Zone I, the load transfer developed in Zone II was considerably reduced and failed to show the marked increase with the large shaft movement. It is not known what the results would have been had the shaft been perfectly straight and the concrete slab had not been present. Undoubtedly, there would have been some increase in the lateral pressure caused by the normal load transfer from the shaft to the soil of Zone I. The amount of increase would probably be very dependent on the properties of the particular overlying soil. Perhaps in the tests to be conducted in sandy soils at Test Sites V and VI, a better understanding of the shaft soil interaction in sands will evolve.

The silts and silty clay were located in Zones III and IV. Since the level of instrumentation between the two zones gave erratic results, only an average load transfer in the zones could be measured. Using the average shear strengths obtained from the triaxial tests and the average load transfer, an α factor of approximately one is obtained. Again, as was the case of the sands, the values of load transfer used were the values for 0.2 of an inch of shaft movement. The very silty

soils indicated the same trend as did the sands, that is, a much greater load transfer was developed with the increasing shaft movements. There is a discrepancy in the shear strength obtained by the triaxial test and the THD cone penetrometer for these two soil zones, particularly for Zone IV. If the average shear strength obtained from the THD Cone penetrometer is used, an α factor of approximately 0.8 is measured for the zones.

It appears that the sands and silty clays act much the same. For a shaft movement of 0.2 of an inch, the measured α factor or product of α and $\bar{k}$ for these soils was between 0.8 and 1.0. At larger shaft movements, the load transfer increased, giving an α factor or product of α and $\bar{k}$ which appears to be much higher than one. The additional load transfer is most likely to be due, not to larger α factors but to greater confining pressures imposed from soil layers above the granular soil. The loss in the ultimate capacity of the shaft from Test 2 to Test 7 (Table 6.1) is believed to be caused by the reduction in the confining pressure of the sands and silty soils rather than the loss of support of the removed soil.

Effects of Maintained Load on Load Transfer. The most important benefit of the maintained load test was in the insight gained in the problems associated with long-term testing. The major problem encountered for the test was the maintenance of a constant load. Failures associated with the air compressor caused loss of load (Chapter 6) and the slow settlement of the shaft required that a constant observance of the load be maintained. Some temperature effects on both the settlement gages and on the upper level of Mustran gages could be the source

of some error in the data. The performance of the Mustran cells was satisfactory and gave an indication that the cells would be suitable for any future long-term tests.

The plots of the load transfer versus time for Tests 1, 3, and 6 are contained in Appendix D. About the only trend noticable was a reduction of the load transfer in the top portion of the shaft. The support lost in this portion of the shafts appeard to have been picked up by the base of the shaft. The greatest changes in load transfer were recorded when the load dropped and then reapplied, such as was the case in Test 3 during the fourteenth hour of load maintenance. When the load was dropped and reapplied, the base load went from 260 kips to 296 kips.

Base Load. The measured base load at failure in all tests was approximately 210 tons. The plots of the base load-settlement curves for Tests 2 and 7 are contained in Fig. 7.10 and 7.11, respectively. Using a base diameter of 50 inches, the average soil stress at failure would be 214 psi. Based on an average soil shear strength of 20 psi for the soil zone below the base, an N factor of 10.7 is obtained. This value of N is consistent with the results of the SH 225 tests.

Although the value of N computed for the HB&T Test Shaft agreed with the findings of Skempton (1951), the observed base load-settlement curve failed to correlate with the computed base load-settlement curve based on the procedure presented by Skempton. The poor correlation is believed to be caused principally by the poor quality of the soil data. The silty layer of soil from approximately 63-65 feet produced triaxial stress-strain curves, which made the average stress-strain curves for

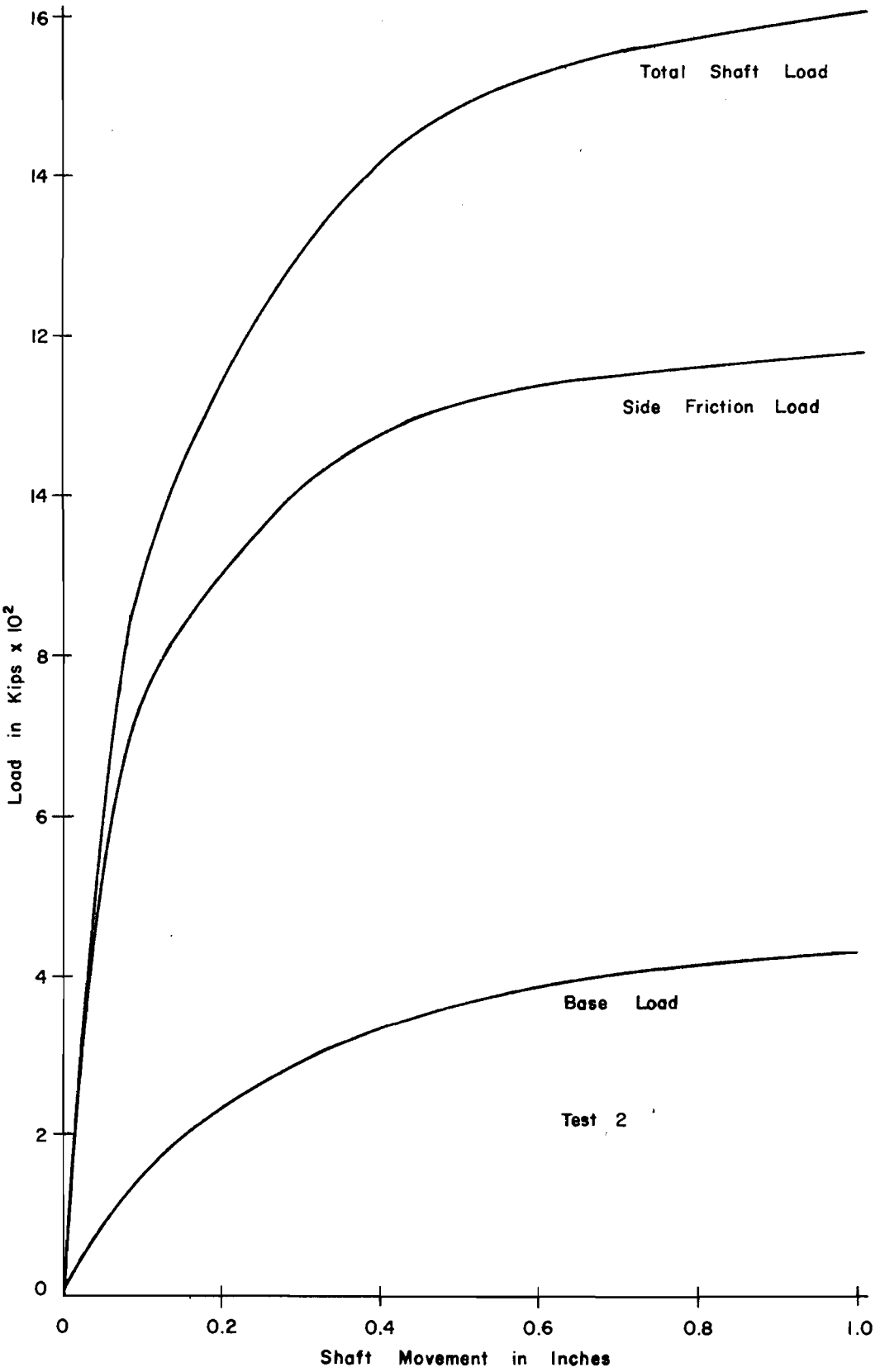

Fig. 7.10. Separation of Load into Base and Side Components for Test 2

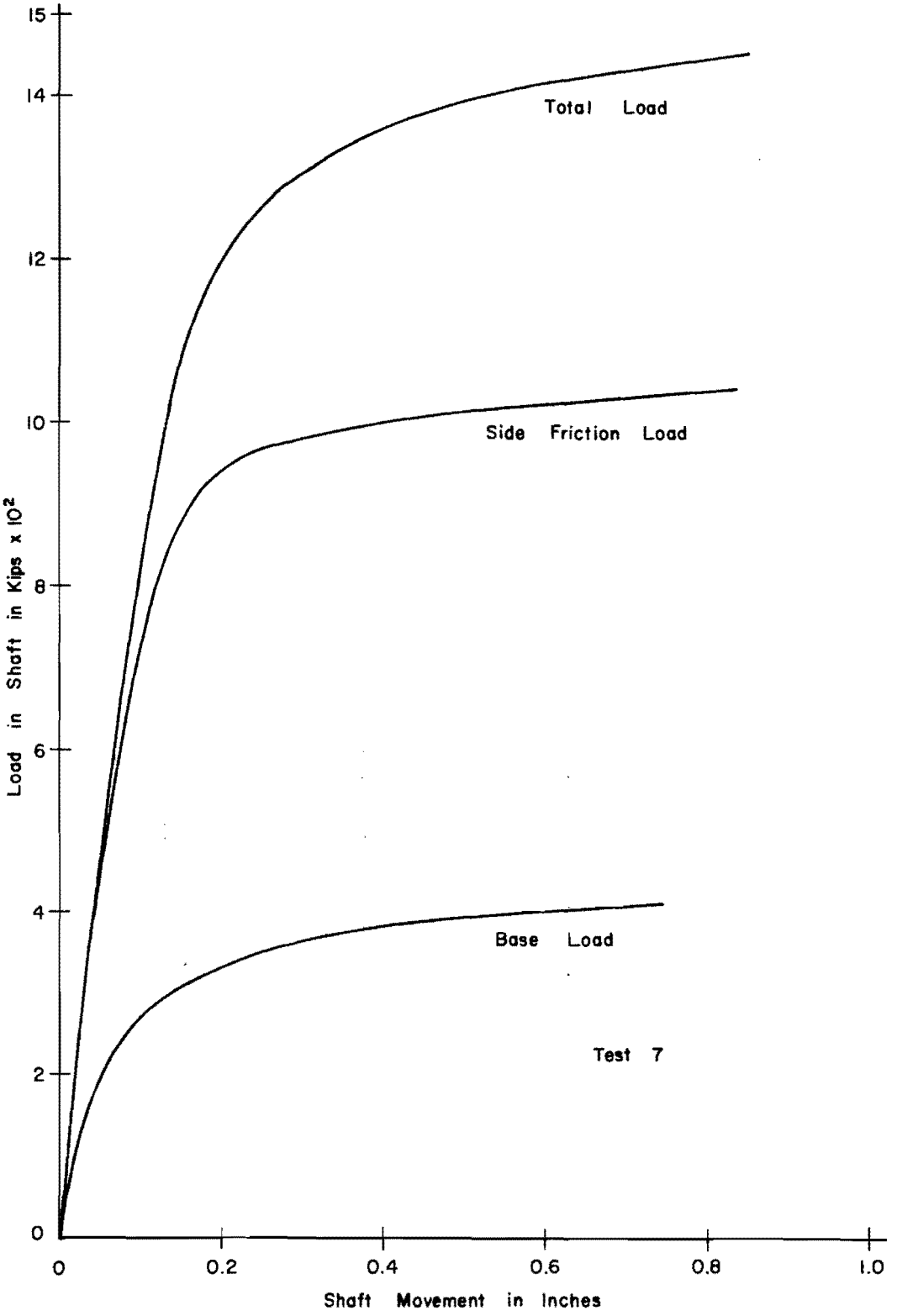

Fig. 7.11. Separation of Load into Base and Side Components for Test 7

Zone VII less stiff. If the computations for the base load-settlement curves are made utilizing the stress-strain curves for the stiff clay of Zone VII, then much better correlation is obtained. Even using the stiffer stress-strain curves the observed base load-settlement curve was stiffer than the computed curve.

Analytical Treatment of the HB&T Test Shaft

Three analytical analyses were made for the HB&T shaft based on three different sets of load-transfer curves. The analyses were made utilizing a digital computer employing a numerical technique similar to that presented by Coyle and Reese (1966).

The first analysis was based directly on the load-transfer curves obtained in Test 2 (Fig. D.11). For the second analysis, synthetic load-transfer curves were constructed by modifying the curves from Test 2. The modification consisted of setting the maximum load transfer to the load transfer developed at a shaft movement of 0.2 of an inch. A shaft movement of 0.2 of an inch was chosen because it was felt that this would eliminate any possible effects of the protrusions and increases in confining pressure caused by the shaft movement. Also eliminated, was the load transfer at the ground surface due to surface slab and compacted fill. This analysis should represent a conservative estimate of the load-carrying characteristics of an ideal test shaft. The third analysis utilized the basic soil properties in the attainment of load-transfer curves. The α factor for sands and silts was 1.0 and for clays was 0.6. For the sand, an α factor of 1.0 means that the lateral pressure is equal to the overburden pressure, or in other words, that

$\bar{k}$ is equal to 1.0. The curves were constructed employing a two-point system, the maximum load transfer, developing at shaft movements of 0.2 inches for clays and 0.4 inches for silts and sands. These movements are approximately ten times the strain at the peak shear strength, as obtained in the triaxial tests. The middle plot point was determined by using three-fourths of the maximum load transfer being developed at one-half of the shaft movement used for the maximum load transfer.

The two sets of synthetic load-transfer curves used in Analyses 2 and 3 are presented in Fig. 7.12 and 7.13, respectively.

The bottom load-settlement curve from Test 2 was used in Analysis 1. For analyses 2 and 3, the base support was reduced in proportion to the reduction in the area from a base 50 inches in diameter to a base 36 inches in diameter. This reduction in base support reduced the ultimate capacity of the shaft by approximately 100 tons.

The comparisons of the actual load-settlement curves and load-distribution curves obtained in Test 2 and in the analytical analysis are presented in Figs. 7.14 and 7.15, respectively. The results from Analysis 1 illustrates that if the load-transfer curves can be defined, then the analytical approach presented by Reese and Coyle (1966) can be employed to obtain accurate load-settlement curves and load-distribution curves for drilled shafts.

Had the test shaft been drilled perfectly straight with no tapering or protrusions, it is felt that the secondary effects occurring with large shaft movements would be minimized. The load-settlement curve and load-distribution curves presented for Analysis 2 then probably more closely represent the curves which would have been obtained

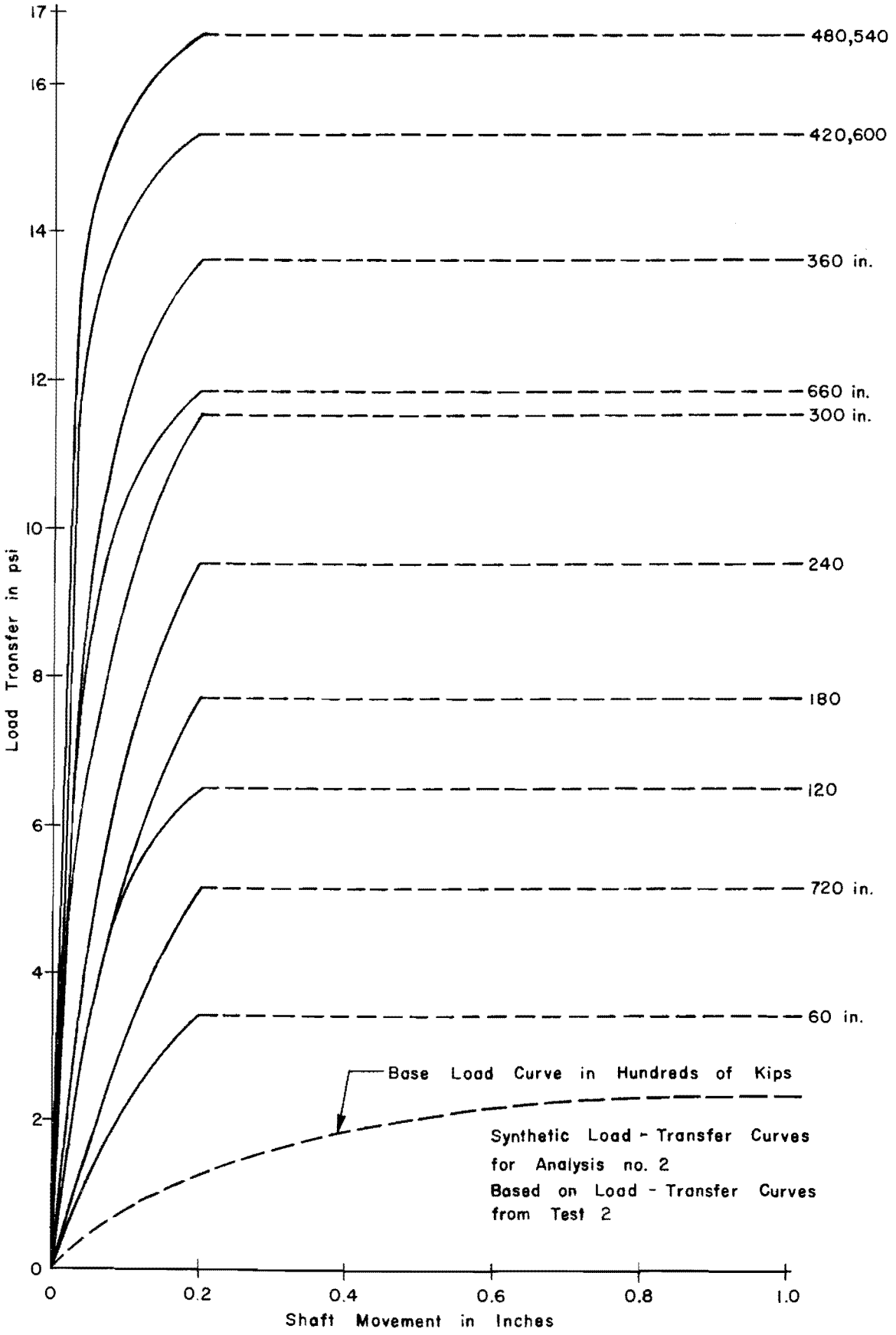

Fig. 7.12. Synthetic Load-Transfer Curves for Analysis 2

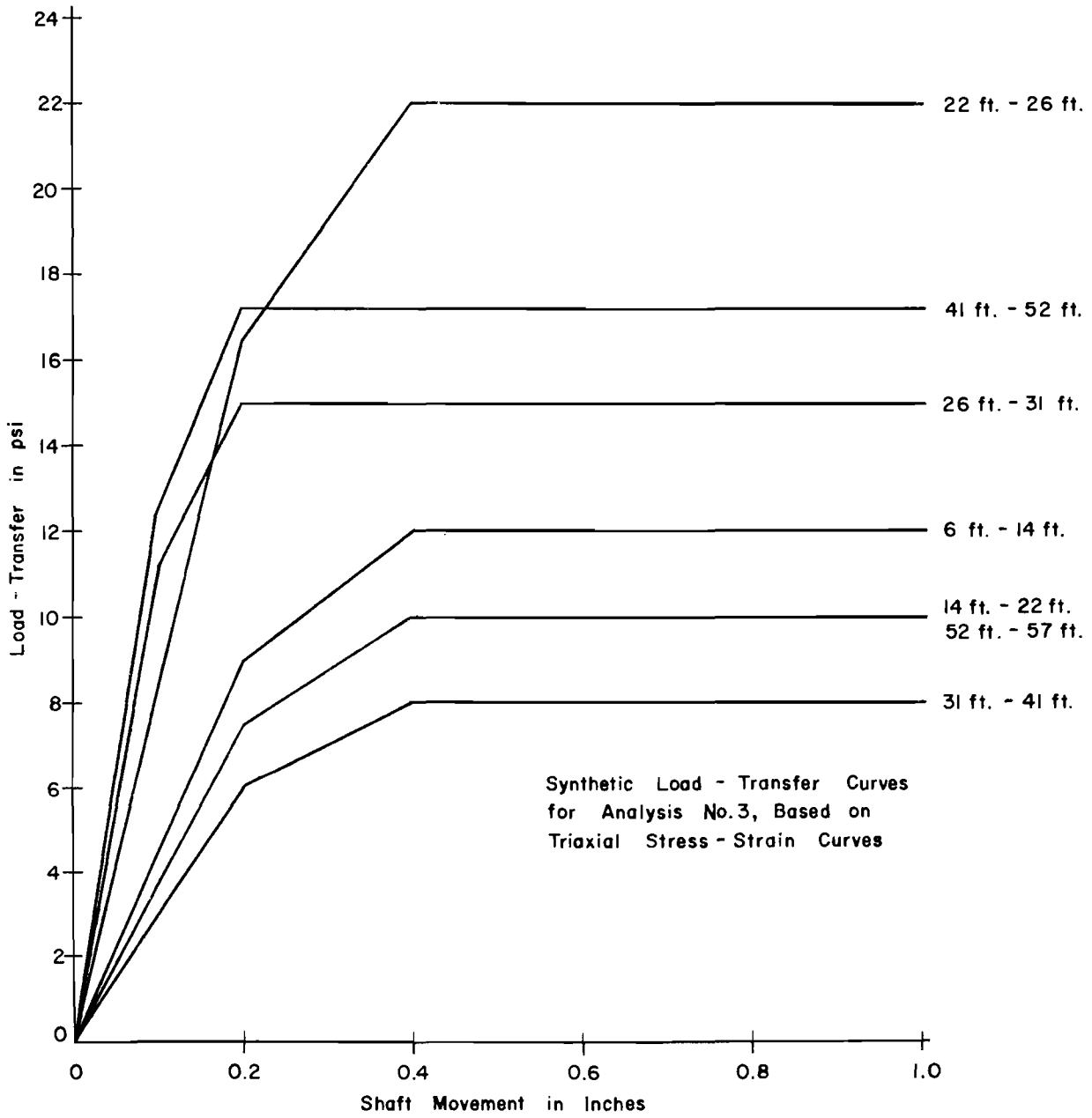

Fig. 7.13. Synthetic Load-Transfer Curves for Analysis 3

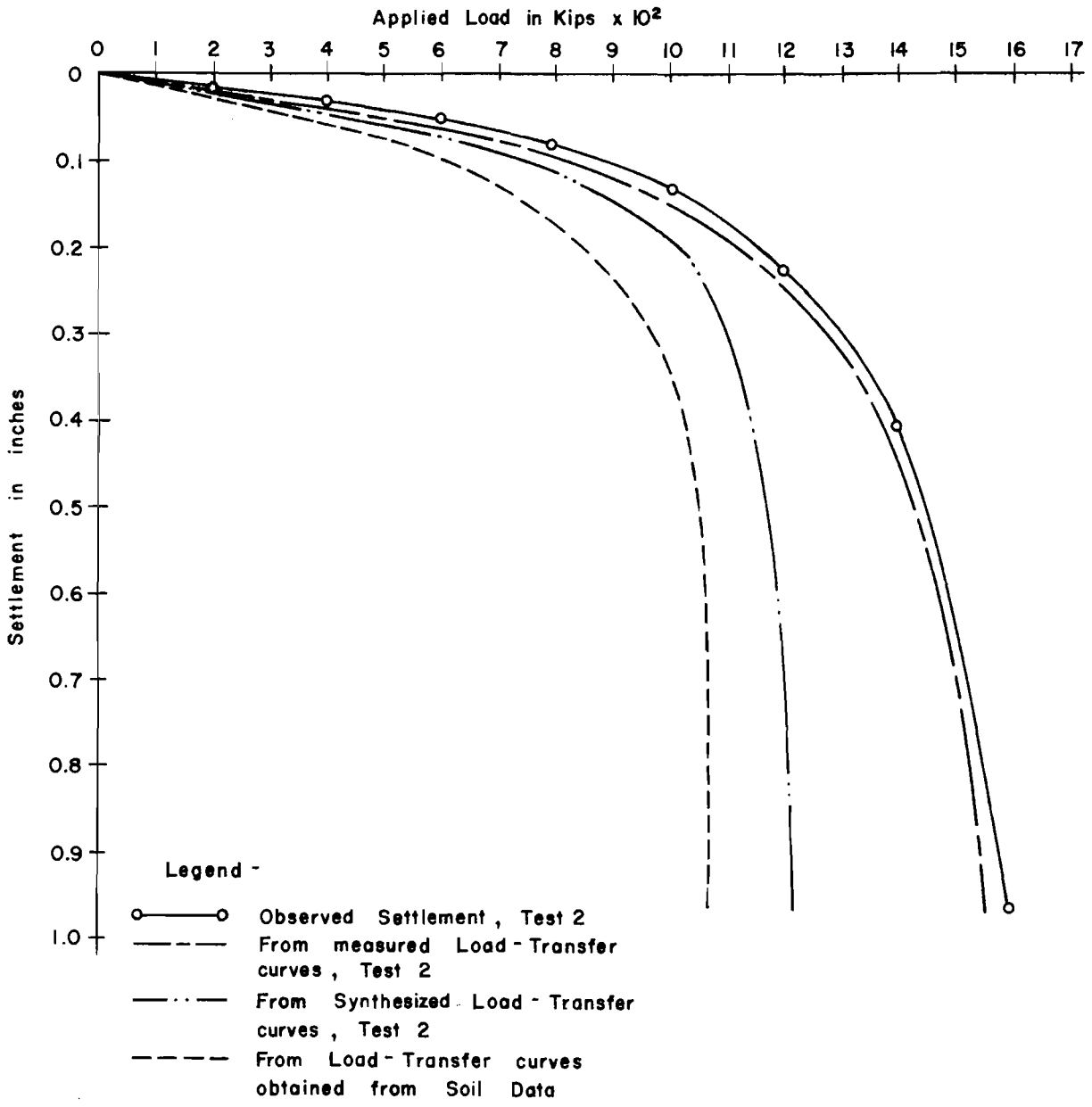

Fig. 7.14. Load-Settlement Curves from Test 2 and Analytical Treatment

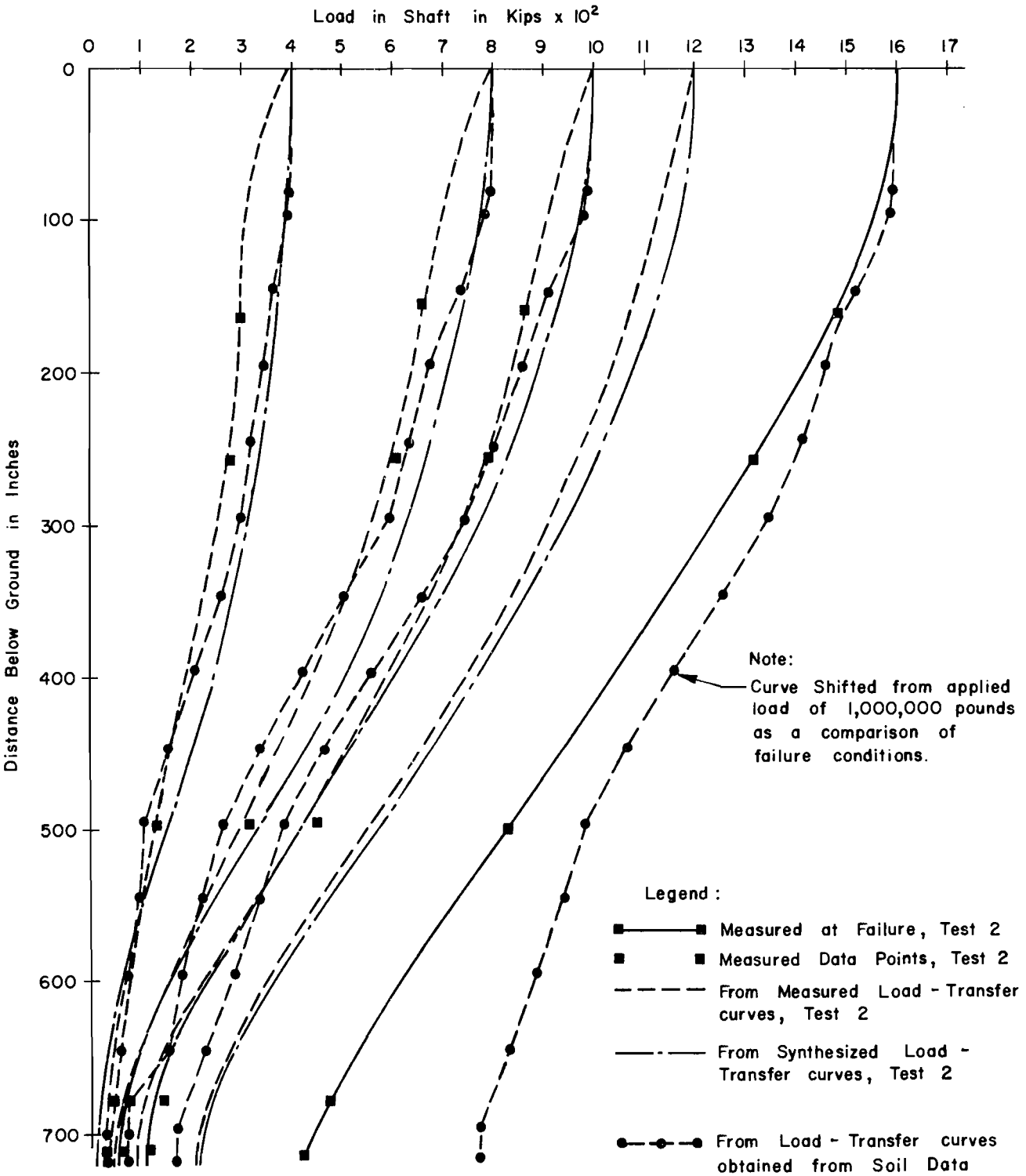

Fig. 7.15. Load-Distribution Curves from Test 2 and Analytical Treatment

had the shaft been an ideal test shaft. The formations of enlargements and protrusions in a test shaft can actually cause results which may give a false sense of security. The proper instrumentation of any test shaft to be used as a basis of design is well advised. The relative cost of the instrumentation is small compared to the cost of most structures employing drilled shafts and can give invaluable information for the true shaft behavior.

Analysis 3 demonstrates that even with crude load-transfer curves realistic load-settlement curves and load-distribution curves can be obtained. The analysis was purposely made conservative, as probably would be the case in an actual design, by completely eliminating any load transfer in the top three diameters and the bottom two diameters of the shaft. In the comparison of the load-distribution curves at failure obtained in the analytical analysis and in Test 2, the largest discrepancy is seen to occur in the multilayered soil of Zone VI. The soil data for this zone is very poor and it is possible that more support is provided than was anticipated.

At the present time the major drawback to realistic design of drilled shafts is the attainment of good soil data and correlation of these data to load-transfer curves. O'Neill and Reese (1970) obtained good correlation at the SH 225 Test Site of load transfer to soil shear strength, but this site was chosen for the ideal soil conditions. At typical construction sites, such as the HB&T Test Site, attainment of the soil properties becomes more difficult. Only through a vigorous research program, involving many test shafts, will procedures for design of drilled shafts evolve that may be used with full confidence.

Factors of Safety

Factors of safety must be applied to the design of drilled shafts to reflect uncertainties in the soil data, design procedures, construction procedure, and loading conditions. Based on the results of Test 2, a plot (Fig. 7.16) was constructed presenting the relationship between the factors of safety for the shaft, the side shear, and the base. Also from the plot for each factor of safety, the load taken out along the side and the base load may be determined. The example illustrated in the plot is for a shaft factor of safety of two. Using the plot as indicated, a factor of safety of 1.7 is obtained for the side friction with a load of 750 kips being taken out in side friction. The resulting base factor of safety is 6.4 with a base load of 70 kips.

The assignment of a factor of safety should be based on the amount of risk involved by the use of the particular foundation type. The use of drilling mud in the construction of a drilled shaft designed on the basic side friction would increase the risk of the shaft and, therefore, should be assigned a higher factor of safety. Likewise, the quality of the soil data available for the shaft design should also be a consideration in the determination of the factor of safety. For a location, such as the HB&T Test Site, a minimum factor of 2.5 or possibly as high as 3.0 should be used in the design. For instance, if a factor of safety of 2.5 is assigned to the Elysian Street Shaft; the factor of safety for the side friction would still be only 2.0. With only the limited amount of data available on shafts constructed in silts and sands, a conservative design must be employed. Even with the most conservative design, the benefits gained in the utilization of drilled shafts has been clearly demonstrated.

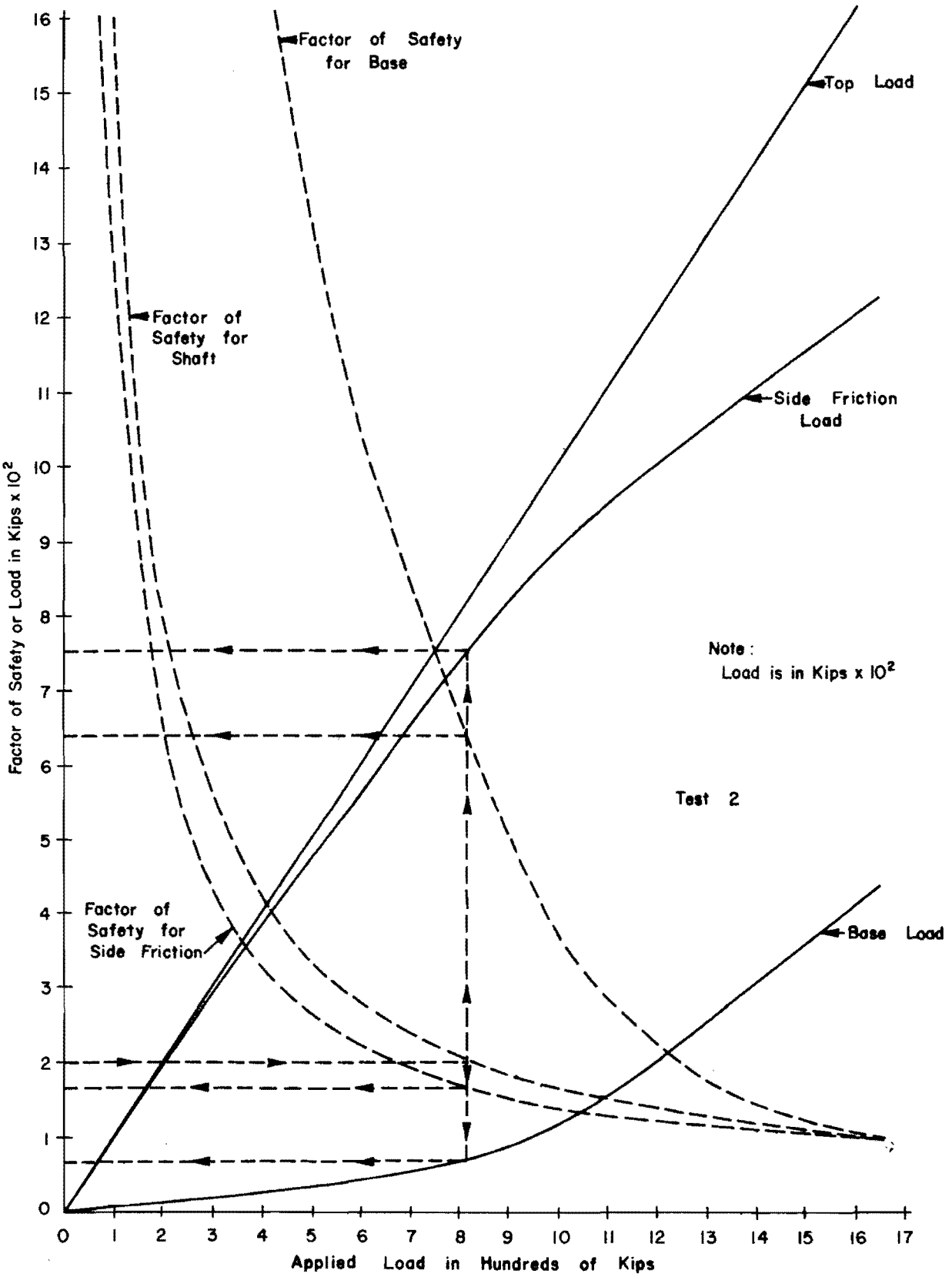

Fig. 7.16. Relationship between Total Factors of Safety and factors of Safety for Base and Side

CHAPTER VIII

CONCLUSIONS AND RECOMMENDATIONS

Although the use of drilled shafts is not new, the design of such shafts only for shear developed along the side of the shaft is still not a widely accepted practice. The economical advantages of the drilled shaft have been clearly described. With economy as a goal, there is a hazard in the use of drilled shafts before the pitfalls involved in their use are fully understood. Construction that employs drilling mud sharply increases the risk of a loss in the shearing resistance along the sides for the shaft.

In the research being conducted by The University of Texas at Austin, two straight drilled shafts, which had been constructed employing drilling fluid, were tested. The study of these two shafts represents a first step toward the understanding of the problems associated with the use of the drilling fluid and its effects on the performance of the shaft. The study also added to knowledge concerning the basic interaction between the soil and shaft.

Based on the inspection and testing of the HB&T Test Shaft plus the inspection of the SH 225 Test Shaft, the following conclusions and recommendations are presented.

Conclusions

1. Even for long-term tests, the Mustran instrumentation system provides an adequate method for the measurement of axial loads in a drilled shaft. The gages are easy to install, and they

are very stable, and highly reliable. The sensitivity is such that adequate readout is obtained. The major problem in the system is that the correlation between gage readings and load in the shaft is dependent on the concrete modulus of elasticity and the shaft area. The most probable source of error develops from differences in the shaft diameters at the gage levels. For this reason, gages should not be placed at locations where caving is likely.

2. Load-transfer curves can be developed from data giving basic soil properties. Such curves may be employed in existing analytical procedures to predict the settlement and load distribution of a drilled shaft. One of the major problems in the design of a drilled shaft for a typical construction site is the attainment of accurate measurements of the soil properties.
3. Near the surface and near the bottom of the shaft, the shear stresses developed along the sides of the shaft are greatly reduced.
4. The stress developed on the base of the shaft was found to be 10 times the shear strength of the soil under the base.
5. In a layered soil system the confining pressure in the cohesionless soil zones is increased by stresses imposed on the overlying soil. As a result, the shear stress developed in the cohesionless soils will continue to increase with increasing shaft settlement.
6. The shear strength reduction factor for clay was found to be approximately 0.6.

7. When proper construction techniques are employed, drilling mud has no detrimental effects on the load carrying characteristics of a drilled shaft. The concrete properties and concrete placement procedure are the two most critical factors involved in the construction process. The elimination of the effects of the drilling mud is accomplished when concrete, having the correct properties, is placed in the proper manner. The drilling mud will then be completely displaced and a vigorous scouring of the borehole wall by the rising concrete will ensue. Should drilling mud be trapped between the concrete and borehole wall, it would virtually eliminate the development of any shear load transfer in the vicinity of the trapped drilling mud.
8. The use of casing in placing the concrete involves a greater risk of trapping drilling mud than does the procedure of placing the concrete under the drilling mud by the use of a tremie or concrete pump. When casing is used in the construction process, the higher the head of concrete at the bottom of the casing the more positive will be the displacement of the drilling mud. Any method of increasing the pressure in the concrete at the bottom of the shaft would be beneficial.
9. The use of very fluid concrete will aid in obtaining good displacement of the drilling mud. A concrete slump of 6 inches should be considered an absolute minimum. Additives to retard concrete setting and to render the concrete more plastic are valuable aids.

10. Regardless of the procedures used, a competent, constant, and vigilant inspection of the complete construction process is an absolute necessity.

Recommendations

1. Mustran cells are recommended for the instrumentation of any future test shaft. Such instrumentation allows a complete evaluation of the test shaft and its load carrying characteristics. The results from such tests might lead to the future understanding of drilled shafts and to design procedures that can be used with confidence.
2. Better techniques are necessary for the determination of in situ soil properties, particularly for soil in which undisturbed sampling is impossible.
3. For the design of drilled shafts, shear strength reduction factors for side shear strength of 0.6 for clay and 0.8 for sand and silts should be employed. No reliance should be placed on load transfer developing within three shaft diameters of the surface or one diameter of the base. The base capacity may be estimated by using a stress on the base 10 times the shear strength of the soil beneath the base.
4. In troublesome soils, drilling mud may continue to be utilized in the construction of drilled shafts. For shafts designed on the basis of side friction, the procedure used in placing the concrete should be examined very critically. Competent inspection is necessary at all times during the construction process.

REFERENCES

Barker, W. R., and Reese, L. C. (1969), Instrumentation for Measurement of Axial Load in Drilled Shafts, Research Report 89-6, Center for Highway Research, The University of Texas at Austin, Austin, Texas, November, 1969.

Burland, J. B. (1963), Discussion in Grouts and Drilling Muds In Engineering Practice, Butterworths, London, 1963, pp. 223-225.

Campbell, D. B., and Hudson, W. R. (1969), The Determination of Soil Properties In Situ, Research Report 89-7, Center for Highway Research, The University of Texas at Austin, Austin, Texas, November, 1969.

Chuang, J. W., and Reese, L. C. (1969), Studies of Shearing Resistance Between Cement Mortar and Soil, Research Report 89-3, Center for Highway Research, The University of Texas at Austin, Austin, Texas, May, 1969.

Coyle, H. M., and Reese, L. C. (1966), "Load Transfer for Axially Loaded Piles in Clay," Journal of the Soil Mechanics and Foundations Division, A.S.C.E., Vol. 92, No. SM2, March, 1966.

Ehlers, C. J., Reese, L. C., and Anagnos, J. N. (1969), The Nuclear Method of Soil-Moisture Determination at Depth, Research Report 89-4, Center for Highway Research, The University of Texas at Austin, Austin, Texas June, 1969.

Fernandez-Renau, L. (1965), Discussion in Proceedings of the Sixth International Conference on Soil Mechanics and Foundation Engineering, Vol. III, 1965, pp. 495-496.

Gatlin, Carl (1960), Petroleum Engineering, Prentice-Hall, Inc., Englewood Cliffs, N. J., 1960.

Gibbs, H. J., and Holtz, W. G. (1957), "Research on Determining the Density on Sands by Spoon Penetration Testing," Proceedings of the Fourth International Conference of Soil Mechanics and Foundation Engineering, Vol. I, Butterworths, London, 1957.

Greer, D. M. (1969), "Drilled Piers State of the Art, 1969," W.C.A. Geotechnical Bulletin, Vol. III, No. 2, Woodward-Clyde and Associates, New York, September, 1969.

Hobbs, N. B. (1957), "Unusual Necking of Cast-in-situ Concrete Piles," Proceedings of the Fourth International Conference on Soil Mechanics and Foundation Engineering, Vol. II, Divisions 3b-6 and Reports, Butterworths, London, 1957, pp. 40-42.

The I.C.O.S. Company in the Underground Works (1969), Aldo Bellini and Carlo De Micheli, Milan, Italy, 1969.

Komornik, A., and Wiseman, G. (1967), "Experience with Large Diameter Cast-in-Situ Piling," Proceedings, Third Asian Regional Conference on Soil Mechanics and Foundation Engineering, Jerusalem Academic Press, Israel, 1967.

McKinney, J. R., and Gray, G. R. (1963), "The Use of Drilling Mud in Large Diameter Construction," Symposium by the British National Society of the International Society of Soil Mechanics and Foundation Engineering, Butterworths, London, 1963.

Neville, A. M. (1963), Properties of Concrete, Wiley, New York, 1963.

O'Neill, M. W., and Reese, L. C. (1970), Behavior of Axially Loaded Drilled Shafts in Beaumont Clay, Research Report 89-8, Center for Highway Research, The University of Texas at Austin, Austin, Texas, 1970.

Palmer, D. J., and Holland, G. R. (1966), "The Construction of Large Diameter Bored Piles with Particular Reference to London Clay," Proceedings of the Symposium on Large Bored Piles, Institution of Civil Engineers, London, February, 1966.

Pandey, V. J. (1967), "Some Experiences with Bored Piling," Journal of the Soil Mechanics and Foundations Division, A.S.C.E., Vol. 93, No. SM5, September, 1967, Part 1.

Peck, R. B., Hanson, W. E., and Thornburn, T. H. (1953), Foundation Engineering, Wiley, New York, 1953.

Reese, L. C., Brown, J. C., and Dalrymple, H. H. (1968), Instrumentation for Measurements of Lateral Earth Pressure in Drilled Shafts, Research Report 89-2, Center for Highway Research, The University of Texas at Austin, Austin, Texas, September, 1968.

Reese, L. C., and Hudson, W. R. (1968), Field Testing of Drilled Shafts to Develop Design Methods, Research Report 89-1, Center for Highway Research, The University of Texas at Austin, Austin, Texas, April, 1968.

Rogers, Walter F., (1963), Composition and Properties of Oil Well Drilling Fluids, Third Edition, Gulf Publishing Company, Houston, Texas, 1963.

Seed, H. B., and Reese, L. C. (1957), "The Action of Soft Clay Along Friction Piles," Transactions, A.S.C.E., Vol. 122, 1957.

Skempton, A.W. (1951), "The Bearing Capacity of Clays," Proceedings of the Building Research Congress, 1951, Division I, Building Research Congress, London, 1951.

Skempton, A. W. (1959), "Cast-in-Situ Bored Piles in London Clay," Geotechnique, Vol. IX, No. 4, London, December, 1959.

Texas Highway Department, (1970), Personal communication with Mr. Horace Hoy of the Texas Highway Department, 1970.

Texas Highway Department (1964), Foundation Exploration and Design Manual, State Highway Department of Texas, Bridge Division, January, 1964.

Tomlinson, M. J. (1969), Foundation Design and Construction, Second Edition, Wiley-Interscience, New York, 1969.

Vijayvergiya, V. N., Hudson, W. R., and Reese, L. C. (1969), Load Distribution for a Drilled Shaft in Clay Shale, Center for Highway Research, The University of Texas at Austin, Austin, Texas, March, 1969.

Whitaker, T., and Cooke, R. W. (1966), "An Investigation of the Shaft and Base Resistance of Large Bored Piles in London Clay," Proceedings of the Symposium on Large Bored Piles, Institution of Civil Engineers, London, February, 1966.

APPENDIX A

SOIL DATA

1. Boring Logs

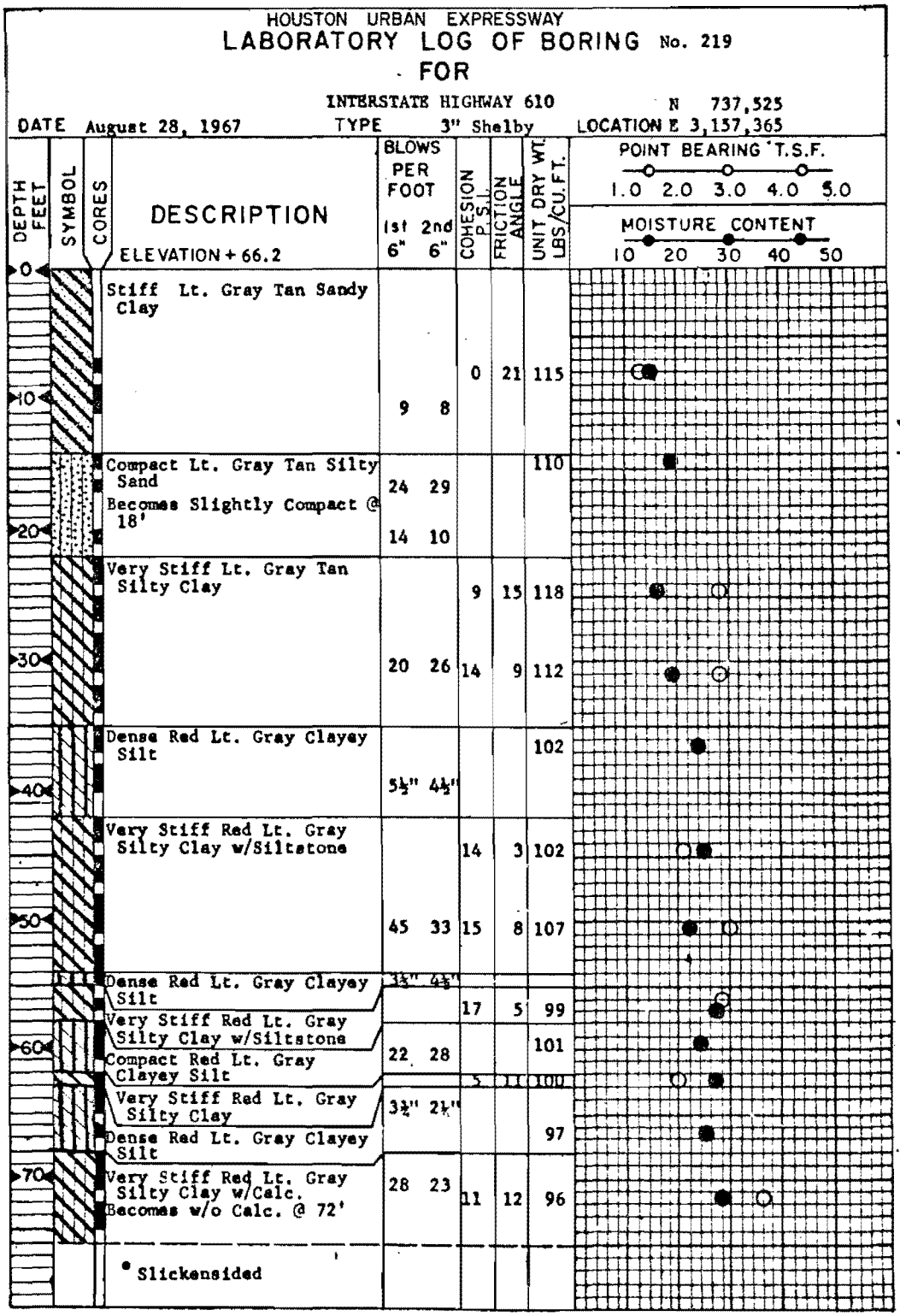

Fig. A.1. Boring Log for Hole THD 219

Texas Highway Department
Form 554

DRILLING REPORT

(For use with Undisturbed Sampling & Testing)

Sheet 1 of 3

County Harris | Structure Overpass for HB & T Railroad | District No. 12
Highway No. IH 610 (North Loop) | Hole No. HBT - 1 | Date May 22, 1969
Control 271-14 | Station 303 + 95 | Grd. Elev. + 66.2
Project No. 3-5-65-89 | Loc. from Centerline Rt. 37' Lt. | Grd. Water Elev. +54

Elev. (Ft.)	Depth (Ft.)	Samples†	Log	THD PEN. TEST No. of Blows 1st 6"	2nd 6"	Sample Number	Lat. Pressure & Ult. Stress (psi)	Wet Density (pcf)	Moisture Content (%)	Liquid Limit (%)	Plasticity Index (%)	DESCRIPTION OF MATERIAL AND REMARKS	
												8" Concrete Slab	
												Compacted Shale	
	5												
						HBT-1-1						Lt. gray & tan sandy clay	
						2			16	37	19	" " " " "	SC
				5	5								
						3			17	30	8	" " " " "	SC
	10								--	24	Nil	Lt. gray & tan clayey sand	
						4						" " " " "	SM
		0		16	19							Silty Sand	
												" "	
				20	22							" "	
	15											" "	
		0		20	25							" "	
												" "	
		0		35	26							" "	
												" "	
	20					5			16	38	26	Lt. gray & tan silty clay	CL
						6			15	32	21	" " " " "	CL
		0		11	14							" " " " "	
						7			15	40	27	" " " " "	CL
	25					8			16	42	24	" " " " "	CL
						9			-	-	-	" " " " "	
		0		12	13							" " " " "	
						10			17	48	29	Lt. gray & tan clay	CL
						11			-	-	-	Red & Gray Clay with Calcareous deposits	
	30					12			16	42	30	" " " " " "	CL

Driller _____ Logger _____ Title _____

†Indicate each foot by shading for core recovery, leaving blank for no core recovery, and crossing (X) for undisturbed laboratory samples taken.

28-850 F3*

Fig. A.2. Boring Log for Hole HBT 1

Texas Highway Department
[illegible] 554

DRILLING REPORT

(For use with Undisturbed Sampling & Testing)

Sheet 2 of 3

County _____ Structure _____ District No. _____

Highway No. _____ Hole No. HBT-1 Date _____

Control _____ Station _____ Grd. Elev. _____

Project No. _____ Loc. from Centerline _____ Rt. _____ Lt. _____ Grd. Water Elev. _____

Elev. (Ft.)	Depth (Ft.)	Samples†	Log	THD PEN. TEST No. of Blows 1st 6"	THD PEN. TEST No. of Blows 2nd 6"	Sample Number	Lat. Pressure & Ult. Stress (psi)	Wet Density (pcf)	Moisture Content (%)	Liquid Limit (%)	Plasticity Index (%)	DESCRIPTION OF MATERIAL AND REMARKS	
	30	0		22	27								
						HBT-1-13			19	34	17	Red & gray very silty clay	CL
						14			-	-	-	Red & gray clayey silt	
						15			-	-	-	" " " "	
	35					16			-	-	-	" " " "	
						17			17	27	Nil	" " " "	
		0		3 3/4	5 3/4							Very stiff red & gray silty clay	ML
												" " " " " "	
												" " " " " "	
	40	0		34	31							" " " " " "	
												" " " " " "	
						18			-	-	-	Very stiff red & gray clay	
						19			29	-	-	" " " " "	
						20			-	-	-	" " " " "	
	45	0		16	18							" " " " "	
												" " " " "	
						21			22	71	51	" " " " "	CH
						22			-	-	-	" " " " "	
						23			-	-	-	" " " " "	
				50	40							Red silty clay	
	50					24			-	61	41		CH
						25			26	36	17	Red clayey silt with calcareous deposits	CL
						26			-	58	42	Red silty clay with calcareous deposits	CH
		0		31	27							" " "	
						27			25	46	31	" " "	CL
	55											" " "	
						28			32	77	55	" " "	CH
				40	60/41/2							" " "	
						29			22	35	17	Red clayey silt	CL
						30			-	78	55	Red silty clay with slickensides	CH
	60												

Driller _____ Logger _____ Title _____

†Indicate each foot by shading for core recovery, leaving blank for no core recovery, and crossing (X) for undisturbed laboratory samples taken.

SS-550 F 291 2-68 1000

Fig. A.2. (Continued)

Texas Highway Department
Form 554

DRILLING REPORT

(For use with Undisturbed Sampling & Testing)

Sheet 3 of 3

County _____ Structure _____ District No. _____
Highway No. _____ Hole No. HBT-1 Date _____
Control _____ Station _____ Grd. Elev. _____
Project No. _____ Loc. from Centerline _____ Rt. _____ Lt. _____ Grd. Water Elev. _____

Elev. (Ft.)	Depth (Ft.)	†Samples	Log	THD PEN. TEST No. of Blows 1st 6"	THD PEN. TEST No. of Blows 2nd 6"	Sample Number	Lat. Pressure & Ult. Stress (psi)	Wet Density (pcf)	Moisture Content (%)	Liquid Limit (%)	Plasticity Index (%)	DESCRIPTION OF MATERIAL AND REMARKS	
	60					HBT-1-31			23	83	60	Stiff Red Clay with Calcareous deposits	CH
						32			31	32	14	Red clayey silt with calcareous deposits	CL
		0		5 1/4	6 1/4							" " " " " "	
						33			22	26	Nil	" " " " " "	ML
	65	0		26	42							Red clayey silt	
												" " "	
		0		21	22							" " "	
						34			24	80	58	Red silty clay	CH
		0		21	23							" " "	
						35			30	85	68	" " "	CH
	70					36			30	90	68	" " "	CH
						37							

Driller _____ Logger _____ Title _____

†Indicate each foot by shading for core recovery, leaving blank for no core recovery, and crossing (X) for undisturbed laboratory samples taken.

28-850 F291

Fig. A.2. (Continued)

Texas Highway Department
Form 554

DRILLING REPORT

(For use with Undisturbed Sampling & Testing)

Sheet 1 of 3

County Harris — Structure Overpass for HB & T Railroad — District No.
Highway No. IH 610 (North Loop) — Hole No. HBT - 2 — Date November 3, 1969
Control 271 - 14 — Station 303 + 95 — Grd. Elev. 66.0'
Project No. 3-5-65-89 — Loc. from Centerline — Rt. 5' — Lt. — Grd. Water Elev. +54

Elev. (Ft.)	Depth (Ft.)	Samples	Log	THD PEN. TEST No. of Blows 1st 6"	THD PEN. TEST No. of Blows 2nd 6"	Sample Number	Lat. Pressure & Ult. Stress (psi)	Wet Density (pcf)	Moisture Content (%)	Liquid Limit (%)	Plasticity Index (%)	DESCRIPTION OF MATERIAL AND REMARKS	
	0											9" Concrete slab with 15" shale	
												fill material	
						HBT-2-1			-	-	-	Red silty clay	
	5												
						2			20	35	18	Silty Clay	SC
						3			19	30	12	" "	SC
						4			-	29	9	Clayey Silt	SC
						5			-	-	-	" "	
	10					6			18	21	3	Sandy silt	SM
						7			-	-	-	" "	
						8			-	-	-	" "	
						9			-	-	-	Silty Sand	SM
	0			20	19							" "	
	15											" "	
												" "	
												" "	
	0			21	22							" "	
												" "	
	20											" "	
												" "	
						10			-	-	-	Gray-red silty clay	
						11			14	30	18	Mottled gray-red silty clay	CL
						12			15	36	25	" " " " "	CL
	25					13			20	44	27	Silty clay becoming less silty	CL
						14			-	-	-	Mottled gray-red clay w slickensides	
						15			24	57	33	" " " " "	
						16			22	58	38	Same with calcareous deposits	
	30					17			21	49	34	" " " "	CL

Driller _____ Logger _____ Title _____

†Indicate each foot by shading for core recovery, leaving blank for no core recovery, and crossing (X) for undisturbed laboratory samples taken.

Fig. A.3. Boring Log for Hole HBT 2

Texas Highway Department
Form 554

DRILLING REPORT
(For use with Undisturbed Sampling & Testing)

Sheet 2 of 3

County _____ Structure _____ District No. _____
Highway No. _____ Hole No. HBT - 2 Date _____
Control _____ Station 303 + 95 Grd. Elev. _____
Project No. _____ Loc. from Centerline Rt. 5' Lt. _____ Grd. Water Elev. _____

Elev. (Ft.)	Depth (Ft.)	† Samples	Log	THD PEN. TEST No. of Blows 1st 6"	THD PEN. TEST No. of Blows 2nd 6"	Sample Number	Lat. Pressure & Ult. Stress (psi)	Wet Density (pcf)	Moisture Content (%)	Liquid Limit (%)	Plasticity Index (%)	DESCRIPTION OF MATERIAL AND REMARKS	
	30					HBT-2-18			-	-	-	Gray & red clay with silt seam at top	
						19			19	35	16	Silty clay becoming more silty	CL
						20			20	30	12		CL
						21			20	26	6	Red & gray mattled clayey silt	CL
												Clayey silt very little cla,	
	35												
												" " " " "	
						22			23	33	13	" " " " "	CL
						23			20	27	9	Clayey silt with many calcareous deposits	CL
												Clayey silt with silt stone lens	
	40											" " " " " "	
												Out of silt at 41'	
						24			26	-	-	Clay slickensided with calcareous deposits	
						25			23	69	39	" " " " "	CH
						26			28	-	-	Red clay very slickensided	
	45					27			-	-	-	" " " "	
						28			-	-	-	with calcareous deposits	
						29			25	-	-	" " "	
						30			22	63	33	" " "	CH
						31			20	-	-	" " "	
						32			-	-	-	" " "	
	50					33			24	25	4	6" layer of silt at 50' & 52'	CL
						34			22	-	-	Silty-clay with silt lens	
						35			-	-	-	" " " "	
						36			-	-	-	Silt layer 53' & 54'	
						37			-	-	-	Clay with slickensides at 55'	
	55					38			23	-	-	6" layer sandy-clayey silt	
						39			17	24	5	Clayey silt	CL
						40			-	-	-	" "	
												silt	
	60					41			19	69	32	"	CH

Driller _____ Logger _____ Title _____

†Indicate each foot by shading for core recovery, leaving blank for no core recovery, and crossing (X) for undisturbed laboratory samples taken.

29-850 F291 2-69 10M

Fig. A.3. (Continued)

Texas Highway Department
Form 554

DRILLING REPORT
(For use with Undisturbed Sampling & Testing)

Sheet 3 of 3

County _____ Structure _____ District No. _____
Highway No. _____ Hole No. HBT-2 Date _____
Control _____ Station 303 + 95 Grd. Elev. _____
Project No. _____ Loc. from Centerline Rt. 5' Lt. _____ Grd. Water Elev. _____

Elev. (Ft.)	Depth (Ft.)	Samples†	Log	THD PEN. TEST No. of Blows 1st 6"	THD PEN. TEST No. of Blows 2nd 6"	Sample Number	Lat. Pressure & Ult. Stress (psi)	Wet Density (pcf)	Moisture Content (%)	Liquid Limit (%)	Plasticity Index (%)	DESCRIPTION OF MATERIAL AND REMARKS	
	60					HBT-2-42			21	63	36	Silty clay	CH
						43			29	40	21	Stiff red clay with calcareous deposits	CL
						44			18	64	33	" " " " " "	CH
												Clayey-silt	
						45			26	36	17	Clayey-silt	CH
	65					46			-	25	3	" "	CL
												Silt	
						47			-	-	-	Stiff red clay with slickensides	
						48			30	67	44	" " " " "	CH
						49			30	-	-	" " " " "	
	70												

Driller _____ Logger _____ Title _____

†Indicate each foot by shading for core recovery, leaving blank for no core recovery, and crossing (X) for undisturbed laboratory samples taken.

29-850 1'2M1 2-69 10M

Fig. A.3. (Continued)

2. Stress-Strain Curves

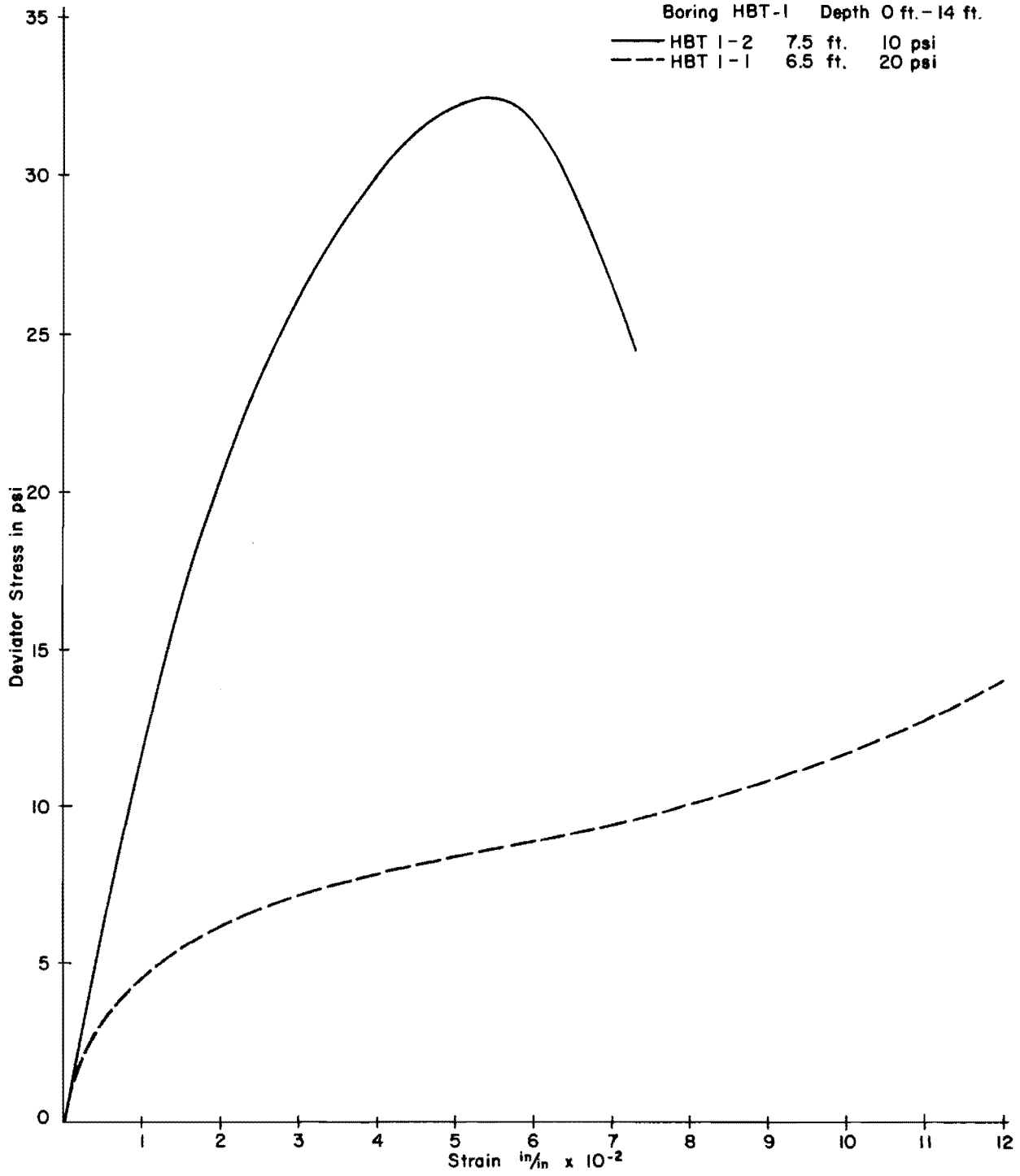

Fig. A.4. Stress-Strain Curves

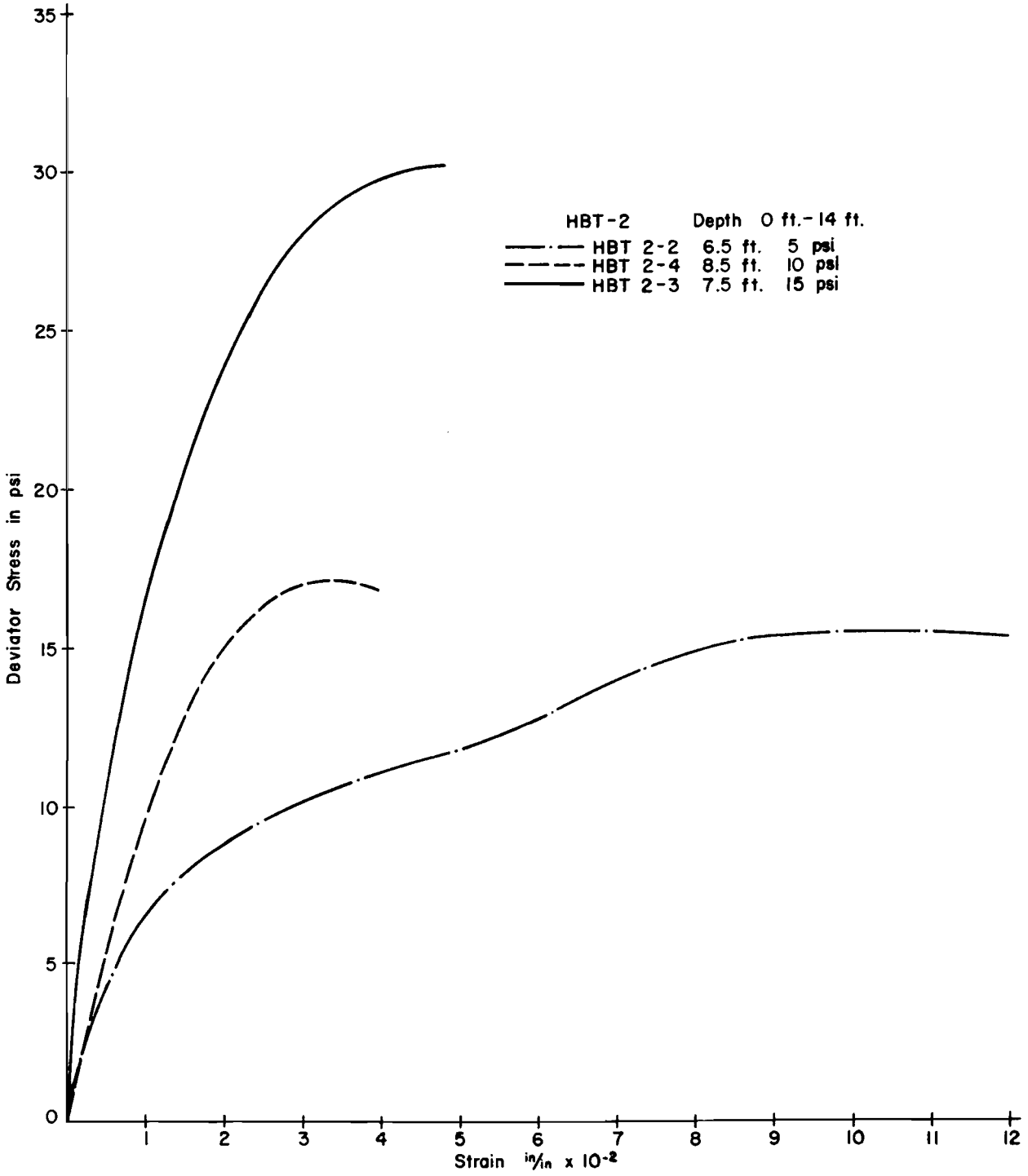

Fig. A.5. Stress-Strain Curves

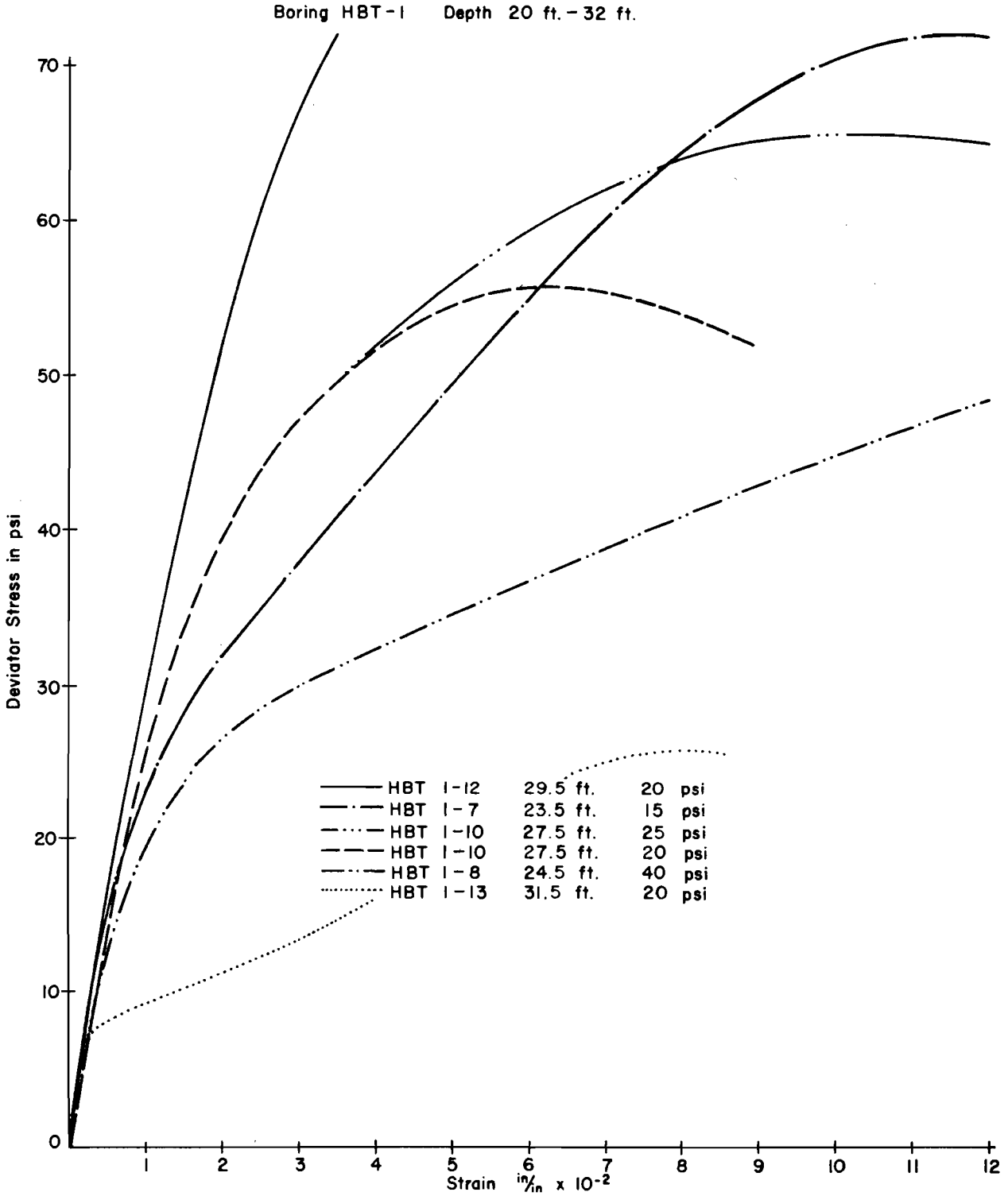

Fig. A.6. Stress-Strain Curves

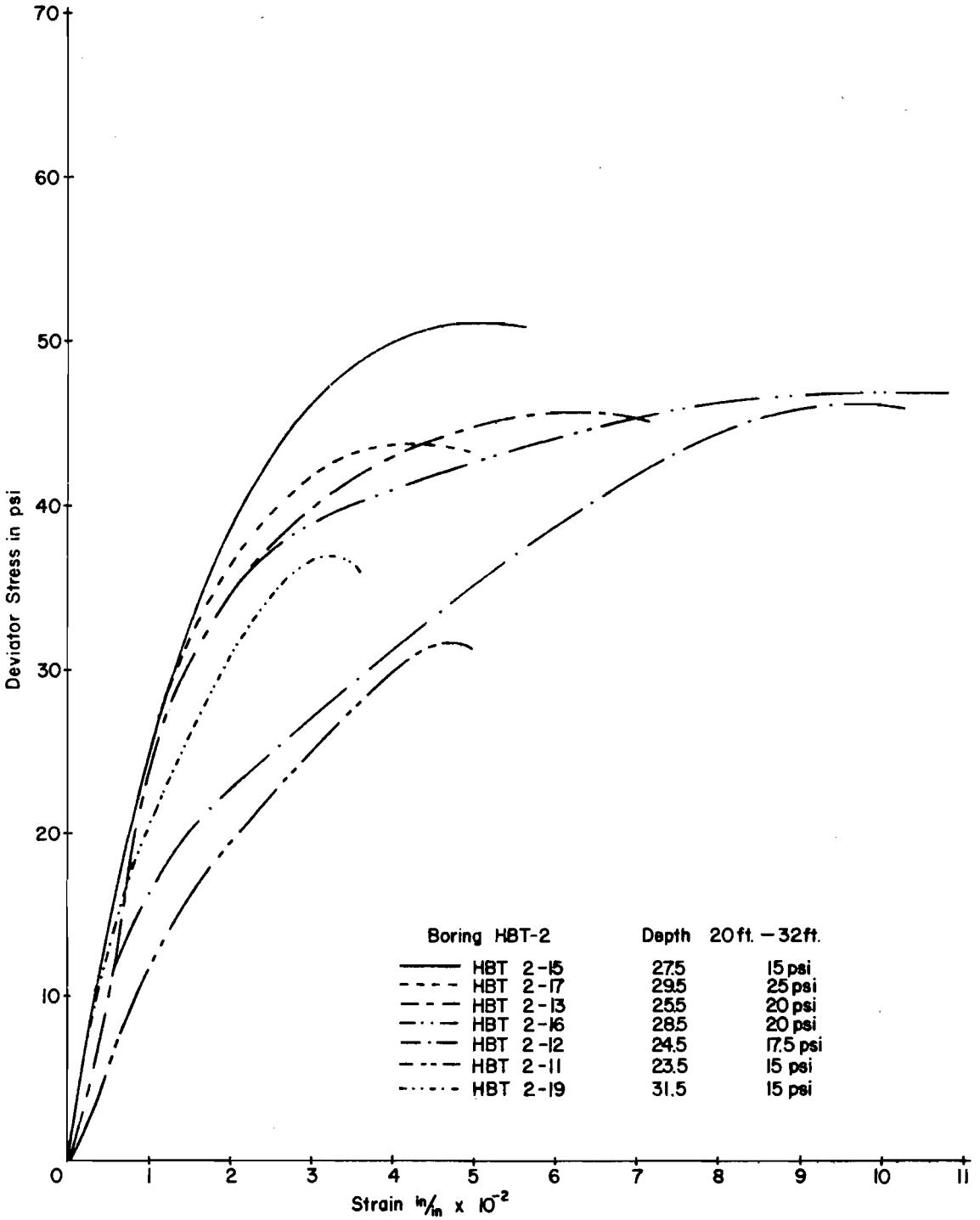

Fig. A.7. Stress-Strain Curves

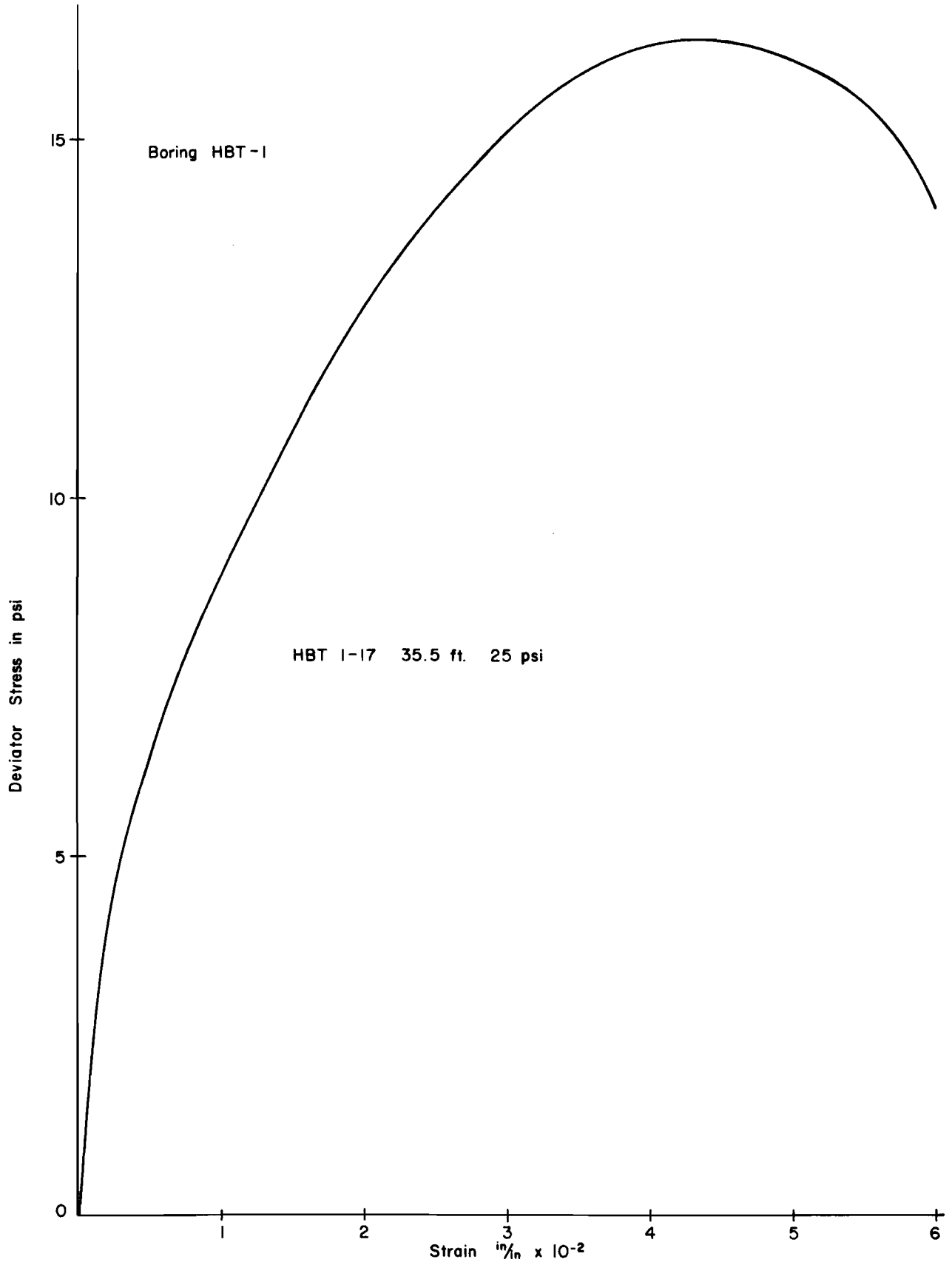

Fig. A.8. Stress-Strain Curves

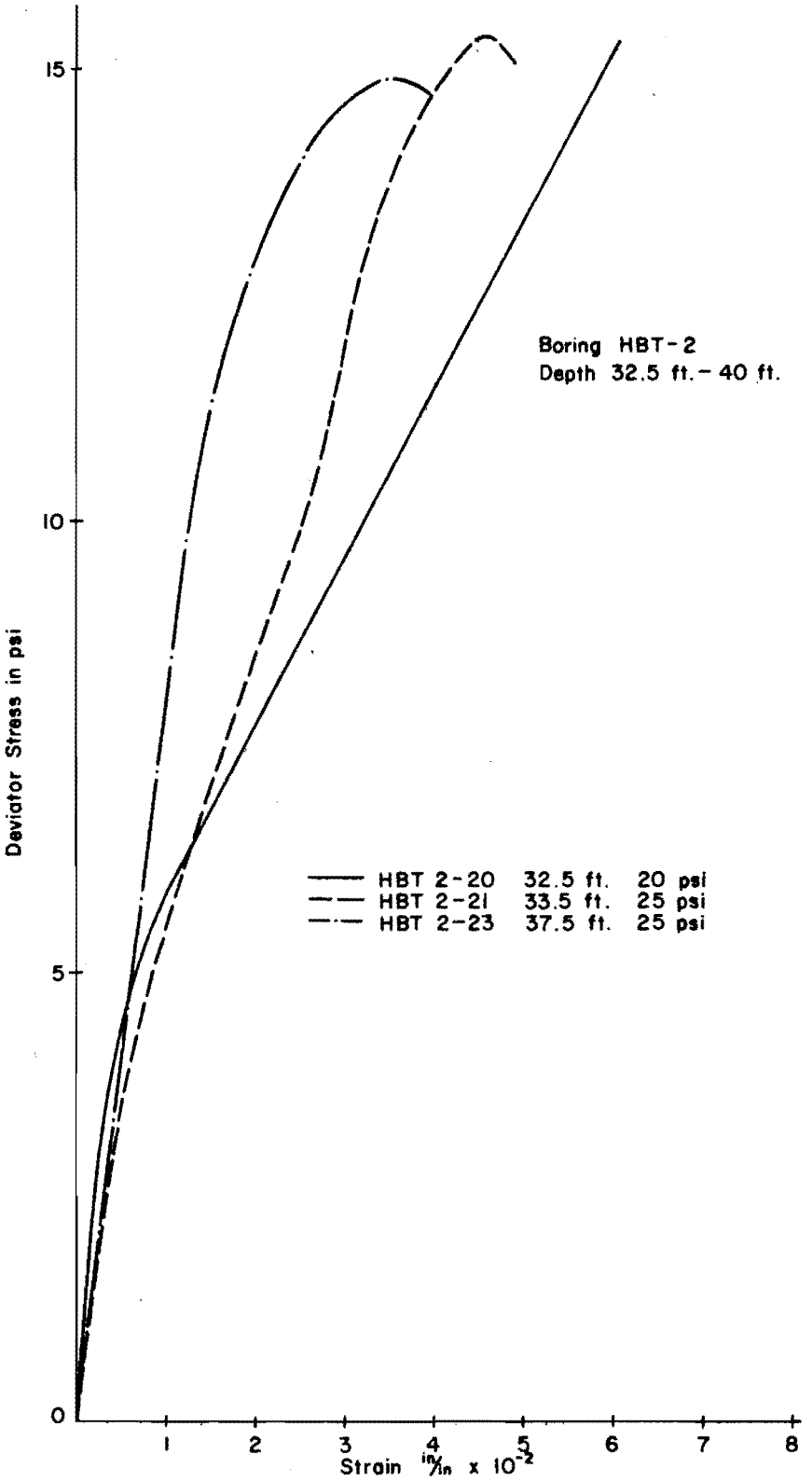

Fig. A.9. Stress-Strain Curves

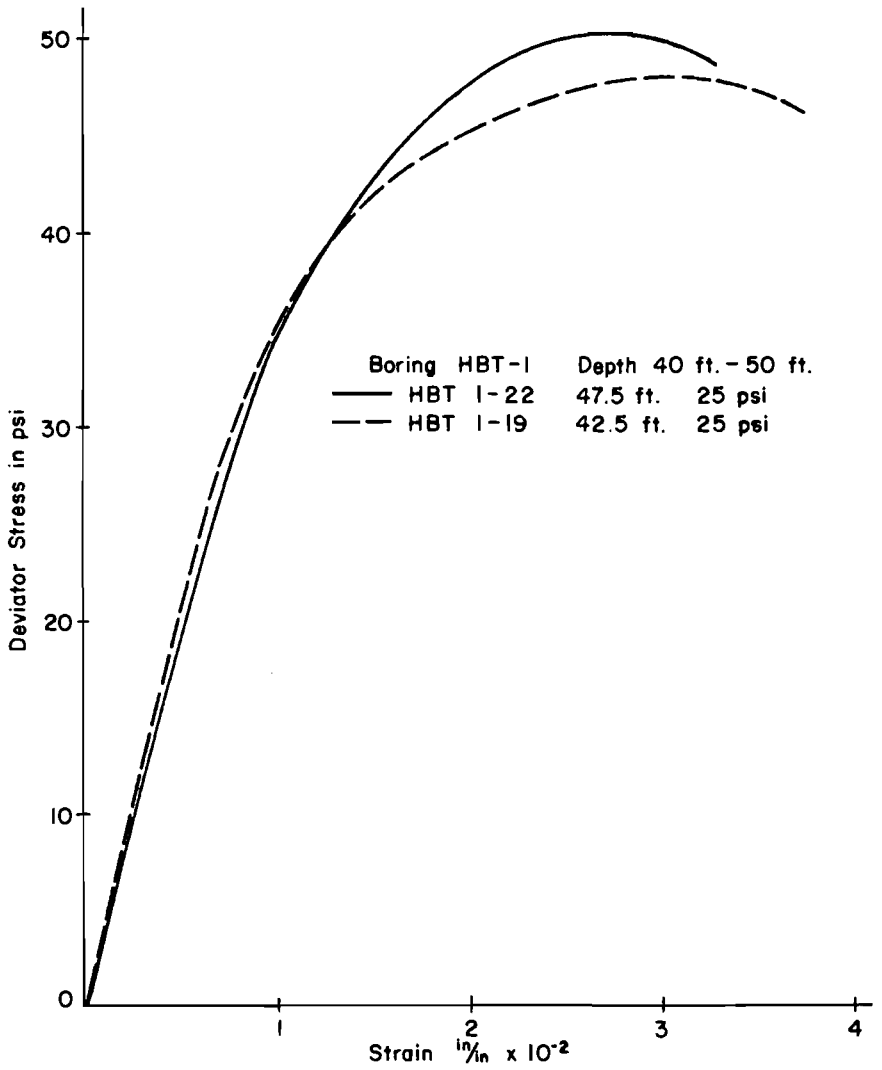

Fig. A.10. Stress-Strain Curves

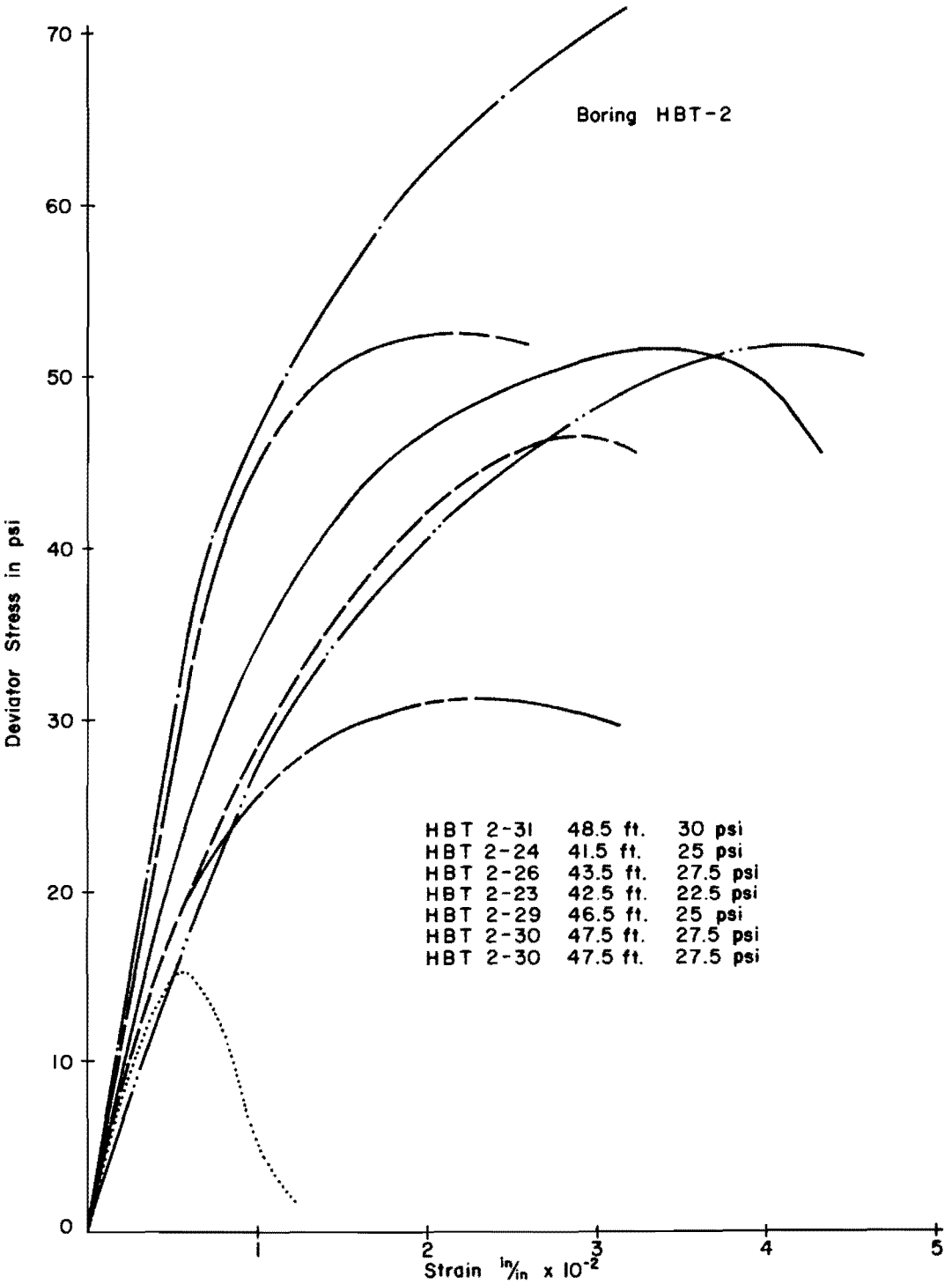

Fig. A.11. Stress-Strain Curves

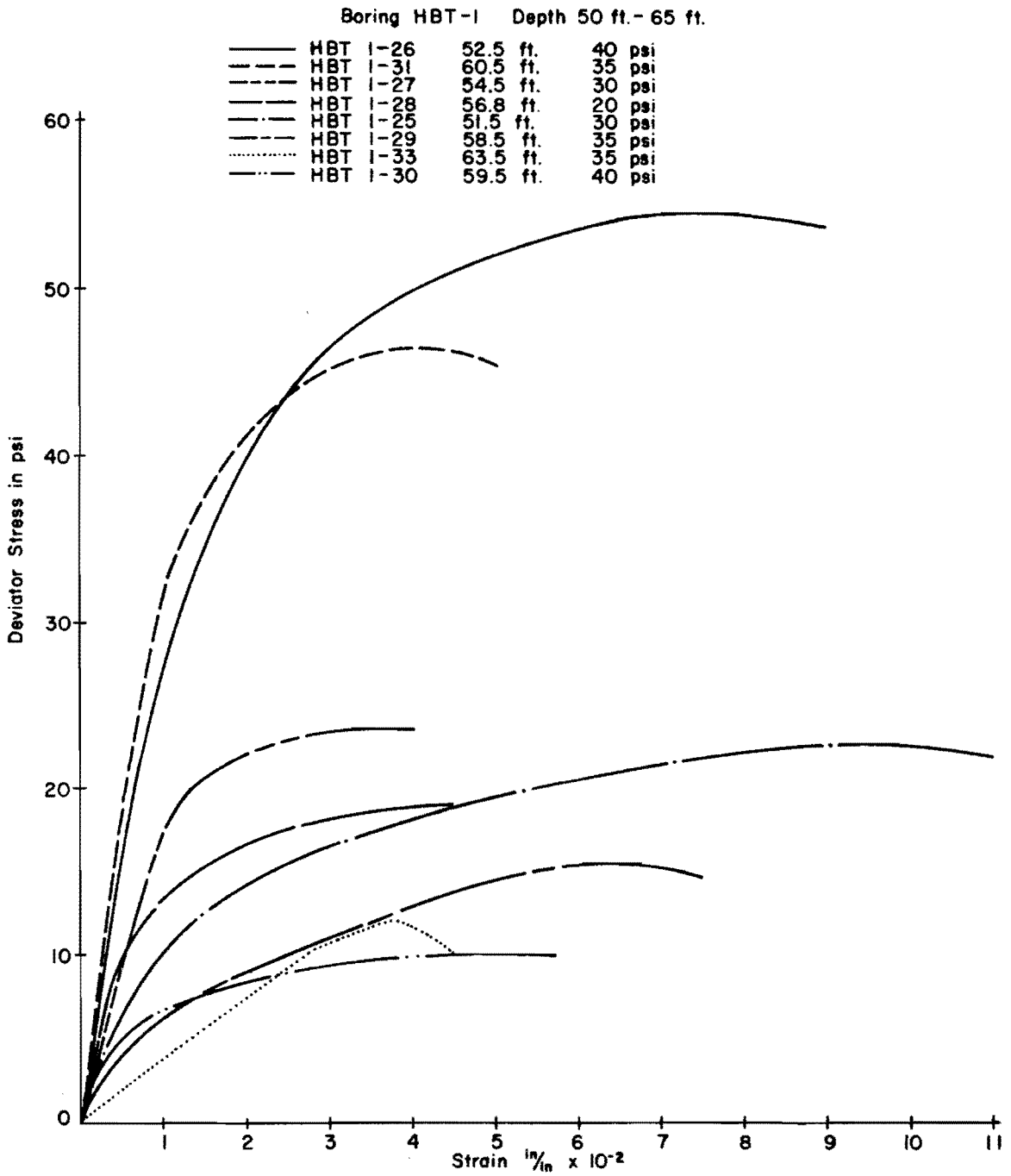

Fig. A.12. Stress-Strain Curves

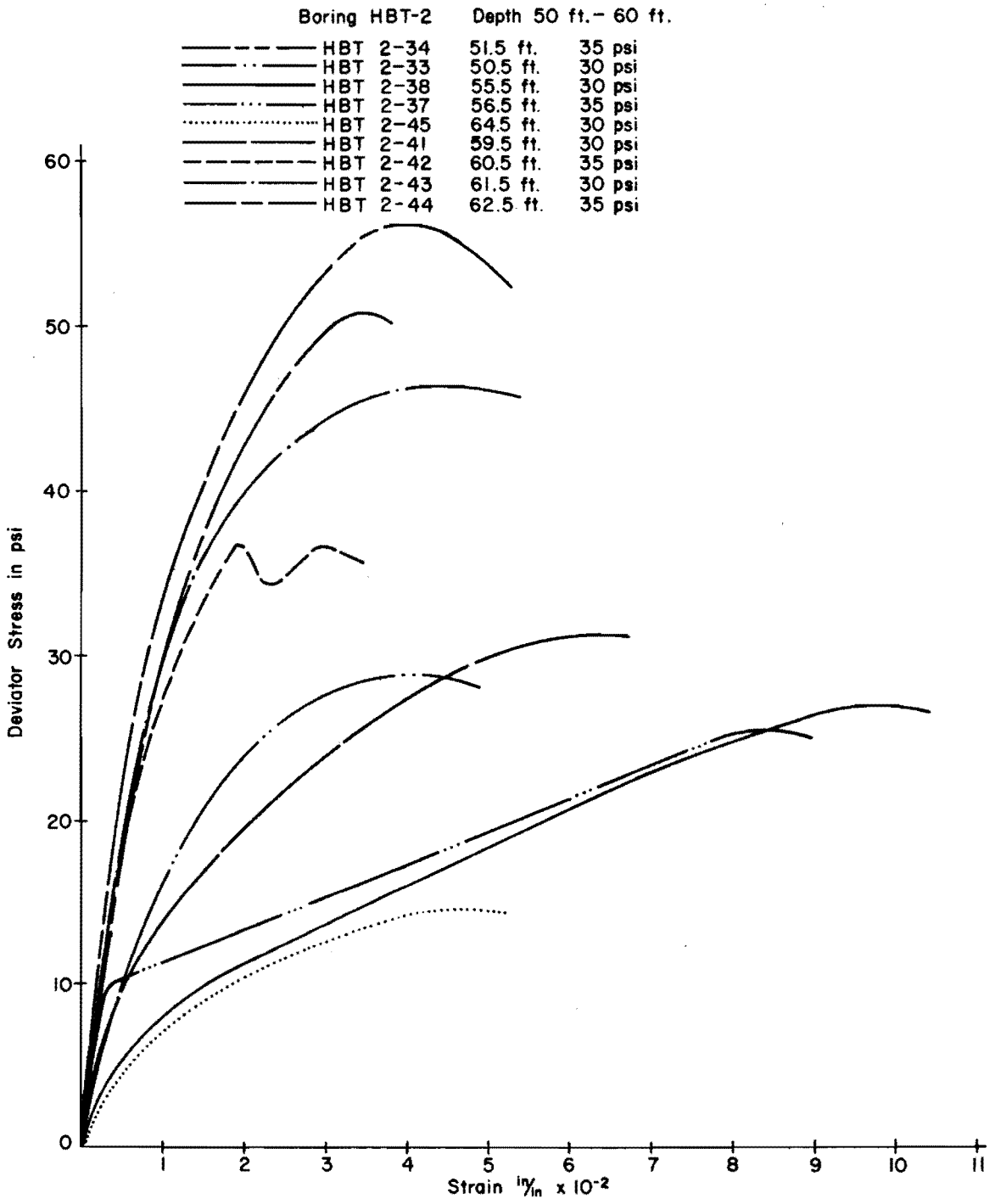

Fig. A.13. Stress-Strain Curves

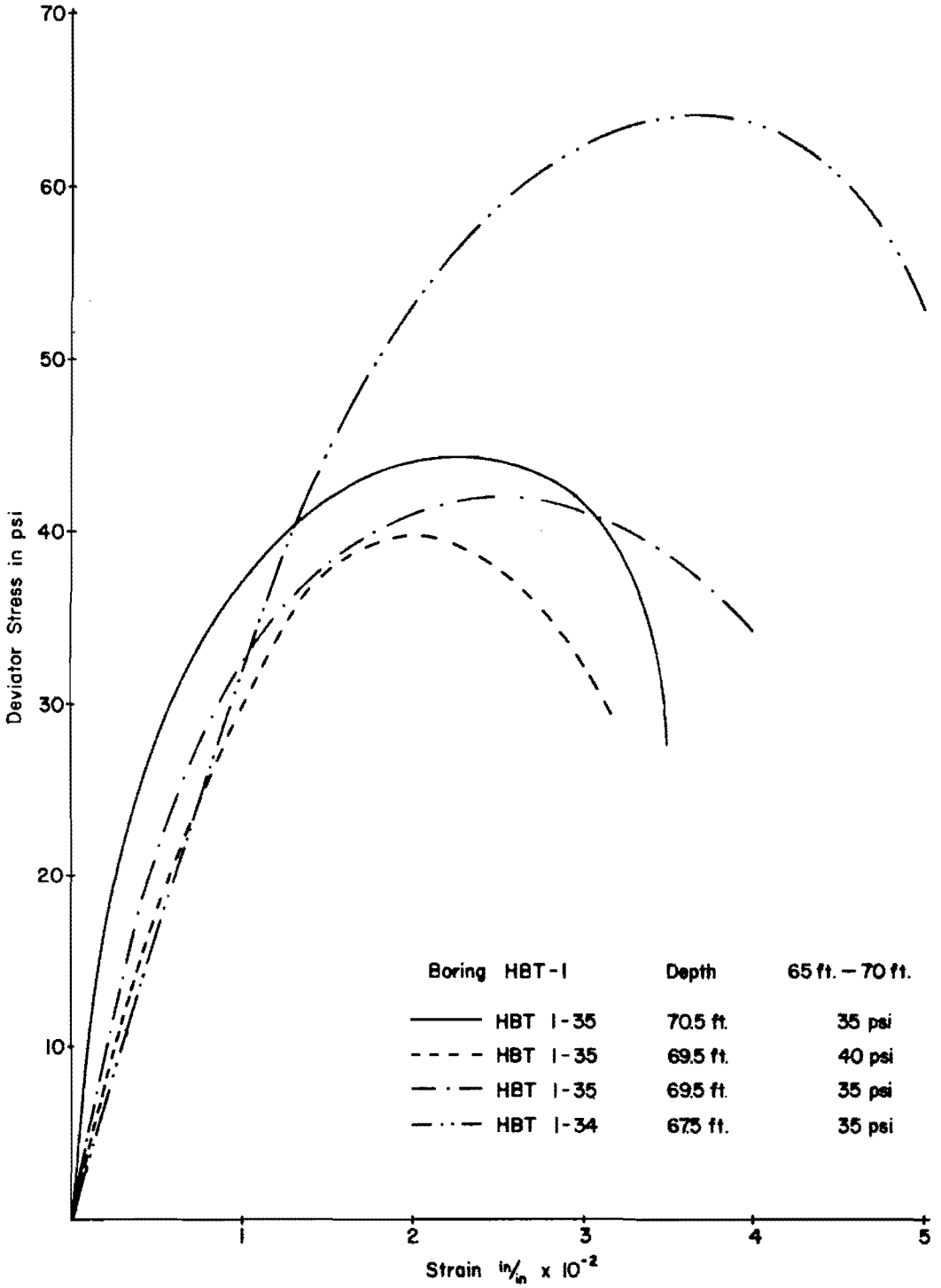

Fig. A.14. Stress-Strain Curves

APPENDIX B

GAGE MONITORING DATA

1. Gage Response to Concrete Curing

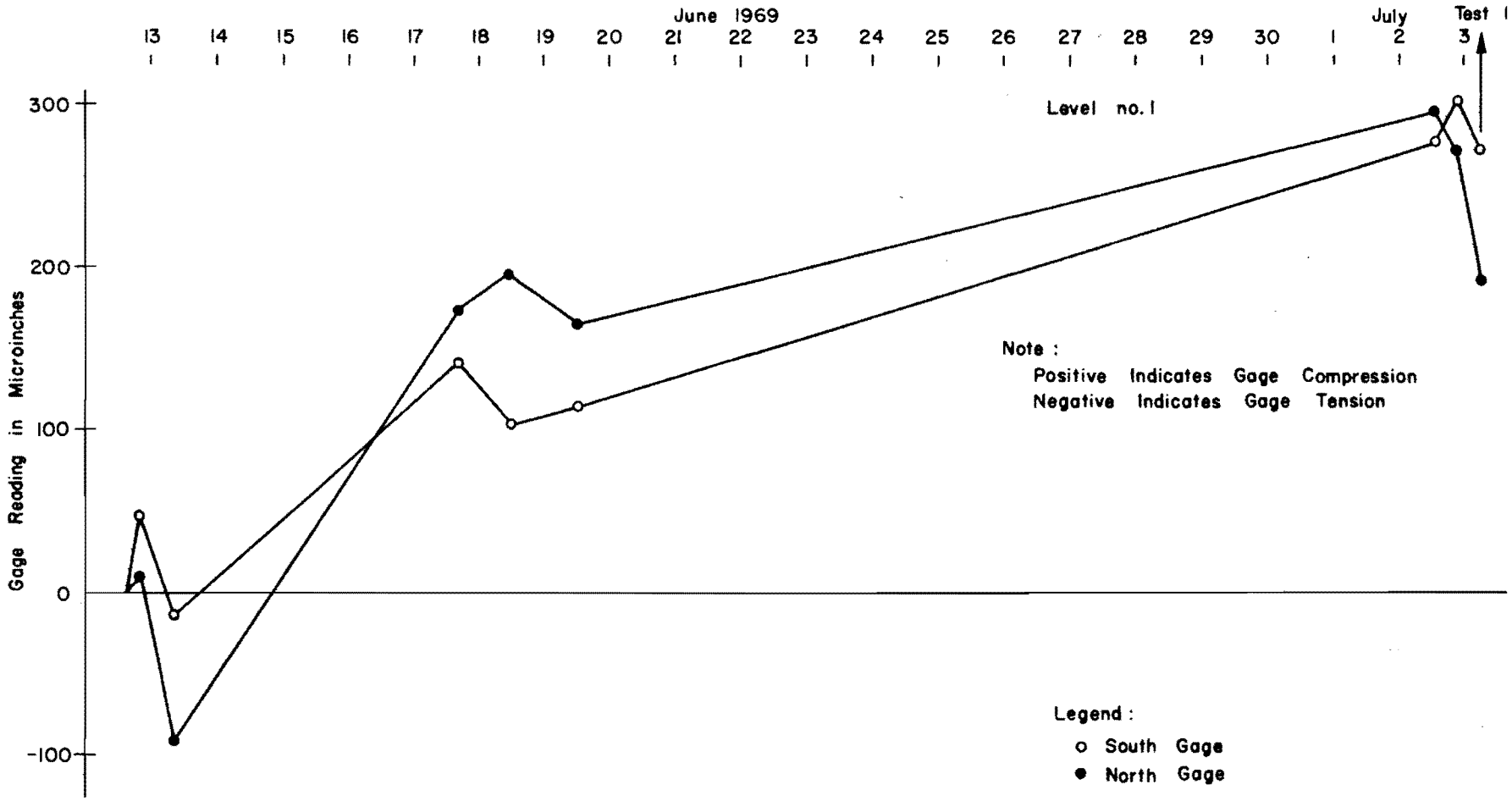

Fig. B.1. Mustran Gage Response to Concrete Curing

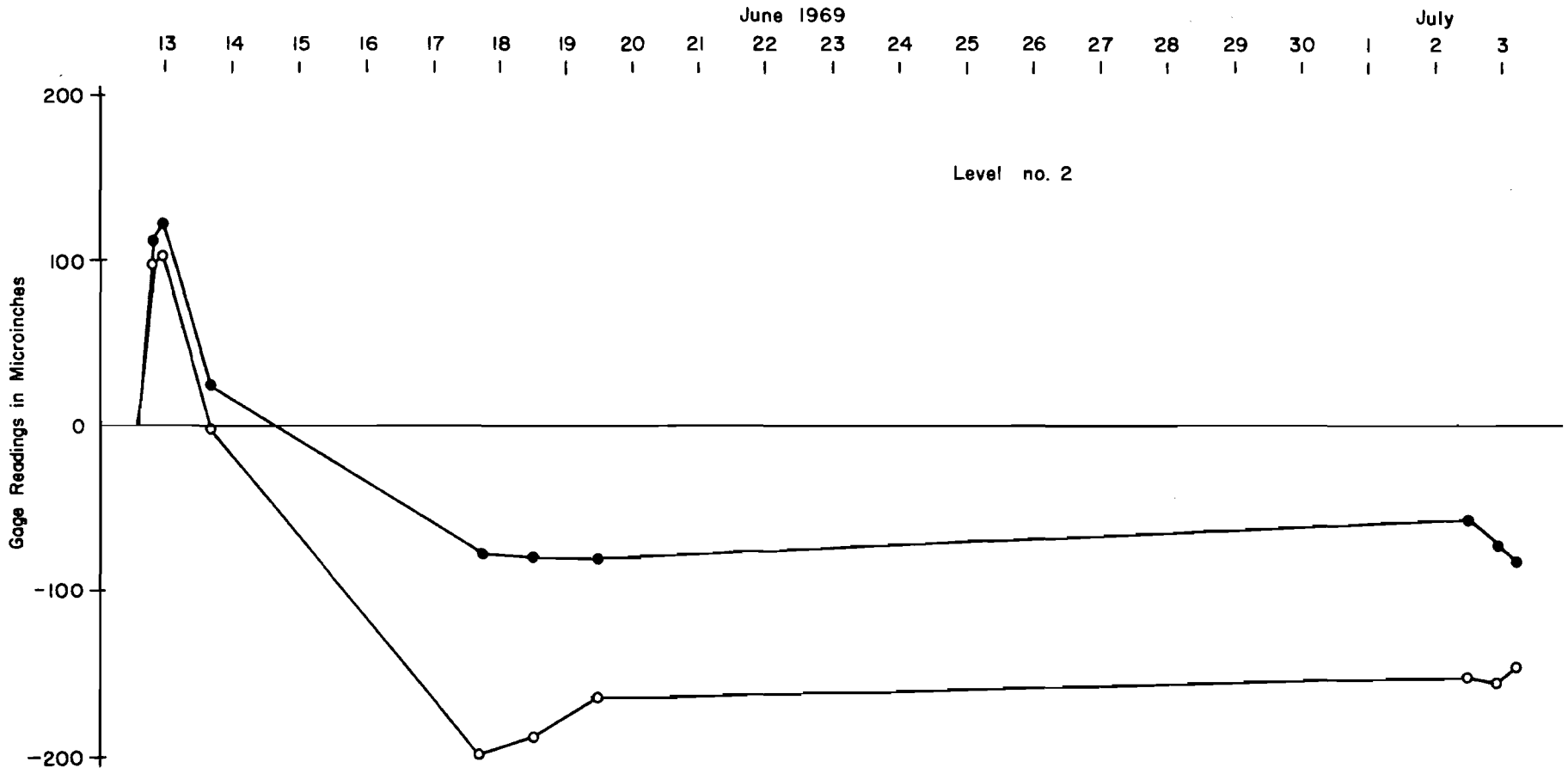

Fig. B.2. Mustran Gage Response to Concrete Curing

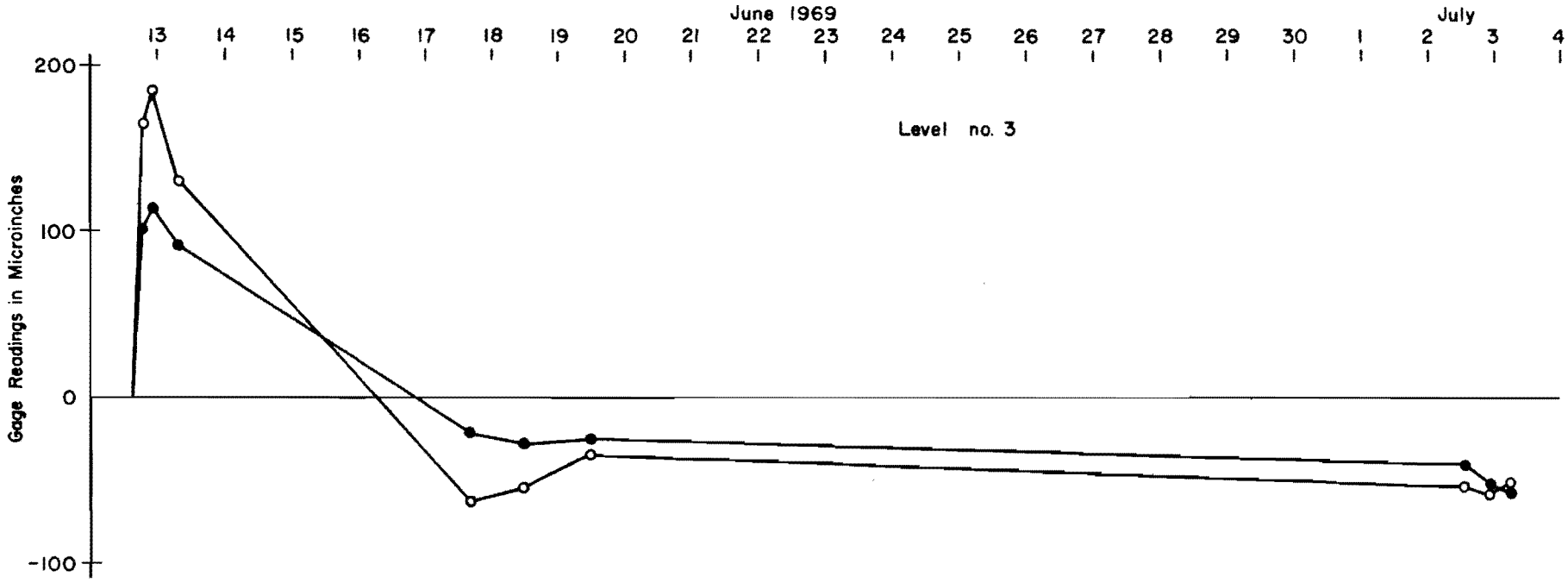

Fig. B.3. Mustran Gage Response to Concrete Curing

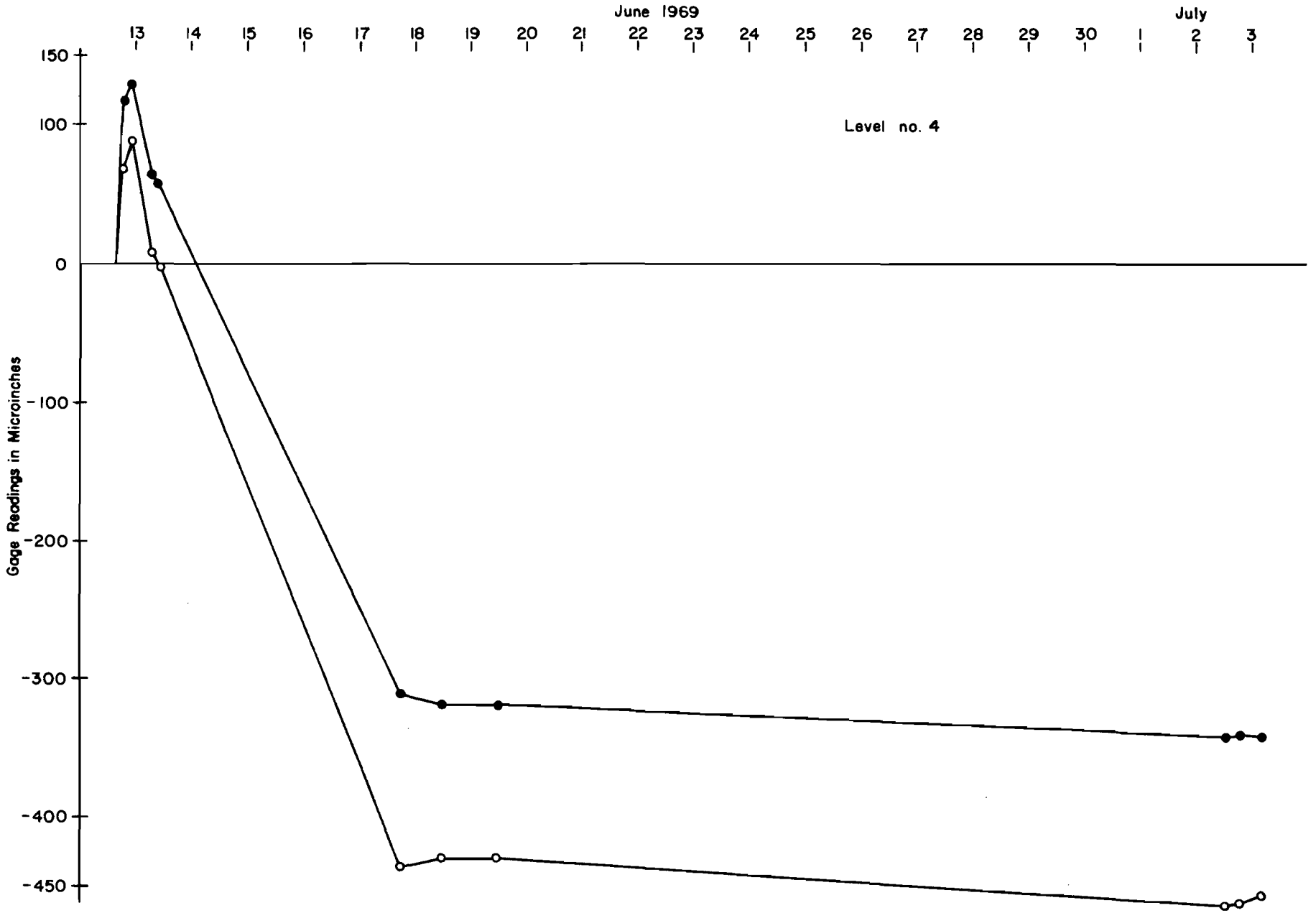

Fig. B.4. Mustran Gage Response to Concrete Curing

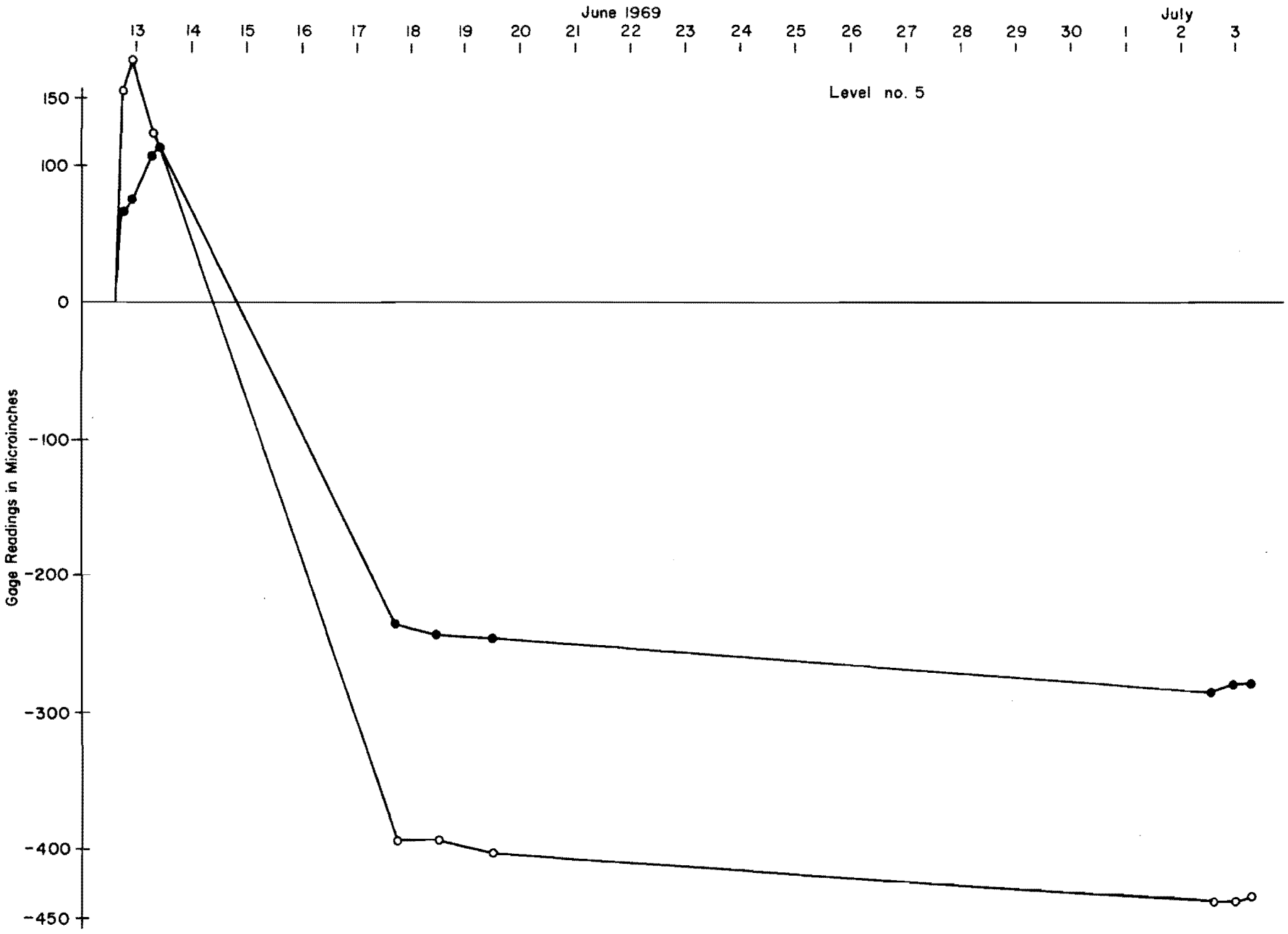

Fig. B.5. Mustran Gage Response to Concrete Curing

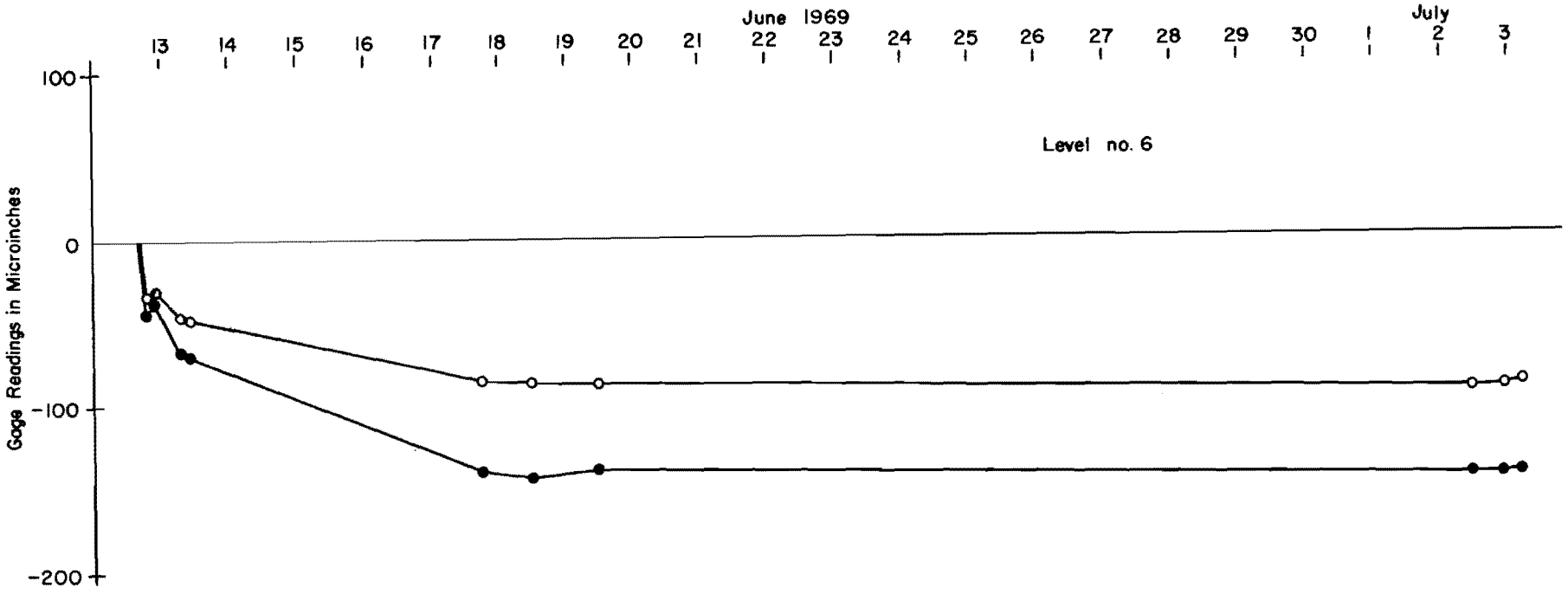

Fig. B.6. Mustran Gage Response to Concrete Curing

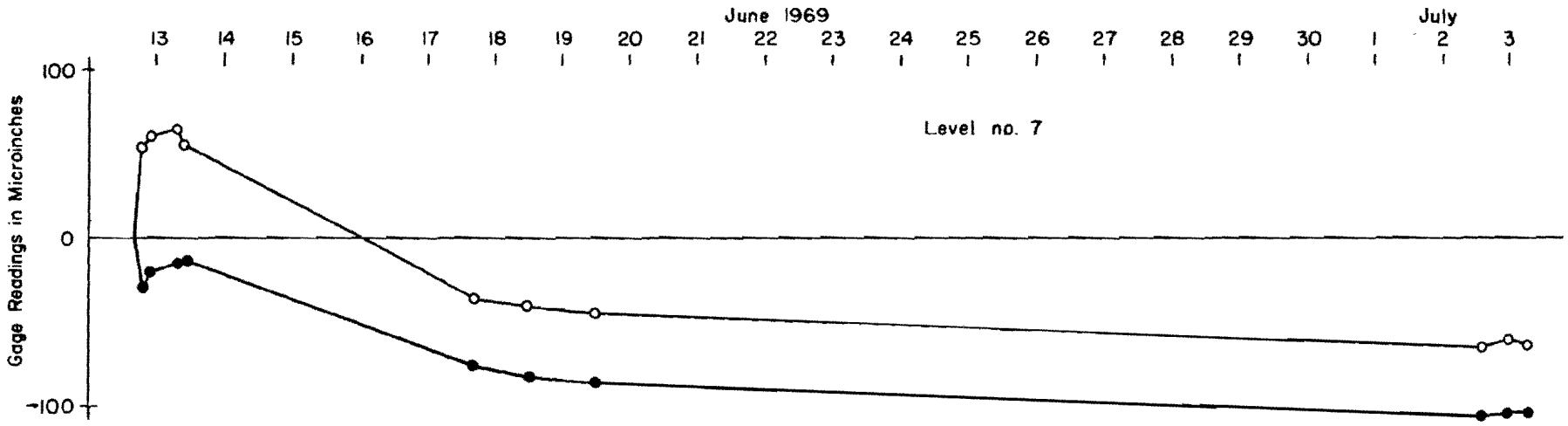

Fig. B.7. Mustran Gage Response to Concrete Curing

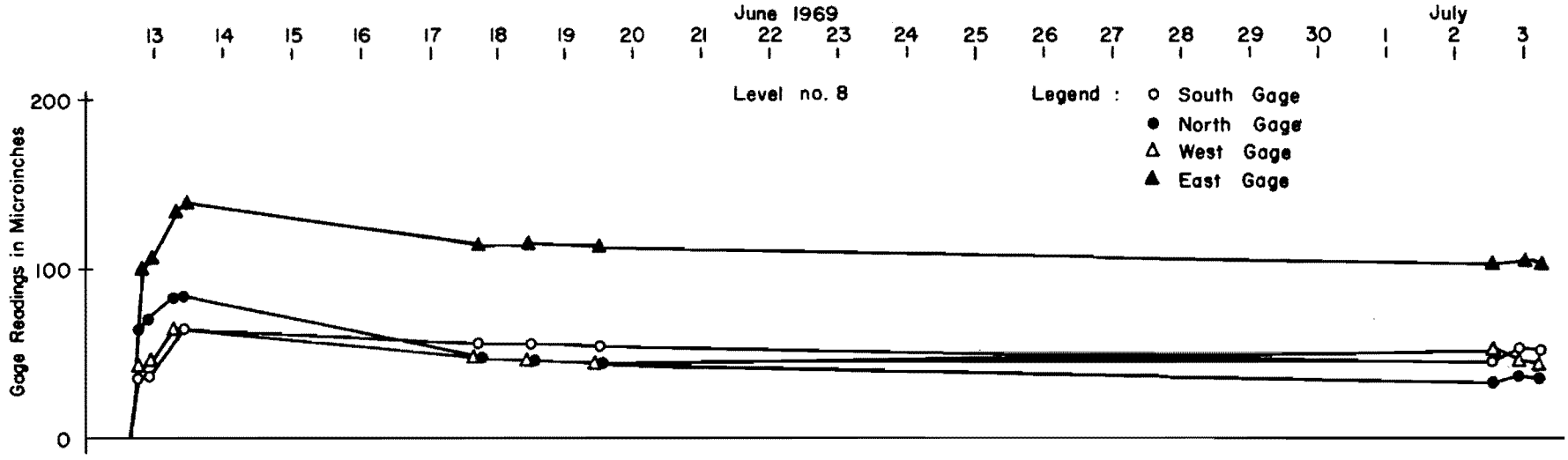

Fig. B.8. Mustran Gage Response to Concrete Curing

2. Data from 24-Hour Monitoring of Mustran Gages

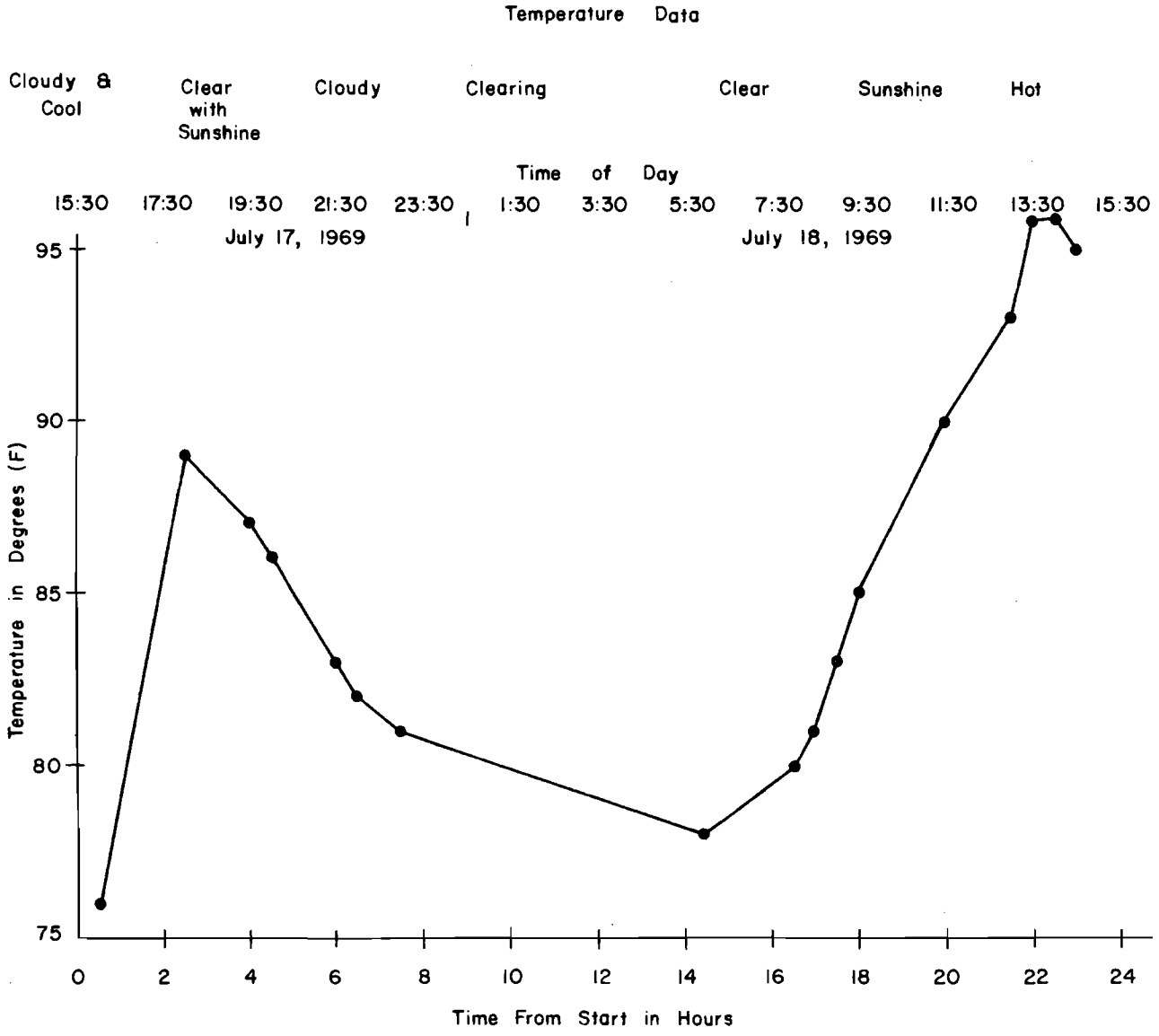

Fig. B.9. Temperature Curve During 24 Hour Monitoring

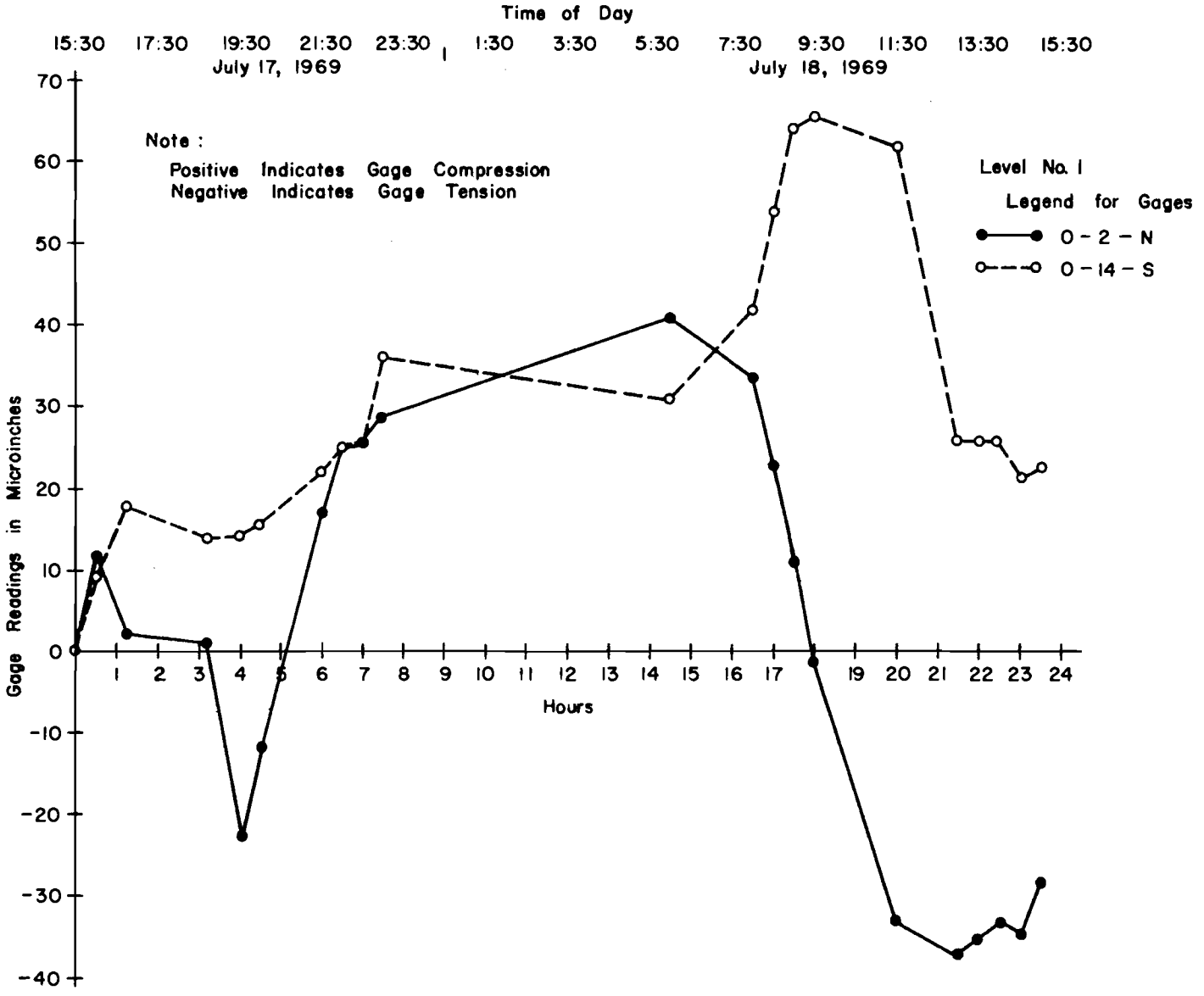

Fig. B.10. Mustran Gage Readings

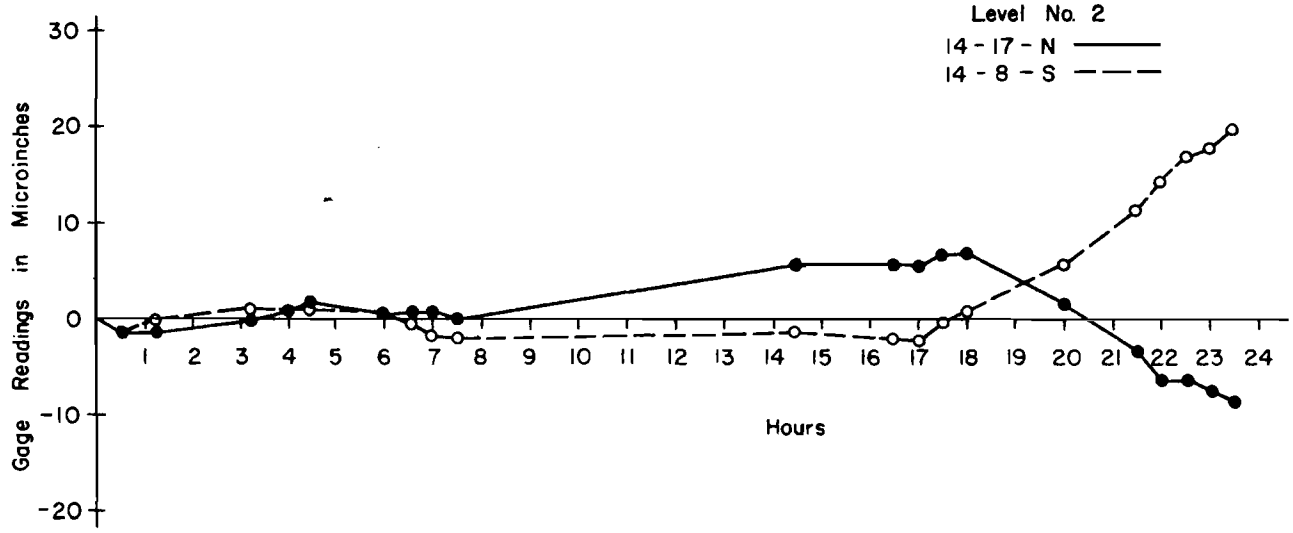

Fig. B.11. Mustran Gage Readings

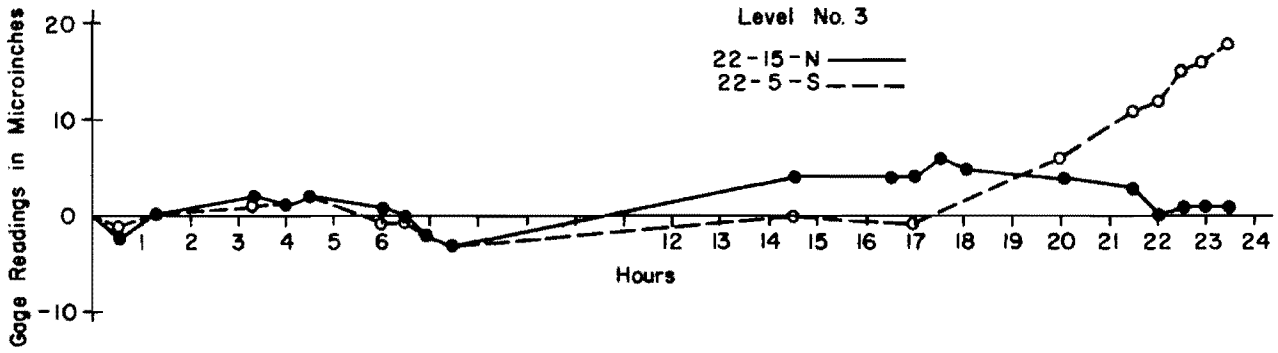

Fig. B.12. Mustran Gage Readings

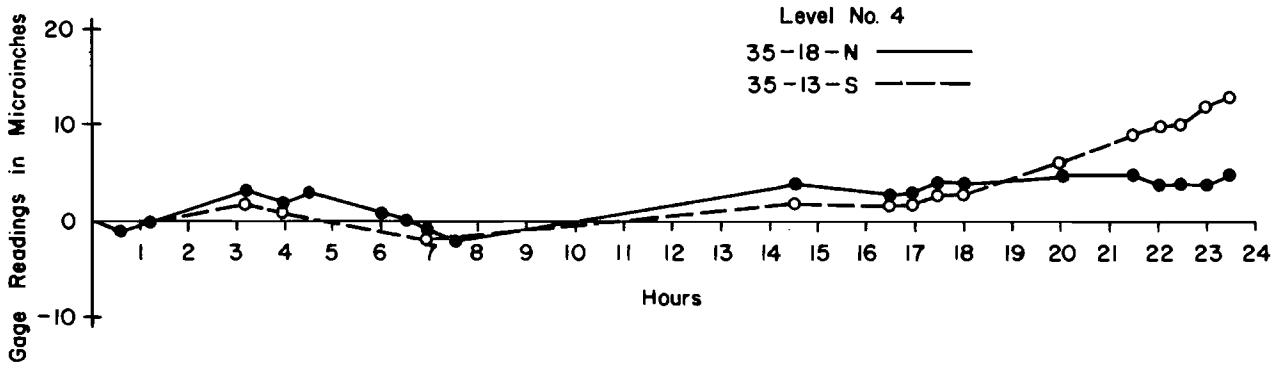

Fig. B.13. Mustran Gage Readings

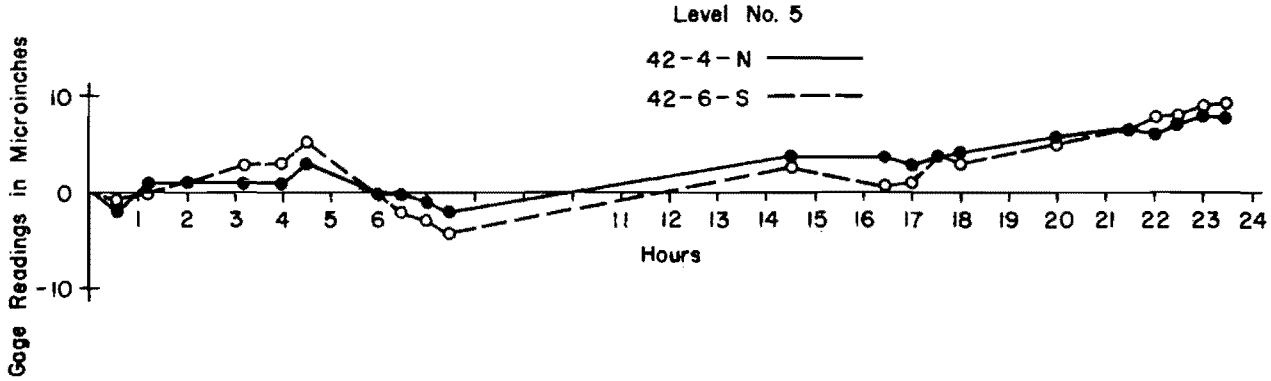

Fig. B.14. Mustran Gage Readings

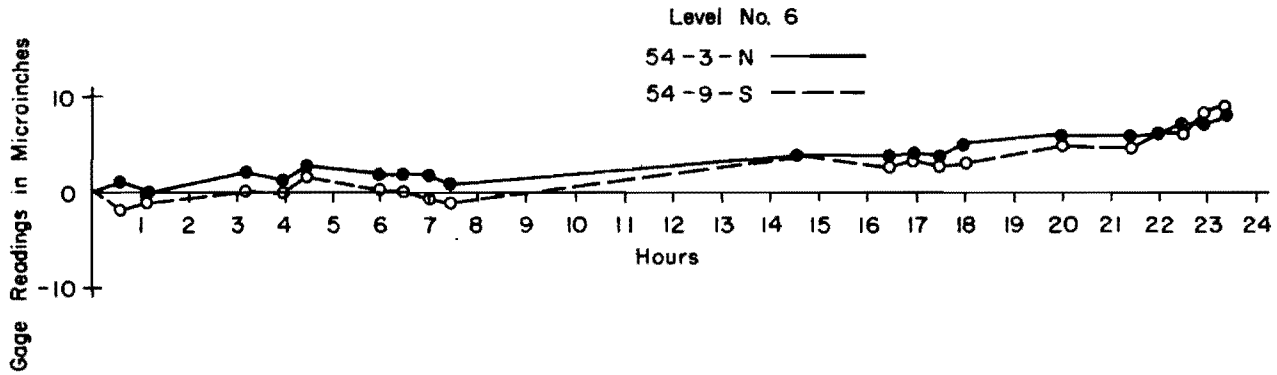

Fig. B.15. Mustran Gage Readings

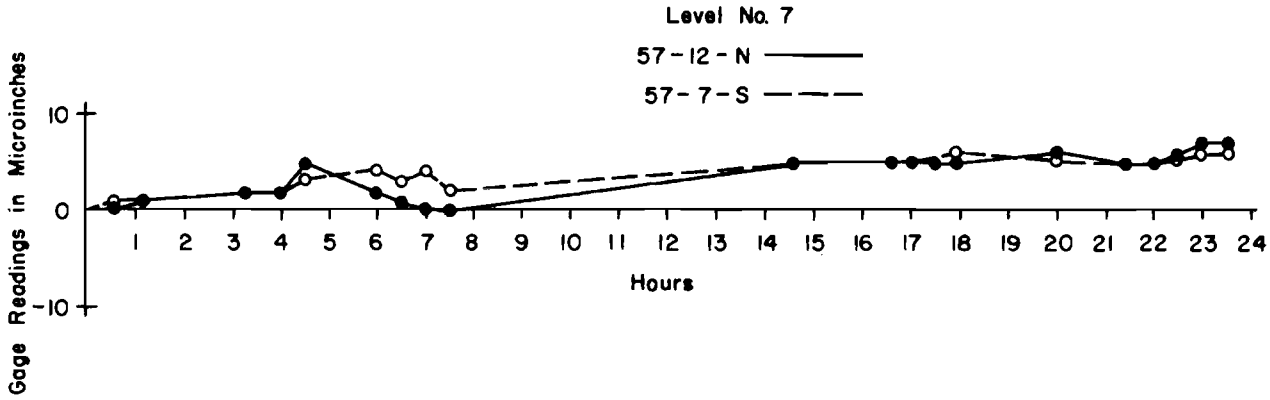

Fig. B.16. Mustran Gage Readings

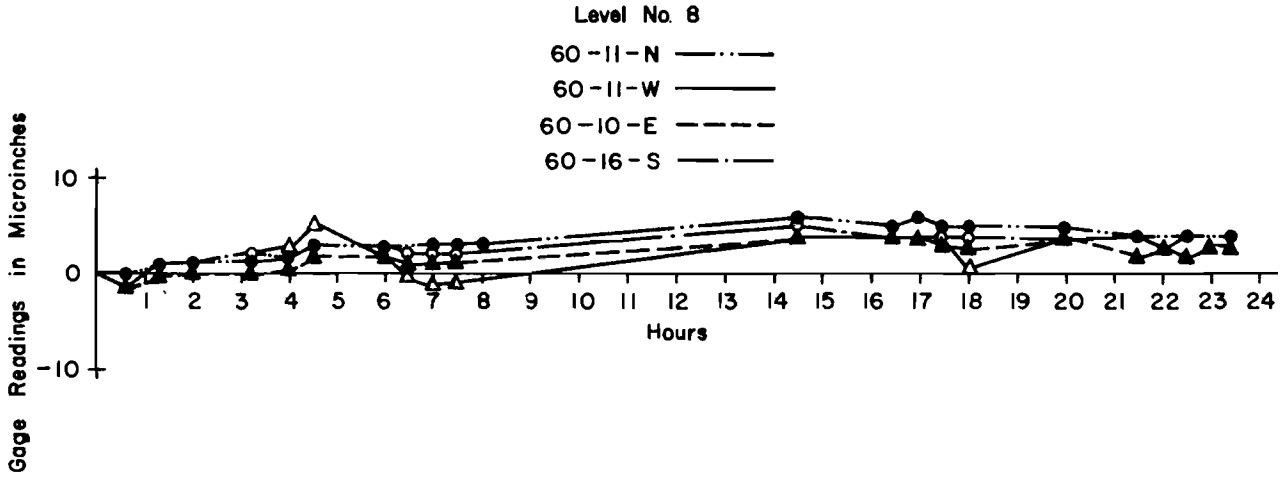

Fig. B.17. Mustran Gage Readings

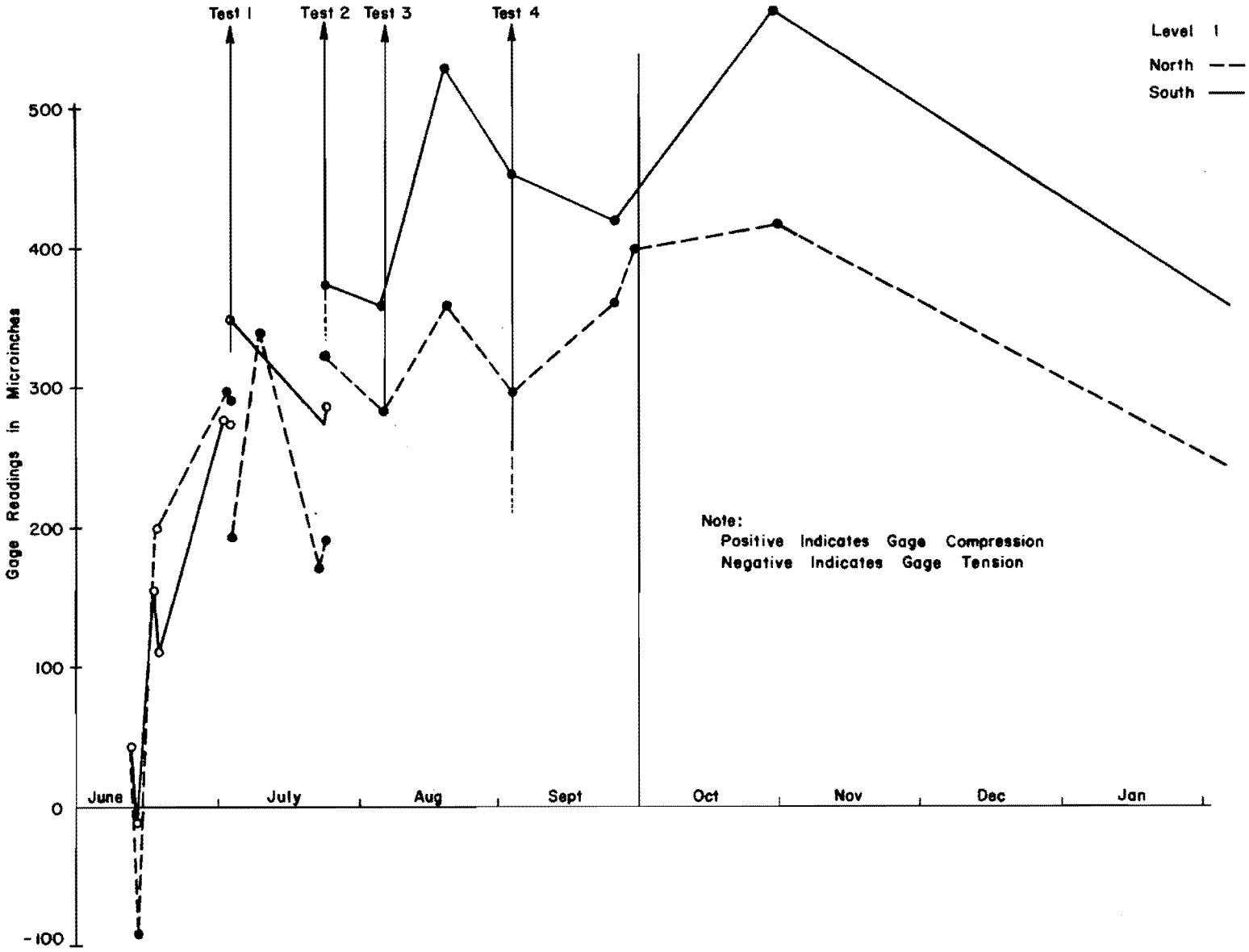

Fig. B.18. Long Term Stability of Mustran Gage

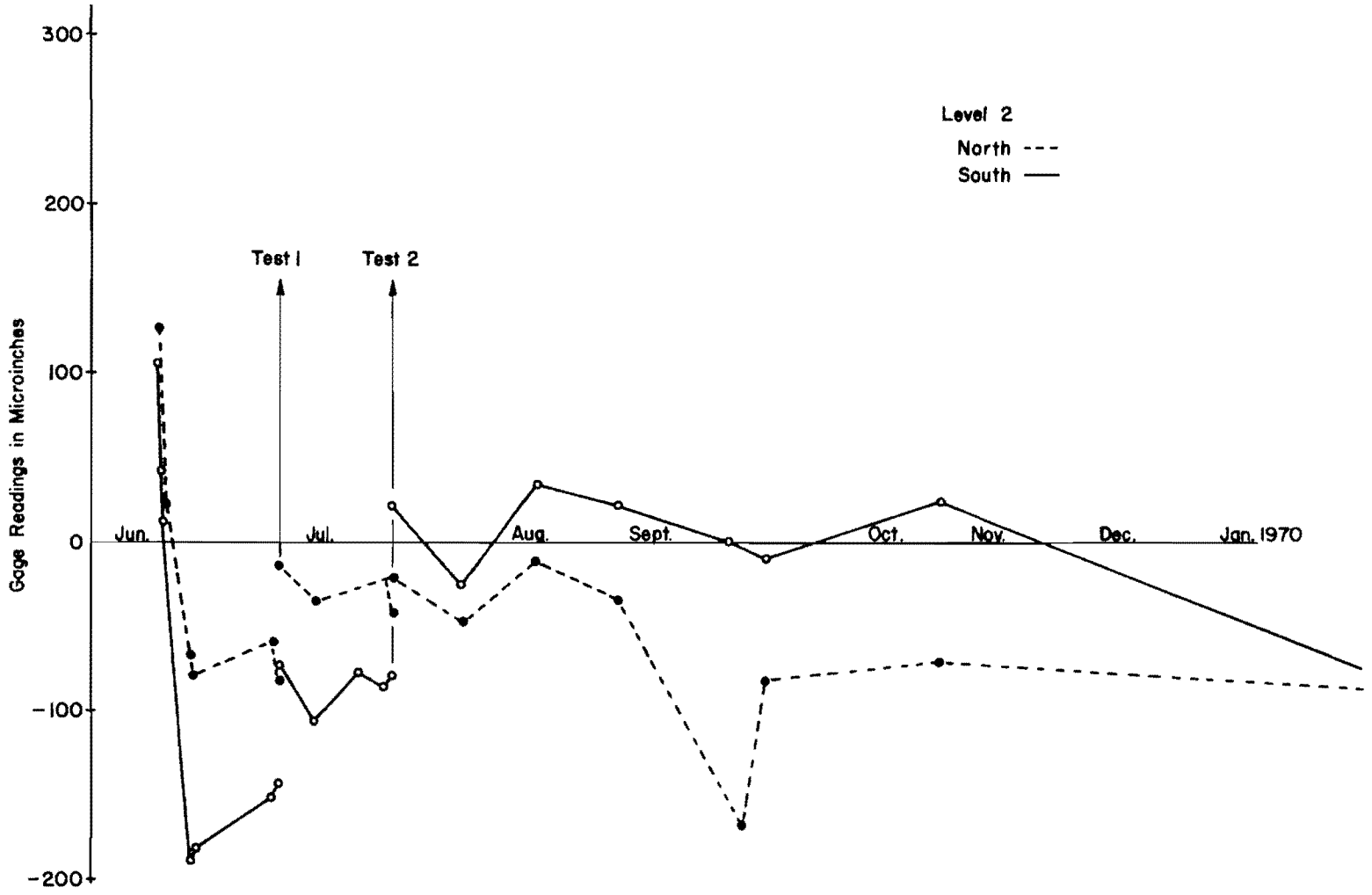

Fig. B.19. Long Term Stability of Mustran Gage

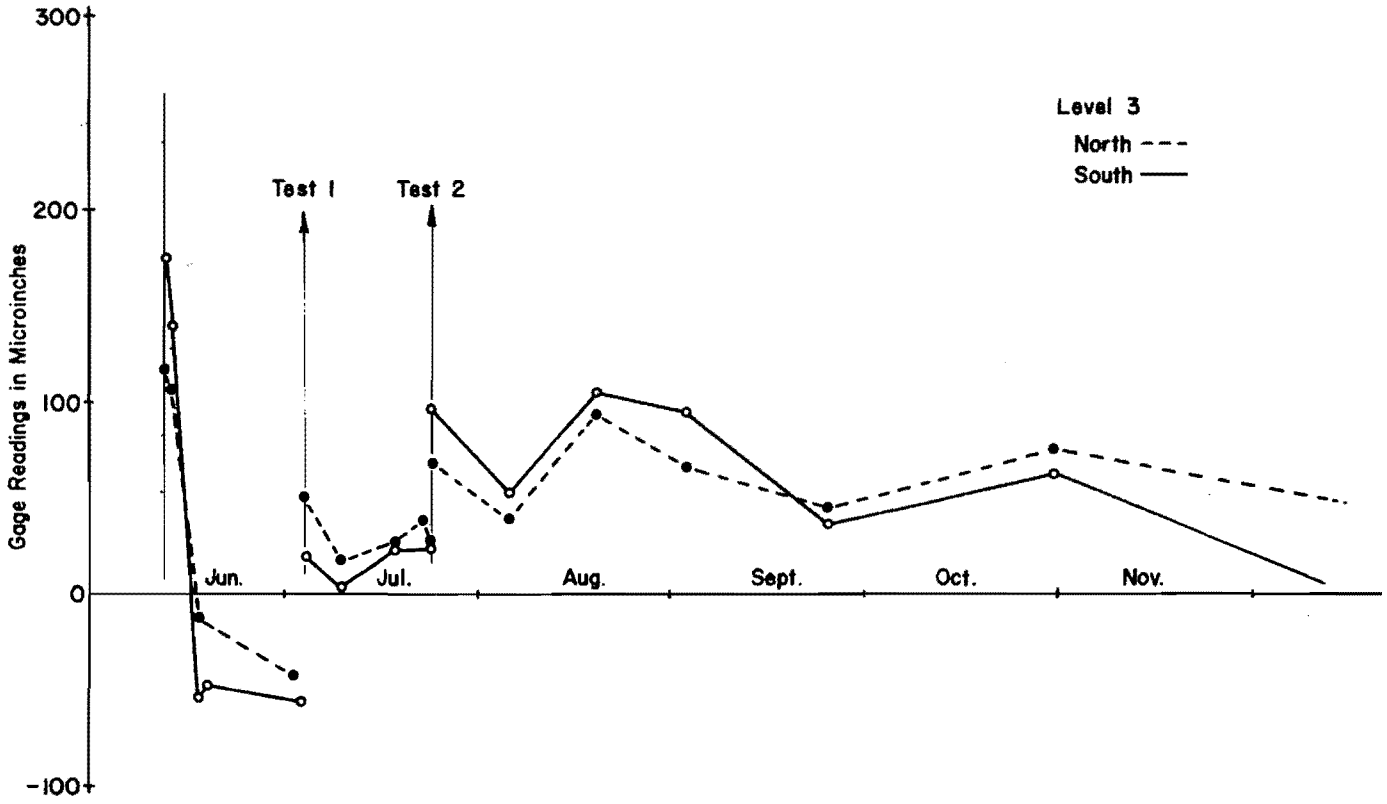

Fig. B.20. Long Term Stability of Mustran Gage

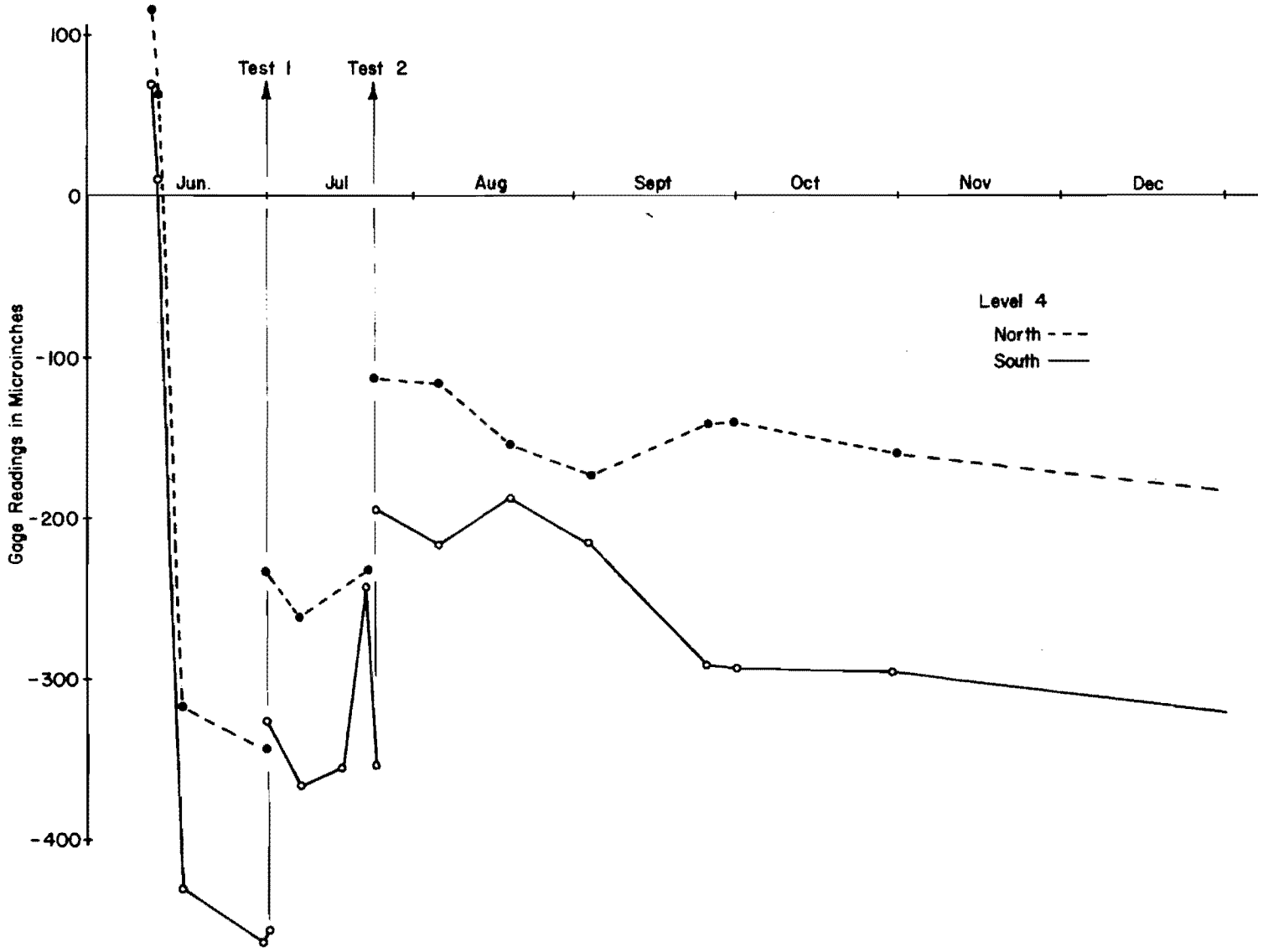

Fig. B.21. Long Term Stability of Mustran Gage

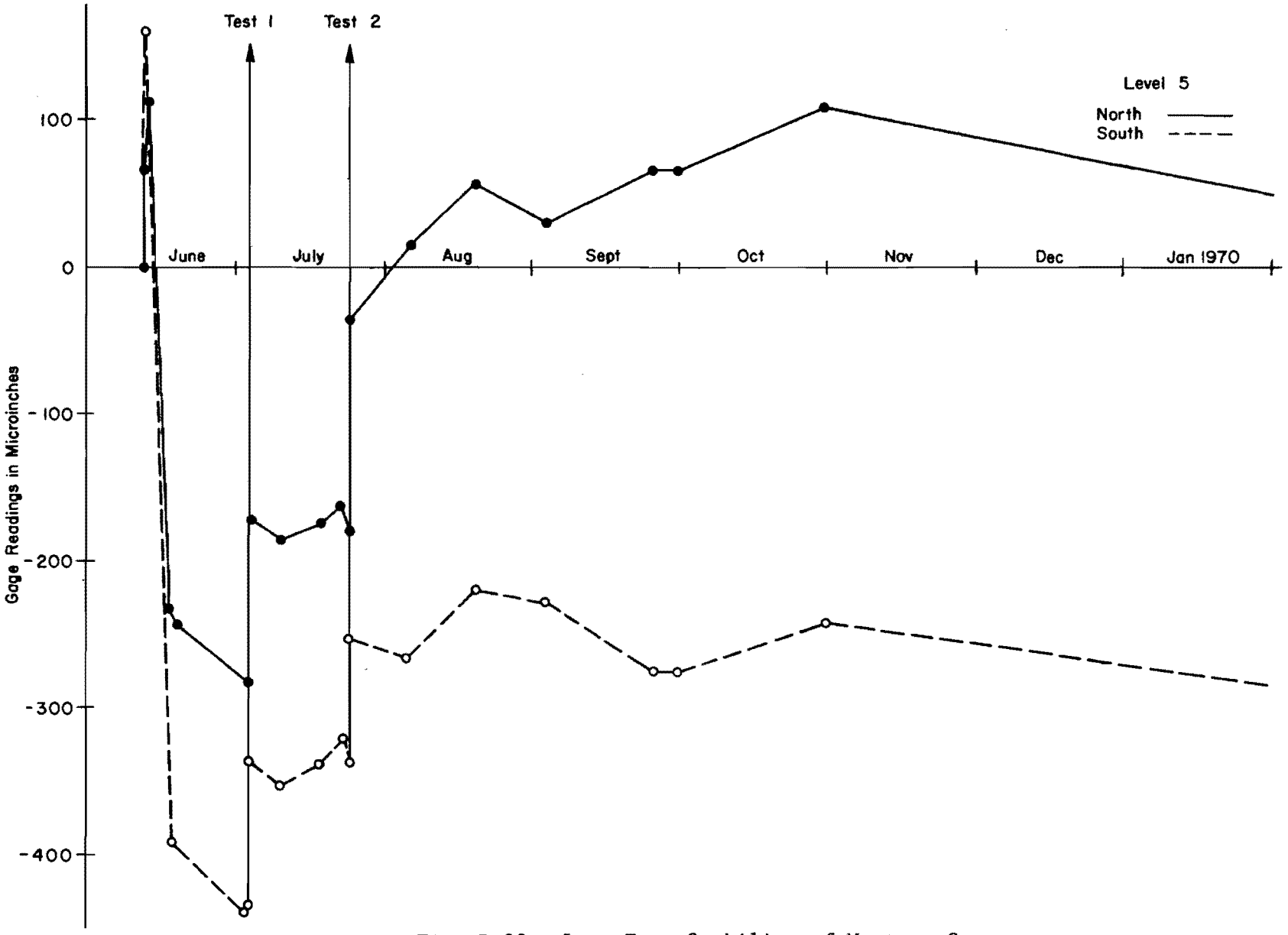

Fig. B.22. Long Term Stability of Mustran Gage

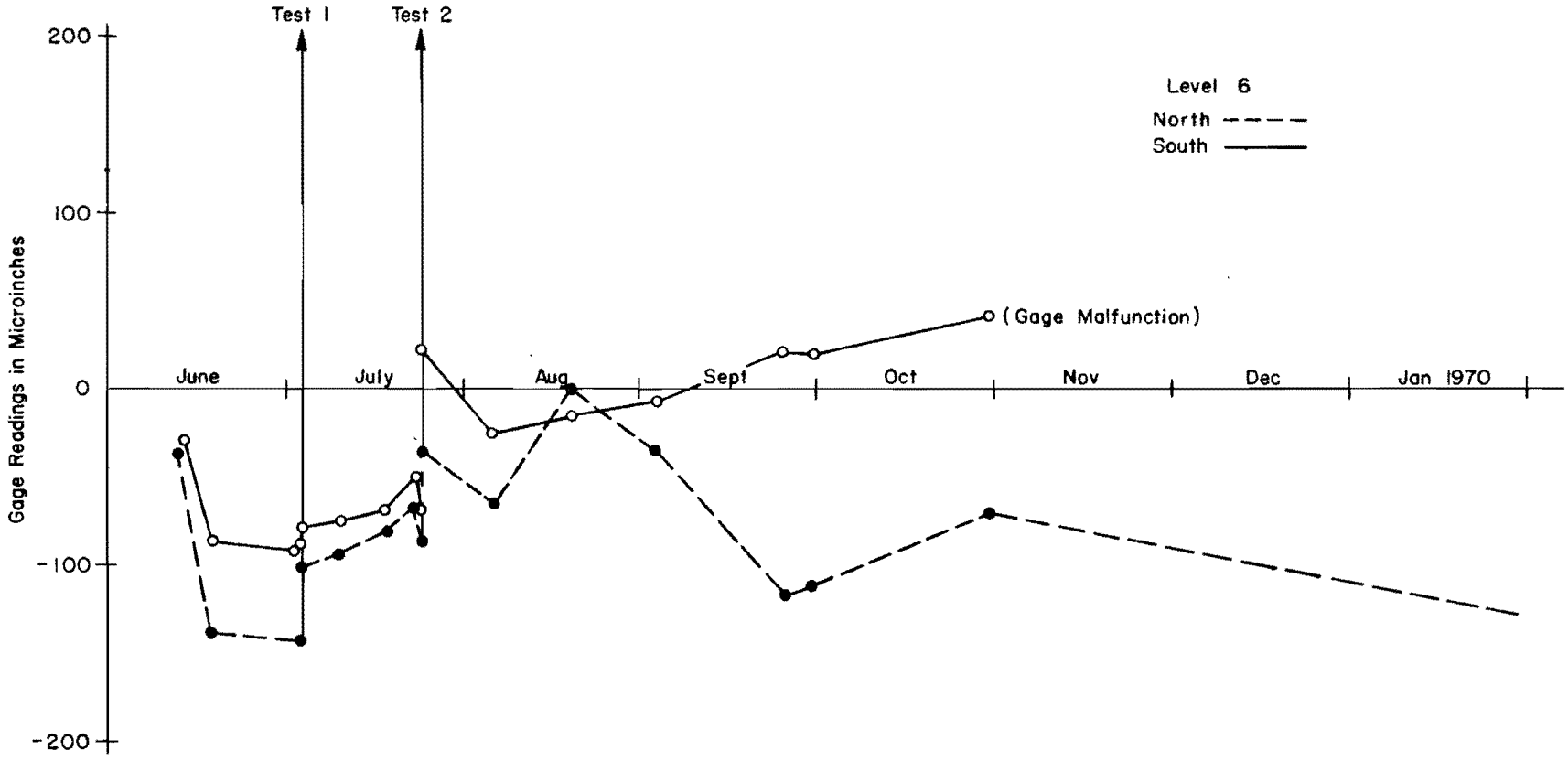

Fig. B.23. Long Term Stability of Mustran Gage

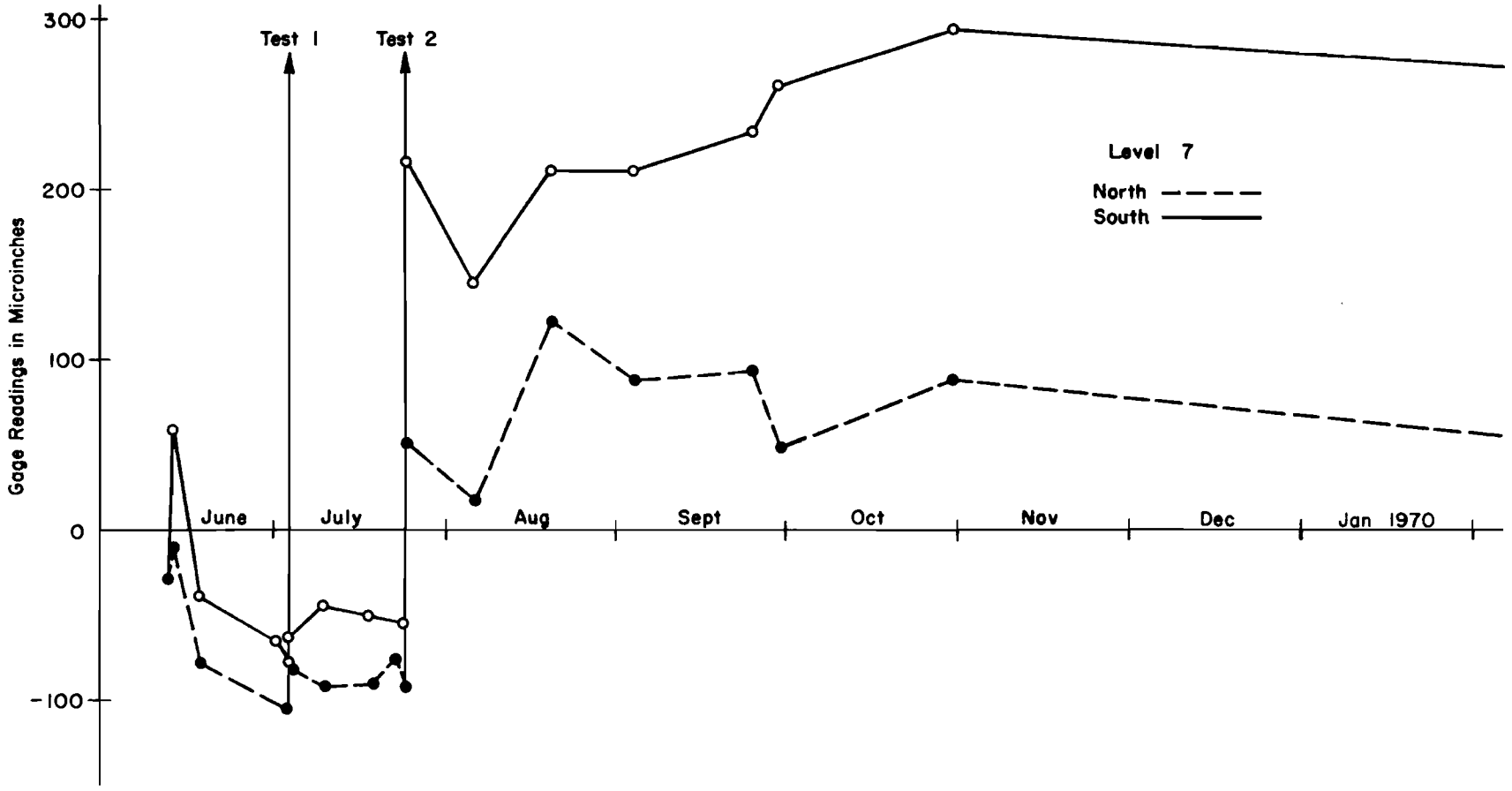

Fig. B.24. Long Term Stability of Mustran Gage

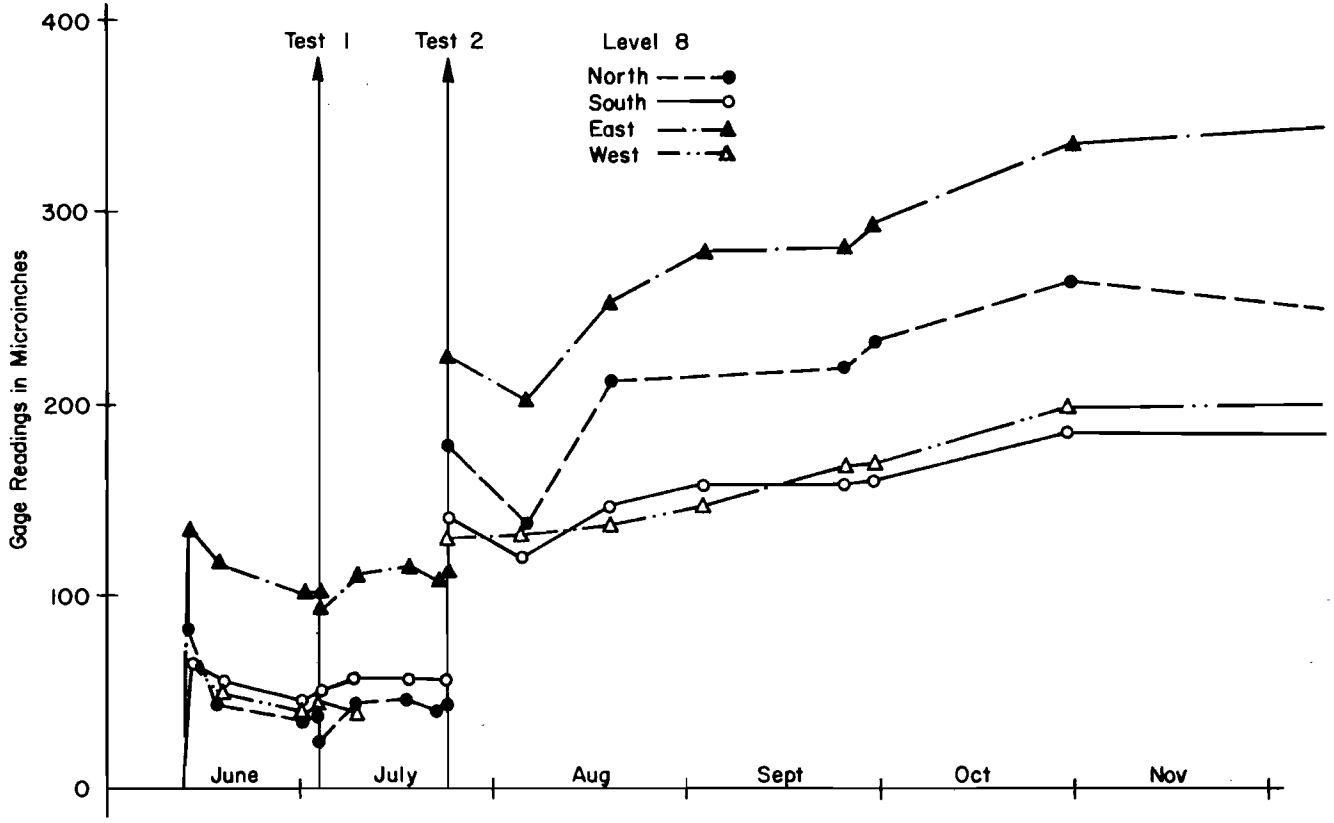

Fig. B.25. Long Term Stability of Mustran Gage

APPENDIX C

GAGE RESPONSE DATA

1. Gage Response for Test 2

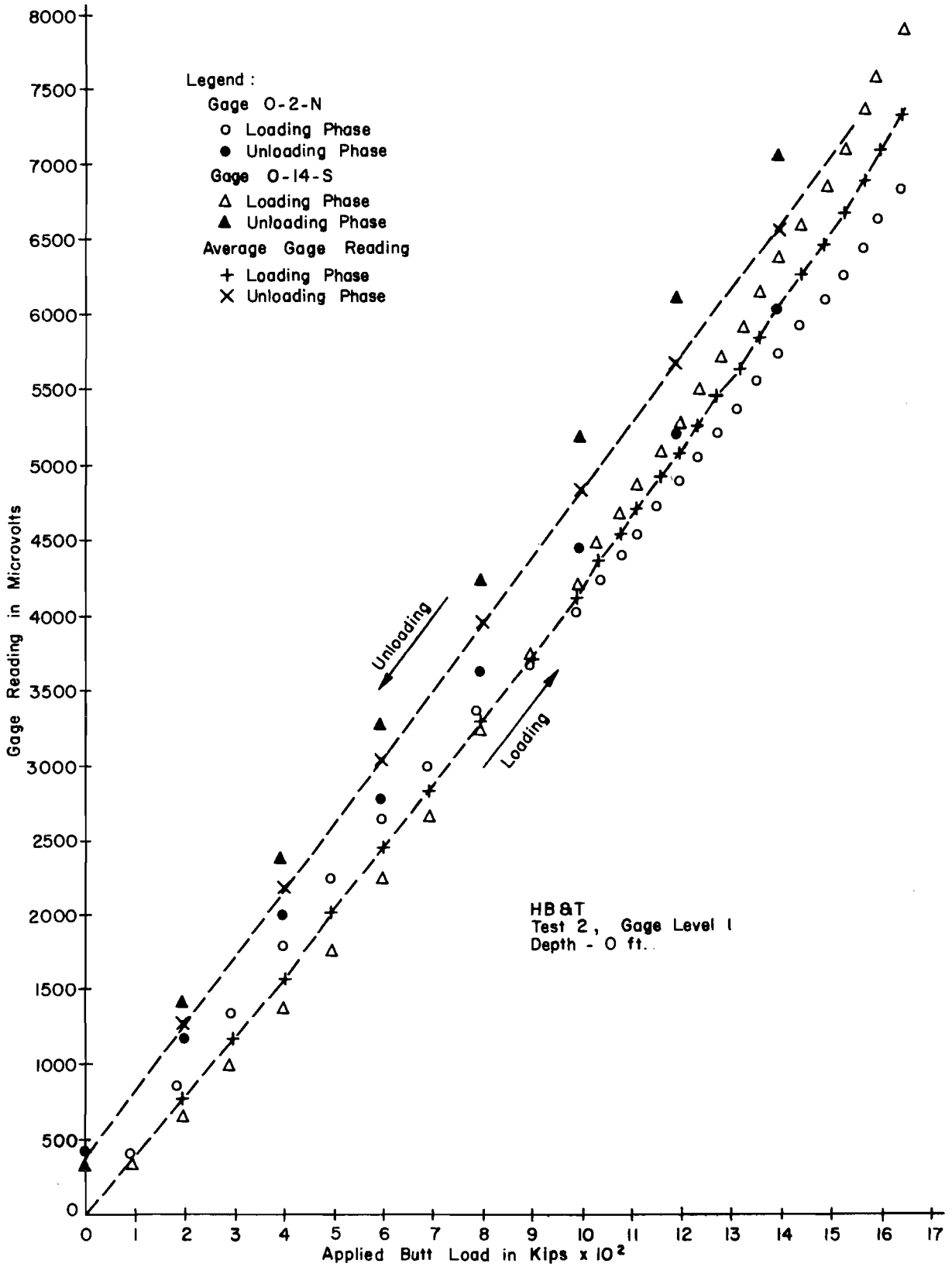

Fig. C.1. Gage Response for Test 2

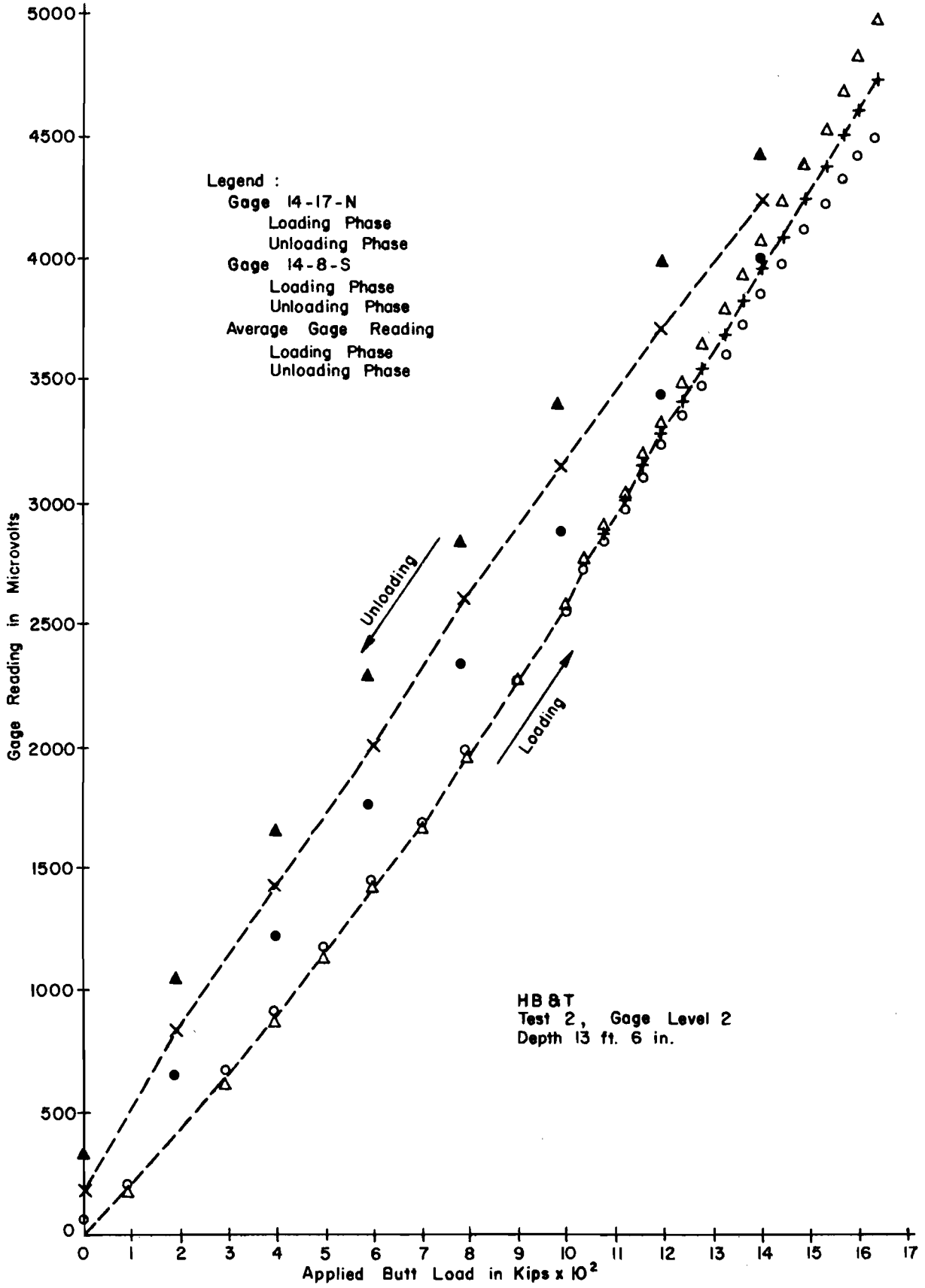

Fig. C.2. Gage Response for Test 2

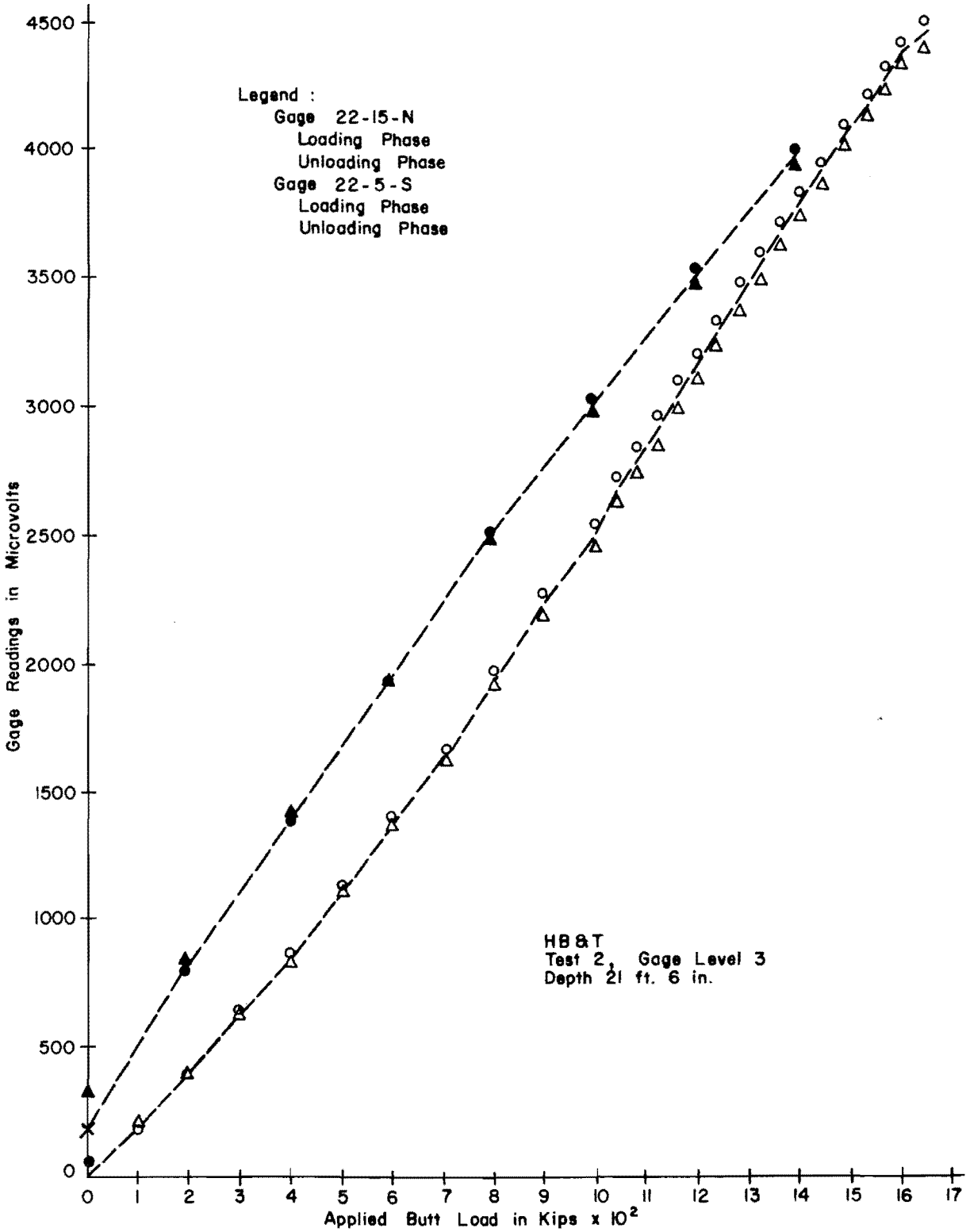

Fig. C.3. Gage Response for Test 2

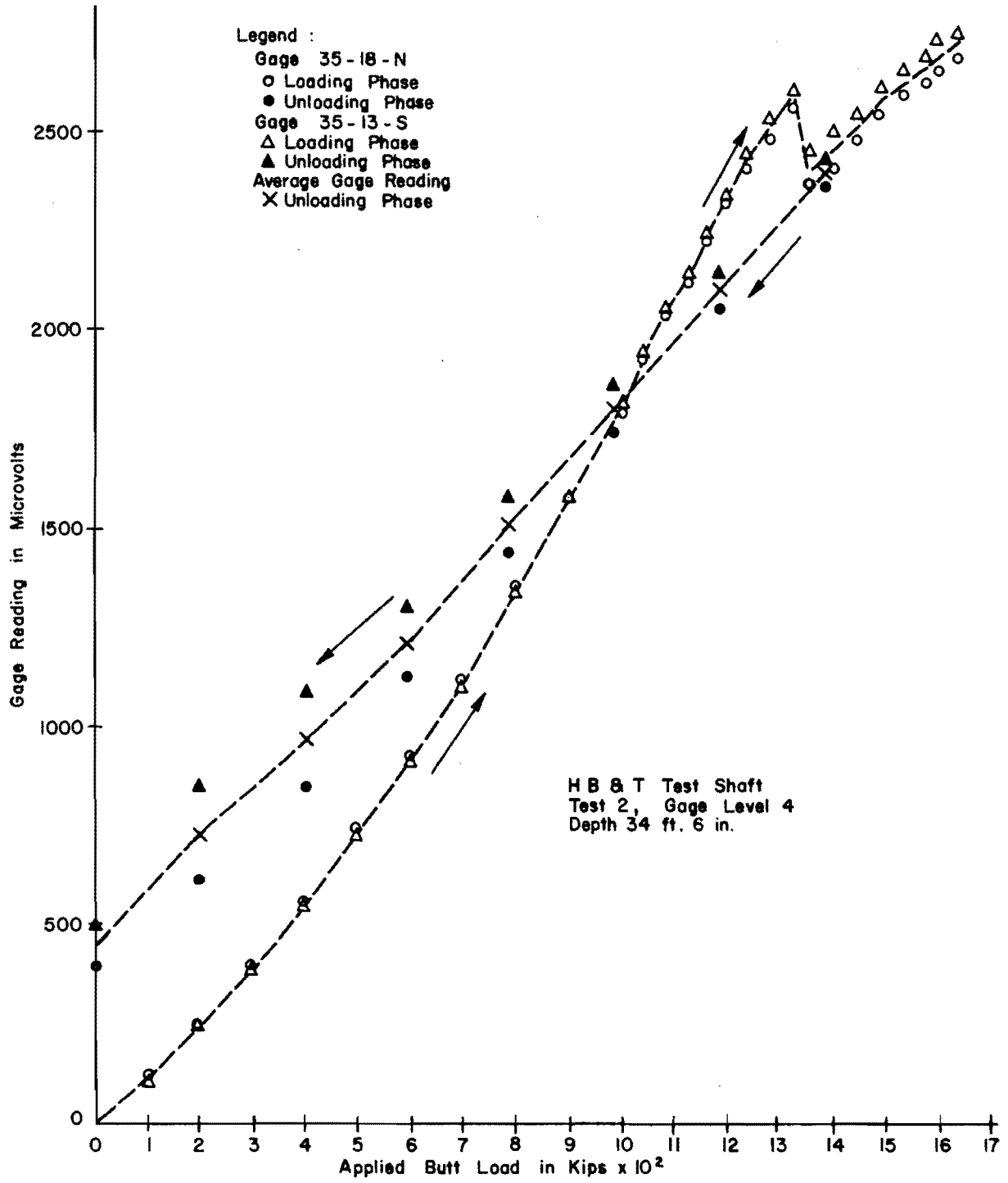

Fig. C.4. Gage Response for Test 2

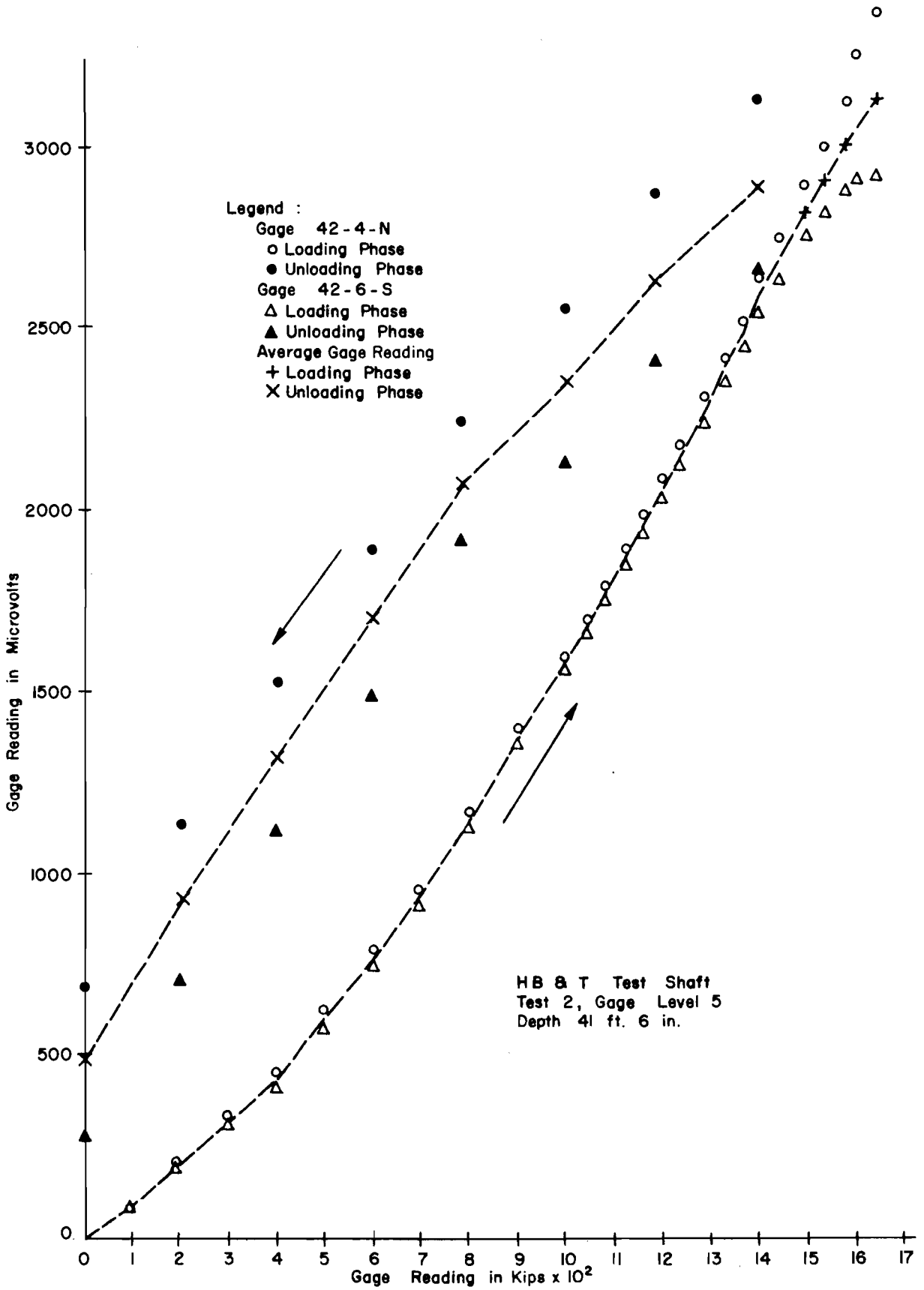

Fig. C.5. Gage Response for Test 2

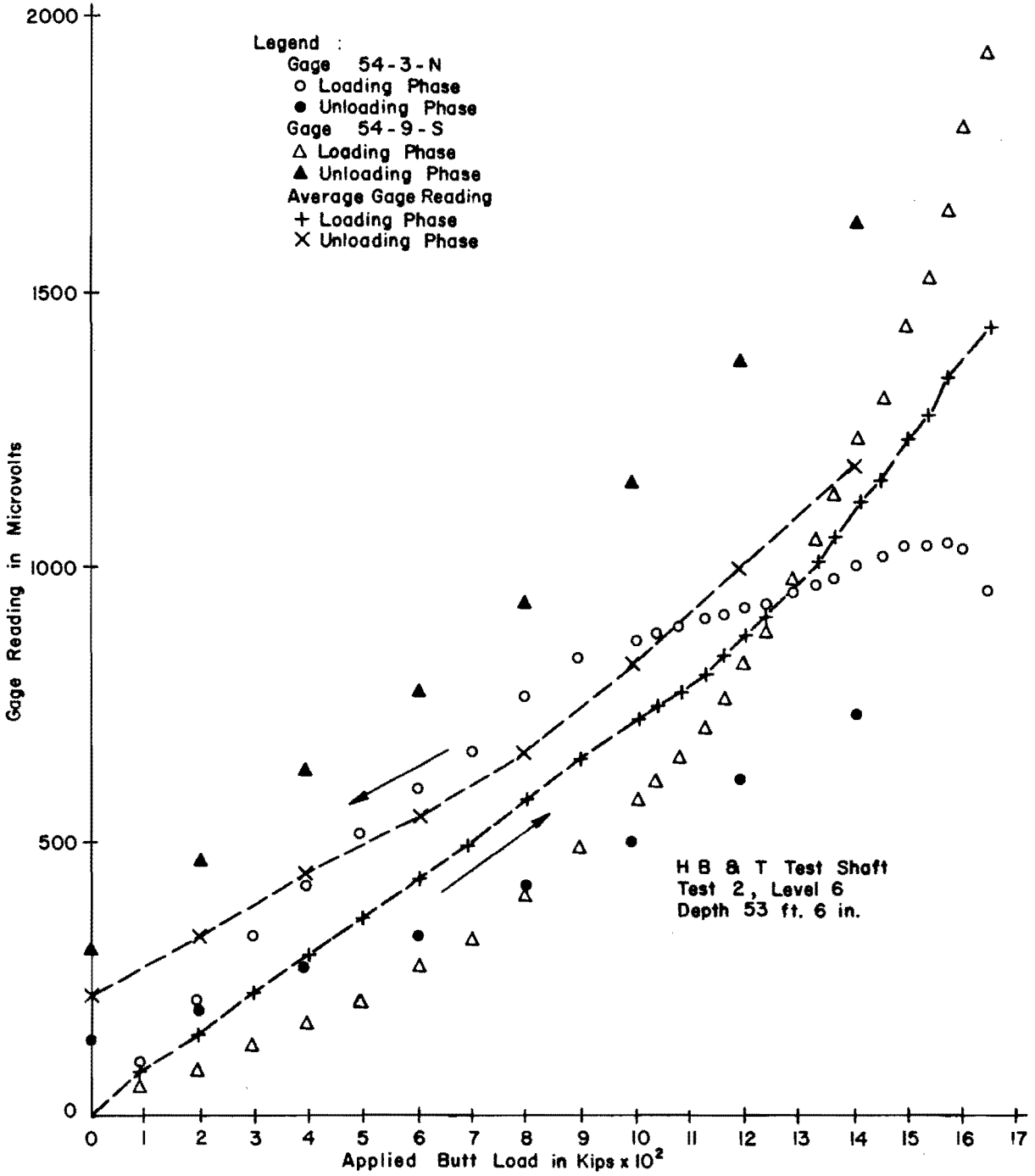

Fig. C.6. Gage Response for Test 2

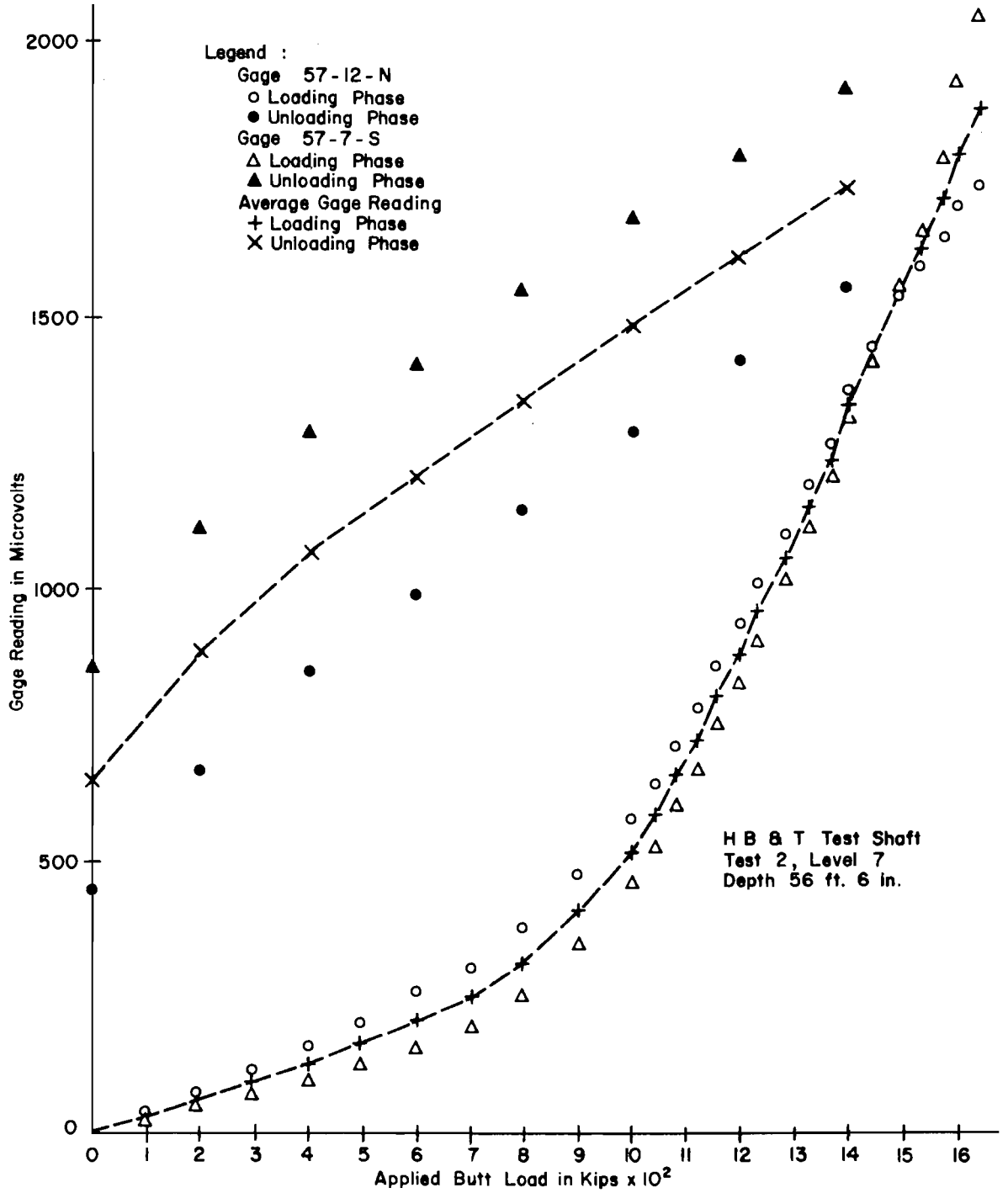

Fig. C.7. Gage Response for Test 2

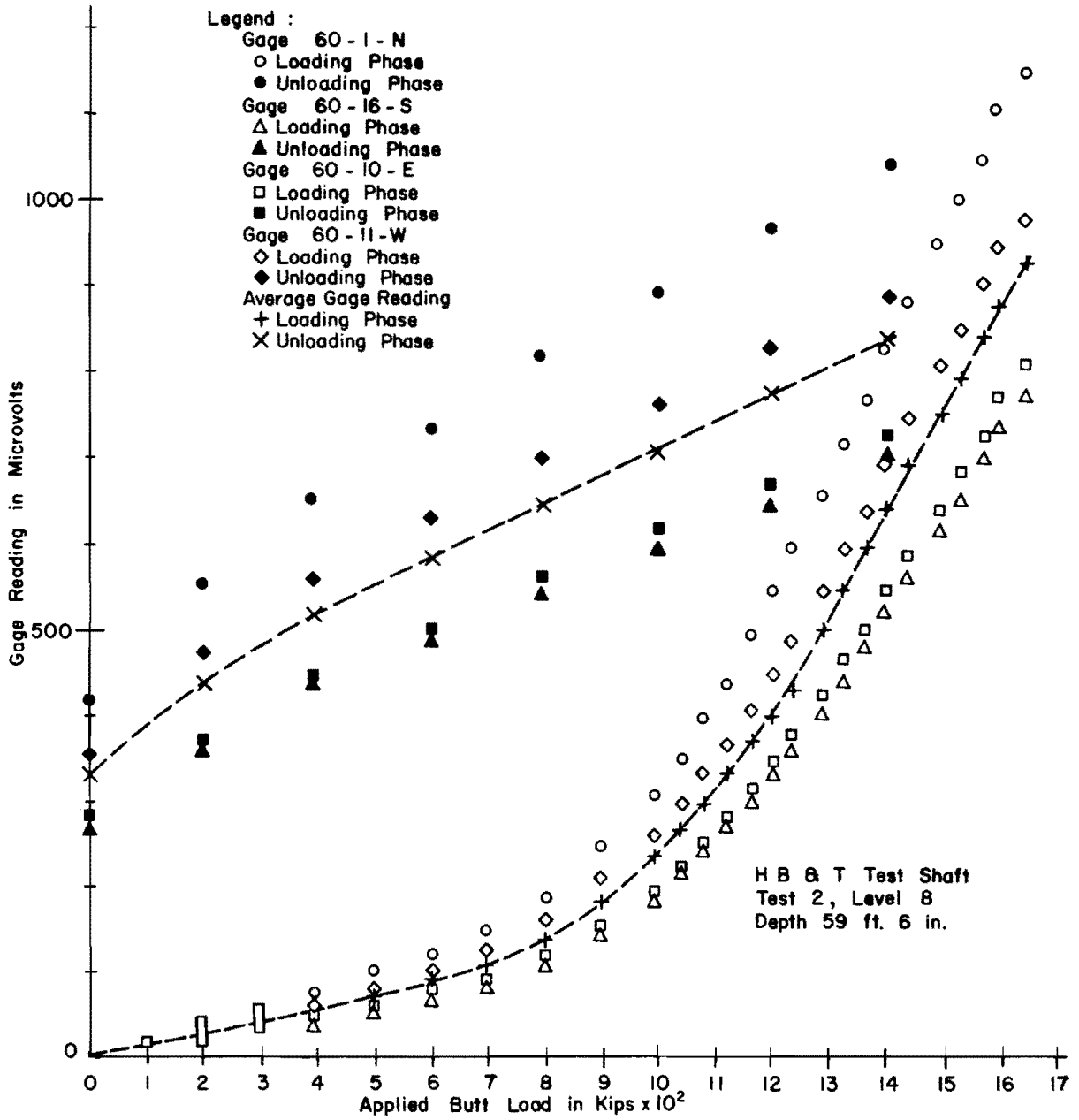

Fig. C.8. Gage Response for Test 2

2. Gage Response for All Tests

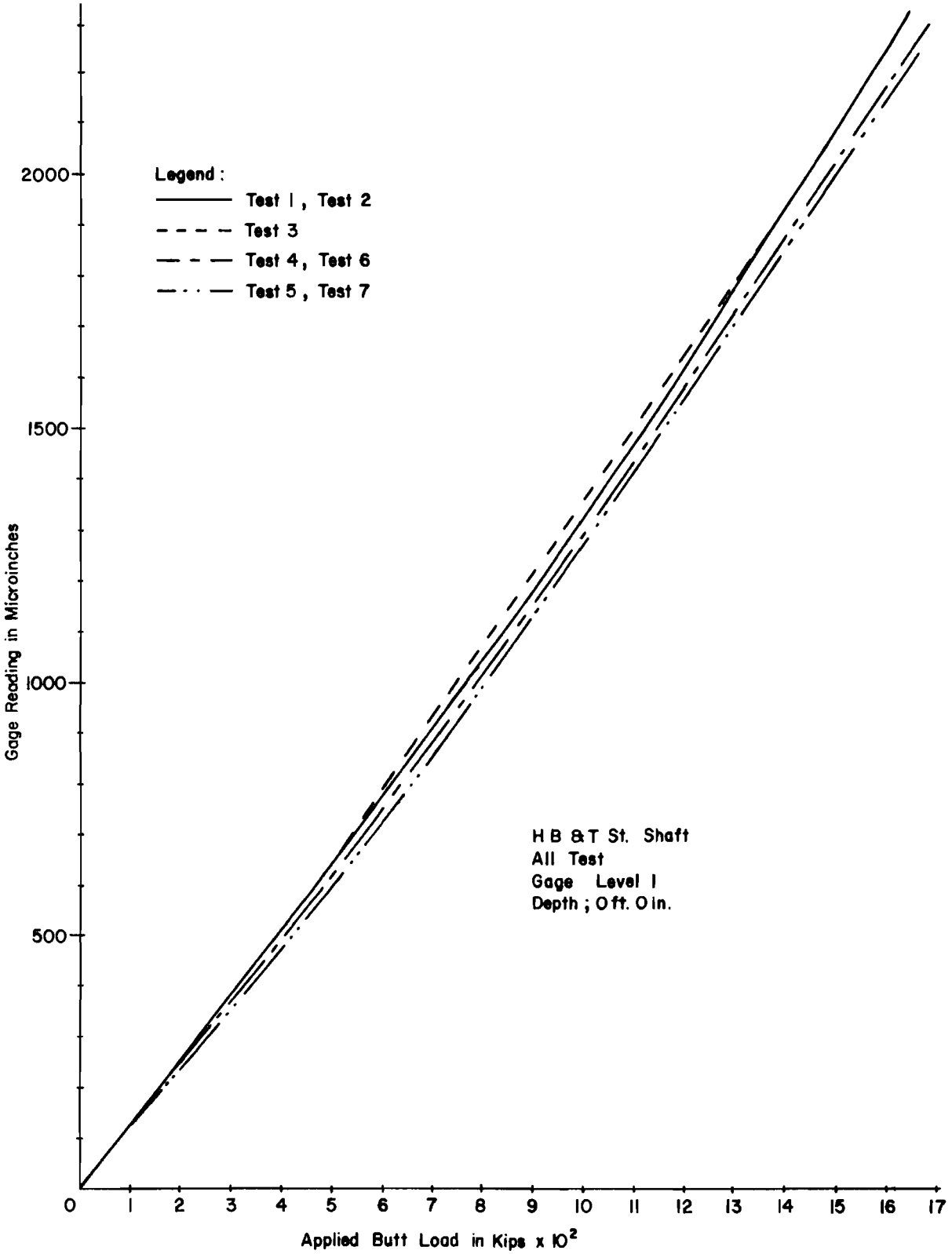

Fig. C.9. Gage Response for all Tests

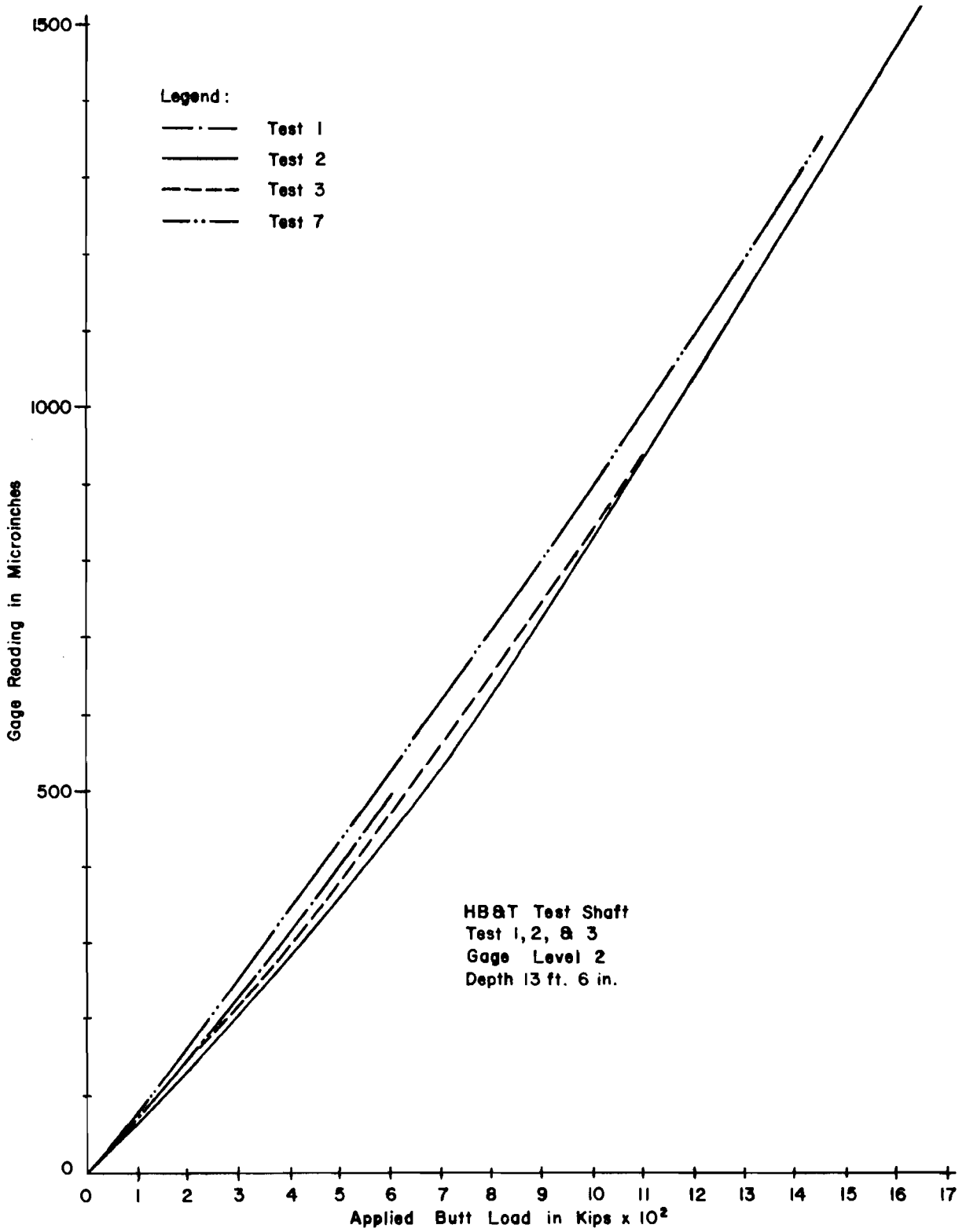

Fig. C.10. Gage Response for all Tests

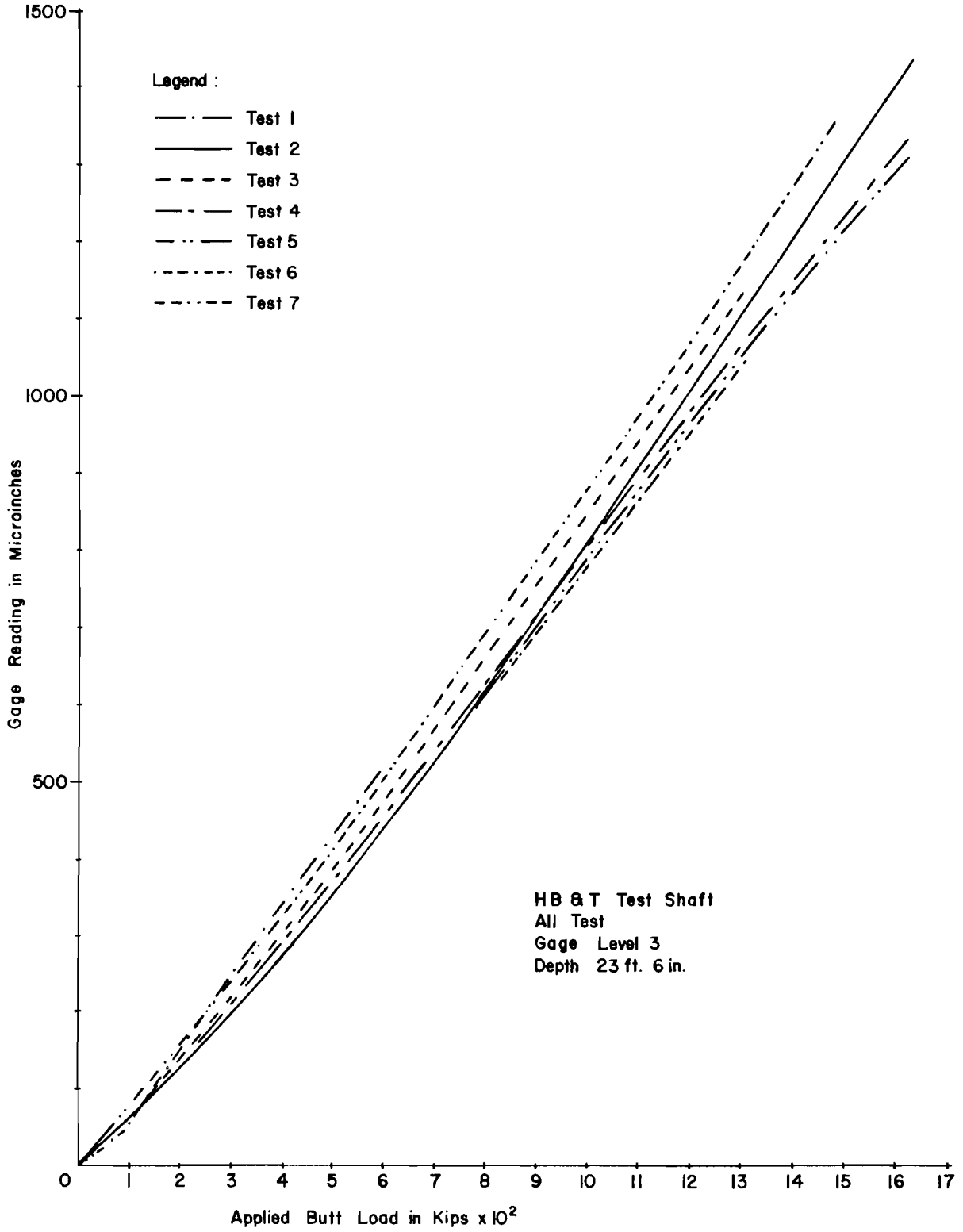

Fig. C.11. Gage Response for all Tests

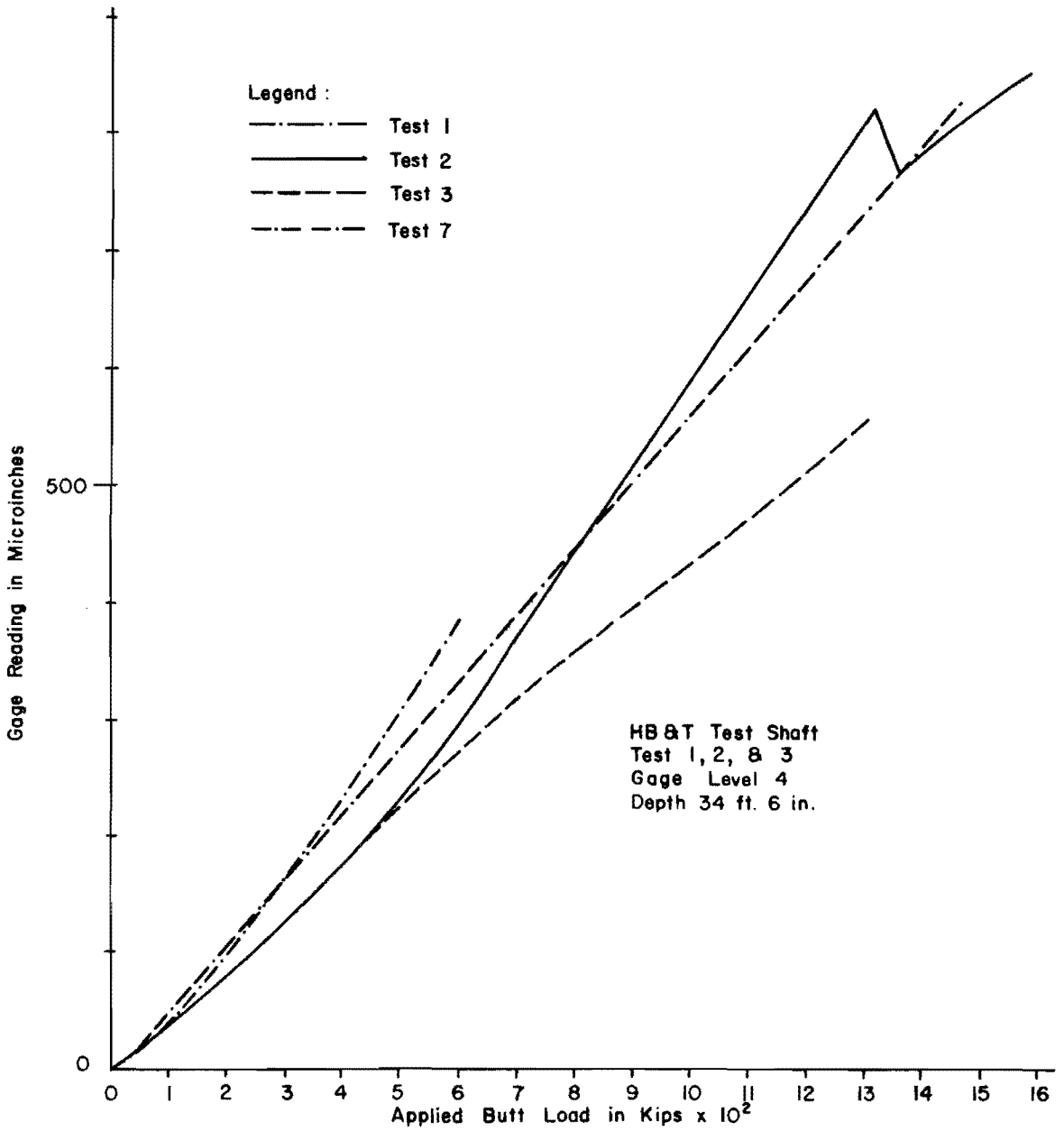

Fig. C. 12. Gage Response for all Tests

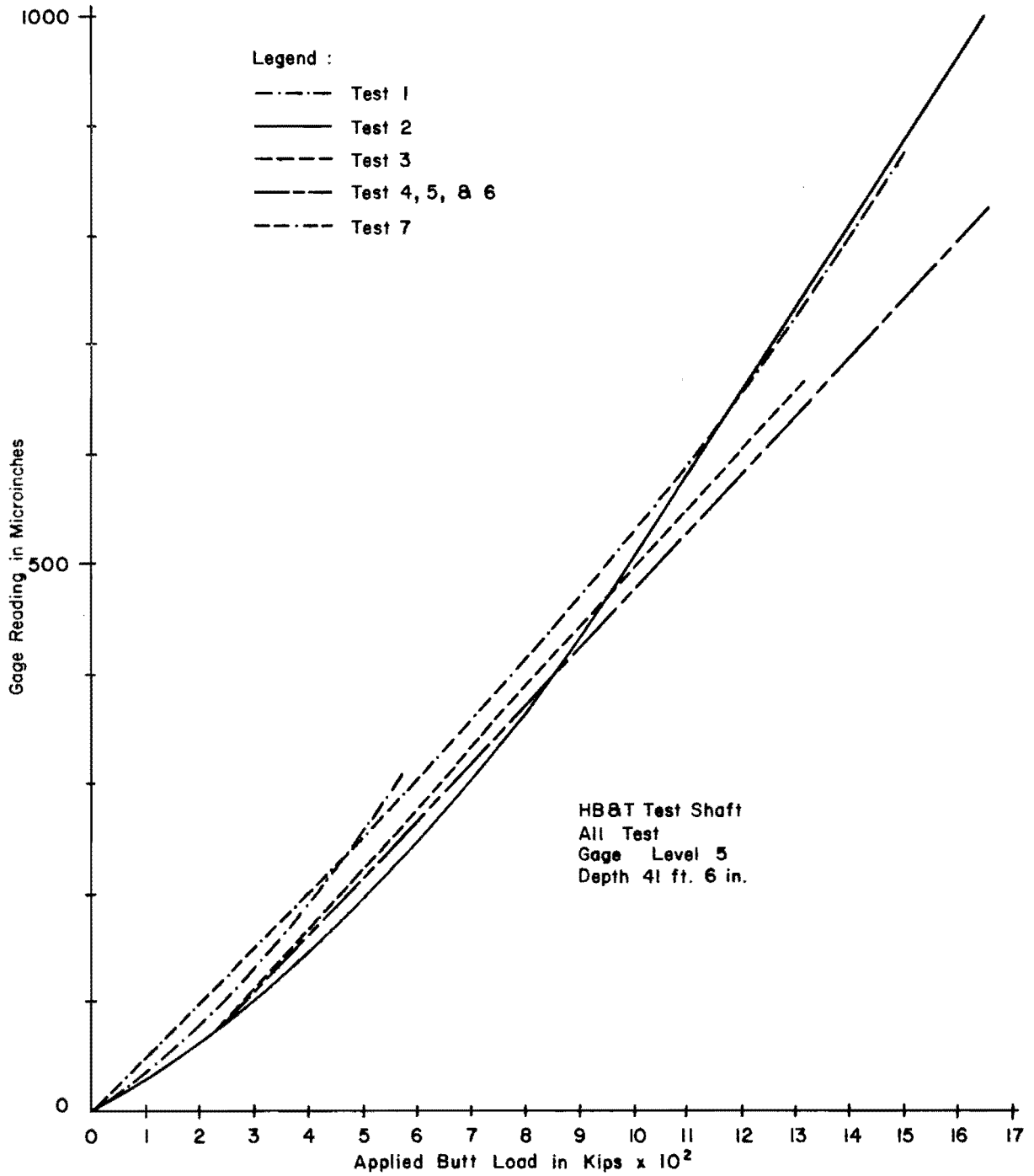

Fig. C.13. Gage Response for all Tests

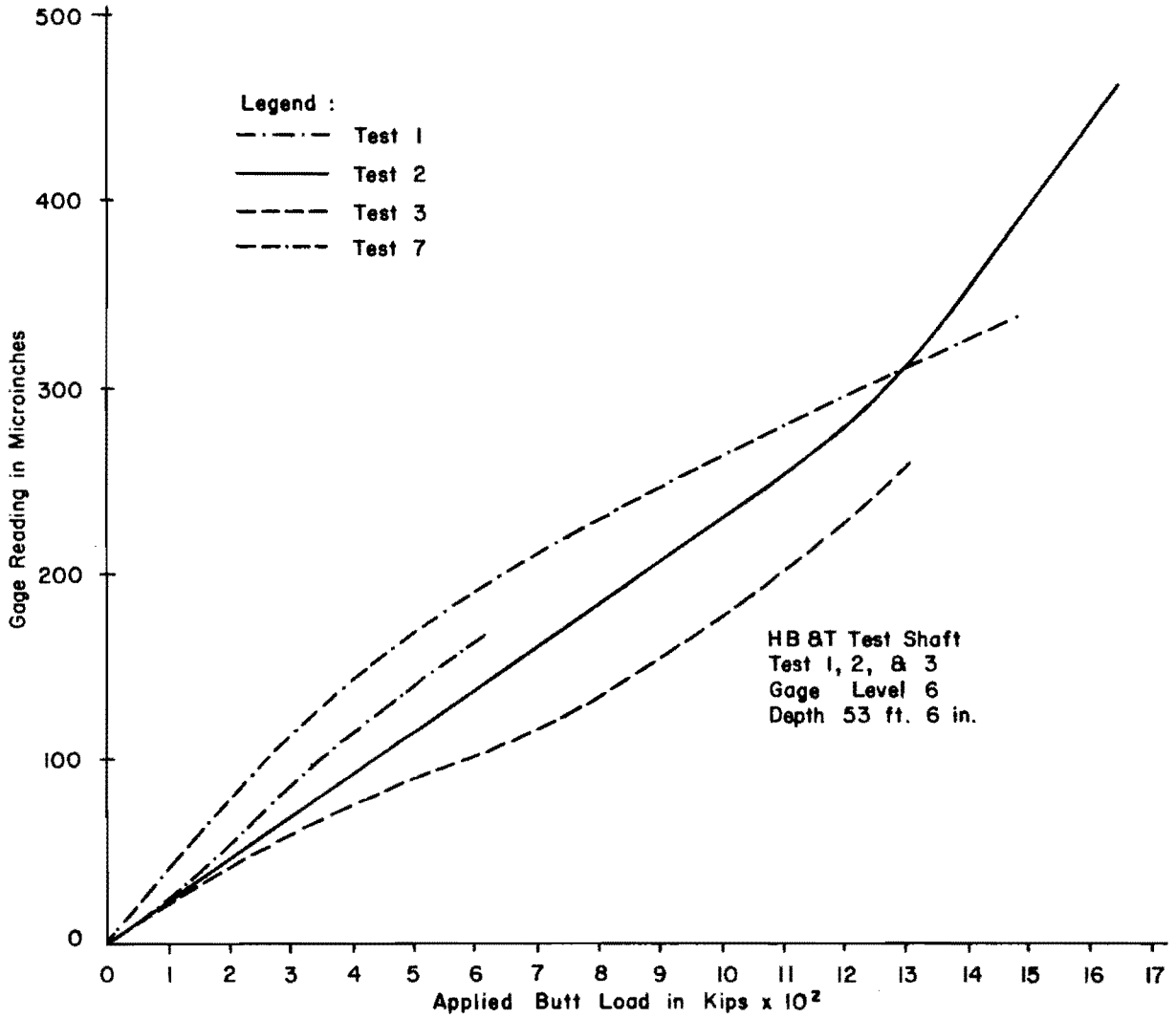

Fig. C.14. Gage Response for all Tests

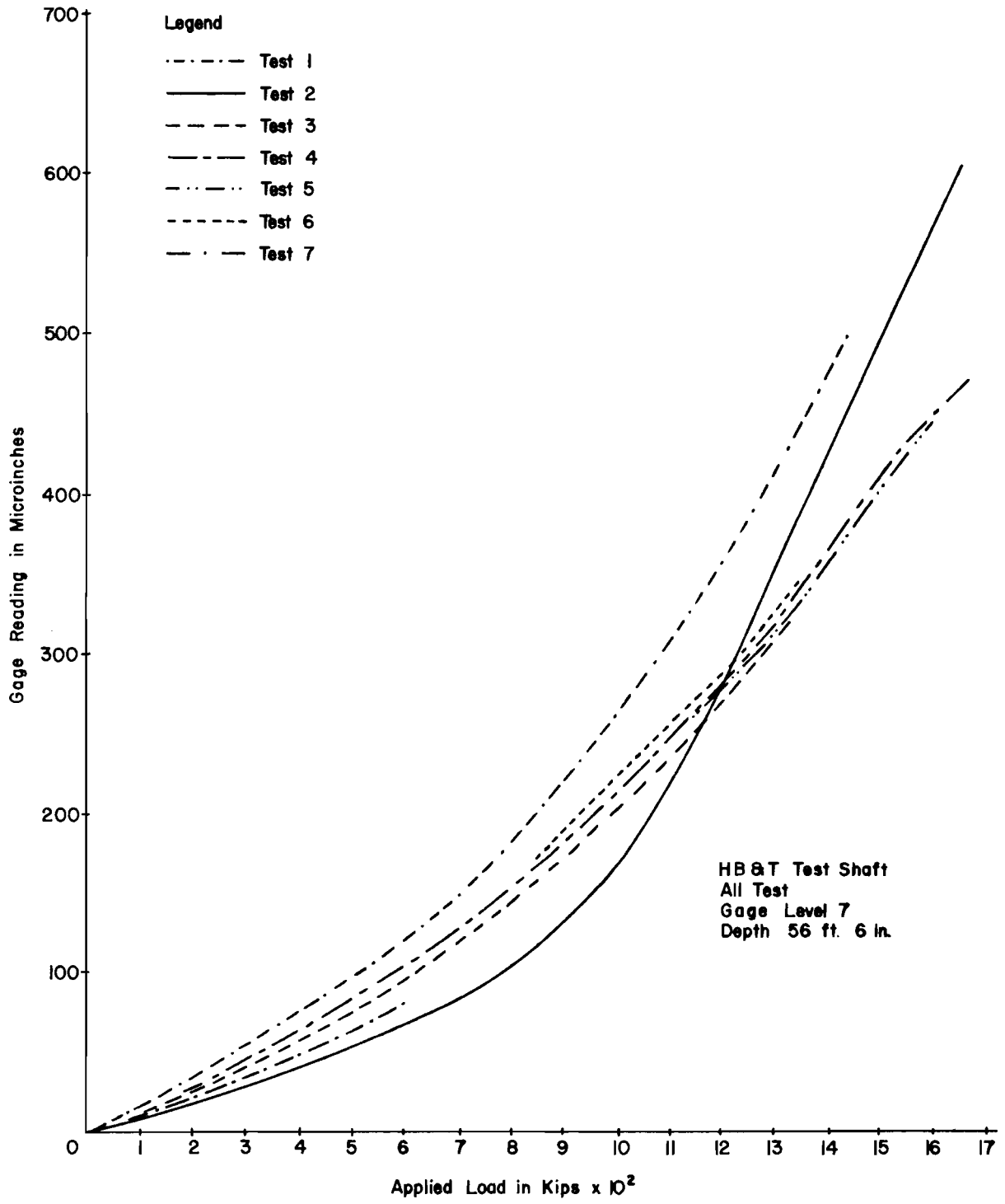

Fig. C.15. Gage Response for all Tests

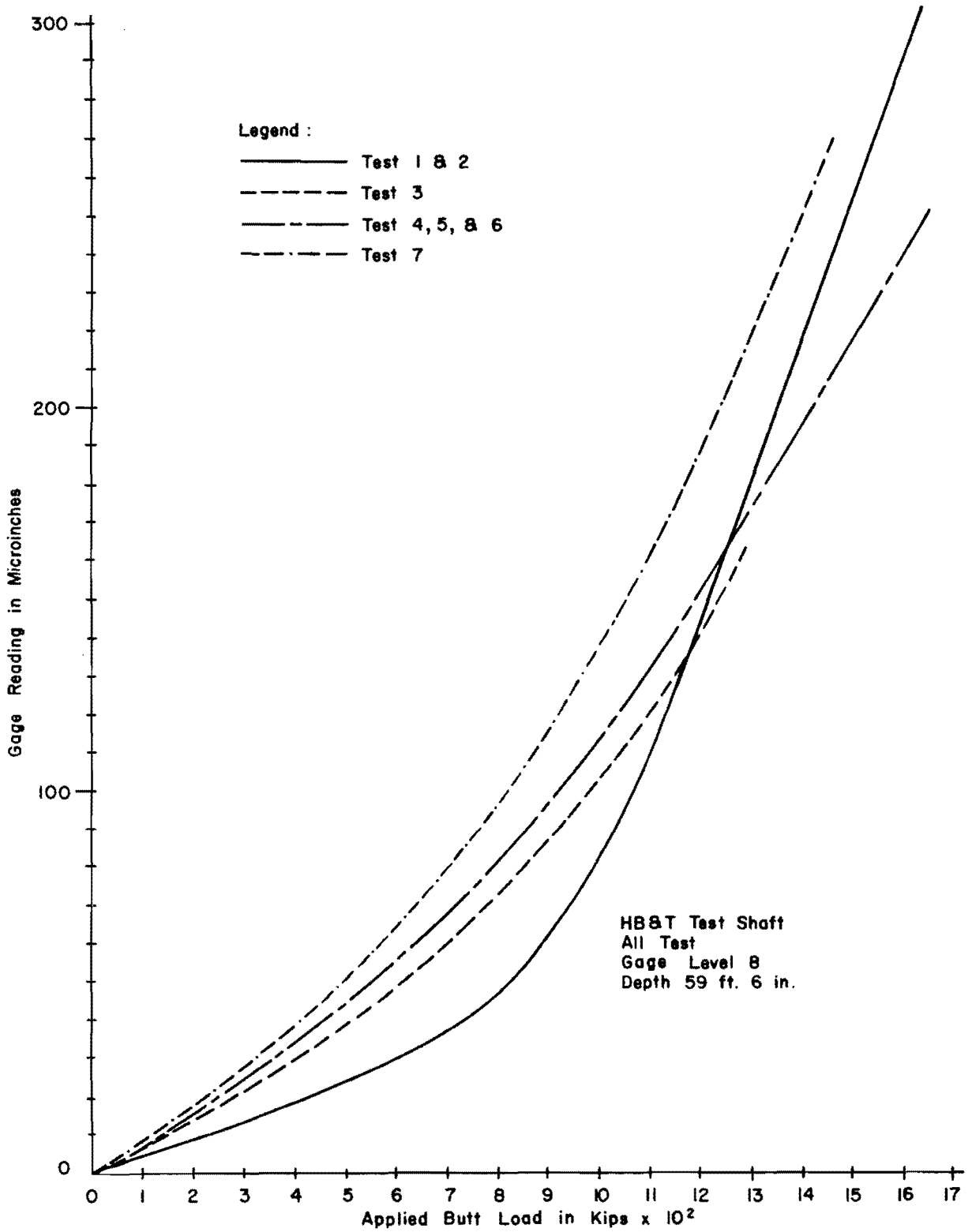

Fig. C.16. Gage Response for all Tests

3. Results of Maintained Load of Test 3

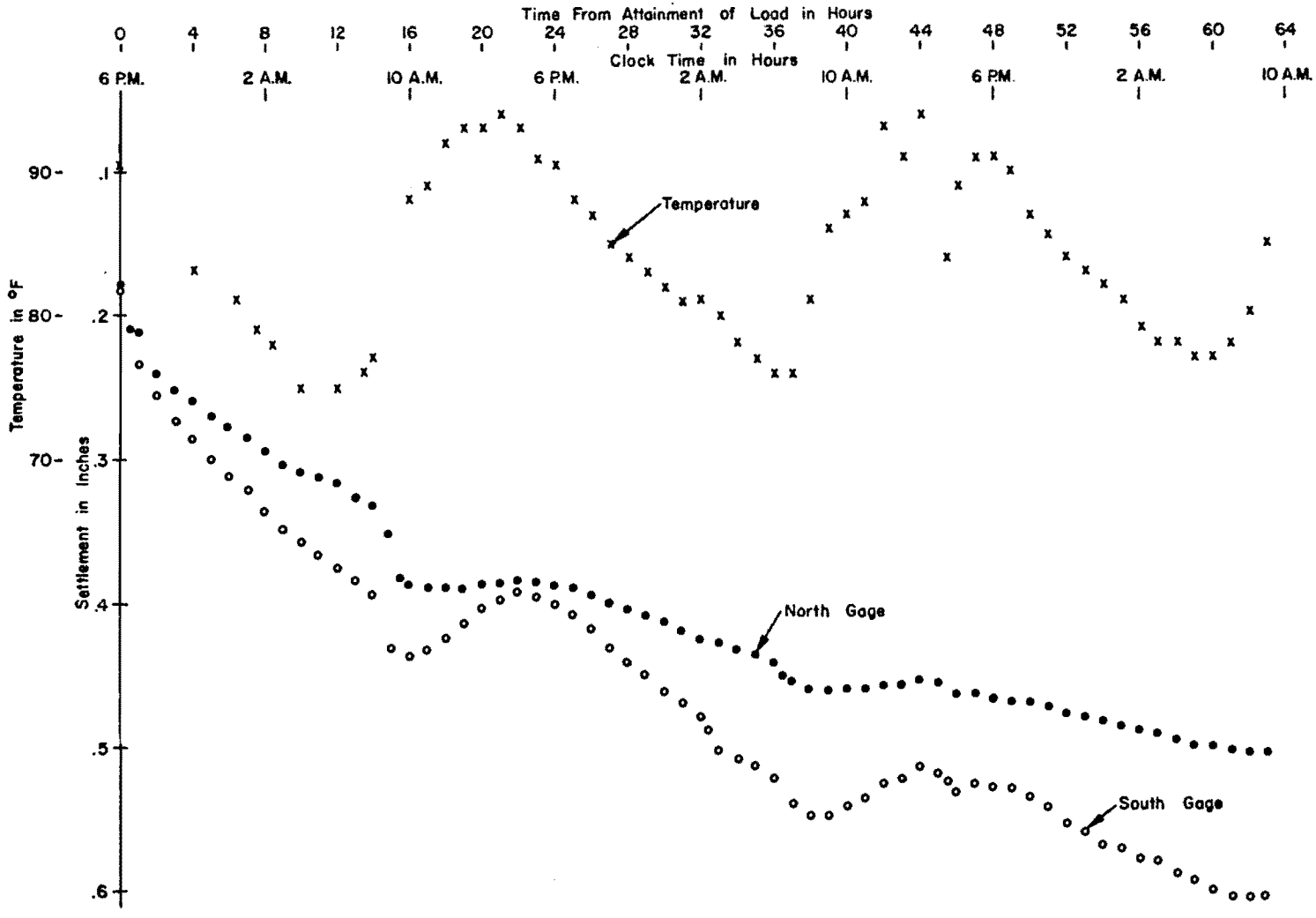

Fig. C.17. Temperature and settlement Gage Changes During Maintained Load of Test 3

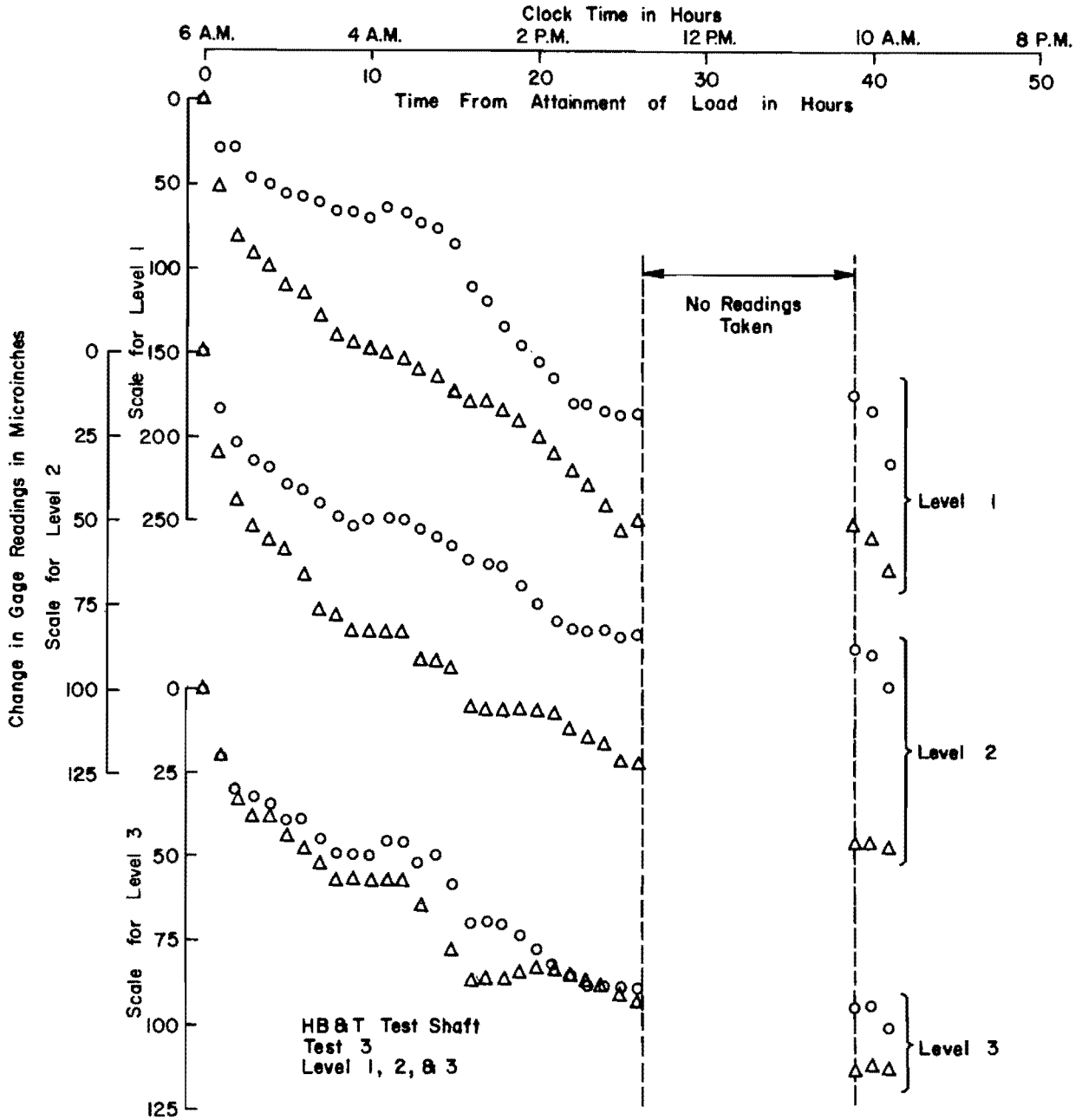

Fig. C.18. Changes in Mustran Gage Reading During Maintained Load of Test 3

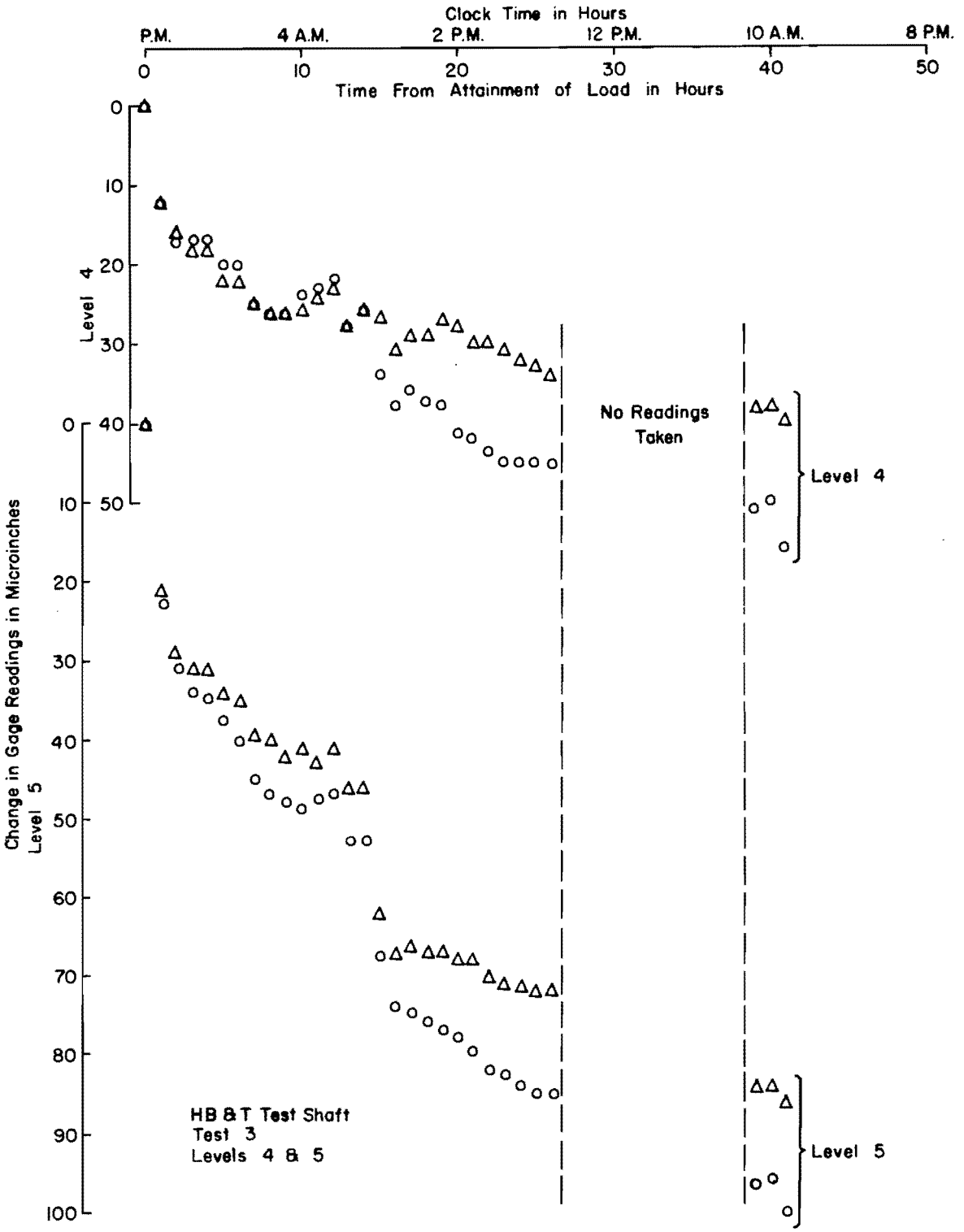

Fig. C.19. Changes in Mustran Gage Reading During Maintained Load of Test 3

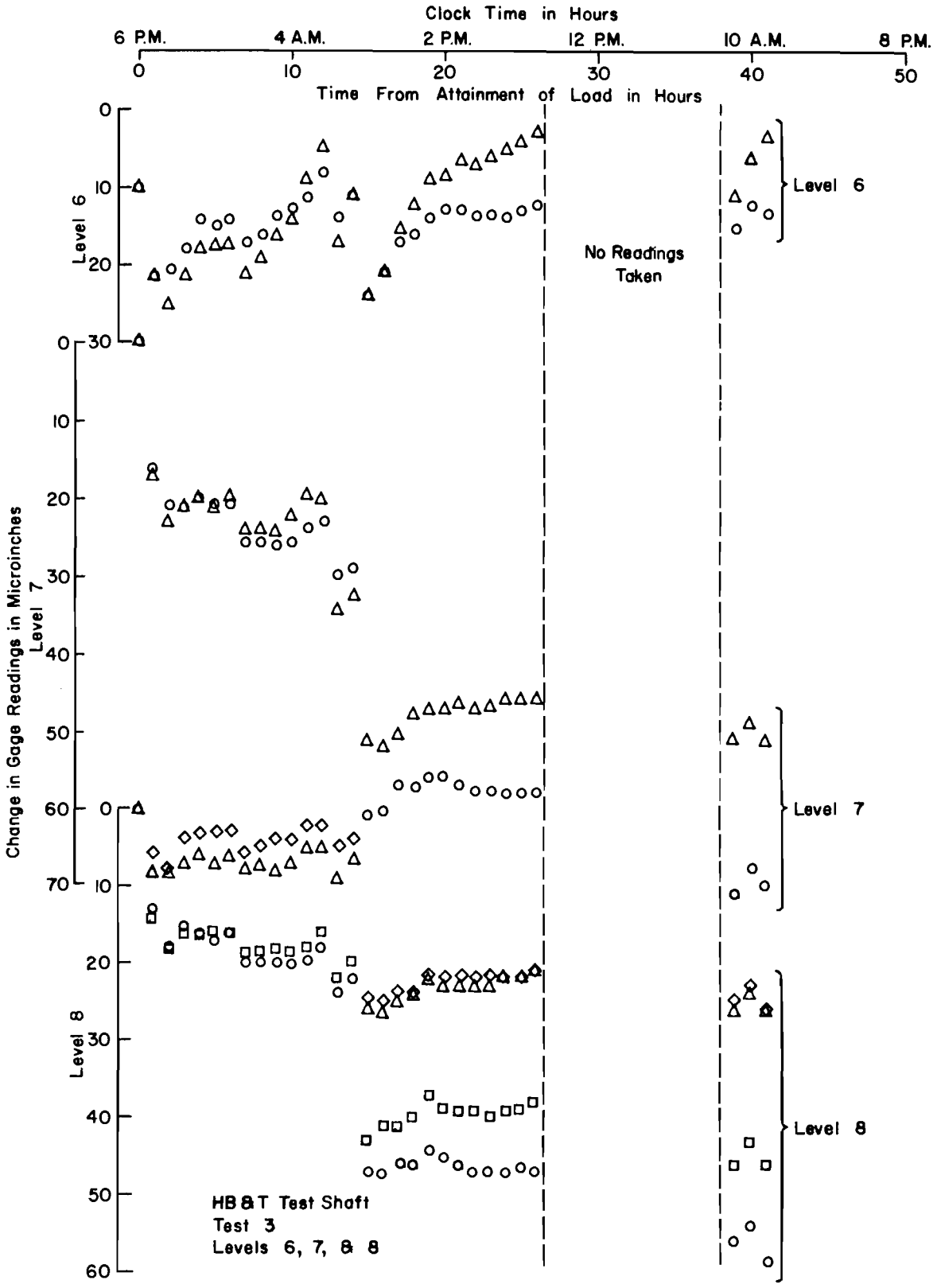

Fig. C.20. Changes in Mustran Gage Reading During Maintained Load of Test 3

4. Results of Maintained Load of Test 6

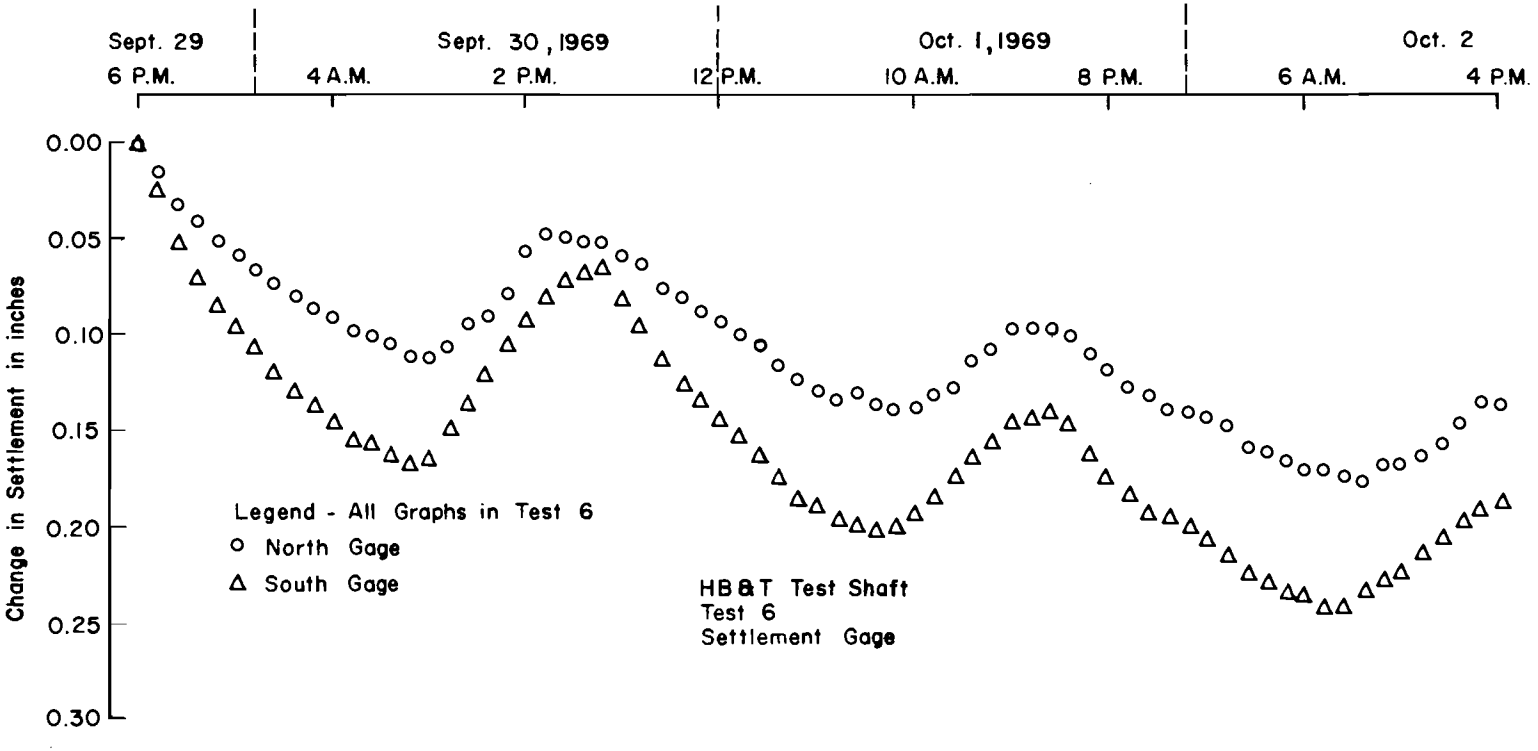

Fig. C.21. Settlement Gage Change during Maintained Load of Test 6

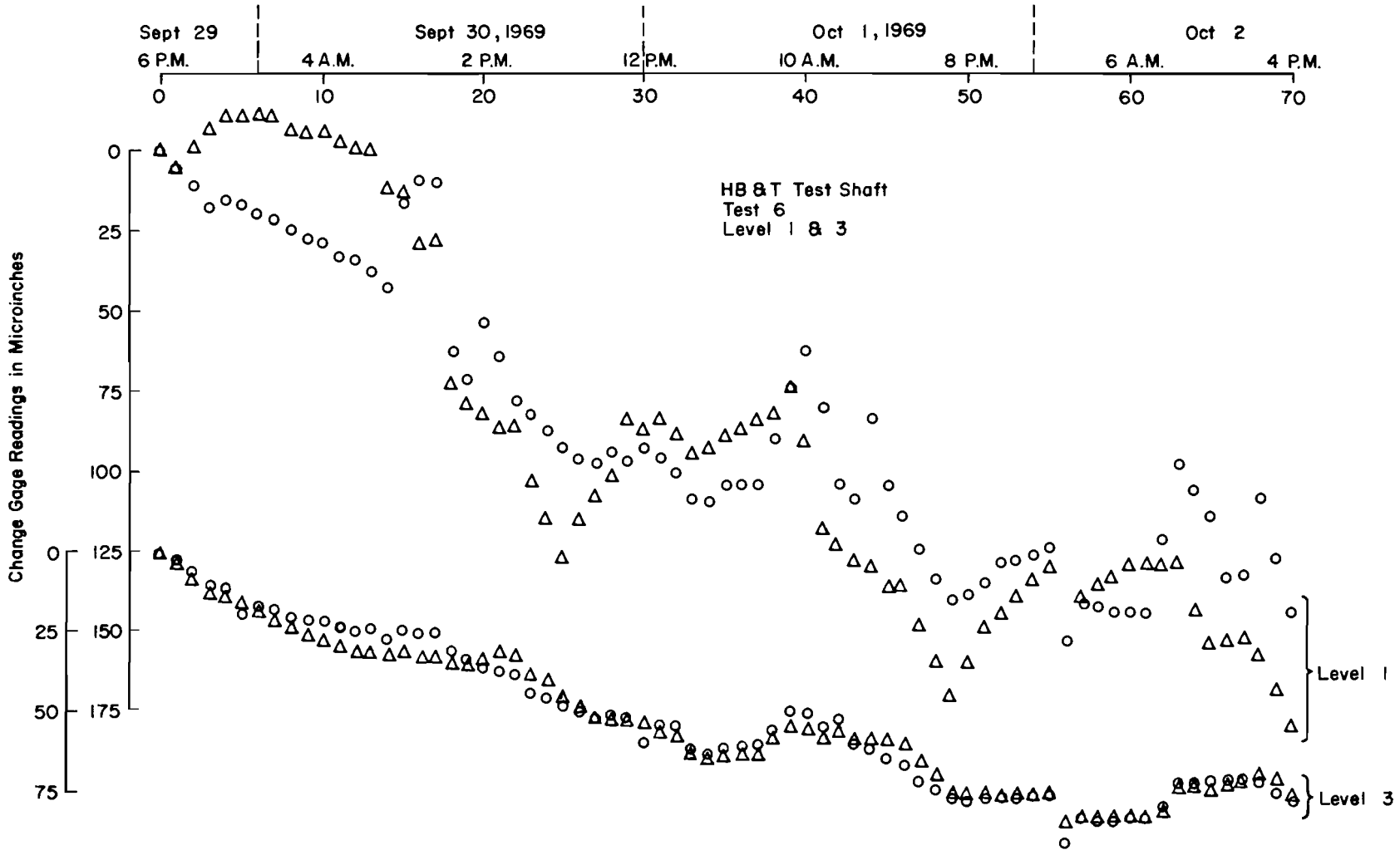

Fig. C.22. Changes in Mustran Gage Readings During Maintained Load of Test 6

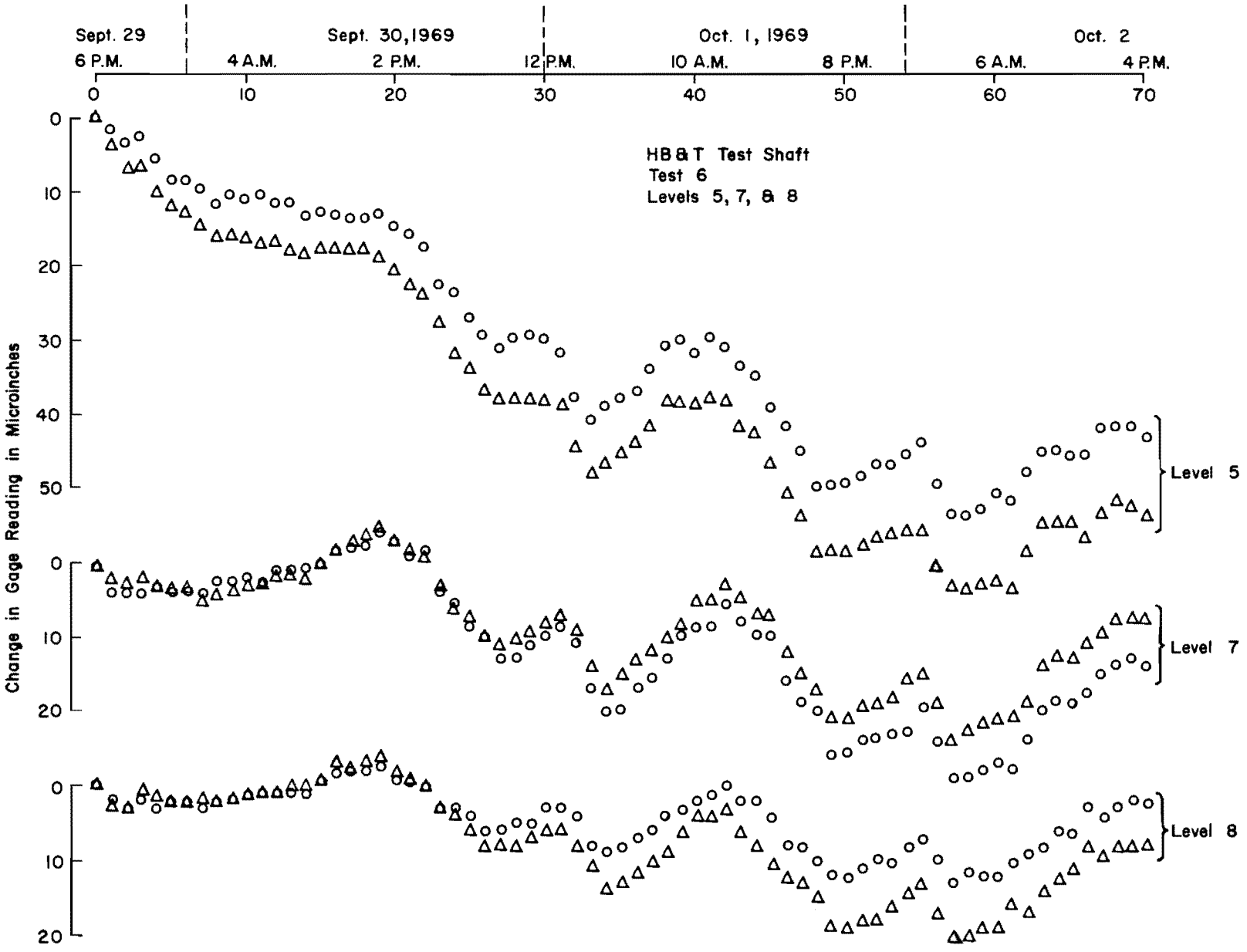

Fig. C.23. Changes in Mustran Gage Readings During Maintained Load of Test 6

5. Gage Response for Test 7

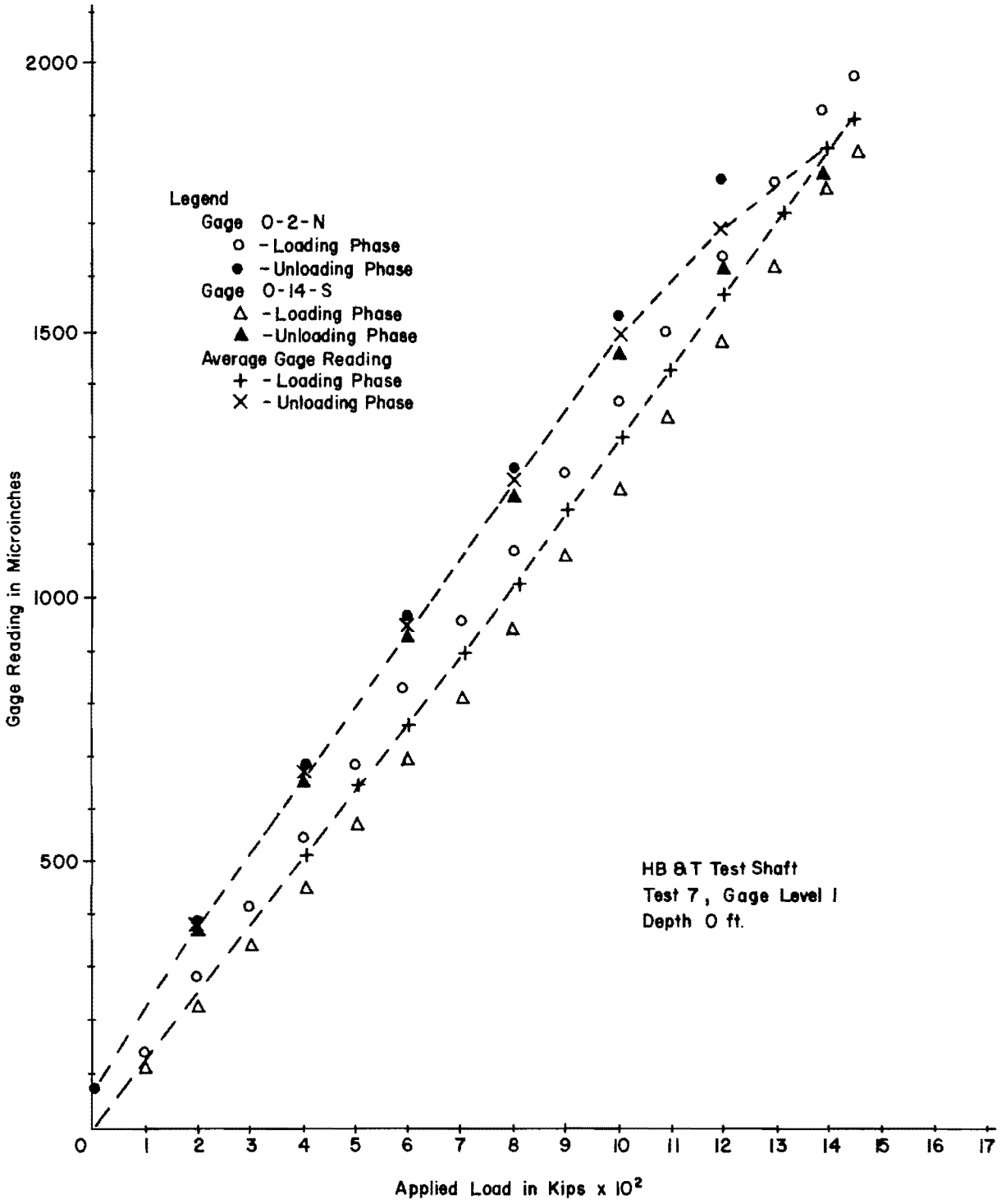

Fig. C.24. Gage Response for Test 7

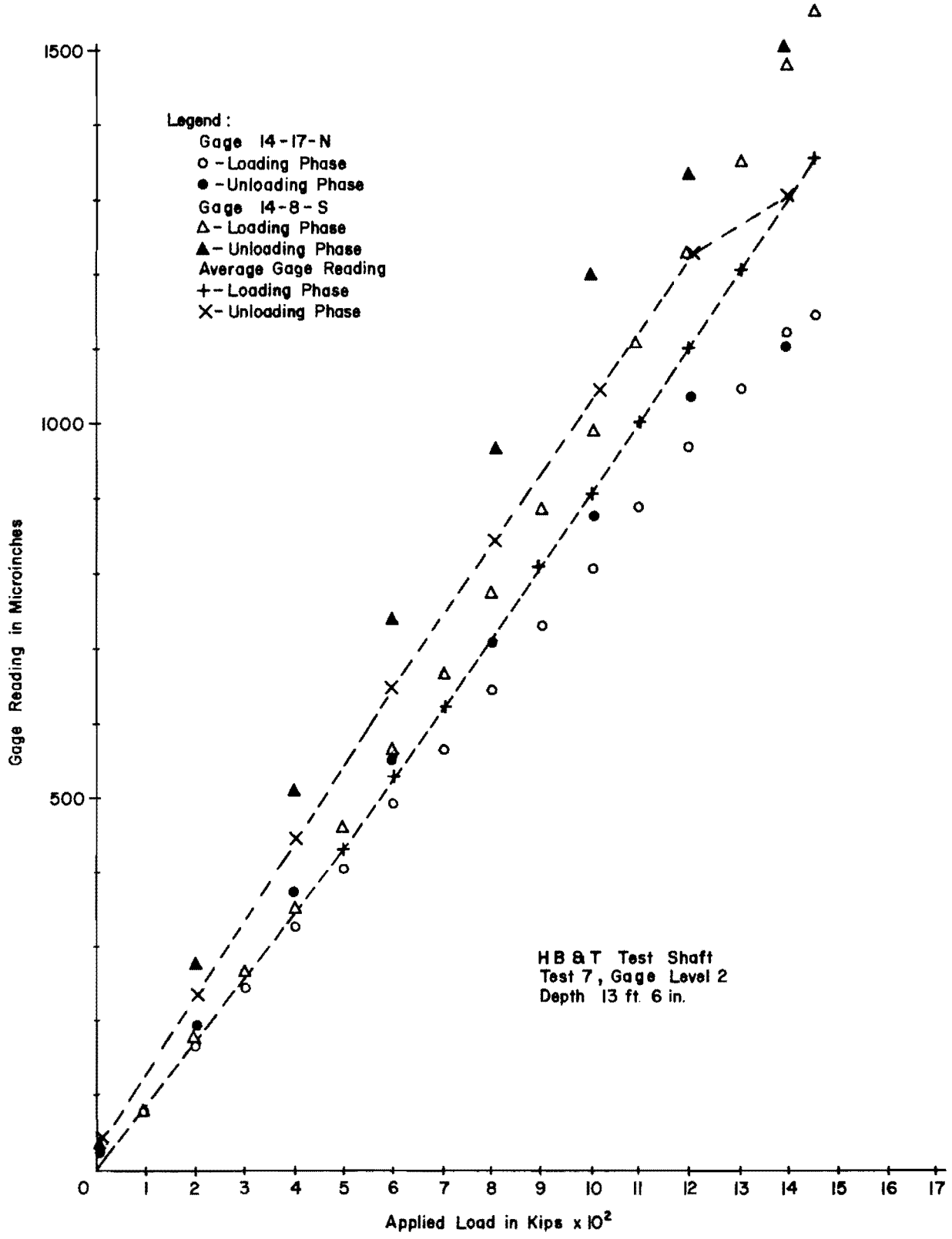

Fig. C.25. Gage Response for Test 7

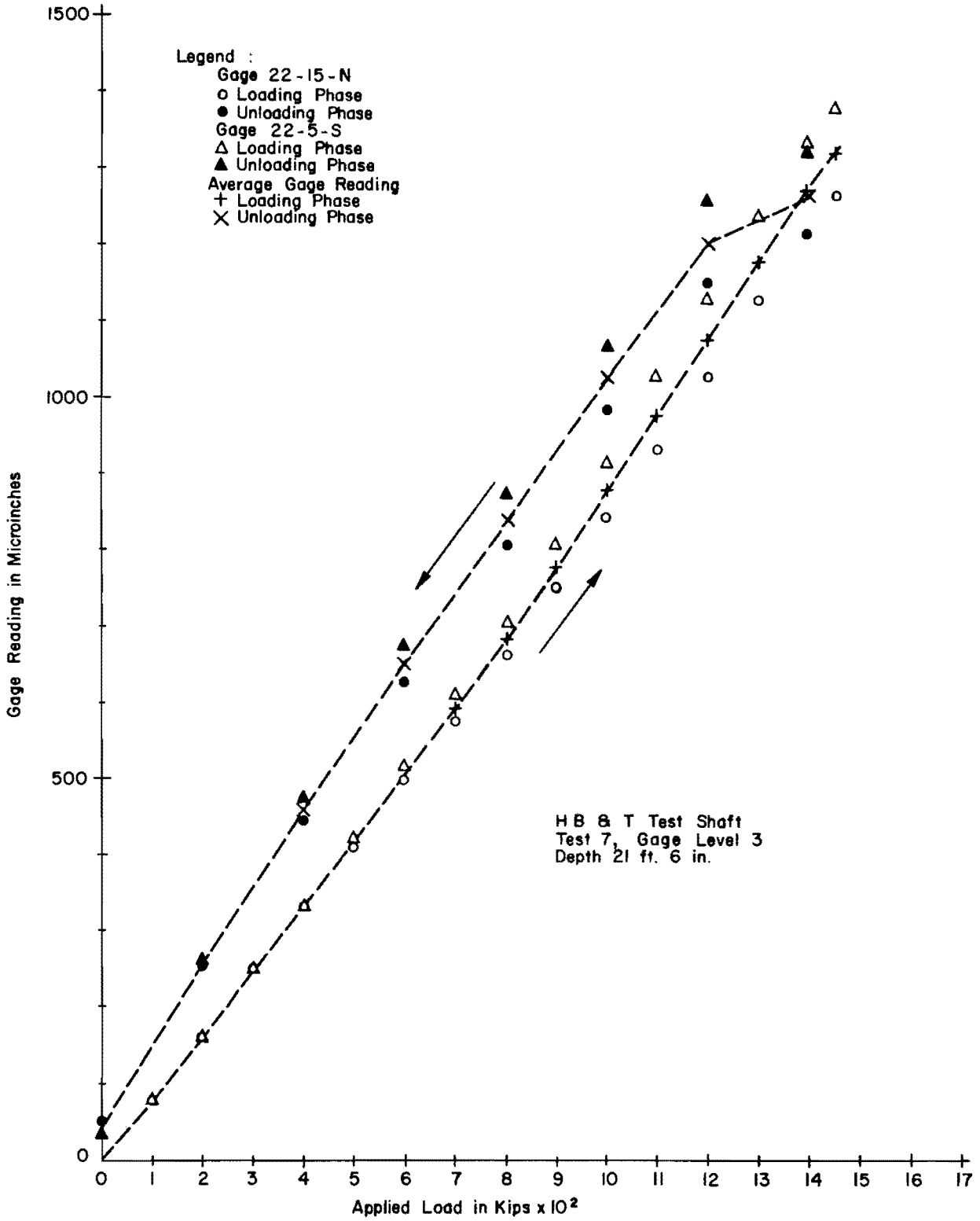

Fig. C.26. Gage Response for Test 7

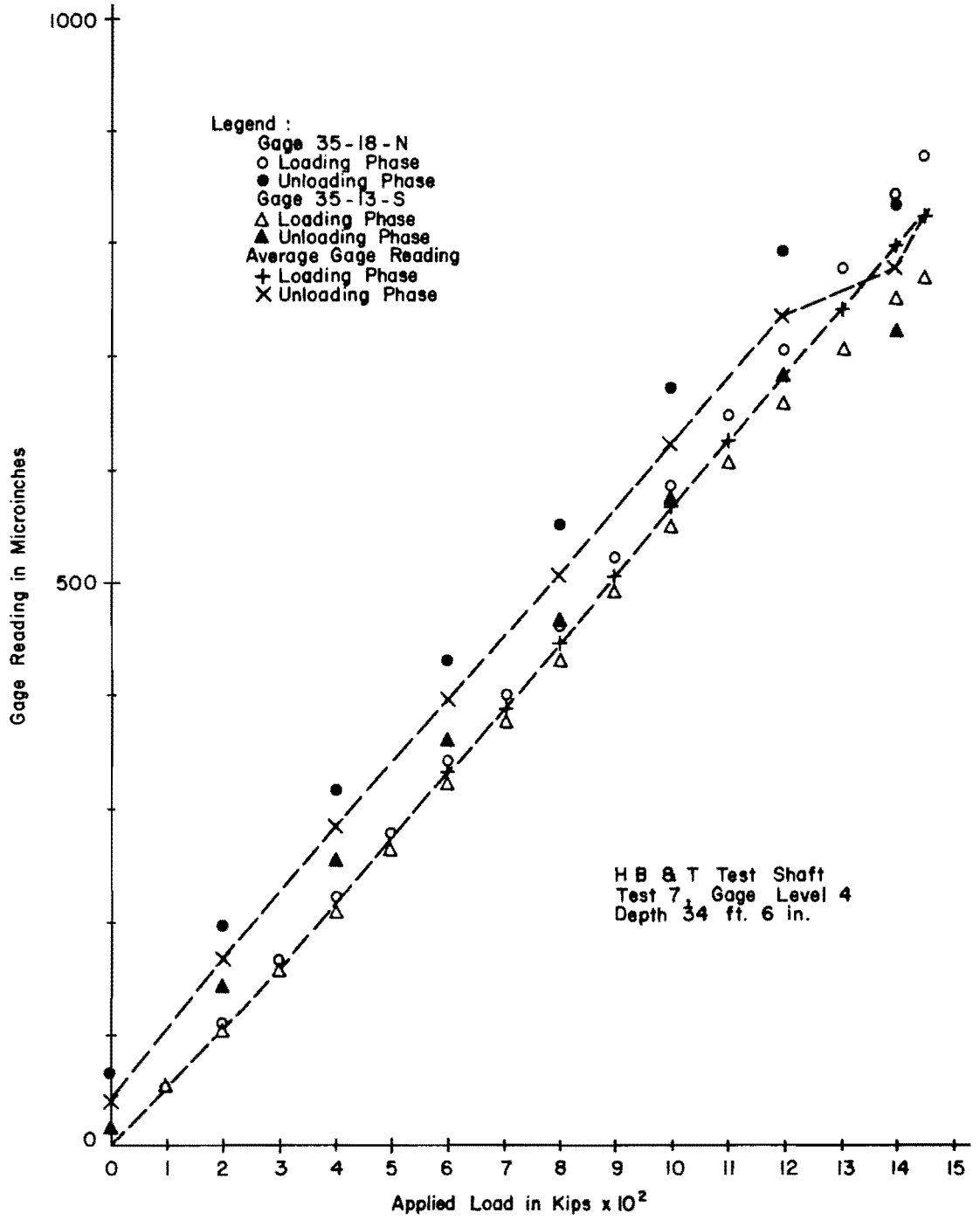

Fig. C.27. Gage Response for Test 7

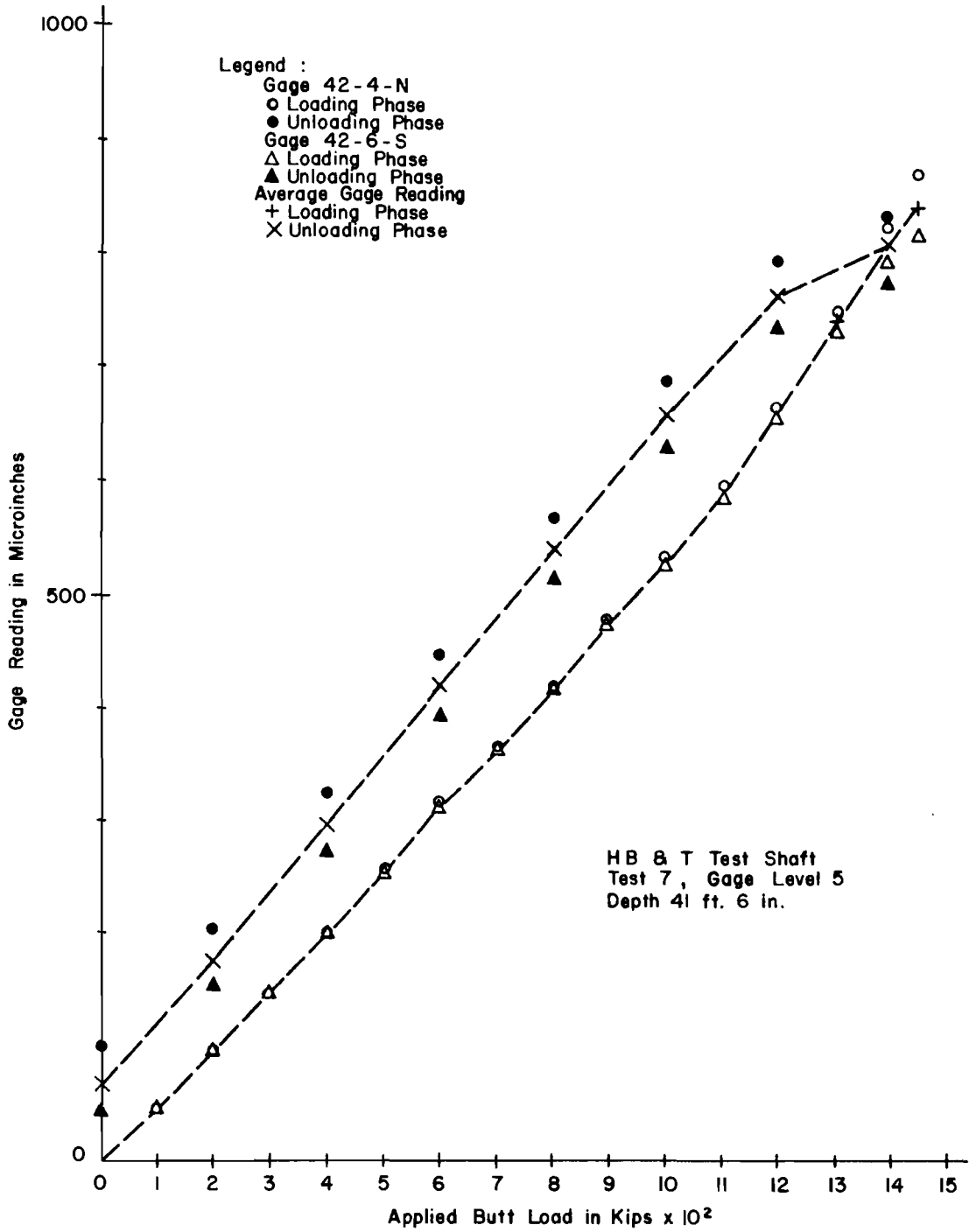

Fig. C.28. Gage Response for Test 7

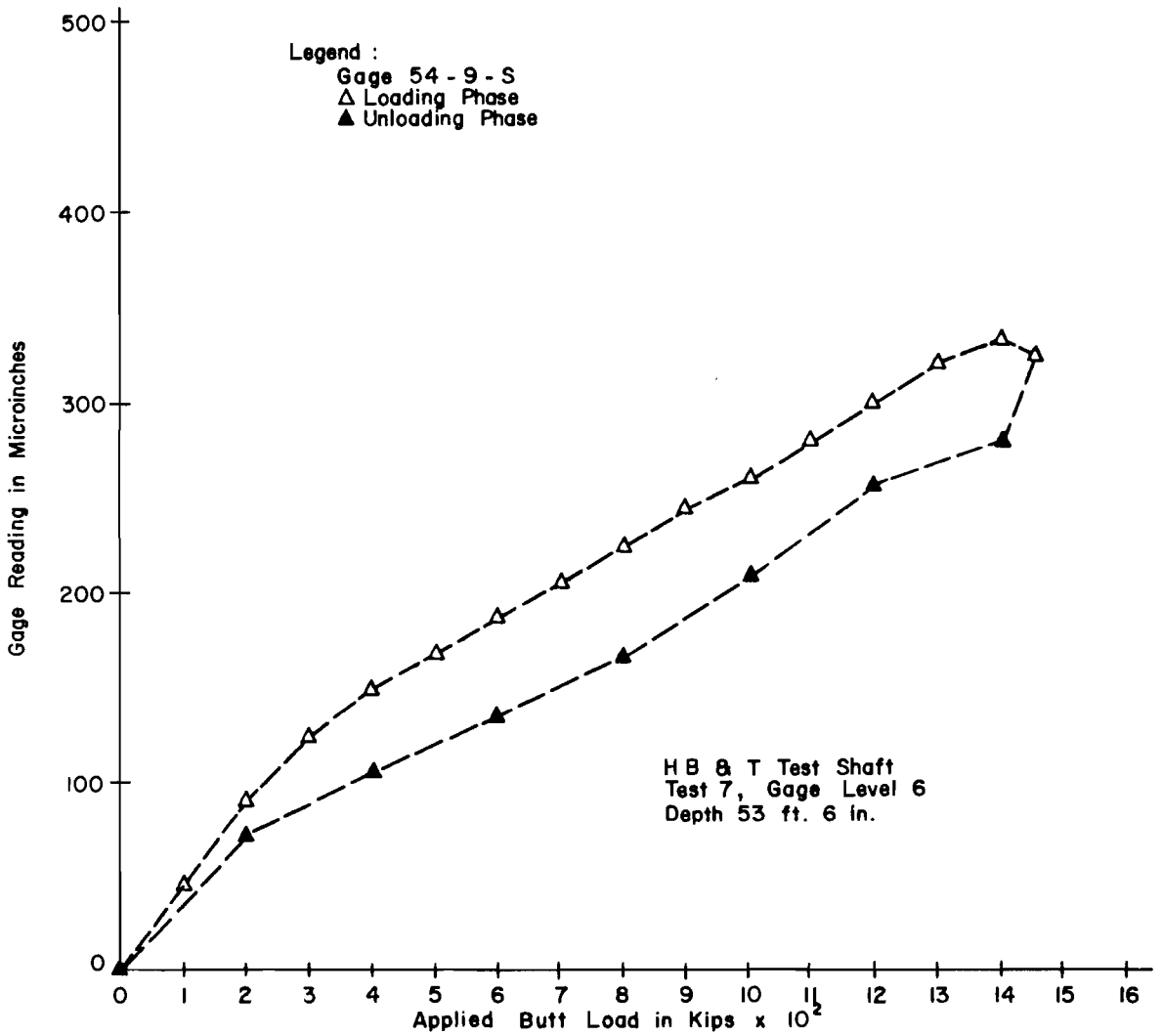

Fig. C.29. Gage Response for Test 7

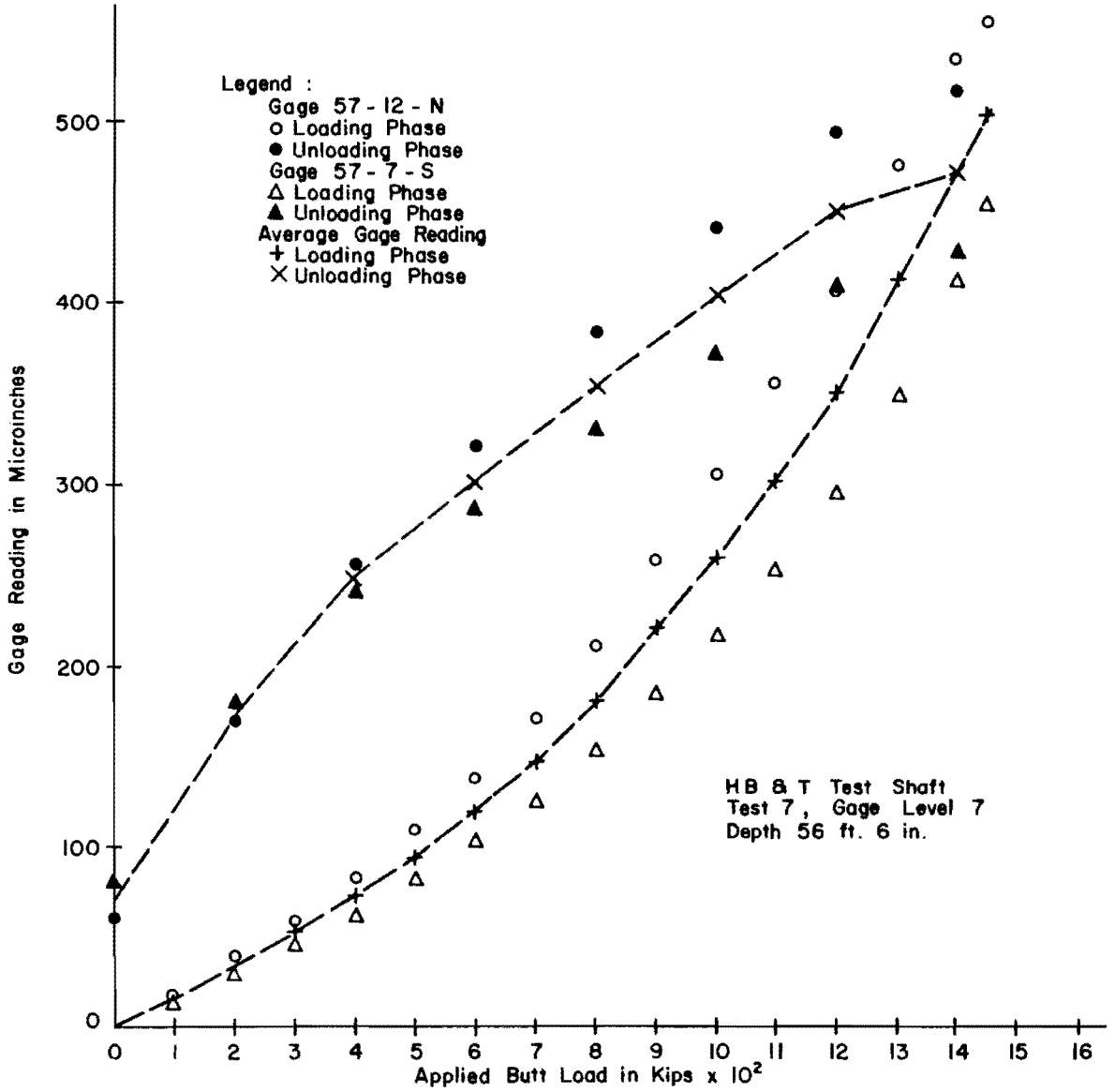

Fig. C.30. Gage Response for Test 7

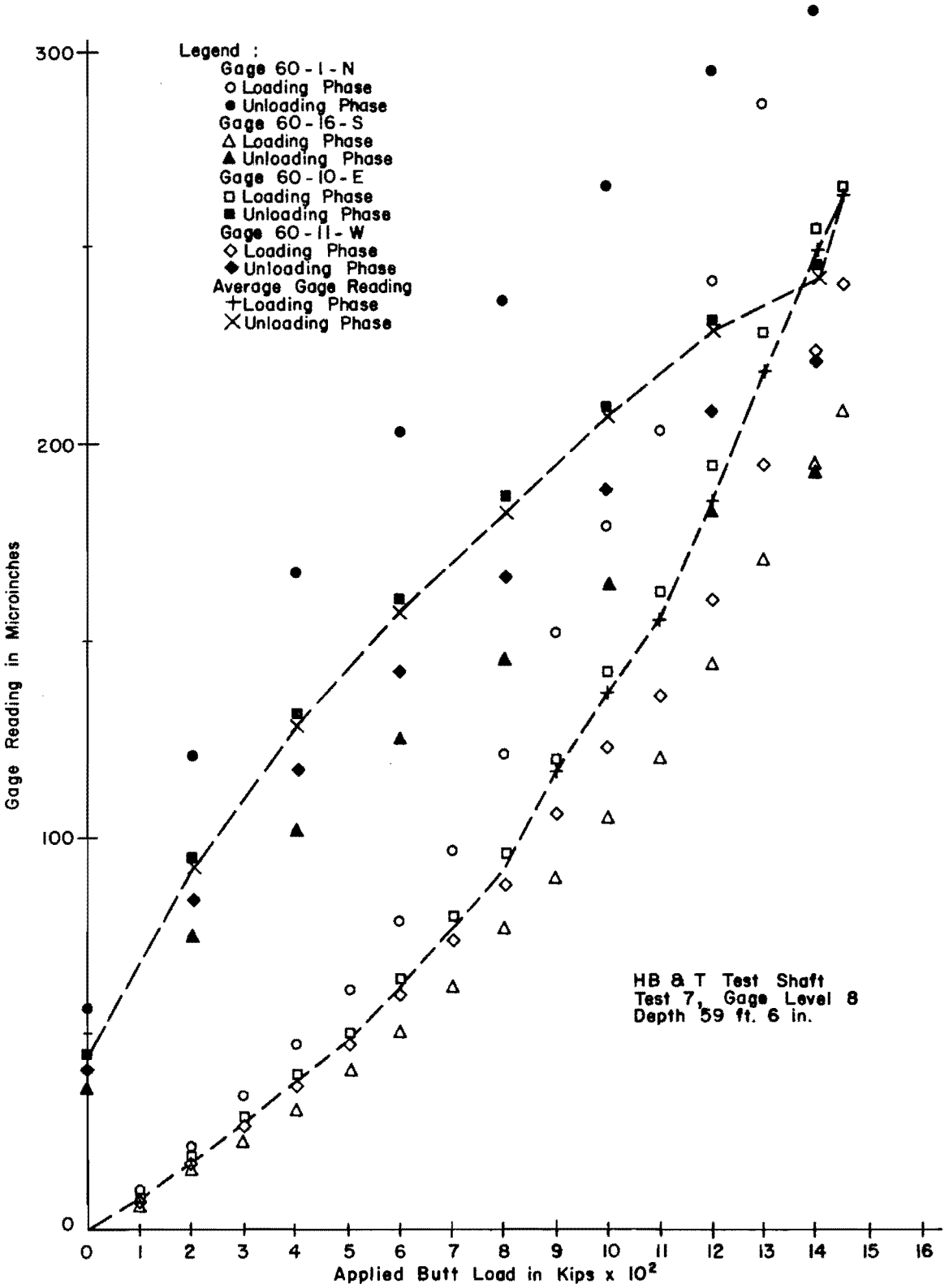

Fig. C.31. Gage Response for Test 7

APPENDIX D

LOAD-DISTRIBUTION AND LOAD-TRANSFER CURVES

1. Load-Distribution Curves

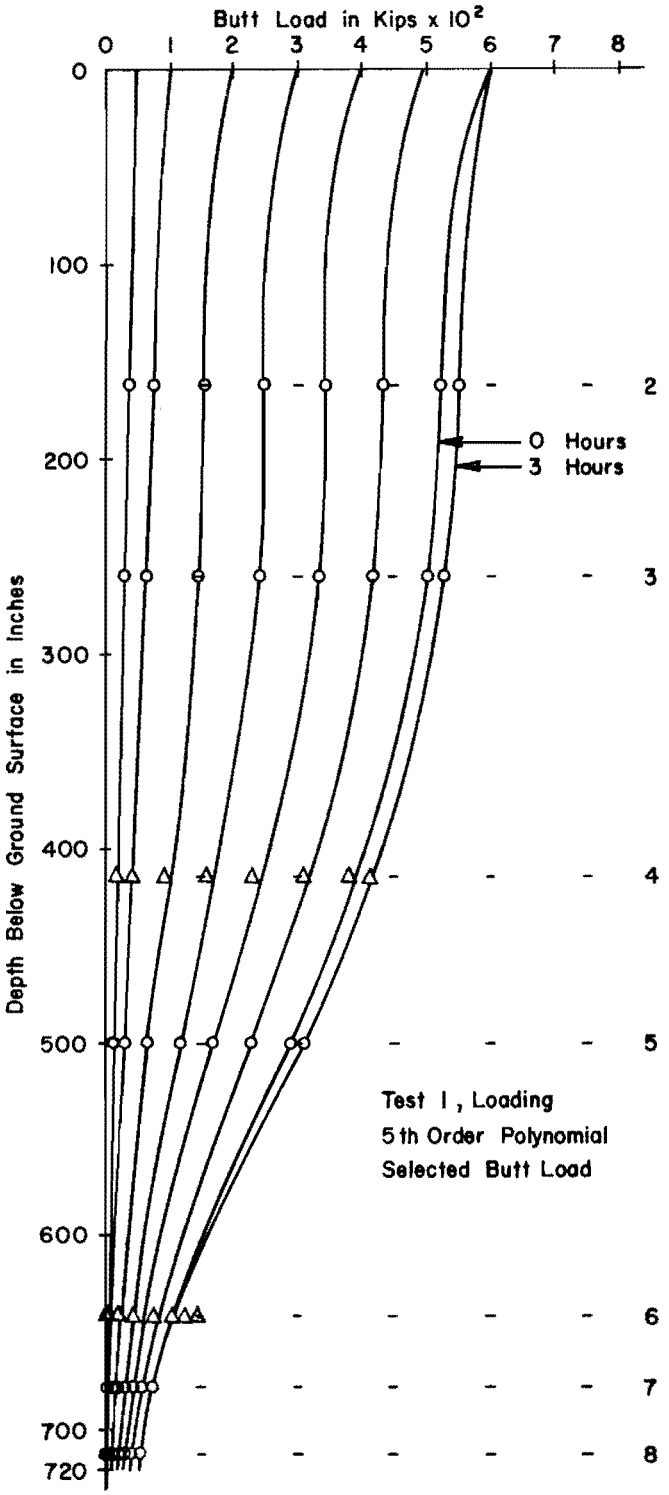

Fig. D.1. Load-Distribution Curves

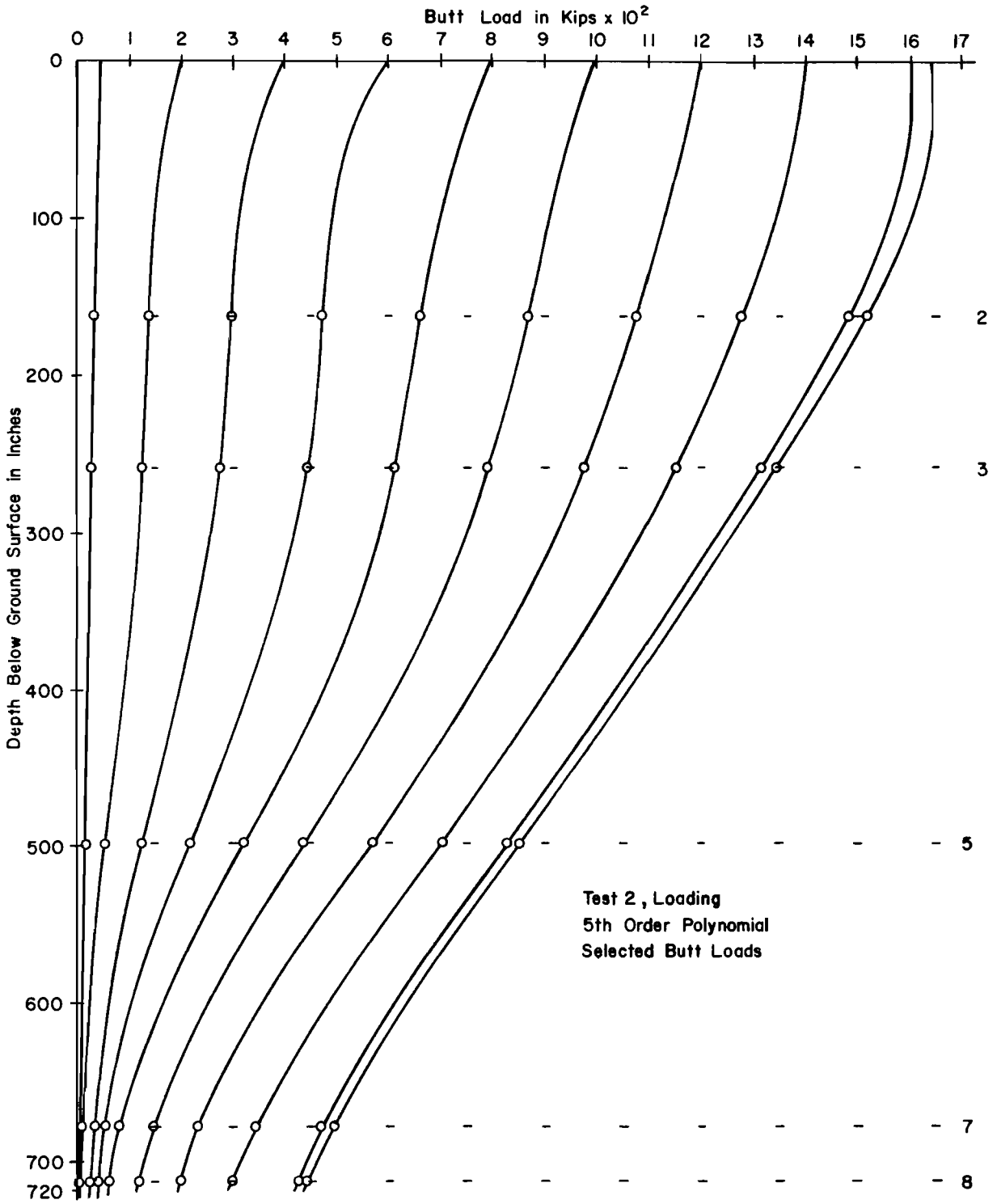

Fig. D.2. Load-Distribution Curves

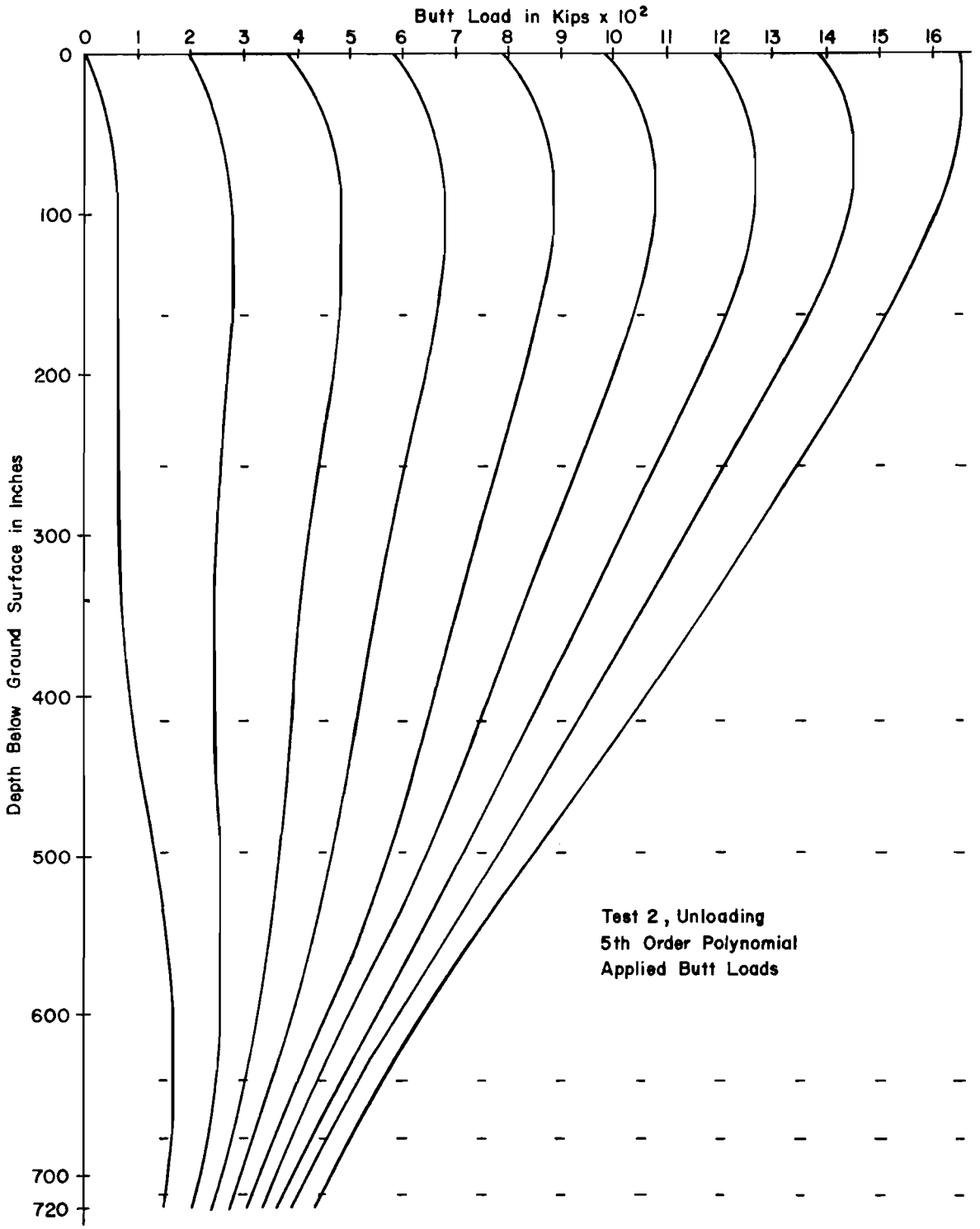

Fig. D.3. Load-Distribution Curves

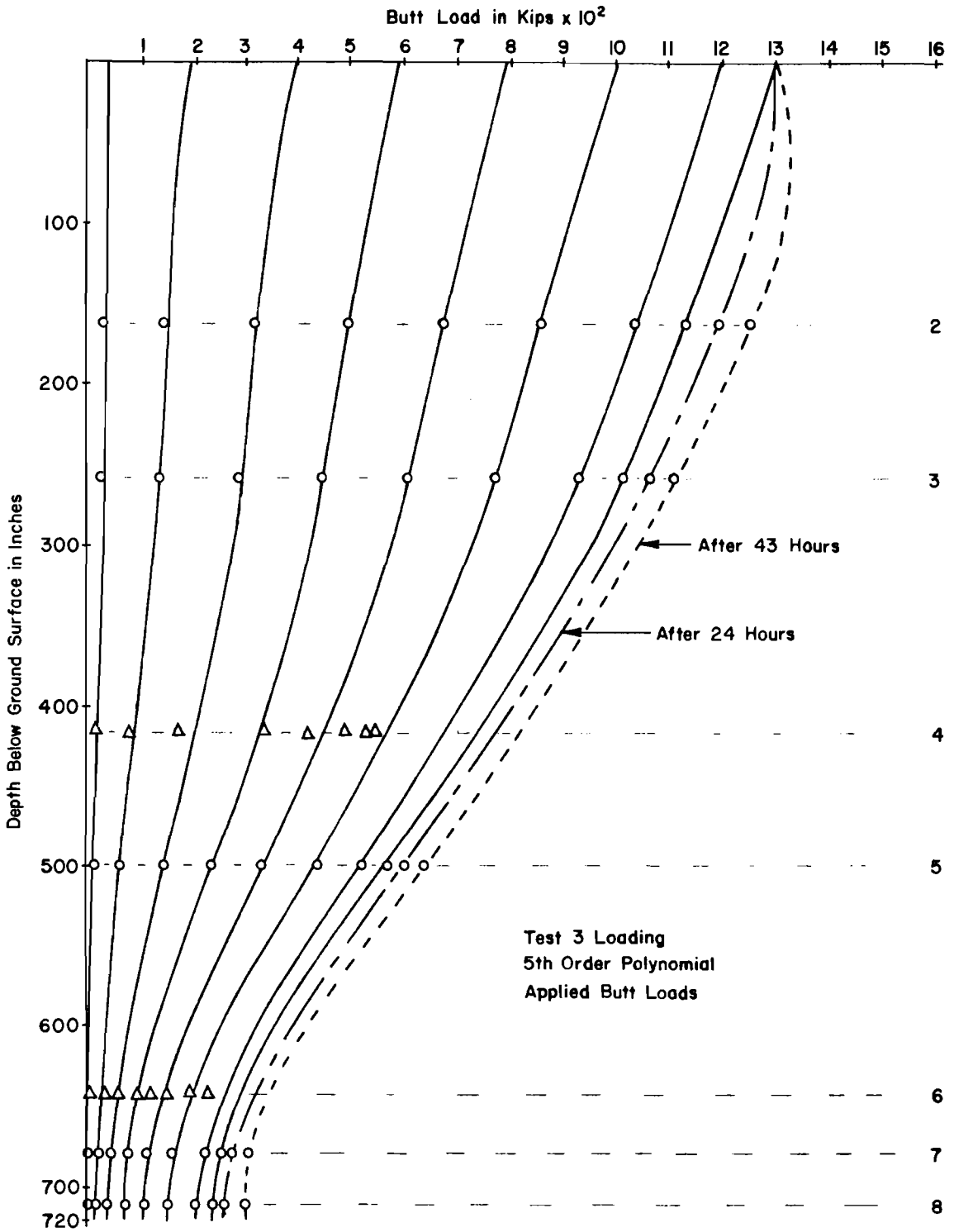

Fig. D.4. Load-Distribution Curves

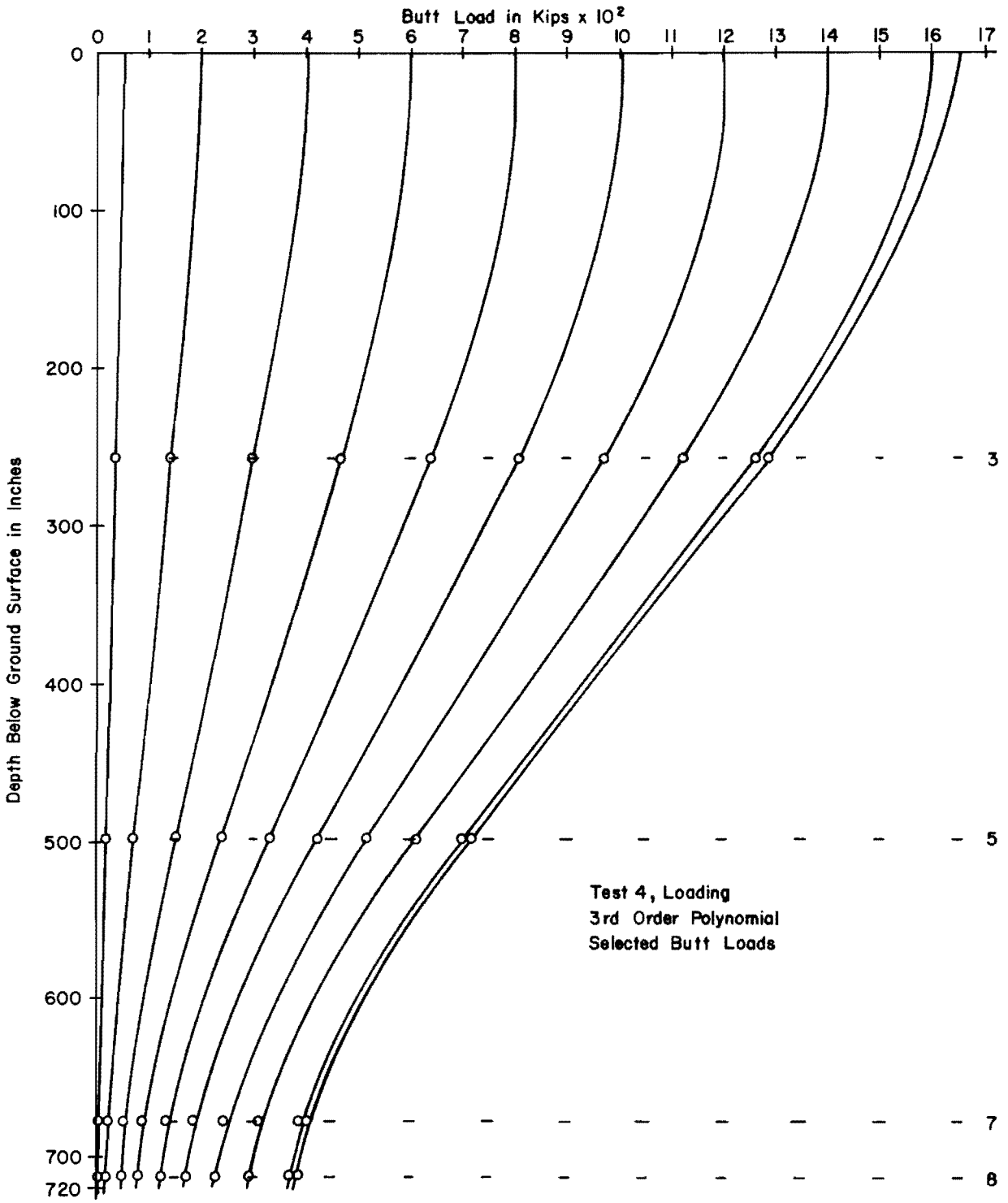

Fig. D.5. Load-Distribution Curves

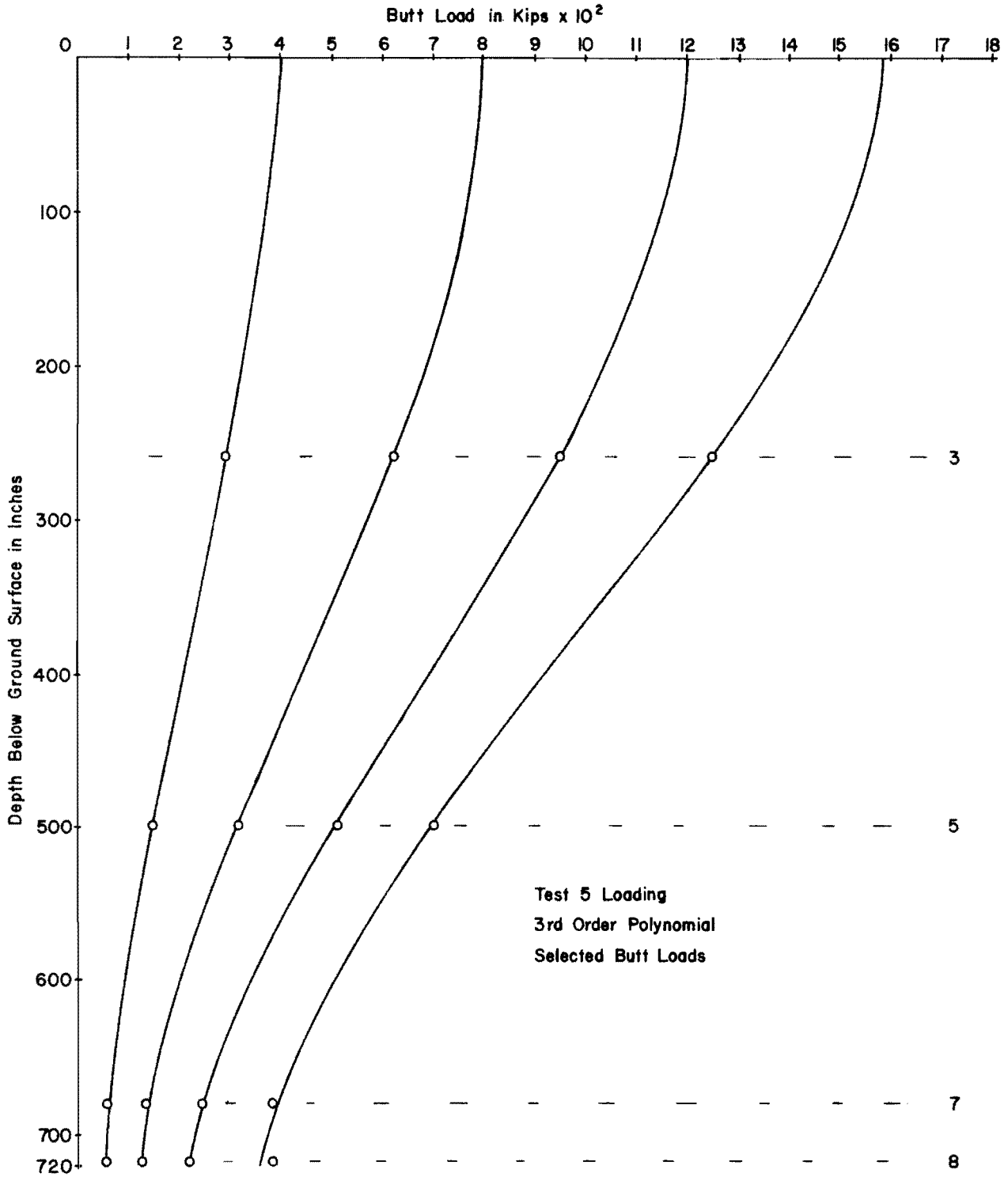

Fig. D.6. Load-Distribution Curves

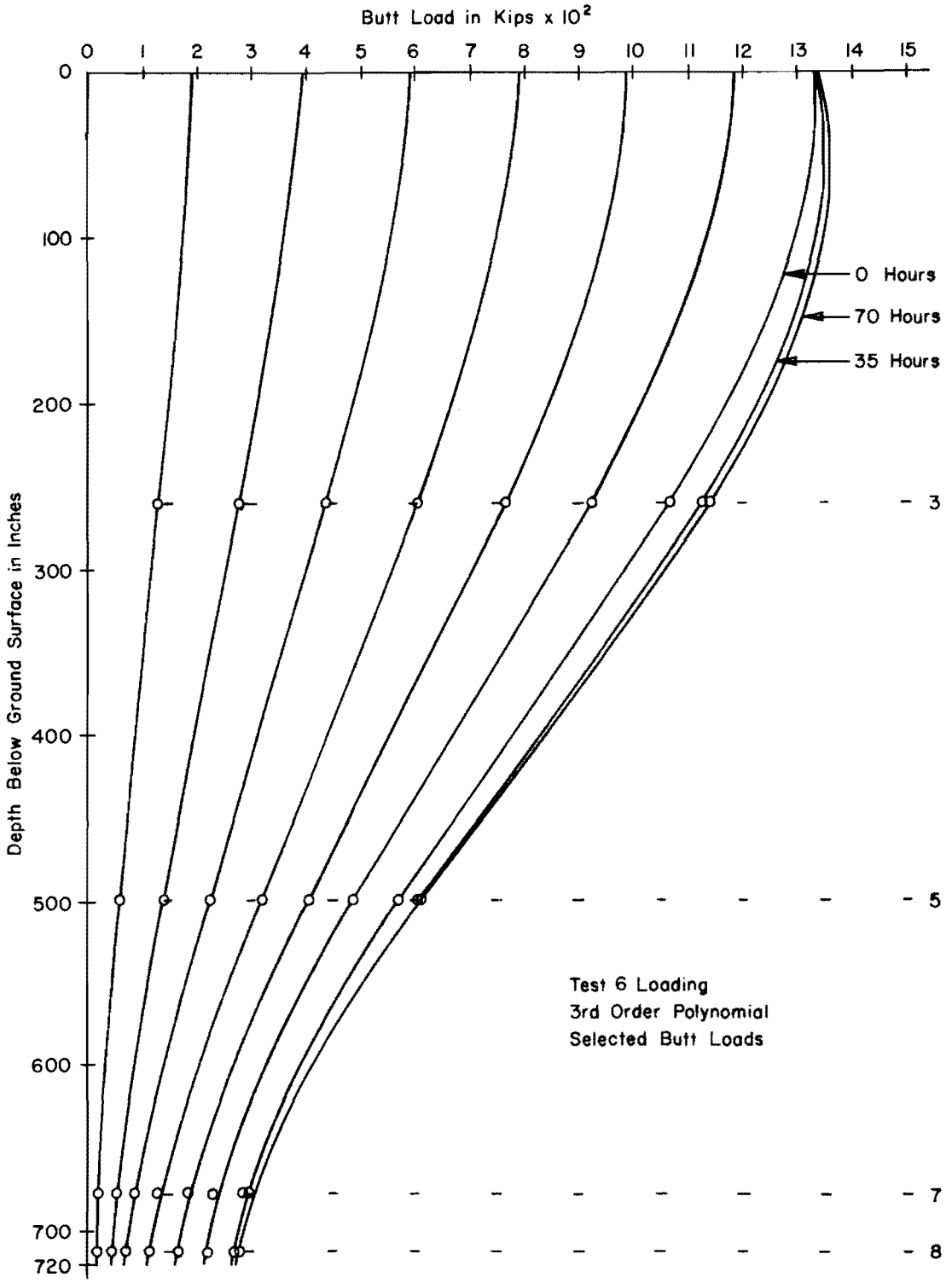

Fig. D.7. Load-Distribution Curves

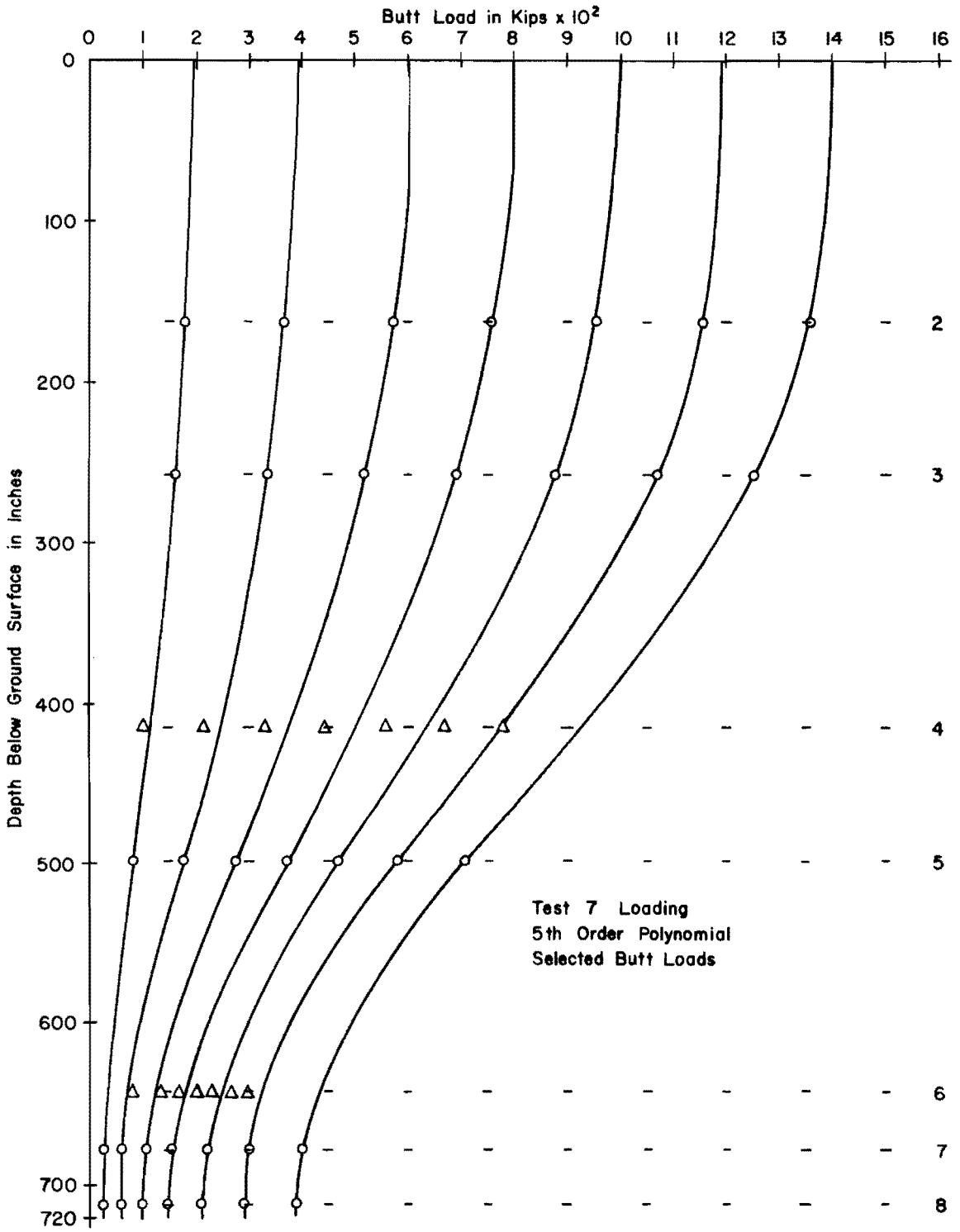

Fig. D.8. Load-Distribution Curves

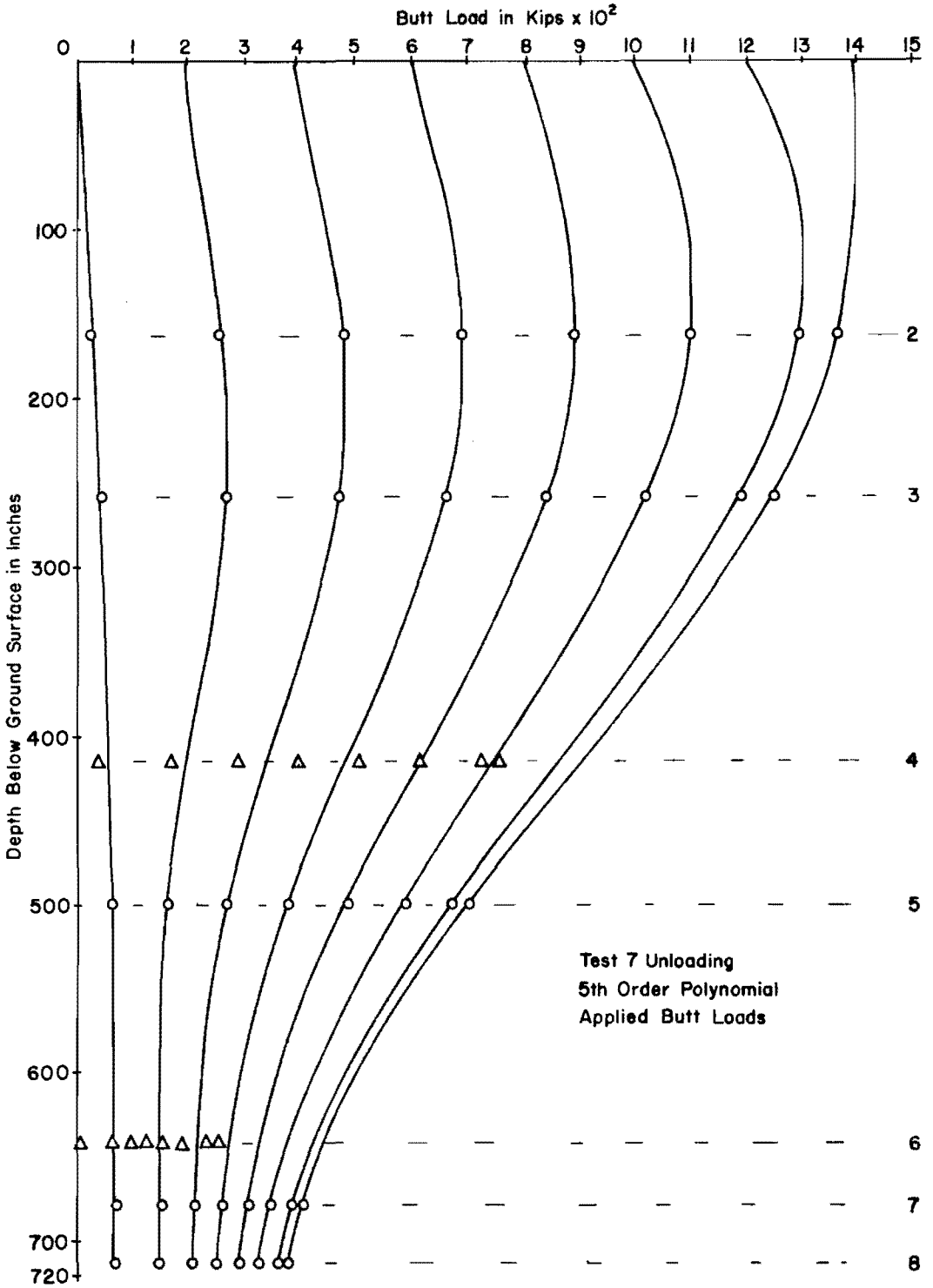

Fig. D.9. Load-Distribution Curves

2. Load-Transfer Curves

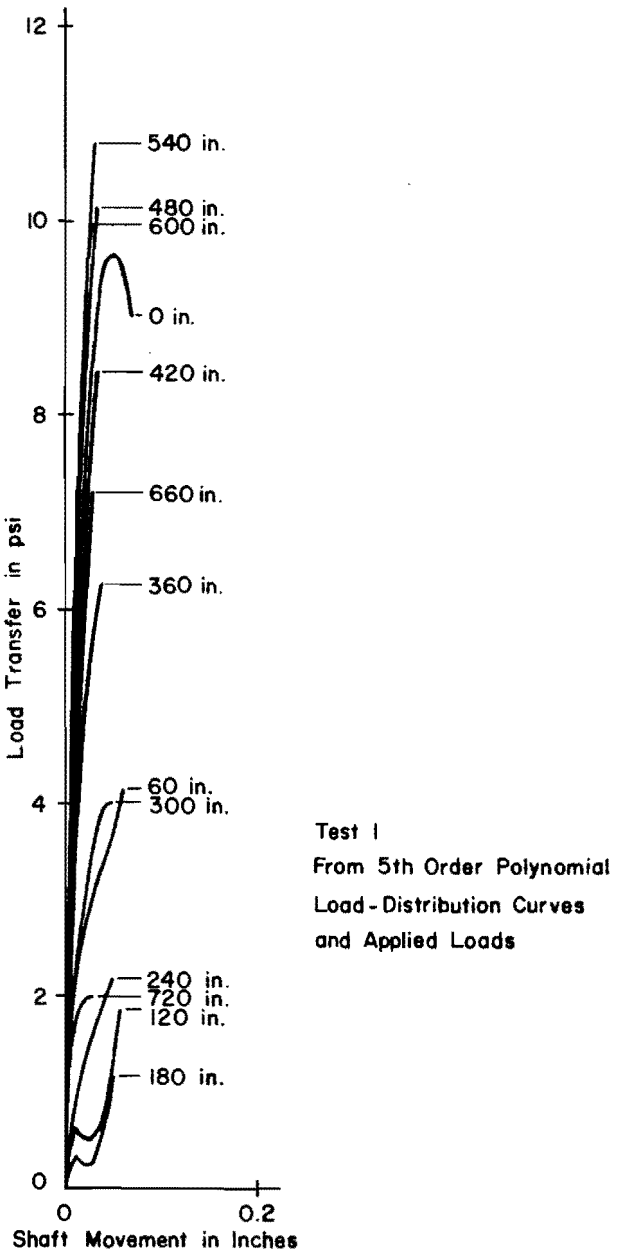

Fig. D.10. Load-Transfer Curves

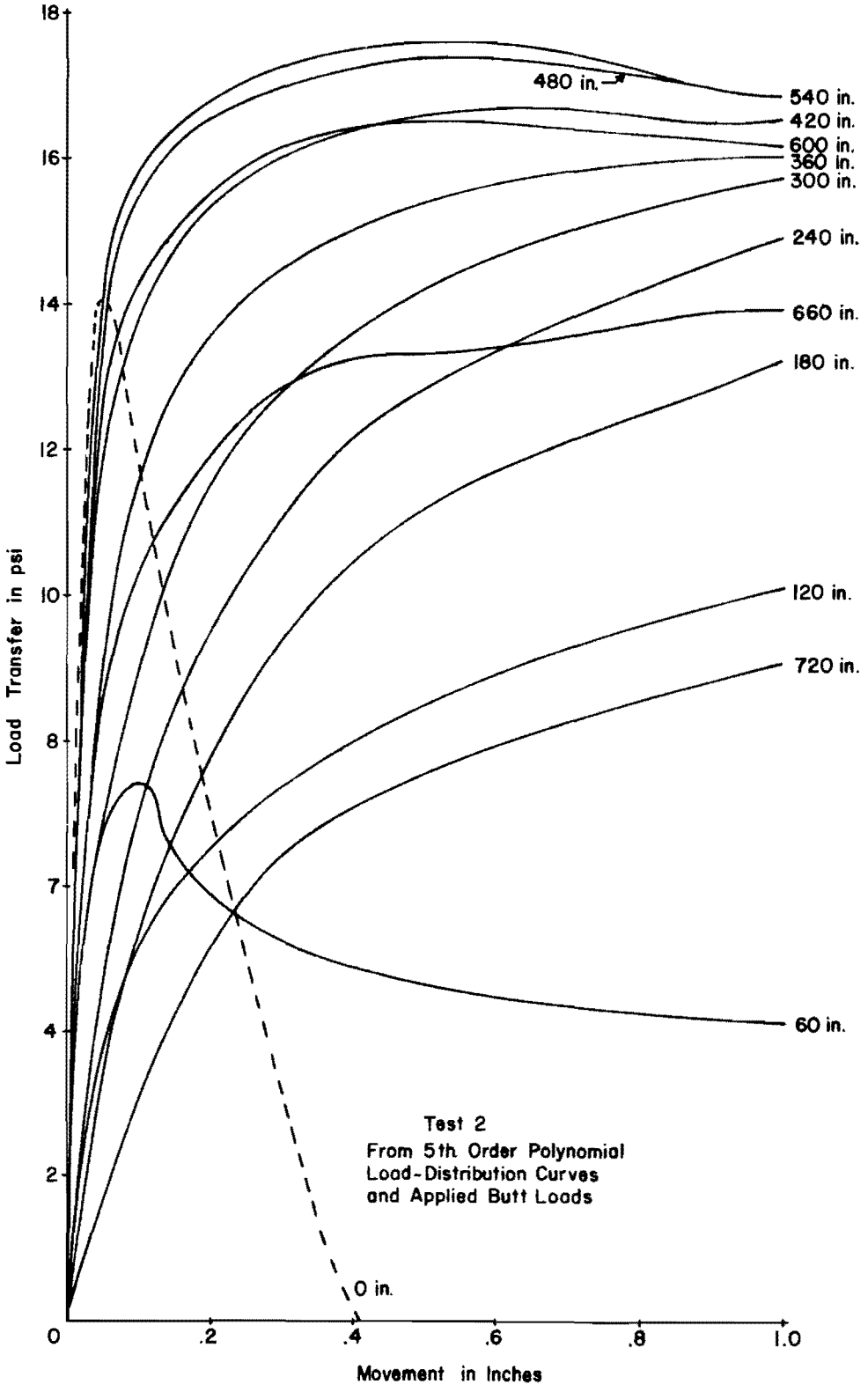

Fig. D.11. Load-Transfer Curves

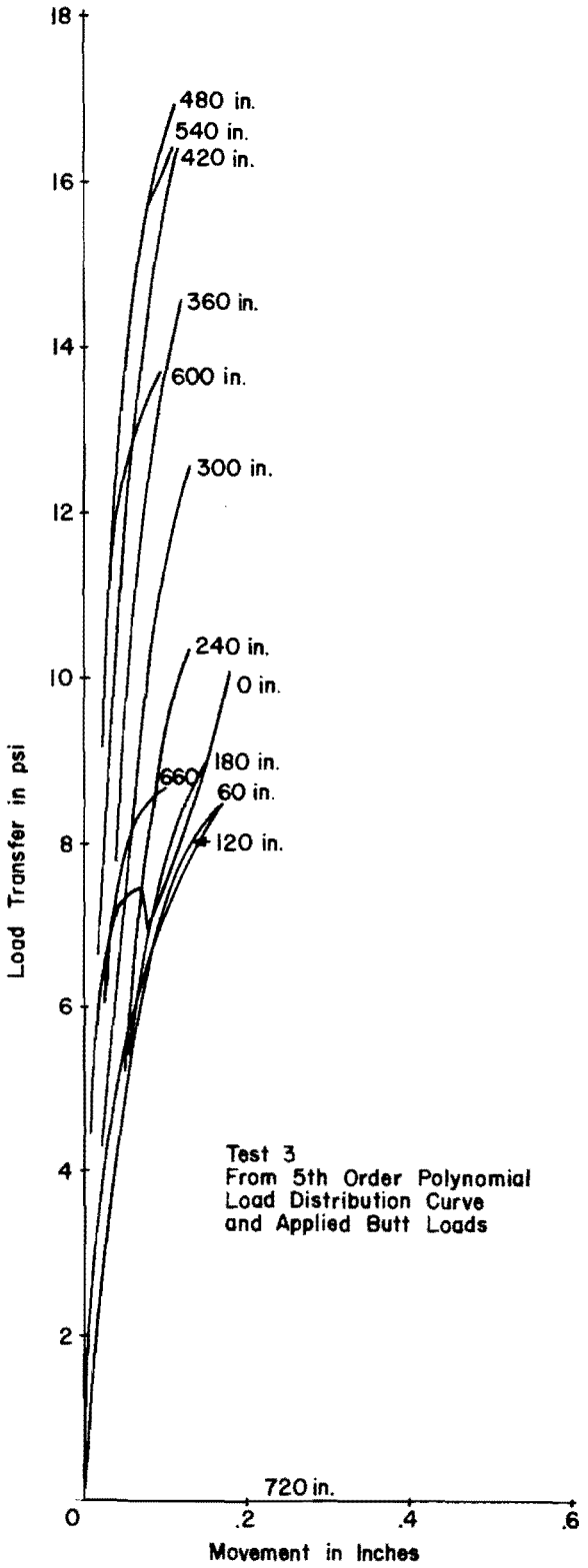

Fig. D.12. Load-Transfer Curves

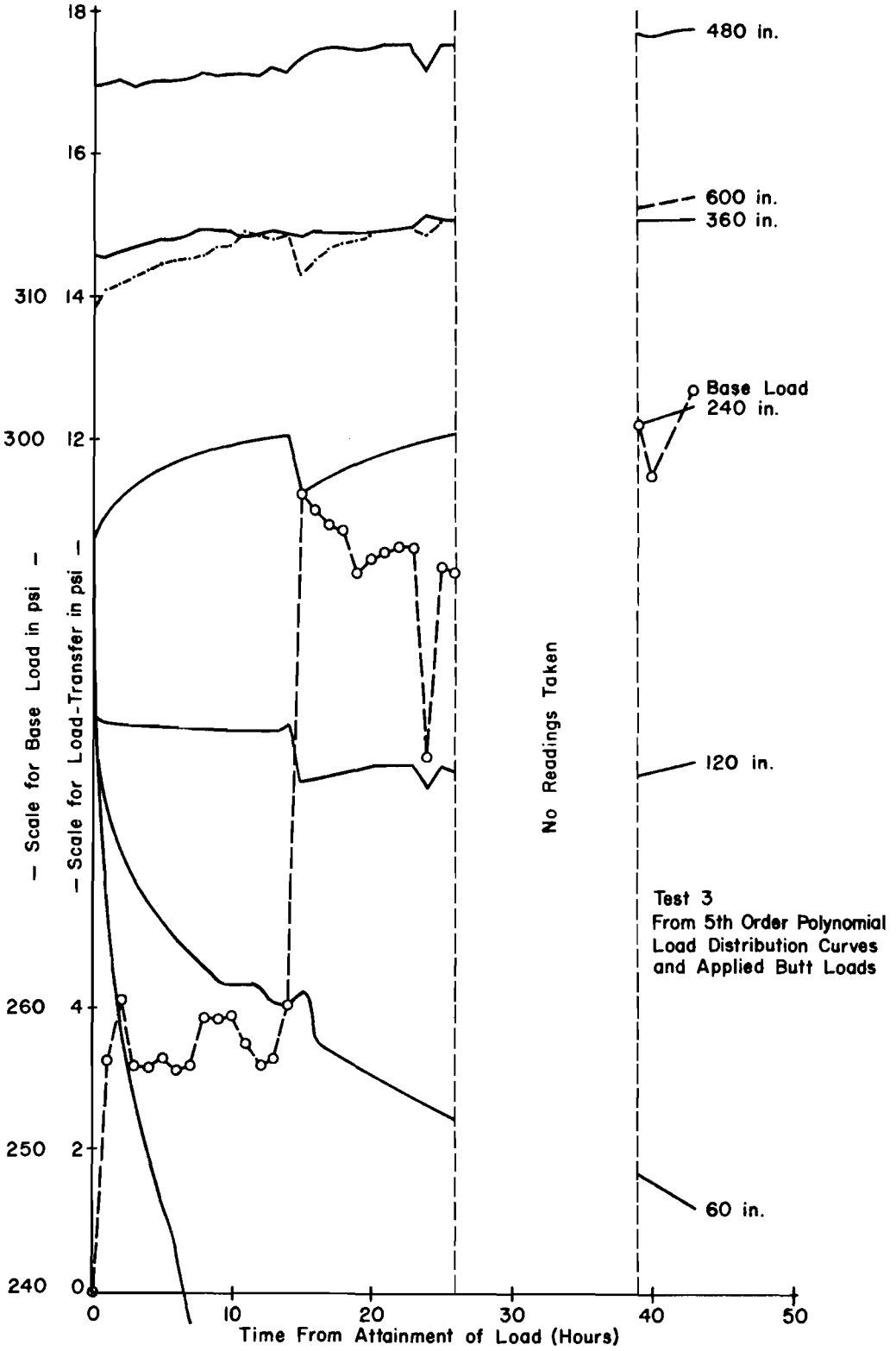

Fig. D.13. Load-Transfer Curves

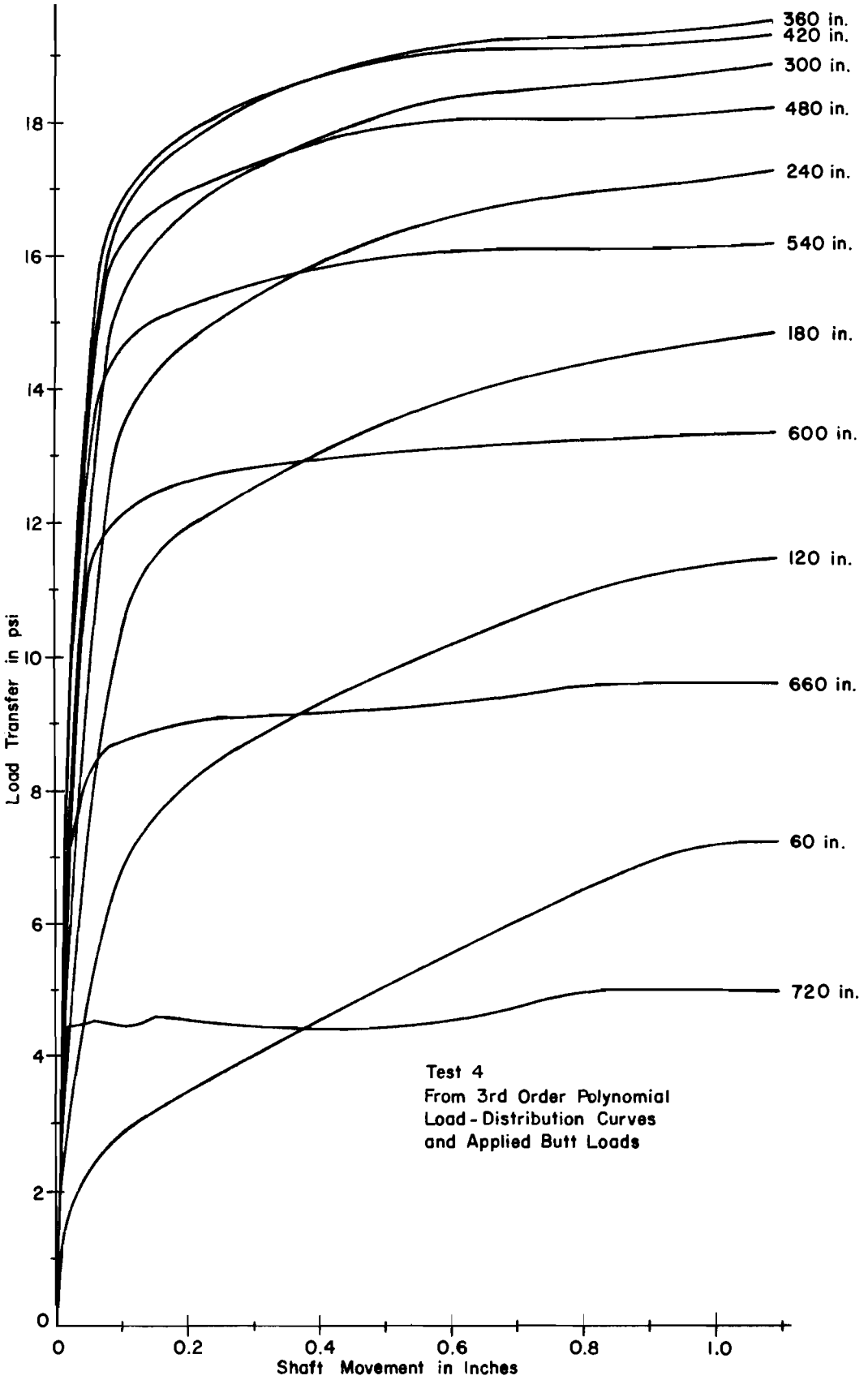

Fig. D.14. Load-Transfer Curves

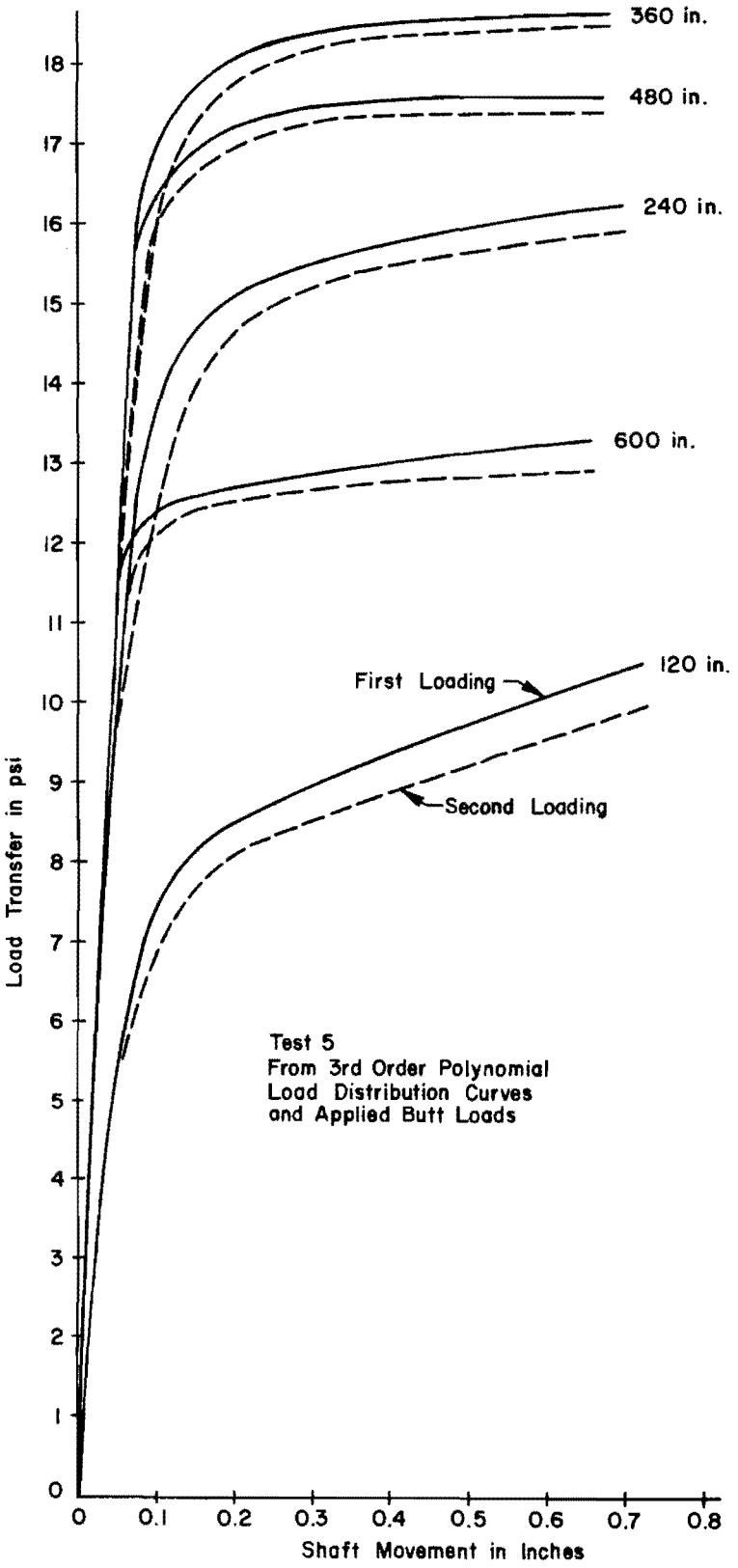

Fig. D.15. Load-Transfer Curves

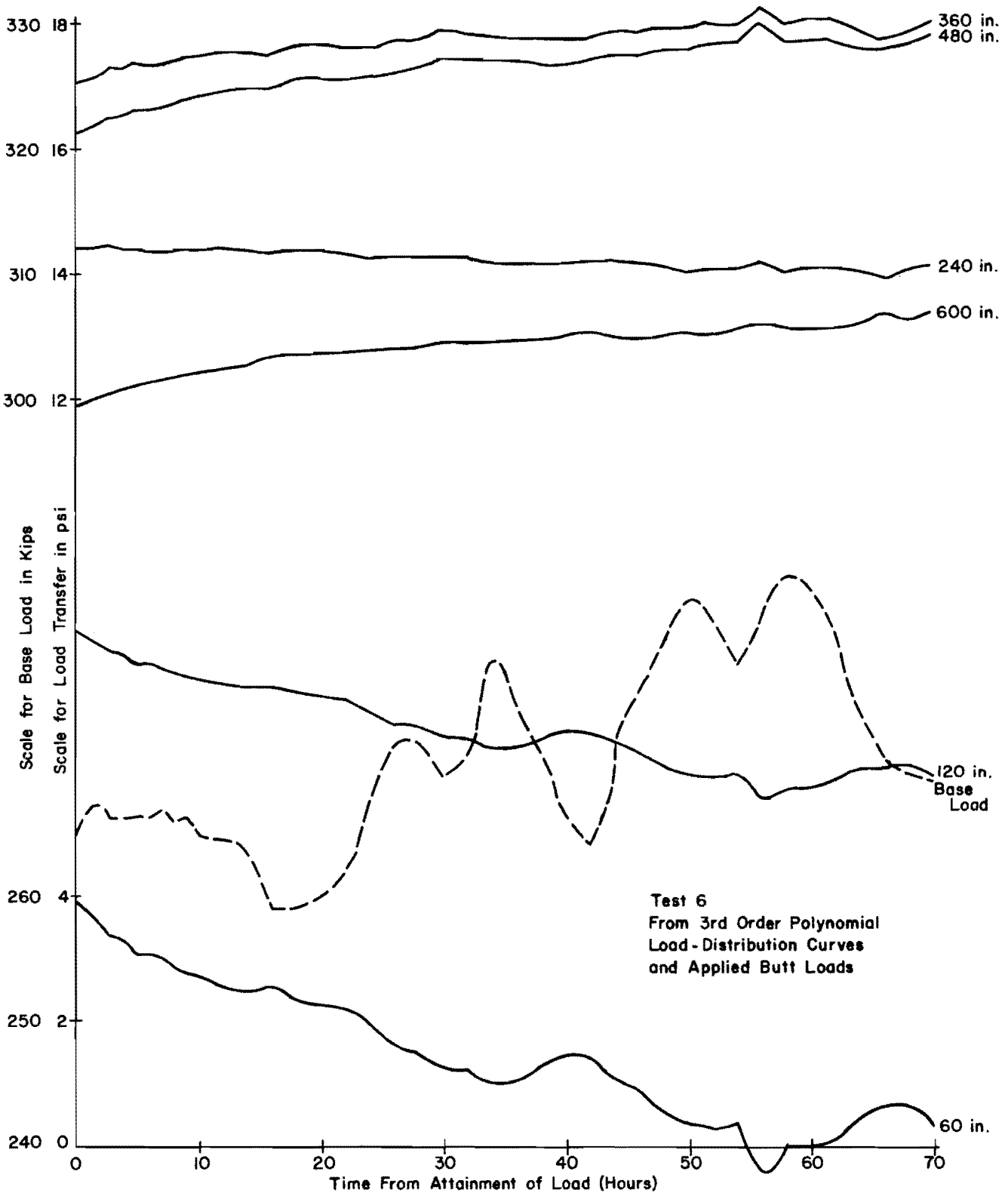

Fig. D.16. Load-Transfer Curves

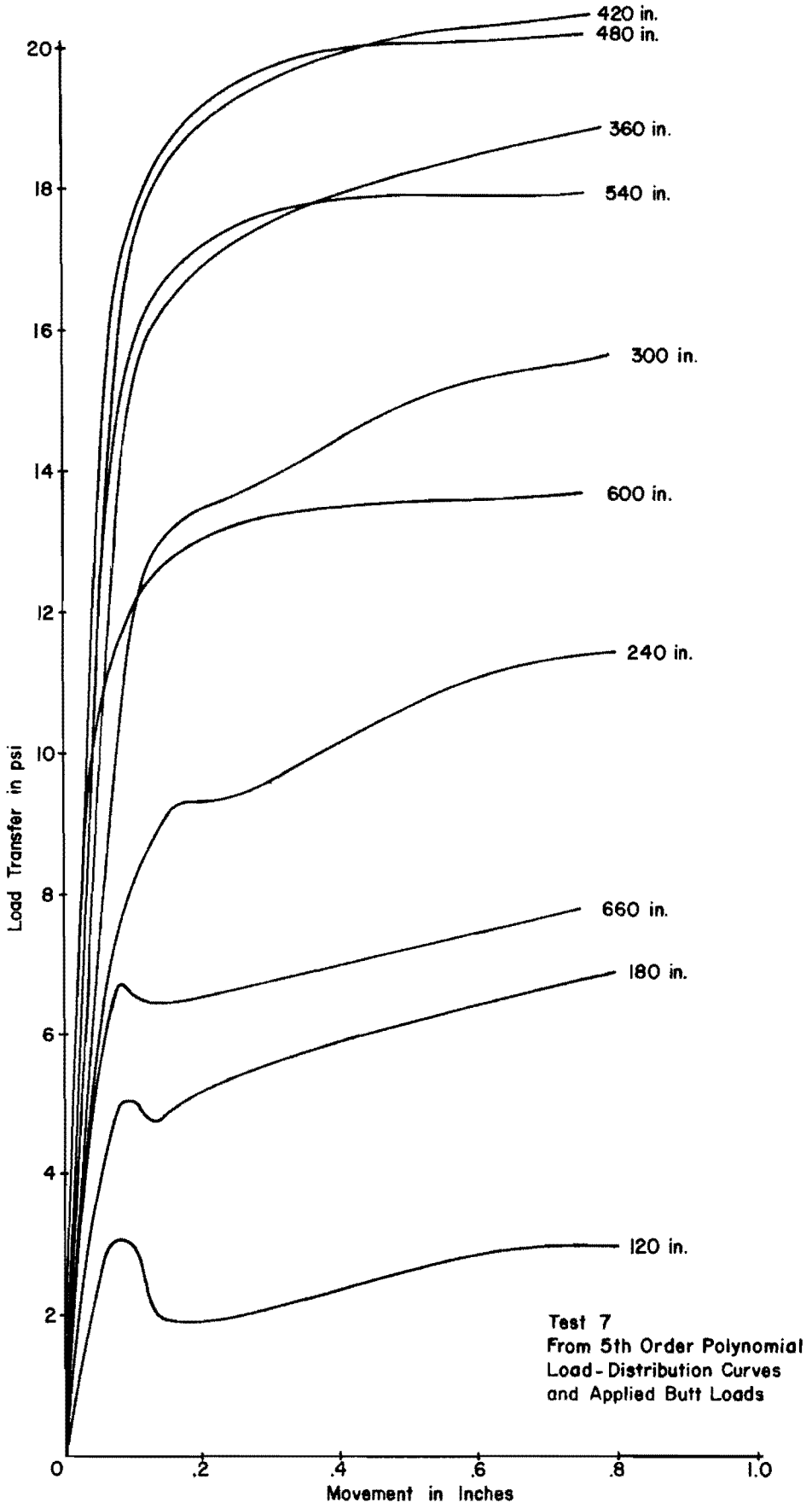

Fig. D.17. Load-Transfer Curves

APPENDIX E

PROGRAM DARES

1. Explanation of Input Tables

The input data to the program is by tables, each table containing a specific type of information. At the beginning of each table is a table header card which gives the table number and the number of cards contained in the table. All tables except Tables 4, 7, and 9 are essential to the operation of the program and must be in proper order.

Table 1 contains the alphanumeric test identification which is to be printed at the beginning of the data output. The identifier may be up to five cards long.

Table 2 contains the basic shaft information, that is, the shaft length and diameter, area of steel in the shaft, and the modulus of elasticity of the concrete. The shaft length is the length below ground surface and may be input in either feet or inches. The diameter input should be the average diameter of the shaft and is input in inches. The area of the steel is input in inches and the modulus of the concrete is input in pounds per square inch.

Table 3 contains the gage information by gage levels, thus there must be one card for each gage level. A gage level may contain up to a maximum of four gages. The distance from the ground surface to the gage level, the number of gages at the level, the weight to be applied to the level data in the curve fitting process, the shaft diameter at the gage level, and the initial load in the shaft at the level must be input on each card. For each gage in the level a code (JSIGN) is input which indicates the polarity of the gage, a blank or zero would mean that the gage goes more positive with compression.

Table 4 contains the calibration constants for any gage levels which are calibrated from an outside source. There should be one card for each level to receive an outside calibration. The level number, which refers to the order in which the gage information appears in Table 3, and the calibration constant for the level are input on a single card. If no calibration constants are to be input, the table, along with the table header card, is omitted.

Table 5 contains the program control information. The following information is input:

a. Total number of load increments (number of sets of test data) in the test.

b. Number of load increments in the loading phase of the test.

c. Number of load increments in the unloading phase of the test. This value may be zero if necessary.

d. Order of the calibration polynomial. This may be left blank if outside calibration constants are furnished.

e. Order of the load-distribution polynomial. If the load distribution is not desired, this value should be left blank.

f. Order of the polynomial fitting the gage data. If the best fit polynomial is not to be calculated, this is to be left blank.

g. A scale factor for scaling of data to desired units. This factor is especially useful when comparing two different tests in which the data are in different units. When no scaling is desired 1.0 may be input, or it may be left blank (a zero scaling factor may not be used).

h. The distance between print out points for the load distribution curves. This value must be in inches and may or may not be even. The first point printed out will always be at the ground surface and the last point at the tip of the shaft.

i. A multiplication factor for converting the load input for the applied load to load in pounds. This allows the load to be input in any units such as tons, or pressure units.

Table 6 contains the settlement gage information and requires only one card. The number of the gages and the average distance, in either feet or inches, from the gages to the ground surface are input.

Table 7 contains the distance in inches from the ground surface to the location of each load transfer curve which is desired. This distance must be even multiples of the incremental distance in Table 5. There should be one card for each curve; if no curves are to be computed, the table is omitted.

Table 8 contains the test data by load increments, one set of data for each load increment. In place of the number cards in the table, the number of cards in a set of data for a load increment is input. This should be equal to the number of gage levels plus three. The first card serves as an alphanumeric identifier for the set. In the first ten space word, the nominal load is read. On the second card the applied load is read. This value is multiplied by the multiplication factor from Table 5 to obtain the applied load in pounds. Next comes one data card for each gage level which contains gage readings for the load increment. These must be always in the same order as the gage levels were listed in Table 3. The first set of data is the zero reference data. The difference in the

gage readings and the zero reference is multiplied by the scale factor from Table 5. The last card in the set contains the settlement gage data.

Table 9 contains the selected loads for load-distribution curves. There should be one card for each selected applied load. A best fit polynomial for the gage data is required in order to obtain load-distribution curves for these selected applied loads. The value of load should be input in pounds.

2. Guide to Input Variables by Tables

TABLE 1	(Maximum number of cards is five)
CO	Alphanumeric used as problem identifier
TABLE 2	(One card only)
PILELF	Shaft length in feet (from ground surface)
PILELI	Shaft length in inches (from ground surface) (Note: shaft length equal to PILELF + PILELI)
DMTR	Shaft diameter in inches
STAR	Steel area in square inches
ECONC	Modulus for concrete (PSI)
TABLE 3	(Maximum number of cards is 20, one card is required for each gage level)
XMF	Distance from ground to gage level in feet
XMI	Distance from ground to gage level in inches
IVM	Number of gages in gage level (Maximum number is four)
WM	Weight of gage level in load-distribution fit
JSIGN	Indicator for direction of gage reading. Blank or zero indicates that the reading goes more positive with compression. A one indicates the reading goes more negative with compression. One JSIGN is read for each gage in the gage level.
PMI	Initial load at level in pounds
DIAM	Shaft diameter at the gage level (the calibration constant for the level will be modified by the inverse of the ratio of the shaft area at the gage level to the shaft area at the calibration level)
TABLE 4	(One card per calibration to be read)
L	Level number
CALM	Outside calibration for gage level L
TABLE 5	(One card only)
NL	Total number of load increments in test (maximum 100)
NU	Number of load increments in loading phase (maximum 50)
NR	Number of load increments in unloading phase
NOR	Order of curve fit for calibration curve (maximum 5)
MOR	Order of curve fit for load distribution curves (maximum 5)
LOR	Order of curve fit for gage data (maximum 5)
SCALE	Factor to scale gage readings
XDIST	Incremental distance along shaft for print out of load distribution data
PMULT	Multiplication factor for applied load

TABLE 6	(One card only)
NSG	Number of settlement gages (maximum 4)
DSGGF	Distance from ground level to settlement gages (in feet)
DSGGI	Distance from ground level to settlement gages (in inches) (Note: distance equals DSGGF + DSGGI)
TABLE 7	(Maximum number of cards is 30)
XTZ	Distance from ground surface to point on shaft where the print out of a load-transfer curve is desired. This distance will be rounded to the nearest multiple of XDIST.
TABLE 8	(Number of cards equals NLM + 3, where NLM is the number of gage levels)

FIRST CARD OF DATA SET

Comment Alphanumeric identifier (the nominal load should be in the first 10 spaces)

SECOND CARD OF DATA SET

P	Reading for applied load (applied load in pounds equals P x PMULP)
NEXT NLM CARDS	(One card per gage level)
RD	Gage readings (one reading per gage)

LAST CARD OF DATA SET

RD	Settlement gage readings (one reading per settlement gage)
TABLE 9	(One card for each selected butt load)
PP	Selected butt load for load distribution curves (in pounds)

GUIDE TO DATA INPUT

TABLE HEADER CARD - ONE CARD AT THE START OF EACH TABLE

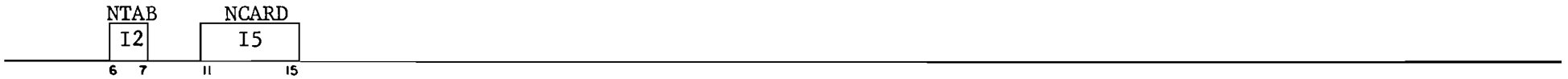

TABLE 1 TEST IDENTIFICATION (UP TO A TOTAL OF 5 CARDS MAY BE USED)

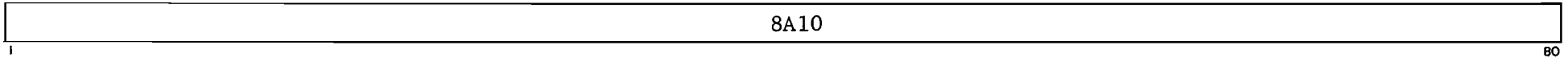

TABLE 2 SHAFT INFORMATION (ONE CARD ONLY)

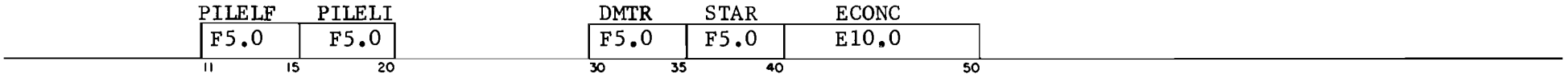

TABLE 3 GAUGE INFORMATION (ONE CARD PER GUAGE LEVEL)

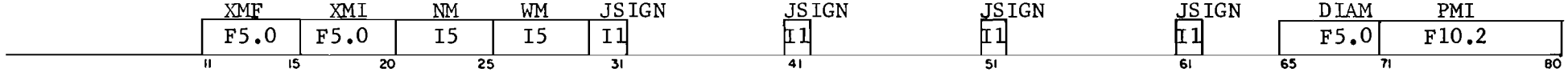

TABLE 4 INDIVIDUAL GAUGE LEVEL CALIBRATION CONSTANT FROM OUTSIDE SOURCE (ONE CARD FOR EACH LEVEL USING OUTSIDE CALIBRATION)

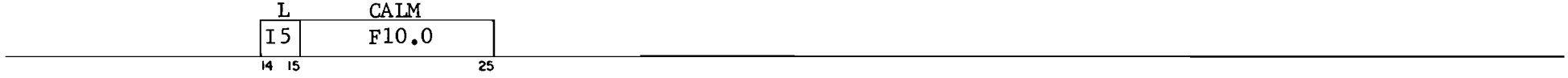

TABLE 5 PROGRAM CONTROL INFORMATION (ONE CARD ONLY)

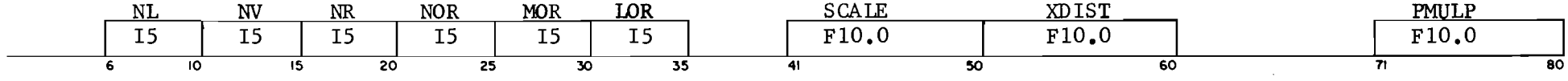

TABLE 6 SETTLEMENT GAUGE INFORMATION (ONE CARD ONLY)

NSG	DSGGF	DSGGI
I5	F5.0	F5.0
6–10	10–15	15–20

TABLE 7 DISTANCES TO LOAD-TRANSFER CURVES

XTZ
F10.0
11–20

TABLE 8 TEST DATA BY LOAD INCREMENTS (NCARD IS THE NUMBER OF CARDS PER SET OF DATA)

COMMENT
4A10
1–40

(One comment at start of each set of data. Put nominal load in first alphanumeric word)

P
F10.0
11–20

(Applied load. One card per set of data)

RD	RD	RD	RD
F10.0	F10.0	F10.0	F10.0
11–20	20–30	30–40	40–50

(Gauge readings. One card for each gauge level per set of data)

RD	RD	RD	RD
F10.0	F10.0	F10.0	F10.0
11–20	20–30	30–40	40–50

(Settlement gauge readings. One card per set of data)

TABLE 9 SELECTED APPLIED LOADS FOR LOAD-DISTRIBUTION CURVES

PP
F10.0
11–20

4. Program Listing

```
      PROGRAM DARES    (INPUT,OUTPUT)
      DIMENSION COMMENT(100,4),CO(40),NM(20),WM(20),JSIGN(20,4),
     1          PMI(20),XM(20),CALM(20),XTZ(30),P(100),RD(4),
     2          AVRD(100,20),RDTEM(20,4),DIF(4),SGZ(4),AVST(100),
     3          COMM(8) ,ACAL(6) ,SGZT(6) ,T(30,50) ,Z(30,50),
     4          AG(20,6) ,PP(50) ,STGR(100) ,STBT(100) ,DIAM(20)
C
      COMMON/BLKA/ X(100),Y(100), A(6), W(100)
C
C
C----INFORMATION CONCERNING INPUT BY TABLES
C
C----TABLE 1 - CONTAINS COMMENT CARDS. UP TO 5 CARDS MAY BE USED
C    DATA INPUT BY FORMAT 8001, 8A10
C
C----TABLE 2 - INPUT TABLE FOR SHAFT DATA ONE CARD ONLY
C    THE VARIABLES,PILELF,PILELI,DMTR,STAR,ECONC   ARE INPUT BY THE FORMAT 8003
C     10X,2F5.0,10X,2F5.0,E10.0
C
C----TABLE 3 - INPUT TABLE FOR GAUGE DATA ONE CARD FOR EACH GAUGE LEVEL
C     VARIABLES - XMF,XMI,NM,WM,JSIGN,DIAM,PMI,   ARE INPUT
C     FOR EACH GAGE LEVEL
C     BY FORMAT 8006 (10X,2F5.0,I5,F5.0,3(I1,9X),I1,4X,F5.0,F10.0)
C
C----TABLE 4 - INPUT TABLE FOR OUTSIDE CALIBRATION ONE FOR EACH LEVEL
C              WHICH IS TO USE AN OUTSIDE CALIBRATION CONSTANT
C     VARIABLES - L , CALM  INPUT BY FORMAT 8009 ,13X,I2,F10.0
C     THIS TABLE MAY BE OMITTED IF NO OUTSIDE CALIBRATION IS USED
C
C----TABLE 5 - PROGRAM CONTROL DATA ONE CARD ONLY
C     VARIABLES - NL,NU,NR,NOR,MOR,LOR,SCALE,XDIST,PMLLP
C     INPUT BY FORMAT 8066 (5X,6I5,5X,2F10.0,10X,E10.0)
C                  5X,5I5,20X,F10.0,10X,E10.0
C
C----TABLE 6 - SETTLEMENT GAUGE DATA  ONE CARD ONLY
C     VARIABLES - NSG,DSGGF,DSGGI  INPUT BY FORMAT 8013,5X,I5,2F5.0
C
C----TABLE 7 - DEPTHS FOR LOAD-TRANSFER CURVES ONE CARD FOR EACH LOAD-
C     TRANSFER CURVE
C     THE VARIABLE XTZ INPUT BY FORMAT 8016,10X,F10.0
C
C----TABLE 8 - TEST DATA BY LOAD INCREMENTS. NCARD IS NUMBER OF CARDS PER SET
C     EACH SET OF DATA SHOULD CONTAIN ONE COMMENT CARD,ONE CARD FOR THE
C     SETTLEMENT GAUGE.  THE COMMENT CARD IS READ BY FORMAT 8001,4A10.0
C     (THE FIRST ALPHANUMERIC SHOULD BE THE NOMINAL LOAD). THE APPLIED
C     LOAD (P) IS READ BY FORMAT 8016,10X,F10.0.  THE SETTLEMENT GAUGE READINGS
C     ARE READ BY FORMAT 8016,10X,4F10.0
C
C----TABLE 9 - NOT USED IN DARES6S BUT INCLUDED TO MAKE DATA FROM DARES5
C     COMPATIBLE WITH DARES6S. TABLE MAY BE OMITTED.
C
C
C----LIST OF PRINCIPAL VARIABLES USED IN THE PROGRAM DARES6S
C
C--CO-----ALPHANUMERIC USED FOR COMMENT CARDS
C--NTAB---TABLE NUMBER
C--NCARD--NUMBER OF CARDS IN THE TABLE
C--PILELF-SHAFT LENGTH(FROM GROUND SURFACE) IN FEET
```

```
C--PILELI-SHAFT LENGTH(FROM GROUND SURFACE) IN INCHES
C--PILEL--THE LENGTH OF SHAFT COMPUTED BY ADDING PILELF AND PILELI
C--DMTR---DIAMETER OF THE SHAFT IN INCHES
C--STAR---AREA OF STEEL IN THE SHAFT IN SQUARE INCHES
C--ECONC--MODULUS OF THE CONCRETE IN PSI
C--CIRCUM-CIRCUMFERENCE OF THE SHAFT (CALCULATED IN THE PROGRAM)
C--AREA---EFFECTIVE AREA OF THE SHAFT (CALCULATED IN THE PROGRAM)
C--NLM----NUMBER OF LEVELS OF GAUGES(TAKEN FROM NCARD FOR TABLE 3)
C--XMF----DISTANCE FROM GROUND SURFACE TO GAUGE LEVEL IN FEET
C--XMI----DISTANCE FROM GROUND SURFACE TO GAUGE LEVEL IN INCHES
C--XM-----COMPUTED DISTANCE (XMF +XMI) FOR GAUGE LEVEL DEPTH IN INCHES
C--NM-----NUMBER GAUGES FOR AN INDIVIDUAL GAUGE LEVEL
C--WM-----WEIGHT THE DATA FROM A GAUGE LEVEL IS TO BE GIVEN IN LOAD-TRANSFER
C--JSIGN--INDICATOR FOR DIRECTION OF GAUGE DATA. (BLANK MEAN DATA GOES MORE
C          POSITIVE UNDER COMPRESSION, A 1 MEANS DATA GOES MORE POSITIVE
C          UNDER TENSION)
C--PMI----INITIAL LOAD IN SHAFT AT A LEVEL IN POUNDS
C--L------IN TABLE 4 L IS THE INDIVIDUAL GAUGE LEVEL BEING CALIBRATED
C--CALM---CALIBRATION ON INDIVIDUAL GAUGE LEVELS FROM OUTSIDE SOURCE
C--NSG----NUMBER OF SETTLEMENT GAUGES
C--DSGGF--DISTANCE FROM SETTLEMENT GAUGES TO GROUND SURFACE IN FEET
C--DSGGI--DISTANCE FROM SETTLEMENT GAUGES TO GROUND SURFACE IN INCHES
C--DSGG---DISTANCE FROM SETTLEMENT GAUGES TO GROUND (DSGGF + DSGGI)
C--XTZ----DISTANCE FROM GROUND SURFACE TO TZ CURVE (ROUNDED TO NEAREST
C          MULTIPLE OF XDIST
C--NL-----TOTAL NUMBER OF LOADINGS
C--NU-----NUMBER OF LOADINGS IN THE ASCENDING LOADING OF THE SHAFT
C--NR-----NUMBER OF LOADINGS IN THE DECENDING LOADING OF THE SHAFT
C--NOR----ORDER OF THE REGRESSION LINE FOR THE CALIBRATION CURVE
C--MOR----ORDER OF THE REGRESSION LINE FOR THE LOAD TRANSFER CURVE
C--LOR----ORDER OF THE REGRESSION LINE FOR THE GAUGE DATA
C--XDIST--INCREMENTAL DISTANCE ALONG THE SHAFT FOR WHICH DATA POINTS
C          OF LOAD,MOVEMENT AND LOAD TRANSFER ARE PRINTED
C--PMULP--MULTIPLICATION FACTOR FOR MULTIPLYING THE APPLIED LOAD
C          READING TO OBTAIN THE APPLIED LOAD IN POUNDS
C--COMMENT-AN ALPHANUMERIC FOR A COMMENT AT THE BEGINING OF EACH LOADING
C           THE NOMINAL LOAD SHOULD BE THE FIRST ALPHANUMERIC WORD
C--P------ THE APPLIED LOAD IN DIVISIONS (P TIMES PMULP IS THE APPLIED
C           LOAD IN POUNDS )
C--RD-----INDIVIDUAL GAUGE READINGS
C--RDTEM--TEMPORARY STORAGE FOR BEGINNING GAUGE READINGS
C--DIF----DIFFERENCE BETWEEN THE GAUGE READING AND THE INITIAL READING
C--SCALE--SCALE FACTOR BY WHICH DIFFERENCES MAY BE SCALED TO A DESIRED OUTPUT
C--DIAM---THE SHAFT DIAMETER AT THE LOCATION OF GAUGE LEVEL
C  AVRD---AVERAGE OF THE DIFFERENCES FOR THE GAUGES OF A LEVEL
C--SGZ----SETTLEMENT GAUGE READING
C--SGZT---STORAGE FOR THE INITIAL SETTLEMENT GAUGE READING
C--AVST---AVERAGE SETTLEMENT FOR A LOADING
C
C
 8000 FORMAT(5X,I2,3X,I5)
 8001 FORMAT(8A10)
 8002 FORMAT (10X,8A10)
 8100 FORMAT (1H1,//)
 8003 FORMAT(10X,2F5.0,10X,2F5.0,E10.0)
 8004 FORMAT(//,9X,30H PROPERTIES OF THE TEST SHAFT  ,/,
     1       /,14X,30H SHAFT LENGTH (FROM GROUND)--- ,F9.1, 7H INCHES,
     2       /,14X,30H SHAFT DIAMETER ------------- ,F9.1, 7H INCHES,
```

```
     3       /,14X,30H SHAFT CIRCUMFERENCE ---------- ,F9.1, 7H INCHES,
     4       /,14X,30H MODULUS OF CONCRETE ---------- ,E9.1,15H LBS PER S
    5Q INCH ,
     6       /,14X,30H AREA OF STEEL IN SHAFT ------ ,F9.1,11H SQ. INCHE
    7S ,
     8       /,14X,30H EFFECTIVE AREA OF SHAFT ----- ,F9.1,11H SQ. INCHE
    9S )
8005 FORMAT(//,9X,28H SHAFT INSTRUMENTATION DATA ,//,
     1          14X,39H LEV WGT NUMBER  DEPTH SHAFT  INITIAL    ,/,
     2          14X,39H         GAUGES  (INS) DIAM  LOAD(LBS)    /)
8006 FORMAT(10X,2F5.0,I5,F5.0,3(I1,9X),I1,4X,F5.0,F10.0)
8007 FORMAT(15X,I2,F5.1,I4,5X,F5.1,F5.1,F9.0)
8008 FORMAT(//,9X,31H OUTSIDE CALIBRATION CONSTANTS ,/,
     1          14X,21H LEVEL  CAL CONSTANT ,/)
8009 FORMAT(13X,I2,F10.0)
8010 FORMAT(  14X,I4,5X,F10.2)
8011 FORMAT (5X,6I5,5X,2F10.0,10X,E10.0)
8012 FORMAT( /,9X,29H PROGRAM CONTROL INFORMATION ,/,
     1       /,14X,44H TOTAL NUMBER OF APPLIED LOAD INCR,---------,I10,
     2       /,14X,44H NUMBER OF INCREASING LOAD INCR,------------,I10,
     3       /,14X,44H NUMBER OF DECREASING LOAD INCR,------------,I10,
     4       /,14X,44H ORDER OF REGRESSION LINE FOR CALIBRATION---,I10,
     5       /,14X,44H ORDER OF REGRESSION LINE FOR LOAD-DISTRIB--,I10,
     5      /,14X,44H ORDER OF REGRESSION LINE FOR GAUGE DATA----,I10,
     5      /,14X,44H SCALE FACTOR FOR SCALING OF GAUGE READINGS-,F10.3,
     6       /,14X,44H INCREMENTAL DISTANCE FOR LOAD-DISTRIB-----,F10.0
     7          , 8H INCHES ,
     8       /,14X,44H MULTIPLICATION FACTOR FOR LOAD INPUT-------,F10.1
     9          ,10H LBS/DIV.  )
8013 FORMAT(5X,I5,2F5.0)
8014 FORMAT(//,9X,22H SETTLEMENT GAUGE DATA ,//,
     1          14X,36H NUMBER OF SETTLEMENT GAUGES--------,I10,/,
     2          14X,36H DISTANCE FROM GROUND TO GAUGES-----,F10.1,
     3            7H INCHES )
8015 FORMAT(//,9X,46H DISTANCES FROM GROUND TO LOAD-TRANSFER CURVES ,/,
     1          14X,22H CURVE NO. DEPTH(INS)  )
8016 FORMAT(10X,7F10.0)
8017 FORMAT(15X,I5,5X,F10.1)
8018 FORMAT(//,9X,38H STRAIN GAUGE DATA BY LOAD INCREMENTS ,//,
     1          9X,15H  LOAD(NOMINAL)
     1       ,25X,31H LOAD COMPUTED BY USE OF PMULP    ,/,
     2          11X,70H    RDG1 RDG2 RDG3 RDG4   DIF1 DIF2 DIF3 DIF4  AVE
    3RAGE  LEVEL  DEPTH          ,/)
8019 FORMAT(10X,4A10,17H COMPUTED LOAD = ,  F8.0  ,7H POUNDS )
8020 FORMAT(14X,F5.0,17X,F5.0,18X,F5.0,4X,I2,4X,F4.0)
8021 FORMAT(14X,2F5.0,12X,2F5.0,13X,F5.0 , 4X,I2,4X,F4.0)
8022 FORMAT(14X,3F5.0, 7X,3F5.0, 8X,F5.0 ,4X, I2, 4X, F4.0)
8023 FORMAT(14X,4F5.0,2X,4F5.0,3X,F5.0,4X,I2,4X,F4.0)
8024 FORMAT(1H1,//,9X,40H LOAD-SETTLEMENT CURVE FOR TOP OF SHAFT ,/,
     1       /,14X,44H COMPUTED  SETTLEMENT  NOMINAL     OTHER
     2       /,14X,43H LOAD(LBS)    INCHES     LOAD     COMMENTS  /)
8025 FORMAT (14X, F9.0, 2X, F7.4, 4X, 4A10)
8026 FORMAT( 1H1,//,9X,31H COMMENTS ON THE TEST           )
8027 FORMAT (1H1,//,9X,44H CALIBRATION CURVE FOR IN-SHAFT CALIBRATION ,
     1       / 14X,22H CALIBRATION CONSTANTS, /)
8028 FORMAT(/,14X,38H  GAGE     INDICATED       SLOPE OF    ,
     1      (/,14X,38H READING   LOAD (LBS)   CURVE(LBS/DIV),/)
8029 FORMAT(  15X,F5.0,4X,F10.1,7X,F10.2)
```

```
 8030 FORMAT( 9X,44H LOAD-DISTRIBUTION CURVE FOR APPLIED LOAD OF ,
     6           F8.0.//,
     1        14X,26H DATA FROM GAUGES BY DEPTH ,/,
     2          14X,50H LEVEL   DEPTH   MEASURED      COMPUTED        ERROR
     3       ,/,14X,49H  NO.   INCHES   LOAD(LBS)     LOAD(LBS)       (LBS)
 8031 FORMAT(16X,I2,5X,F4.0,3(4X,F9.1))
 8032 FORMAT(//, 9X,30H CONSTANTS FOR REGRESSION LINE ,/)
 8033 FORMAT(   14X, 3H A(,I1, 3H) = , E10.3)
 8034 FORMAT( /, 9X,64H LOAD DISTRIBUTION, SHAFT MOVEMENT AND LOAD TRANS
     1FER ALONG SHAFT , /,
     2        14X,43H DEPTH   LOAD   MOVEMENT      LOAD  TRANSFER ,
     2              19H PERCENT LOAD TO    ,/,
     3        14X,43H  INS.  POUNDS   INCHES        PSI       TSF    ,
     3              19H APPLIED MAXIMUM     ,/)
 8035 FORMAT (15X,F4.0,F9.0,2X,F6.3, 5X,F7.2,2X,F7.3, 2(3X,F5.1))
 8036 FORMAT ( 9X,33H LOAD TRANSFER CURVE FOR DEPTH OF , F5.0,
     1             7H INCHES ,//,
     2         14X,27H  MOVEMENT    LOAD TRANSFER , /
     3         14X,27H   INCHES         PSI        , /)
 8037 FORMAT (17X,F6.3,7X,F7.2)
 8039 FORMAT( 9X,36H REGRESSION LINE FOR GAUGE LEVEL -- ,I2,//,
     1        9X,31H CONSTANTS FOR REGRESSION LINE  )
 8040 FORMAT ( 12X, 4(2X,F10.1),2X,E10.3)
 8041 FORMAT (/ , 9X,45H THE SQUARE OF THE COEFFICIENT OF CORRELATION ,
     1              13H IS EQUAL TO , E10.3 )
 8042 FORMAT(/,14X,59H   APPLIED   AVE GAUGE    COMPUTED      ERROR
     1 SLOPE   ,/,
     2         14X,59H  LOAD(LBS)   READINGS    READINGS
     3OF CURVE ,/)
 8043 FORMAT(1H1,//,9X,41H SELECTED APPLIED LOAD FOR LOAD TRANSFER ,/,
     1             9X,41H BASED ON BEST FIT CURVE FOR GAUGE DATA  ,/,
     2            14X,21H CURVE       APPLIED      ,/,
     3            14X,21HNUMBER      LOAD(LBS)     ,/ )
 8044 FORMAT (1H1,//, 9X,47H LOAD-SETTLEMENT CURVE FOR SHAFT (INTERPOLAT
     1ED),/,14X,47H   APPLIED          TOP        GROUND      BOTTOM
     2   ,/,14X,47H    LOAD         OF SHAFT   SURFACE    OF SHAFT   ,/)
 8045 FORMAT (15X,F10.0,5X,3(F6.3,5X))
 8046 FORMAT (10X,4A10)
C
C
C----INITIALIZE ALL VARIABLES AS NECESSARY
C
                KCAL =  0
                SMAX = HLD = 0.0
                LTR = LEY = 0
                ITZ  = NSG = IOR = NTZ =0
C
C----READ TABLE HEADER AND DETERMINE PROPER READ STATEMENT
C
      PRINT 8100
    2 READ 8000,NTAB,NCARD
        IF(NTAB .EQ. 0) GO TO 100
        GO TO (10,20,30,40,50,60,70,80,90),NTAB
C
C----READ TABLE 1  COMMENT CARDS A TOTAL OF 5 CARDS MAY BE USED
C
   10     DO  11 I = 1,NCARD
               J = I * 8
```

```
                K = J - 7
      READ 8001, (CC(L),L =K,J)
   11 PRINT 8002,(CC(L),L =K,J)
                NC = NCARD
          GO TO 2
C
C----READ TABLE 2  SHAFT DATA ONE CARD ONLY
C
   20 READ 8003,PILELF,PILELI,DMTR,STAR,ECONC
                PILEL = PILELF* 12.0 + PILELI
                CIRCUM = DMTR * 3.1416
                AREA = (DMTR/2.0) ** 2 * 3.1416 + (STAR*30000000./ECONC
     1                )- STAR
          PRINT 8004,PILEL,DMTR,CIRCUM,ECONC,STAR,AREA
          GO TO 2
C
C----READ TABLE 3 GAUGE INFORMATION ONE CARD FOR EACH LEVEL
C
   30 PRINT 8005
C
C----SET NUMBER LEVELS OF GAUGES EQUAL TO THE NUMBER OF CARDS IN THE TABLE
C
                NLM = NCARD
          DO 31  I = 1,NCARD
                CALM(I) = 0.0
      READ 8006,XMF,XMI,NM(I),WM(I),(JSIGN(I,K),K=1,4),DIAM(I),PMI(I)
          IF(DIAM(I). EQ. 0.0) DIAM(I) = DMTR
                XM(I) = XMF * 12.0 + XMI
   31 PRINT 8007 , I,WM(I),NM(I),XM(I),DIAM(I), PMI(I)
          GO TO 2
C
C----READ TABLE 4 INDIVIDUAL GAUGE CALIBRATION (IF FURNISHED, TABLE NOT
C                  NECESSARY IF INSHAFT CALIBRATION IS USED)
C
   40 PRINT 8008
                KCAL =  1
          DO 41  I = 1,NCARD
      READ 8009,L,CALM(L)
   41 PRINT 8010,L,CALM(L)
          GO TO 2
C
C----READ TABLE 5 PROGRAM CONTROL INFORMATION (ONE CARD ONLY)
C
   50 READ  8011,NL,NU,NR,NOR,MOR,LOR,SCALE,XDIST,PMULP
          IF(SCALE .EQ. 0.0) SCALE = 1.0
      PRINT 8012,NL,NU,NR,NOR,MOR,LOR,SCALE,XDIST,PMULP
          GO TO 2
C
C----READ TABLE 6 SETTLEMENT GAUGE DATA (ONE CARD ONLY)
C
   60 READ 8013,NSG,DSGGF,DSGGI
                DSGG = DSGGF * 12.0 + DSGGI
      PRINT 8014,NSG,DSGG
          GO TO 2
C
C----READ TABLE 7 DEPTHS FROM GROUND TO LOAD-TRANSFER CURVES
C                  (ONE CARD PER CURVE)
C
```

```
   70      CONTINUE
           IF (NLM * NCARD .GT. 14) PRINT 8100
      PRINT 8015
           DO  71 I = 1,NCARD
      READ 8016,XTZ(I)
                   ZZ = XTZ(I) / XDIST
C
C-----ROUND XTZ TO NEAREST MULTIPLE OF XDIST
C
                   IZ = ZZ
                   ROUND = ZZ - IZ
           IF(ROUND .GT. 0.5) IZ = IZ +1
                   XTZ(I) = XDIST * IZ
           IF (XTZ(I) .GT. PILEL) XTZ(I) = PILEL
   71 PRINT 8017,I,XTZ(I)
                   NTZ = NCARD
           GO TO 2
C
C----READ TABLE 8 TEST DATA BY LOAD INCREMENTS(NCARD IS NO. OF CARDS PER
C                   SET OF DATA INCLUDING THE COMMENT CARD)
C
   80 PRINT 8100
           DO 81 I = 1,NC
                   J = I * 8
                   K = J - 7
   81 PRINT 8002,(CO(L),L = K,J)
      PRINT 8018
           DO 85  I = 1,NL
      READ 8001,(COMMENT(I,J),J = 1,4)
      READ 8016,P(I)
                   P(I) = P(I) * PMULP
           IF(I .EQ. 1) P1 = P(I)
                   P(I) = P(I) - P1
      PRINT 8019,(COMMENT(I,J),J = 1,4), P(I)
           DO 84  J = 1,NLM
                   KK = NM(J)
      READ 8016,(RD(K),K = 1,KK)
C
C-----TAKE DIFFERENCES BETWEEN GAUGE READINGS AND INITIAL READING AND
C          AVERAGE
C
                   AVRD(I,J) = 0.0
           DO 83  K = 1,KK
           IF(I.EQ.1) RDTEM(J,K) = RD(K)
                   DIF(K) = RD(K) - RDTEM(J,K)
C
C----SCALE DIFFERENCES TO DESIRED SCALE
C
                   DIF(K) = DIF(K) * SCALE
           IF(JSIGN(J,K) .NE. 0) DIF(K) = - DIF(K)
   83              AVRD(I,J) = DIF(K) + AVRD(I,J)
                   AVRD(I,J) = AVRD(I,J)/KK
C
C----PRINT GAUGE DATA (FORMAT USED DEPENDS ON NUMBER OF GAUGES
C    IN THE GAUGE LEVEL)
C
           GO TO (86,87,88,89),KK
   86 PRINT 8020,(RD(K),K=1,KK),(DIF(K),K=1,KK),AVRD(I,J)
```

```
     1        ,J,XM(J)
              GO TO 84
   87 PRINT 8021,(RD(K),K=1,KK),(DIF(K),K=1,KK),AVRD(I,J)
     1        ,J,XM(J)
              GO TO 84
   88 PRINT 8022,(RD(K),K=1,KK),(DIF(K),K=1,KK),AVRD(I,J)
     1        ,J,XM(J)
              GO TO 84
   89 PRINT 8023,(RD(K),K=1,KK),(DIF(K),K=1,KK),AVRD(I,J)
     1        ,J,XM(J)
   84         CONTINUE
              IF(NLM + 2.EQ. NCARD) GO TO 92
C
C-----READ SETTLEMENT GAUGES AND DETERMINE AVERAGE SETTLEMENT
C
         READ 8016,(SGZ(K),K = 1,NSG)
                   AVST(I) = 0.0
              DO 82  K = 1,NSG
              IF(I.EQ.1) SGZT(K)= SGZ(K)
   82              AVST(I) = SGZ(K) - SGZT(K) + AVST(I)
                   AVST(I) =-AVST(I)/NSG
              IF(HLD.LT.P(I)) HLD = P(I)
              IF(SMAX.LT.AVST(I)) SMAX = AVST(I)
   85         CONTINUE
         PRINT 8024
              DO 91  I = 1,NL
   91 PRINT 8025, P(I),AVST(I), (COMMENT(I,J),J=1,4)
   92         CONTINUE
              GO TO 2
   90              LTR = NCARD
         PRINT 8043
              DO 95 I = 1,LTR
         READ 8016,PP(I)
         PRINT 8017,I,PP(I)
   95         CONTINUE
              GO TO 2
  100         CONTINUE
C
C----FIT CALIBRATION GAUGES(LEVEL NO. 1) WITH POLYNOMIAL OF ORDER NOR

              IF(NOR.EQ.0.AND.KCAL.NE.0) NOR = 1
              IF(NOR.EQ.0.AND.KCAL.EQ.0) GO TO 301
              DO 110 I = 1,NU
                   X(I) = AVRD(I,1)
                   Y(I) = P(I)
  110              W(I) = 1.0
C
C-----SET KEY = 0  TO FREE SLOPE AT ORIGIN
C
                   KEY = 0
C
C-----SET ORIGIN OF CALIBRATION TO 0.0  (PS = 0.0)
C
                   PS  = 0.0
                   SLOPE = 0.0
                   JJ = 0
C
C-----CALL THE CURVE FIT SUBROUTINE TO DETERMINE THE CONSTANTS FOR THE
```

```
C      CALIBRATION CURVE
C
           CALL POLY(PS,NU,NOR,KEY,SLOPE,JJ)
                  KK = NOR + 1
       PRINT 8027
           DO 120 I = 1,KK
                  J = I - 1
C
C-----PRINT OUT THE CALIBRATION CONSTANTS
C
       PRINT 8033, J,A(I)
  120              ACAL(I) = A(I)
C
C----COMPUTE DELTA SUCH THAT NO MORE THAN 40 POINTS OF THE CALIBRATION
C     CURVE ARE PRINTED
C
                  DELTA = 200.0
  121             X(1) = DELTA * 40
           IF(AVRD(NU,1).GT.X(1)) GO TO 122
                  DELTA = DELTA / 2
           GO TO 121
  122             DELTA = DELTA * 2
       PRINT 8028
                  GR = 0.0
C
C-----PRINT OUT DATA POINTS FOR THE CALIBRATION CURVE AT INTERVALS OF
C      #DELTA# DIVISIONS
C
           DO 130 I = 1,40
                  PX = ACAL(1)
                  SL = ACAL(2)
          DO 131 K = 1,NOR
                  PX = PX + ACAL(K+1) * GR ** K
           IF(K.GE.NOR) GO TO 131
                  SL = SL +(ACAL(K+2) * (K+1) * GR ** K)
  131     CONTINUE
       PRINT 8029,GR,PX,SL
           IF(GR.GT.AVRD(NU,1)) GO TO 132
  130              GR = GR + DELTA
  132     CONTINUE
                  AE = AREA * ECONC
C----START FITTING DATA WITH BEST CURVE OF ORDER IOR
           IF(MOR .EQ. 0) GO TO 301
           DO 140 I = 1,NLM
                  X(I) = XM(I)
  140             W(I) = WM(I)
           DO 200 I = 2,NL
       PRINT 8100
           IF(LEY .NE. 1) PRINT 8046,  (COMMENT(I,J),J=1,4)
C
C-----PRINT OUT THE APPLIED LOAD
C
       PRINT 8030,P(I)
                  SY = 0.0
C
C-----CALCULATE AND PRINT OUT THE LOAD IN THE SHAFT AT GAUGE POINTS
C
           DO 150 J = 1,NLM
```

```
          IF(CALM(J).EQ.0.0) GO TO 154
                Y(J) = CALM(J) * AVRD(1,J) + PMI(J)
          GO TO 153
  154     CONTINUE
                Y(J) = PMI(J)
          DO 155 K = 1,NOR
  155           Y(J) = Y(J)+ ACAL(K+1) * AVRD(I,J) ** K
  153     CONTINUE
                Y(J) = Y(J) * (DIAM(J) ** 2) / (DIAM(1) **2)
                SY = Y(J) + SY
  150     CONTINUE
                SY = SY /NLM
C
C-----SET THE ORIGIN OF LOAD DISTRIBUTION CURVE AT THE APPLIED LOAD
C
                PS = P(I)
C
C-----SET KEY OF SLOPE(KEY =0 SLOPE NOT SET, KEY = 1 SLOPE AT ORIGIN SET
C     TO BE EQUAL TO SLOPE)
C
             KEY=0
                SLOPE = 0
                JJ = I
C
C-----CALL CURVE FIT SUBROUTINE TO DETERMINE CONSTANTS FOR
C     LOAD DISTRIBUTION CURVE
          CALL POLY(PS,NLM,MOR,KEY,SLOPE,JJ)
                SSY = 0.0
                SSE = 0.0
          DO 157  J= 1,NLM
                YC    = A(1)
                JJ = MOR + 1
          DO 156  K = 2,JJ
  156           YC    = YC    + A(K) * XM(J) ** (K-1)
                ERR = Y(J) - YC
                SSE = ERR ** 2  + SSE
                SSY =  SSY + (Y(J) - SY) ** 2
                ERR = - ERR
      PRINT 8031,J,X(J),Y(J),YC   ,ERR
  157 CONTINUE
                RSQ = (SSY - SSE) / SSY
      PRINT 8041,RSQ
                XDIS  = 0.0
      PRINT 8032
C-----PRINT CONSTANTS FOR LOAD-DISTRIBUTION CURVE
          DO 135 J = 1,JJ
                K = J - 1
  135 PRINT 8033,K,A(J)
      PRINT 8034
                L = 1
C-----CALCULATE AND PRINT AT POINTS ALONG THE SHAFT THE LOAD,SHAFT MOVEM
C     ENTS AND LOAD TRANSFER
          DO 170 J = 1,100
          IF(XDIS .GT. PILEL) XDIS  = PILEL
                XLOAD = A(1)
                XDIR  = A(2)
                XINT  = 0.0
          DO 160 K = 1,JJ
```

```
                XINT  = XINT  + (A(K) * XDIS  ** K) / K
          IF(K . GE.JJ) GO TO 160
                XLOAD = XLOAD +  A(K+1) * XDIS  ** K
          IF (K.GE.MOR)   GO TO 160
                XDIR  = XDIR  + (A(K+2) * XDIS  ** K) * (K+1)
  160     CONTINUE
                XMOV  = AVST(I) - (XINT + DSGG * P(I))/AE
                XTRA  = - XDIR / CIRCUM
                TSF   =  XTRA  * 0.072
          IF(P(I) .EQ. 0.0) P(I) = 0.0001
                PERA = (XLOAD / P(I) ) * 100.0
                PERM = (XLOAD / HLD  ) * 100.0
      PRINT  8035, XDIS ,XLOAD,XMOV,XTRA,TSF,PERA,PERM
          IF(XDIS .EQ. 0.0) STGR(I) = XMOV
          IF(XDIS .EQ. PILEL) STBT(I) = XMOV
          IF(NTZ.EQ.0) GO TO 165
          IF(I.GT.NU) GO TO 165
          IF(L.GT.NTZ) GO TO 165
C-----PICK OUT DATA TO BE REPRINTED FOR LOAD-TRANSFER CURVES
          IF(XDIS .NE.XTZ(L))  GO TO 165
                T(L,I) = XMOV
                Z(L,I) = XTRA
                L = L + 1
  165     CONTINUE
          IF(XDIS.GE.PILEL) GO TO 200
  170           XDIS  =  XDIS + XDIST
  200     CONTINUE
          IF(NTZ.EQ.0) GO TO 301
          IF(LEY .EQ . 1) GO TO 198
                P(1) = 0.0
                STGR(1) = 0.0
                STBT(1) = 0.0
                XLOAD = 10000.0
                XDIS = 0.0
          DO 175 I = 1,10
          IF(XLOAD*50.0 .LT. HLD) XLOAD = XLOAD * 2.0
          IF(XLOAD .EQ. 20000.0) XLOAD = 25000.0
  175     CONTINUE
      PRINT 8044
                K = 1
          DO 180 I = 1,100
          DO 185 J = K,NU
                K = J
                L = K + 1
          IF(XDIS .GE. P(K) .AND. XDIS .LE. P(L)) GO TO 186
  185     CONTINUE
  186     CONTINUE
                CONST = (XDIS - P(K))/ (P(L) - P(K))
                GROUND = STGR(K) + (STGR(L) -STGR(K)) * CONST
                BOTTOM = STBT(K) + (STBT(L) - STBT(K)) * CONST
                TOP = AVST(K) + (AVST(L) - AVST(K)) * CONST
      PRINT 8045, XDIS ,TOP, GROUND, BOTTOM
          IF(XDIS  .EQ. HLD) GO TO 199
                XDIS = XDIS + XLOAD
          IF(XDIS .GT. HLD) XDIS = HLD
  180     CONTINUE
  199     CONTINUE
  198     CONTINUE
```

```
          DO 300 I = 1,NTZ
          T(I,1) = 0.0
          Z(I,1) = 0.0
      PRINT 8100
      PRINT 8036,XTZ(T)
C-----INTERPOLATE AND PRINT LOAD-TRANSFER CURVES AT INTERVALS OF
C     SHAFT MOVEMENTS OF DMOV
                DMOV = 0.005
          XMOV = 0.0
                L = 1
          DO 250 J = 1,100
          IF(J.EQ.21) DMOV = 0.01
          IF(J.EQ.31) DMOV = 0.10
          IF(XMOV.GT.T(I,NU)) XMOV = T(I,NU)
          DO 220 K = L,NU
                L = K
          IF(XMOV.GE.T(I,L).AND.XMOV.LE.T(I,L+1)) GO TO 222
  220     CONTINUE
  222           ZZ = (Z(I,L+1)-Z(I,L))*(XMOV-T(I,L))/(T(I,L+1)-T(I,L))
                ZZ = Z(I,L) + ZZ
  225 PRINT 8037,XMOV,ZZ
          IF(XMOV .GE. T(I,NU)) GO TO 300
  250           XMOV = XMOV + DMOV
  300    CONTINUE
  301     CONTINUE
C-----FIT GAUGE WITH LEAST-SQUARES POLYNOMIAL OF ORDER LOR
          IF(LEY .EQ. 1) GO TO 1000
          IF(LOR .EQ. 0 ) GO TO 1000
          DO 309 I = 1,NU
                W(I) = 1.0
  309           X(I) = P(I)
                KK   = LOR +1
          DO 350 I = 1,NLM
                SY =0
          DO 310 J = 1,NU
                SY = SY + AVRD(J,I)
  310           Y(J) = AVRD(J,I)
                SY = SY /NU
                JJ = 1
C-----FREE SLOPE AT THE ORIGIN (KEY = 0)
                KEY = 0
                SLOPE =0.0
C-----SET ORIGIN OF POLYNOMIAL AT 0 (PS = 0)
                PS    =0.0
C-----CALL SUBROUTINE TO DETERMINE CONSTANTS FOR BEST-FIT POLYNOMIAL
          CALL POLY(PS,NU,LOR,KEY,SLOPE,JJ)
      PRINT 8100
                SSE = 0.0
                SSY = 0.0
      PRINT 8039,I
          DO 311 K =1,KK
                AG(I,K) = A(K)
                L =K-1
  311 PRINT 8033,L,A(K)
      PRINT 8042
          DO 320 J = 1,NU
                SLOPE = A(2)
                YC    =  0.0
```

```
          DO 321 K = 2,KK
                YC    = YC    + A(K) * X(J) ** (K-1)
          IF(K.GE.KK) GO TO 321
                SLOPE = SLOPE + K * X(J)**(K-1) * A(K+1)
  321     CONTINUE
C-----COMPUTE ERRORS AND CORRELATION OF CURVE FIT
                ERR = Y(J) - YC
                SSE = SSE + ERR ** 2
                SSY = SSY + (Y(J) - SY) ** 2
                ERR = - ERR
C-----PRINT DATA ON CURVE OF GAUGE DATA
      PRINT 8040,X(J),Y(J),YC ,ERR,SLOPE
  320     CONTINUE
                RSQ = (SSY - SSE) / SSY
      PRINT 8041,RSQ
  350     CONTINUE
          IF(LTR.EQ.0.OR.MOR.EQ.0) GO TO 1000
                NL = LTR + 1
                LEY = 1
          DO 390 J = 1,LTR
          DO 380 I = 1 , NU
                K = I
          IF(PP(J) .GT. P(NU))     GO TO 388
          IF(PP(J) .GE. P(I) .AND. PP(J) .LE. P(I+1)) GO TO 389
  380     CONTINUE
  388     CONTINUE
                K = NU - 1
  389     CONTINUE
C-----COMPUTE SETTLEMENT GAUGE READING AND GAUGE READING
C     FOR EACH SELECTED APPLIED LOAD
          X(J) = AVST(K)+(AVST(K+1)-AVST(K))*(PP(J)-P(K))/(P(K+1)-P(K))
  390     CONTINUE
          DO 400 I = 1,LTR
                AVST(I+1) = X(I)
C-----TRANSFER SELECTED LOADS TO THE STORAGE FOR APPLIED
                P(I+1) = PP(I)
          DO 400 J = 1,NLM
                AVRD(I+1,J) = 0.0
          DO 400 K = 1,LOR
                AVRD(I+1,J )= AVRD(I+1,J) + AG(J,K+1) *PP(I) ** K
  400     CONTINUE
C     LOAD AND RETURN TO PORTION OF PROGRAM FOR
C     COMPUTING LOAD-DISTRIBUTION CURVES.
          GO TO 132
 1000     CONTINUE
      END
```

```
      SUBROUTINE POLY (P,NPT,IOR,KEY,SLOPE,JJ)
      COMMON/BLKA/ X(100),Y(100), A(6), W(100)
      DIMENSION                       SS(6,6),SQ(100,10),C(6),SUM(11)
            KK = IOR * 2
            NN = IOR + 1
      IF(JJ .GT. 2) GO TO 109
C----CLEAR STORAGE
      DO 100 I = 1,NN
  100       SUM(I) = SUM(I+IOR) = 0.0
C----RAISE X#S TO PROPER POWER AND SUM
      DO 110 I = 1,NPT
            SUM(1) = SUM(1) + 1
      DO 110 J = 1,KK
            SQ(I,J) =(X(I) ** J) * W(I)
  110       SUM(J+1)= SQ(I,J)+ SUM(J+1)
  109 CONTINUE
      DO 115 I = 1,NN
  115       C(I) = 0.0
      DO 120 I = 1,NPT
            C(1) = C(1) + Y(I)
      DO 120 J = 2,NN
  120       C(J) = C(J) + Y(I) * SQ(I,J-1)
      DO 130 I = 1,NN
      DO 130 J = 1,NN
  130       SS(I,J) = SS(J,I) = SUM(I+J-1)
C----SET ORIGIN TO PROPER VALUE
      DO 140 I = 1,NN
  140       SS(1,I) = 0.0
            SS(1,1) = 1.0
             C(1) = P
C----IF KEY = 1 THEN SET SLOPE AT ORIGIN TO#SLOPE#
      IF(KEY  .NE. 1) GO TO 151
      DO 150 I = 1,NN
  150       SS(2,I) = 0.0
            C(2)    = SLOPE
            SS(2,2) = 1.0
  151 CONTINUE
C----CALL SUBROUTINE TO SOLVE SYSTEM OF EQUATIONS
      CALL SOLVE(NN,SS,C,A)
    RETURN
    END
```

```
      SUBROUTINE  SOLVE  (N,A,C,X)
      DIMENSION A(6,6),V(6,6),U(6,6),C(6),P(21),X(6),S(6)
          IF(N.GT.1) GO TO 10
              X(1) = C(1)/A(1,1)
         GO TO 90
   10     CONTINUE
      DO 20 I=1,N
   20 V(1,1) =A(I,1)
      DO 30 J = 1,N
   30 U(1,J) =A(1,J)/V(1,1)
      DO 31  J=2,N
   31 V(1,J) = 0
      DO 32 I=2,N
   32 U(I,1) = 0
      DO 65 JJ =2,N
      DO 52 I=2,N
      J = JJ
      IF (J-I) 49,49,51
   49 K= J-1
      SUM =0
      DO 50 M = 1,K
      PROD = V(I,M) * U(M,J)
   50 SUM = PROD + SUM
      V(I,J) = A(I,J) - SUM
      GO TO 52
   51 V(I,J) = 0
   52 CONTINUE
      DO 65 J = 2,N
      I = JJ
      IF (J-I) 62,63,54
   54 K = I-1
      SUM = 0
      DO 55 M = 1,K
      PROD =  V(I,M) * U(M,J)
   55 SUM = PROD + SUM
      U(I,J) = (A(I,J)-SUM)/V(I,I)
      GO TO 65
   62 U(I,J) = 0
      GO TO 65
   63 U(I,J) = 1
   65 CONTINUE
      P(1) = C(1)/V(1,1)
      DO 70 I = 2,N
      K = I - 1
      SUM = 0
      DO 75 M = 1,K
      PROD = V(I,M) * P(M)
   75 SUM = PROD + SUM
   70 P(I) = (C(I)-SUM)/V(I,I)
      X(N) = P(N)
      DO 80 K=2,N
      I = N+1- K
      SUM = 0
      L = I + 1
      DO 85 M =  L,N
      PROD = U(I,M) * X(M)
   85 SUM = PROD + SUM
   80 X(I) = P(I) - SUM
   90     CONTINUE
      RETURN
      END
```

5. Sample Data

```
TABLE 1        4
HB AND T     SHAFT TEST NO.2. CONDUCTED ON 17 JULY 1969
TEST CONDUCTED BY PERSONNEL FROM THE UNIVERSITY OF TEXAS
SHAFT LOADED TO FAILURE. LOAD APPLIED IN 50 TON INCREMENTS
TO 600 TONS THEN IN 20 TON INCREMENTS.
TABLE 2        1
              60                    40 15.6 5.200E 06
TABLE 3        9
           1    0     0     2 1.0 1          1                          36
           2 13.5           2 1.0 1          1                       41.8
           3 21.5           2 1.0 1          1                       40.5
           4 34.5           2 0.0 1          1
           5 41.5           2 1.0 1          1                          38
           6 53.5           2 0.0 1          1                           3
           7 56.5           2 1.0 1          1                          37
           8 59.4           2 1.0 1          1                          50
           9 59.4           2 1.0 1                                     50
TABLE 5        1
          35   27    8     3    5    5          .319          30              49.3E+00
TABLE 6        1
           2          16
TABLE 7       13
                    00
           2         60
           3        120
           4        180
           5        240
           6        300
           7        360
           8        420
           9        480
          10        540
          11        600
          12        660
          13        720
TABLE 8       12
0   TONS
                    +  22
                    -  41      +   6
                    -  14      -   7
                       0       -   2
                       0       -   8
                    -   3      -  10
                    +  21      -   3
                    -  19      -   2
                    -   4      -   1
                    -   3      -   5
                   1.878      1.490
50  TONS
                   +1952
                    - 438      - 335
                    - 214      - 194
                    - 187      - 187
                    - 114      - 125
```

	- 84	- 99
	- 69	- 48
	- 50	- 20
	- 18	- 19
	- 12	+ 13
	1.872	1.485
100 TONS		
	+3980	
	- 909	- 645
	- 431	- 396
	- 395	- 391
	- 248	- 254
	- 186	- 214
	- 184	- 82
	- 89	- 47
	- 28	- 29
	- 21	+ 30
	1.866	1.479
150 TONS		
	+6017	
	-1385	- 988
	- 673	- 624
	- 626	- 619
	- 399	- 396
	- 305	- 335
	- 300	- 125
	- 131	- 69
	- 35	- 45
	- 34	+ 48
	1.858	1.471
200 TONS		
	+7985	
	-1837	-1347
	- 917	- 859
	- 862	- 849
	- 550	- 549
	- 417	- 471
	- 395	- 162
	- 175	- 99
	- 48	- 60
	- 42	+ 69
	1.849	1.462
250 TONS		
	10152	
	-2286	-1772
	-1181	-1132
	-1133	-1112
	- 735	- 734
	- 574	- 631
	- 492	- 207
	- 223	- 125
	- 59	- 80
	- 54	+ 94
	1.838	1.452
300 TONS		
	+1221	

	-2703	-2242
	-1461	-1411
	-1409	-1378
	- 924	- 923
	- 745	- 799
	- 574	- 267
	- 278	- 161
	- 78	- 102
	- 70	+ 113
	1.827	1.441
350 TONS		
	+1407	
	-3030	-2672
	-1710	-1667
	-1664	-1621
	-1110	-1110
	- 910	- 968
	- 640	- 319
	- 322	- 197
	- 92	- 121
	- 83	+ 140
	1.820	1.428
400 TONS		
	+1616	
	-3408	-3210
	-2000	-1970
	-1967	-1909
	-1341	-1344
	-1131	-1186
	- 747	- 400
	- 399	- 256
	- 116	- 156
	- 108	+ 178
	1.799	1.411
450 TONS		
	+1825	
	-3738	-3706
	-2290	-2285
	-2271	-2195
	-1578	-1584
	-1359	-1414
	- 814	- 492
	- 495	- 351
	- 151	- 206
	- 147	+ 236
	1.776	1.388
500 TONS		
	+2015	
	-4066	-4170
	-2565	-2574
	-2538	-2452
	-1792	-1818
	-1558	-1611
	- 849	- 575
	- 601	- 465
	- 195	- 261

	- 190	+ 304
	1.749	1.360
520 TONS		
	+2110	
	-4283	-4458
	-2744	-2776
	-2718	-2627
	-1934	-1949
	-1661	-1715
	- 862	- 616
	- 666	- 535
	- 221	- 294
	- 215	+ 344
	1.731	1.342
540 TONS		
	+2190	
	-4436	-4651
	-2856	-2913
	-2836	-2742
	-2036	-2054
	-1748	-1805
	- 871	- 658
	- 732	- 608
	- 252	- 332
	- 242	+ 390
	1.711	1.322
560 TONS		
	+2280	
	-4589	-4850
	-2993	-3052
	-2959	-2851
	-2126	-2147
	-1837	-1897
	- 882	- 707
	- 801	- 674
	- 280	- 366
	- 268	+ 438
	1.691	1.303
580 TONS		
	+2353	
	-4767	-5086
	-3127	-3205
	-3092	-2988
	-2229	-2250
	-1926	-1993
	- 893	- 766
	- 879	- 754
	- 315	- 406
	- 298	+ 488
	1.668	1.279
600 TONS		
	+2439	
	-4901	-5259
	-3238	-3336
	-3207	-3106
	-2320	-2344

	-2021	-2090
	- 908	- 824
	- 953	- 831
	- 347	- 445
	- 329	+ 537
	1.644	1.266
620 TONS		
	+2507	
	-5078	-5476
	-3369	-3487
	-3330	-3223
	-2410	-2448
	-2113	-2183
	- 910	- 879
	-1030	- 914
	- 381	- 486
	- 360	+ 591
	1.616	1.227
640 TONS		
	+2613	
	-5250	-5703
	-3504	-3650
	-3472	-3369
	-2475	-2534
	-2235	-2313
	- 935	- 973
	-1128	-1021
	- 426	- 542
	- 403	+ 651
	1.585	1.195
660 TONS		
	+2697	
	-5396	-5878
	-3610	-3779
	-3585	-3480
	-2556	-2607
	-2338	-2420
	- 950	-1059
	-1212	-1118
	- 465	- 590
	- 441	+ 705
	1.549	1.159
680 TONS		
	+2772	
	-5576	-6107
	-3750	-3938
	-3710	-3613
	-2369	-2458
	-2436	-2525
	- 963	-1136
	-1289	-1213
	- 501	- 636
	- 478	+ 756
	1.510	1.120
700 TONS		
	+2853	

	-5767	-6331
	-3867	-4071
	-3818	-3726
	-2411	-2507
	-2535	-2640
	- 982	-1225
	-1383	-1318
	- 544	- 692
	- 519	+ 816
	1.466	1.075
720 TONS		
	+2933	
	-5942	-6563
	-3996	-4220
	-3939	-3849
	-2468	-2554
	-2627	-2748
	- 997	-1306
	-1462	-1417
	- 586	- 742
	- 561	+ 873
	1.413	1.023
740 TONS		
	+3034	
	-6106	-6807
	-4124	-4386
	-4080	-4000
	-2540	-2617
	-2739	-2889
	-1017	-1436
	-1556	-1552
	- 641	- 804
	- 614	+ 941
	1.339	1.047
760 TONS		
	+3112	
	-6290	-7048
	-4239	-4542
	-4203	-4124
	-2587	-2656
	-2807	-2995
	-1019	-1530
	-1610	-1658
	- 681	- 848
	- 652	+ 991
	1.249	0.856
780 TONS		
	+3197	
	-6479	-7299
	-4346	-4680
	-4309	-4221
	-2619	-2687
	-2870	-3121
	-1022	-1652
	-1666	-1791
	- 726	- 899

	- 697	+1049
	1.120	0.726
800 TONS		
	+3235	
	-6667	-7543
	-4433	-4835
	-4407	-4315
	-2653	-2726
	-2908	-3256
	-1009	-1802
	-1720	-1932
	- 773	- 943
	- 737	+1096
	0.943	0.550
820 TONS		
	+3345	
	-6842	-7781
	-4510	-4975
	-4484	-4381
	-2677	-2737
	-2907	-3367
	- 938	-1942
	-1750	-2048
	- 807	- 976
	- 769	+1139
	0.704	0.311
700 TONS R		
	+2815	
	-6067	-6997
	-3982	-4495
	-3997	-3924
	-2356	-2424
	-2653	-3132
	- 712	-1632
	-1574	-1917
	- 728	- 882
	- 694	+1035
	0.655	0.265
600 TONS R		
	+2415	
	-5299	-6098
	-3459	-3969
	-3525	-3470
	-2052	-2149
	-2402	-2866
	- 592	-1379
	-1443	-1799
	- 671	- 821
	- 645	+ 960
	0.674	0.283
500 TONS R		
	+2002	
	-4498	-5174
	-2911	-3411
	-3021	-2982
	-1742	-1867

```
                -2126     -2572
                - 482     -1155
                -1307     -1677
                - 617     - 760
                - 594     + 886
               0.693     0.305
400 TONS R
               +1597
                -3692     -4244
                -2360     -2843
                -2499     -2480
                -1436     -1588
                -1927     -2258
                - 382     - 391
                -1167     -1555
                - 561     - 696
                - 543     + 812
               0.715     0.327
300 TONS R
               +1182
                -2829     -3269
                -1774     -2232
                -1932     -1935
                -1124     -1310
                -1486     -1905
                - 302     - 776
                -1015     -1417
                - 502     - 628
                - 489     + 727
               0.739     0.352
200 TONS R
                +7946
                -2042     -2364
                -1235     -1662
                -1391     -1419
                - 853     -1087
                -1125     -1547
                - 236     - 621
                - 864     -1281
                - 445     - 558
                - 434     + 645
               0.764     0.380
100 TONS R
                +3943
                -1214     -1401
                - 649     -1034
                - 790     - 852
                - 614     - 855
                - 710     -1143
                - 173     - 464
                - 687     -1113
                - 374     - 472
                - 365     + 547
               0.795     0.413
0   RETURN
                +  41
```

	- 481	- 320
	- 62	- 335
	- 139	- 234
	- 387	- 507
	- 278	- 698
	- 114	- 297
	- 464	- 860
	- 279	- 351
	- 269	+ 412
	0.838	0.456
TABLE 9	10	
	50000	
	200000	
	400000	
	600000	
	800000	
	1000000	
	1200000	
	1400000	
	1600000	
	1640000	

6. Sample Output

```
HB AND T    SHAFT TEST NO.2. CONDUCTED ON 17 JULY 1969
TEST CONDUCTED BY PERSONNEL FROM THE UNIVERSITY OF TEXAS
SHAFT LOADED TO FAILURE. LOAD APPLIED IN 50 TON INCREMENTS
TO 600 TONS THEN IN 20 TON INCREMENTS.

PROPERTIES OF THE TEST SHAFT

     SHAFT LENGTH (FROM GROUND)---    720.0 INCHES
     SHAFT DIAMETER ------------      40.0 INCHES
     SHAFT CIRCUMFERENCE ---------   125.7 INCHES
     MODULUS OF CONCRETE ---------  5.2E+06 LBS PER SQ INC
     AREA OF STEEL IN SHAFT ------    15.6 SQ. INCHES
     EFFECTIVE AREA OF SHAFT -----  1331.0 SQ. INCHES

SHAFT INSTRUMENTATION DATA

     LEV WGT NUMBER  DEPTH SHAFT  INITIAL
         GAUGES  (INS) DIAM  LOAD(LBS)

      1  1.0   2       0.0 36.0       -0
      2  1.0   2     162.0 41.8       -0
      3  1.0   2     258.0 40.5       -0
      4  0.0   2     414.0 40.0       -0
      5  1.0   2     498.0 38.0       -0
      6  0.0   2     642.0 30.0       -0
      7  1.0   2     678.0 37.0       -0
      8  1.0   2     712.8 50.0       -0
      9  1.0   2     712.8 50.0       -0

PROGRAM CONTROL INFORMATION

     TOTAL NUMRER OF APPLIED LOAD INCR.--------      35
     NUMBER OF INCREASING LOAD INCR.-----------      27
     NUMBER OF DECREASING LOAD INCR.-----------       8
     ORDER OF REGRESSION LINE FOR CALIBRATION---      3
     ORDER OF REGRESSION LINE FOR LOAD-DISTRIB--      5
     ORDER OF REGRESSION LINE FOR GAUGE DATA----      5
     SCALE FACTOR FOR SCALING OF GAUGE READINGS-    .319
     INCREMENTAL DISTANCE FOR LOAD-DISTRIB-----,     30 INCHES
     MULTIPLICATION FACTOR FOR LOAD INPUT-------   49.3 LBS/DIV.

SETTLEMENT GAUGE DATA

     NUMBER OF SETTLEMENT GAUGES--------      2
     DISTANCE FROM GROUND TO GAUGES-----   16.0 INCHES
```

DISTANCES FROM GROUND TO LOAD-TRANSFER CURVES

CURVE NO.	DEPTH(INS)
1	0.0
2	60.0
3	120.0
4	180.0
5	240.0
6	300.0
7	360.0
8	420.0
9	480.0
10	540.0
11	600.0
12	660.0
13	720.0

HB AND T SHAFT TEST NO.2. CONDUCTED ON 17 JULY 1969
TEST CONDUCTED BY PERSONNEL FROM THE UNIVERSITY OF TEXAS
SHAFT LOADED TO FAILURE. LOAD APPLIED IN 50 TON INCREMENTS
TO 600 TONS THEN IN 20 TON INCREMENTS.

STRAIN GAUGE DATA BY LOAD INCREMENTS

LOAD(NOMINAL) RDG1	RDG2	RDG3	RDG4	DIF1	DIF2	DIF3	DIF4	LOAD COMPUTED BY USE OF PMULP AVERAGE	LEVEL	DEPTH
0 TONS								COMPUTED LOAD =		0 POUNDS
-41	6			-0	-0			0	1	0
-14	-7			-0	-0			0	2	162
0	-2			-0	-0			0	3	258
0	-8			-0	-0			0	4	414
-3	-10			-0	-0			0	5	498
21	-3			-0	-0			0	6	642
-19	-2			-0	-0			0	7	678
-4	-1			-0	-0			0	8	713
-3	-5			-0	0			0	9	713
50 TONS								COMPUTED LOAD =		95149 POUNDS
-438	-335			127	109			118	1	0
-214	-194			64	60			62	2	162
-187	-187			60	59			59	3	258
-114	-125			36	37			37	4	414
-84	-99			26	28			27	5	498
-69	-48			29	14			22	6	642
-50	-20			10	6			8	7	678
-18	-19			4	6			5	8	713
-12	13			3	6			4	9	713
100 TONS								COMPUTED LOAD =		195129 POUNDS
-909	-645			277	208			242	1	0
-431	-396			133	124			129	2	162
-395	-391			126	124			125	3	258
-248	-254			79	78			79	4	414
-186	-214			58	65			62	5	498
-184	-82			65	25			45	6	642
-89	-47			22	14			18	7	678
-28	-29			8	9			8	8	713
-21	30			6	11			8	9	713
150 TONS								COMPUTED LOAD =		295553 POUNDS
-1385	-988			429	317			373	1	0
-673	-624			210	197			204	2	162
-626	-619			200	197			198	3	258
-399	-396			127	124			126	4	414
-305	-335			96	104			100	5	498
-300	-125			102	39			71	6	642
-131	-69			36	21			29	7	678
-35	-45			10	14			12	8	713
-34	48			10	17			13	9	713
200 TONS								COMPUTED LOAD =		392576 POUNDS
-1837	-1347			573	432			502	1	0
-917	-859			288	272			280	2	162
-862	-849			275	270			273	3	258
-550	-549			175	173			174	4	414
-417	-471			132	147			140	5	498
-395	-162			133	51			92	6	642
-175	-99			50	31			40	7	678

```
      -48  -60          14   19          16     8      713
      -42   69          12   24          18     9      713
250 TONS                                COMPUTED LOAD =    499409 POUNDS
    -2286-1772         716  567         642     1        0
    -1181-1132         372  359         366     2      162
    -1133-1112         361  354         358     3      258
     -735 -734         234  232         233     4      414
     -574 -631         182  198         190     5      498
     -492 -207         164   65         114     6      642
     -223 -125          65   39          52     7      678
      -59  -80          18   25          21     8      713
      -54   94          16   32          24     9      713
300 TONS                                COMPUTED LOAD =    600868 POUNDS
    -2703-2242         849  717         783     1        0
    -1461-1411         462  448         455     2      162
    -1409-1378         449  439         444     3      258
     -924 -923         295  292         293     4      414
     -745 -799         237  252         244     5      498
     -574 -267         190   84         137     6      642
     -278 -161          83   51          67     7      678
      -78 -102          24   32          28     8      713
      -70  113          21   38          30     9      713
350 TONS                                COMPUTED LOAD =    692566 POUNDS
    -3030-2672         953  854         904     1        0
    -1710-1667         541  530         535     2      162
    -1664-1621         531  516         524     3      258
    -1110-1110         354  352         353     4      414
     -910 -968         289  306         297     5      498
     -640 -319         211  101         156     6      642
     -322 -197          97   62          79     7      678
      -92 -121          28   38          33     8      713
      -83  140          26   46          36     9      713
400 TONS                                COMPUTED LOAD =    795603 POUNDS
    -3408-3210        1074 1026        1050     1        0
    -2000-1970         634  626         630     2      162
    -1967-1909         627  608         618     3      258
    -1341-1344         428  426         427     4      414
    -1131-1186         360  375         367     5      498
     -747 -400         245  127         186     6      642
     -399 -256         121   81         101     7      678
     -116 -156          36   49          43     8      713
     -108  178          33   58          46     9      713
450 TONS                                COMPUTED LOAD =    898640 POUNDS
    -3738-3706        1179 1184        1182     1        0
    -2290-2285         726  727         726     2      162
    -2271-2195         724  700         712     3      258
    -1578-1584         503  503         503     4      414
    -1359-1414         433  448         440     5      498
     -814 -492         266  156         211     6      642
     -495 -351         152  111         132     7      678
     -151 -206          47   65          56     8      713
     -147  236          46   77          61     9      713
500 TONS                                COMPUTED LOAD =    992310 POUNDS
    -4066-4170        1284 1332        1308     1        0
    -2565-2574         814  819         816     2      162
    -2538-2452         810  782         796     3      258
    -1792-1818         572  577         575     4      414
    -1558-1611         496  511         503     5      498
     -849 -575         278  182         230     6      642
     -601 -465         186  148         167     7      678
     -195 -261          61   83          72     8      713
     -190  304          60   99          79     9      713
```

520 TONS			COMPUTED LOAD =	1039145 POUNDS
-4283-4458	1353 1424		1389	1 0
-2744-2776	871 883		877	2 162
-2718-2627	867 837		852	3 258
-1934-1949	617 619		618	4 414
-1661-1715	529 544		536	5 498
-862 -616	282 196		239	6 642
-666 -535	206 170		188	7 678
-221 -294	69 93		81	8 713
-215 344	68 111		89	9 713
540 TONS			COMPUTED LOAD =	1078585 POUNDS
-4436-4651	1402 1486		1444	1 0
-2856-2913	907 927		917	2 162
-2836-2742	905 874		889	3 258
-2036-2054	649 653		651	4 414
-1748-1805	557 573		565	5 498
-871 -658	285 209		247	6 642
-732 -608	227 193		210	7 678
-252 -332	79 106		92	8 713
-242 390	76 126		101	9 713
560 TONS			COMPUTED LOAD =	1122955 POUNDS
-4589-4850	1451 1549		1500	1 0
-2993-3052	950 971		961	2 162
-2959-2851	944 909		926	3 258
-2126-2147	678 682		680	4 414
-1837-1897	585 602		593	5 498
-882 -707	288 225		256	6 642
-801 -674	249 214		232	7 678
-280 -366	88 116		102	8 713
-268 438	85 141		113	9 713
580 TONS			COMPUTED LOAD =	1158944 POUNDS
-4767-5086	1508 1624		1566	1 0
-3127-3205	993 1020		1007	2 162
-3092-2988	986 953		969	3 258
-2229-2250	711 715		713	4 414
-1926-1993	613 633		623	5 498
-893 -766	292 243		267	6 642
-879 -754	274 240		257	7 678
-315 -406	99 129		114	8 713
-298 488	94 157		126	9 713
600 TONS			COMPUTED LOAD =	1201342 POUNDS
-4901-5259	1550 1680		1615	1 0
-3238-3336	1028 1062		1045	2 162
-3207-3106	1023 990		1007	3 258
-2320-2344	740 745		743	4 414
-2021-2090	644 664		654	5 498
-908 -824	296 262		279	6 642
-953 -831	298 264		281	7 678
-347 -445	109 142		126	8 713
-329 537	104 173		138	9 713
620 TONS			COMPUTED LOAD =	1234866 POUNDS
-5078-5476	1607 1749		1678	1 0
-3369-3487	1070 1110		1090	2 162
-3330-3223	1062 1027		1045	3 258
-2410-2448	769 778		774	4 414
-2113-2183	673 693		683	5 498
-910 -879	297 279		288	6 642
-1030 -914	323 291		307	7 678
-381 -486	120 155		137	8 713
-360 591	114 190		152	9 713
640 TONS			COMPUTED LOAD =	1287124 POUNDS
-5250-5703	1662 1821		1741	1 0

```
    -3504-3650   1113 1162
    -3472-3369   1108 1074
    -2475-2534    790  806
    -2235-2313    712  735
     -935 -973    305  309
    -1128-1021    354  325
     -426 -542    135  173
     -403  651    128  209
660 TONS
    -5396-5878   1708 1877
    -3610-3779   1147 1203
    -3585-3480   1144 1109
    -2556-2607    815  829
    -2338-2420    745  769
     -950-1059    310  337
    -1212-1118    381  356
     -465 -590    147  188
     -441  705    140  226
680 TONS
    -5576-6107   1766 1950
    -3750-3938   1192 1254
    -3710-3613   1183 1152
    -2369-2458    756  782
    -2436-2525    776  802
     -963-1136    314  361
    -1289-1213    405  386
     -501 -636    159  203
     -478  756    152  243
700 TONS
    -5767-6331   1827 2022
    -3867-4071   1229 1296
    -3818-3726   1218 1188
    -2411-2507    769  797
    -2535-2640    808  839
     -982-1225    320  390
    -1383-1318    435  420
     -544 -692    172  220
     -519  816    165  262
720 TONS
    -5942-6563   1882 2096
    -3996-4220   1270 1344
    -3939-3849   1257 1227
    -2468-2554    787  812
    -2627-2748    837  873
     -997-1306    325  416
    -1462-1417    460  451
     -586 -742    186  236
     -561  873    178  280
740 TONS
    -6106-6807   1935 2173
    -4124-4386   1311 1397
    -4080-4000   1302 1275
    -2540-2617    810  832
    -2739-2889    873  918
    -1017-1436    331  457
    -1556-1552    490  494
     -641 -804    203  256
     -614  941    195  302
760 TONS
    -6290-7048   1993 2250
    -4239-4542   1348 1447
    -4203-4124   1341 1315

    1138     2     162
    1091     3     258
     798     4     414
     723     5     498
     307     6     642
     339     7     678
     154     8     713
     168     9     713
COMPUTED LOAD =  1328536 POUNDS
    1793     1       0
    1175     2     162
    1157     3     258
     822     4     414
     757     5     498
     323     6     642
     368     7     678
     167     8     713
     183     9     713
COMPUTED LOAD =  1365511 POUNDS
    1858     1       0
    1223     2     162
    1168     3     258
     769     4     414
     789     5     498
     338     6     642
     396     7     678
     181     8     713
     197     9     713
COMPUTED LOAD =  1405444 POUNDS
    1924     1       0
    1263     2     162
    1203     3     258
     783     4     414
     823     5     498
     355     6     642
     427     7     678
     196     8     713
     213     9     713
COMPUTED LOAD =  1444884 POUNDS
    1989     1       0
    1307     2     162
    1242     3     258
     800     4     414
     855     5     498
     370     6     642
     456     7     678
     211     8     713
     229     9     713
COMPUTED LOAD =  1494677 POUNDS
    2054     1       0
    1354     2     162
    1288     3     258
     821     4     414
     896     5     498
     394     6     642
     492     7     678
     230     8     713
     248     9     713
COMPUTED LOAD =  1533131 POUNDS
    2122     1       0
    1397     2     162
    1328     3     258
```

-2587-2656 825 845
-2807-2995 894 952
-1019-1530 332 487
-1610-1658 508 528
-681 -848 216 270
-652 991 207 318
780 TONS
-6479-7299 2054 2330
-4346-4680 1382 1491
-4309-4221 1375 1346
-2619-2687 835 855
-2870-3121 915 992
-1022-1652 333 526
-1666-1791 525 571
-726 -899 230 286
-697 1049 221 336
800 TONS
-6667-7543 2114 2408
-4433-4835 1410 1540
-4407-4315 1406 1376
-2653-2726 846 867
-2908-3256 927 1035
-1009-1802 329 574
-1720-1932 543 616
-773 -943 245 300
-737 1096 234 351
820 TONS
-6842-7781 2170 2484
-4510-4975 1434 1585
-4484-4381 1430 1397
-2677-2737 854 871
-2907-3367 926 1071
-938-1942 306 619
-1750-2048 552 653
-807 -976 256 311
-769 1139 244 365
700 TONS R
-6067-6997 1922 2234
-3982-4495 1266 1432
-3997-3924 1275 1251
-2356-2424 752 771
-2653-3132 845 996
-712-1632 234 520
-1574-1917 496 611
-728 -882 231 281
-694 1035 220 332
600 TONS R
-5299-6098 1677 1947
-3459-3969 1099 1264
-3525-3470 1124 1106
-2052-2149 655 683
-2402-2866 765 911
-592-1379 196 439
-1443-1799 454 573
-671 -821 213 262
-645 960 205 308
500 TONS R
-4498-5174 1422 1652
-2911-3411 924 1086
-3021-2982 964 951
-1742-1867 556 593
-2126-2572 677 817

835 4 414
923 5 498
469 6 642
518 7 678
243 8 713
262 9 713
COMPUTED LOAD = 1575036 POUNDS
2102 1 0
1436 2 162
1360 3 258
845 4 414
953 5 498
429 6 642
548 7 678
258 8 713
279 9 713
COMPUTED LOAD = 1593770 POUNDS
2261 1 0
1475 2 162
1391 3 258
867 4 414
981 5 498
451 6 642
579 7 678
273 8 713
293 9 713
COMPUTED LOAD = 1648000 POUNDS
2327 1 0
1510 2 162
1414 3 258
862 4 414
999 5 498
462 6 642
602 7 678
284 8 713
305 9 713
COMPUTED LOAD = 1386710 POUNDS
2078 1 0
1349 2 162
1263 3 258
761 4 414
921 5 498
377 6 642
553 7 678
256 8 713
276 9 713
COMPUTED LOAD = 1189510 POUNDS
1812 1 0
1181 2 162
1115 3 258
669 4 414
838 5 498
317 6 642
514 7 678
237 8 713
256 9 713
COMPUTED LOAD = 985901 POUNDS
1537 1 0
1005 2 162
957 3 258
574 4 414
747 5 498

```
     -482-1155      160  367          264     6     642
    -1307-1677      411  534          473     7     678
     -617 -760      196  242          219     8     713
     -594  886      189  284          236     9     713
400 TONS R                       COMPUTED LOAD =   786236 POUNDS
    -3692-4244     1165 1356         1260     1       0
    -2360-2843      748  905          857     2     162
    -2499-2480      797  790          794     3     258
    -1436-1588      458  504          481     4     414
    -1927-2258      614  717          665     5     498
     -382 -391      129  124          196     6     642
    -1167-1555      366  495          431     7     678
     -561 -696      178  222          200     8     713
     -543  812      172  261          216     9     713
300 TONS R                       COMPUTED LOAD =   581641 POUNDS
    -2829-3269      889 1045          967     1       0
    -1774-2232      561  710          636     2     162
    -1932-1935      616  617          616     3     258
    -1124-1310      359  415          387     4     414
    -1486-1905      473  605          539     5     498
     -302 -776      103  247          175     6     642
    -1015-1417      318  451          385     7     678
     -502 -628      159  200          179     8     713
     -489  727      155  234          194     9     713
200 TONS R                       COMPUTED LOAD =   390653 POUNDS
    -2042-2364      638  756          697     1       0
    -1235-1662      389  528          469     2     162
    -1391-1419      444  452          448     3     258
     -853-1087      272  344          308     4     414
    -1125-1547      358  490          424     5     498
     -236 -621       82  197          140     6     642
     -864-1281      270  408          339     7     678
     -445 -558      141  178          159     8     713
     -434  645      137  207          172     9     713
100 TONS R                       COMPUTED LOAD =   193305 POUNDS
    -1214-1401      374  449          412     1       0
     -649-1034      203  328          265     2     162
     -790 -852      252  271          262     3     258
     -614 -855      196  270          233     4     414
     -710-1143      226  361          293     5     498
     -173 -464       62  147          104     6     642
     -687-1113      213  354          284     7     678
     -374 -472      118  150          134     8     713
     -365  547      115  176          146     9     713
0   RETURN                       COMPUTED LOAD =      937 POUNDS
     -481 -320      140  104          122     1       0
      -62 -335       15  105           60     2     162
     -139 -234       44   74           59     3     258
     -387 -507      123  159          141     4     414
     -278 -698       88  219          154     5     498
     -114 -297       43   94           68     6     642
     -464 -860      142  274          208     7     678
     -279 -351       88  112          100     8     713
     -269  412       85  133          109     9     713
```

LOAD-SETTLEMENT CURVE FOR TOP OF SHAFT

COMPUTED LOAD(LBS)	SETTLEMENT INCHES	NOMINAL LOAD	OTHER COMMENTS
0	-0.0000	0 TONS	
95149	.0055	50 TONS	
195129	.0115	100 TONS	
295553	.0195	150 TONS	
392576	.0285	200 TONS	
499409	.0390	250 TONS	
600868	.0500	300 TONS	
692566	.0600	350 TONS	
795603	.0790	400 TONS	
898640	.1020	450 TONS	
992310	.1295	500 TONS	
1039145	.1475	520 TONS	
1078585	.1675	540 TONS	
1122955	.1870	560 TONS	
1158944	.2105	580 TONS	
1201342	.2290	600 TONS	
1234866	.2625	620 TONS	
1287124	.2940	640 TONS	
1328536	.3300	660 TONS	
1365511	.3690	680 TONS	
1405444	.4135	700 TONS	
1444884	.4560	720 TONS	
1494677	.4910	740 TONS	
1533131	.6315	760 TONS	
1575036	.7610	780 TONS	
1593770	.9375	800 TONS	
1648000	1.1765	820 TONS	
1386710	1.2240	700 TONS	R
1189510	1.2055	600 TONS	R
985901	1.1850	500 TONS	R
786236	1.1630	400 TONS	R
581641	1.1385	300 TONS	R
390653	1.1120	200 TONS	R
193305	1.0800	100 TONS	R
937	1.0370	0 RETURN	

SELECTED APPLIED LOAD FOR LOAD TRANSFER
BASED ON BEST FIT CURVE FOR GAUGE DATA

CURVE NUMBER	APPLIED LOAD(LBS)
1	50000.0
2	200000.0
3	400000.0
4	600000.0
5	800000.0
6	1000000.0
7	1200000.0
8	1400000.0
9	1600000.0
10	1640000.0

CALIBRATION CURVE FOR IN-SHAFT CALIBRATION

CALIBRATION CONSTANTS

A(0) = 0.
A(1) = 7.841E+02
A(2) =-8.951E-03
A(3) =-1.007E-05

GAGE READING	INDICATED LOAD (LBS)	SLOPE OF CURVE(LBS/DIV)
0	0.0	784.10
100	78310.3	782.01
200	156381.1	779.31
300	234152.1	776.01
400	311562.9	772.10
500	388553.0	767.60
600	465062.0	762.48
700	541029.5	756.77
800	616395.1	750.45
900	691098.5	743.52
1000	765079.1	735.99
1100	838276.7	727.86
1200	910630.6	719.12
1300	982080.7	709.78
1400	1052566.4	699.83
1500	1122027.4	689.28
1600	1190403.2	678.13
1700	1257633.4	666.37
1800	1323657.7	654.01
1900	1388415.6	641.05
2000	1451846.6	627.48
2100	1513890.5	613.30
2200	1574486.8	598.52
2300	1633575.0	583.14
2400	1691094.8	567.15

50 TONS
LOAD-DISTRIBUTION CURVE FOR APPLIED LOAD OF 95149

DATA FROM GAUGES BY DEPTH

LEVEL NO.	DEPTH INCHES	MEASURED LOAD(LBS)	COMPUTED LOAD(LBS)	ERROR (LBS
1	0	92156.6	95149.0	2992.4
2	162	65202.2	65202.2	.0
3	258	58839.0	58839.0	-.0
4	414	35650.7	38130.8	2480.1
5	498	23681.2	23681.2	.0
6	642	11721.8	7285.1	-4436.7
7	678	6472.7	6472.7	-.0
8	713	7719.5	7116.5	-603.1
9	713	6513.4	7116.5	603.1

THE SQUARE OF THE COEFFICIENT OF CORRELATION IS EQUAL TO 9.954E-01

CONSTANTS FOR REGRESSION LINE

A(0) = 9.515E+04
A(1) =-4.363E+02
A(2) = 2.556E+00
A(3) =-7.585E-03
A(4) = 9.201E-06
A(5) =-3.825E-09

LOAD DISTRIBUTION, SHAFT MOVEMENT AND LOAD TRANSFER ALONG SHAFT

DEPTH INS.	LOAD POUNDS	MOVEMENT INCHES	LOAD PSI	TRANSFER TSF	PERCENT LOAD TO APPLIED	MAXIMUM
0	95149	.005	3.47	.250	100.0	5.8
30	84162	.005	2.41	.173	88.5	5.1
60	76648	.005	1.62	.117	80.6	4.7
90	71633	.004	1.07	.077	75.3	4.3
120	68299	.004	.72	.052	71.8	4.1
150	65975	.004	.53	.038	69.3	4.0
180	64120	.003	.47	.034	67.4	3.9
210	62321	.003	.50	.036	65.5	3.8
240	60274	.003	.60	.043	63.3	3.7
270	57777	.003	.73	.053	60.7	3.5
300	54717	.002	.89	.064	57.5	3.3
330	51059	.002	1.05	.075	53.7	3.1
360	46838	.002	1.19	.086	49.2	2.8
390	42141	.002	1.30	.093	44.3	2.6
420	37104	.002	1.37	.098	39.0	2.3
450	31894	.001	1.39	.100	33.5	1.9
480	26703	.001	1.36	.098	28.1	1.6
510	21733	.001	1.27	.092	22.8	1.3
540	17186	.001	1.13	.082	18.1	1.0
570	13256	.001	.95	.068	13.9	.8
600	10112	.001	.72	.052	10.6	.6
630	7892	.001	.46	.033	8.3	.5
660	6688	.001	.18	.013	7.0	.4
690	6539	.001	-.10	-.007	6.9	.4
720	7416	.001	-.36	-.026	7.8	.5

100 TONS
LOAD-DISTRIBUTION CURVE FOR APPLIED LOAD OF 195129

DATA FROM GAUGES BY DEPTH

LEVEL NO.	DEPTH INCHES	MEASURED LOAD(LBS)	COMPUTED LOAD(LBS)	ERROR (LBS
1	0	189303.2	195129.4	5826.2
2	162	135670.0	135670.0	.0
3	258	123892.4	123892.4	-.0
4	414	76198.7	82627.1	6428.4
5	498	53886.1	53886.1	.0
6	642	24651.9	19168.6	-5483.3
7	678	15189.2	15189.2	-.0
8	713	12543.8	12664.4	120.6
9	713	12785.0	12664.4	-120.6

THE SQUARE OF THE COEFFICIENT OF CORRELATION IS EQUAL TO 9.968E-01

CONSTANTS FOR REGRESSION LINE

A(0) = 1.951E+05
A(1) =-9.060E+02
A(2) = 5.548E+00
A(3) =-1.692E-02
A(4) = 2.137E-05
A(5) =-9.468E-09

LOAD DISTRIBUTION, SHAFT MOVEMENT AND LOAD TRANSFER ALONG SHAFT

DEPTH INS.	LOAD POUNDS	MOVEMENT INCHES	LOAD PSI	TRANSFER TSF	PERCENT LOAD APPLIED	TO MAXIMUM
0	195129	.011	7.21	.519	100.0	11.8
30	172503	.010	4.91	.353	88.4	10.5
60	157357	.010	3.22	.232	80.6	9.5
90	147538	.009	2.06	.149	75.6	9.0
120	141253	.008	1.33	.096	72.4	8.6
150	137042	.008	.95	.068	70.2	8.3
180	133749	.007	.84	.060	68.5	8.1
210	130497	.006	.92	.066	66.9	7.9
240	126656	.006	1.14	.082	64.9	7.7
270	121822	.005	1.44	.103	62.4	7.4
300	115780	.005	1.77	.127	59.3	7.0
330	108488	.004	2.09	.151	55.6	6.6
360	100039	.004	2.38	.171	51.3	6.1
390	90639	.004	2.60	.187	46.5	5.5
420	80578	.003	2.73	.196	41.3	4.9
450	70203	.003	2.76	.199	36.0	4.3
480	59888	.003	2.69	.194	30.7	3.6
510	50011	.002	2.53	.182	25.6	3.0
540	40921	.002	2.28	.164	21.0	2.5
570	32915	.002	1.96	.141	16.9	2.0
600	26206	.002	1.60	.115	13.4	1.6
630	20900	.002	1.22	.088	10.7	1.3
660	16966	.002	.88	.063	8.7	1.0
690	14206	.002	.61	.044	7.3	.9
720	12234	.002	.47	.034	6.3	.7

150 TONS
LOAD-DISTRIBUTION CURVE FOR APPLIED LOAD OF 295553

DATA FROM GAUGES BY DEPTH

LEVEL NO.	DEPTH INCHES	MEASURED LOAD(LBS)	COMPUTED LOAD(LBS)	ERROR (LBS
1	0	290632.1	295553.5	4921.4
2	162	214529.9	214529.9	.0
3	258	196202.1	196202.1	-.0
4	414	121313.8	132132.7	10818.8
5	498	87258.8	87258.8	.0
6	642	38441.0	30660.8	-7780.1
7	678	23639.4	23639.4	-.0
8	713	18091.2	19176.5	1085.3
9	713	20261.8	19176.5	-1085.3

THE SQUARE OF THE COEFFICIENT OF CORRELATION IS EQUAL TO 9.975E-01

CONSTANTS FOR REGRESSION LINE

A(0) = 2.956E+05
A(1) =-1.225E+03
A(2) = 7.528E+00
A(3) =-2.327E-02
A(4) = 2.929E-05
A(5) =-1.284E-08

LOAD DISTRIBUTION, SHAFT MOVEMENT AND LOAD TRANSFER ALONG SHAFT

DEPTH INS.	LOAD POUNDS	MOVEMENT INCHES	LOAD TRANSFER PSI	TSF	PERCENT APPLIED	LOAD TO MAXIMUM
0	295553	.019	9.75	.702	100.0	17.9
30	264980	.018	6.63	.477	89.7	16.1
60	244510	.017	4.36	.314	82.7	14.8
90	231184	.015	2.82	.203	78.2	14.0
120	222533	.014	1.86	.134	75.3	13.5
150	216547	.014	1.38	.100	73.3	13.1
180	211637	.013	1.27	.092	71.6	12.8
210	206592	.012	1.44	.104	69.9	12.5
240	200550	.011	1.79	.129	67.9	12.2
270	192953	.010	2.25	.162	65.3	11.7
300	183515	.009	2.76	.199	62.1	11.1
330	172181	.008	3.25	.234	58.3	10.4
360	159091	.008	3.68	.265	53.8	9.7
390	144543	.007	4.02	.289	48.9	8.8
420	128955	.006	4.23	.305	43.6	7.8
450	112826	.006	4.30	.310	38.2	6.8
480	96701	.005	4.23	.304	32.7	5.9
510	81133	.005	4.01	.289	27.5	4.9
540	66645	.005	3.66	.263	22.5	4.0
570	53692	.004	3.20	.230	18.2	3.3
600	42624	.004	2.66	.192	14.4	2.6
630	33651	.004	2.10	.151	11.4	2.0
660	26800	.004	1.55	.111	9.1	1.6
690	21882	.004	1.08	.078	7.4	1.3
720	18456	.004	.77	.055	6.2	1.1

200 TONS
LOAD-DISTRIBUTION CURVE FOR APPLIED LOAD OF 392576

DATA FROM GAUGES BY DEPTH

LEVEL NO.	DEPTH INCHES	MEASURED LOAD(LBS)	COMPUTED LOAD(LBS)	ERROR (LBS
1	0	390291.8	392575.9	2284.1
2	162	294664.2	294664.2	.0
3	258	269407.1	269407.1	-.0
4	414	168049.9	182126.5	14076.6
5	498	121702.7	121702.7	.0
6	642	49881.0	43933.7	-5947.3
7	678	33407.3	33407.3	-.0
8	713	24843.9	26049.7	1205.8
9	713	27255.5	26049.7	-1205.8

THE SQUARE OF THE COEFFICIENT OF CORRELATION IS EQUAL TO 9.984E-01

CONSTANTS FOR REGRESSION LINE

A(0) = 3.926E+05
A(1) =-1.474E+03
A(2) = 9.161E+00
A(3) =-2.896E-02
A(4) = 3.686E-05
A(5) =-1.628E-08

LOAD DISTRIBUTION, SHAFT MOVEMENT AND LOAD TRANSFER ALONG SHAFT

DEPTH INS.	LOAD POUNDS	MOVEMENT INCHES	LOAD TRANSFER PSI	TSF	PERCENT LOAD TO APPLIED	MAXIMUM
0	392576	.028	11.73	.844	100.0	23.8
30	355854	.026	7.95	.572	90.6	21.6
60	331335	.024	5.22	.376	84.4	20.1
90	315343	.023	3.39	.244	80.3	19.1
120	304822	.022	2.30	.165	77.6	18.5
150	297293	.020	1.78	.128	75.7	18.0
180	290800	.019	1.73	.124	74.1	17.6
210	283869	.018	2.00	.144	72.3	17.2
240	275455	.017	2.49	.180	70.2	16.7
270	264901	.016	3.12	.225	67.5	16.1
300	251882	.014	3.79	.273	64.2	15.3
330	236367	.013	4.43	.319	60.2	14.3
360	218562	.012	4.99	.360	55.7	13.3
390	198872	.011	5.43	.391	50.7	12.1
420	177844	.011	5.70	.410	45.3	10.8
450	156128	.010	5.79	.417	39.8	9.5
480	134425	.009	5.69	.410	34.2	8.2
510	113438	.009	5.41	.390	28.9	6.9
540	93829	.008	4.97	.358	23.9	5.7
570	76170	.008	4.38	.316	19.4	4.6
600	60893	.008	3.71	.267	15.5	3.7
630	48245	.007	3.00	.216	12.3	2.9
660	38240	.007	2.32	.167	9.7	2.3
690	30611	.007	1.75	.126	7.8	1.9
720	24764	.007	1.39	.100	6.3	1.5

Note: Remaining load-distribution data are omitted from the Sample Output.

LOAD-SETTLEMENT CURVE FOR SHAFT (INTERPOLATED)

APPLIED LOAD	TOP OF SHAFT	GROUND SURFACE	BOTTOM OF SHAFT
0	0.000	0.000	0.000
50000	.003	.003	.000
100000	.006	.006	.001
150000	.009	.008	.001
200000	.012	.011	.002
250000	.016	.015	.003
300000	.020	.019	.004
350000	.025	.024	.006
400000	.029	.028	.007
450000	.034	.033	.009
500000	.039	.038	.011
550000	.044	.043	.013
600000	.050	.049	.015
650000	.055	.054	.017
700000	.061	.060	.019
750000	.071	.069	.025
800000	.080	.078	.030
850000	.091	.089	.038
900000	.102	.100	.045
950000	.117	.115	.056
1000000	.132	.130	.067
1050000	.153	.151	.083
1100000	.177	.174	.103
1150000	.205	.202	.127
1200000	.228	.226	.146
1250000	.272	.269	.185
1300000	.305	.302	.214
1350000	.353	.350	.257
1400000	.407	.404	.308
1450000	.469	.465	.364
1500000	.510	.507	.402
1550000	.684	.680	.571
1600000	.965	.961	.847
1648000	1.176	1.173	1.057

LOAD TRANSFER CURVE FOR DEPTH OF 0 INCHES

MOVEMENT INCHES	LOAD TRANSFER PSI
0.000	0.00
.005	3.29
.010	6.53
.015	8.50
.020	10.01
.025	11.14
.030	12.14
.035	13.01
.040	13.53
.045	13.62
.050	13.70
.055	13.75
.060	13.75
.065	13.64
.070	13.52
.075	13.41
.080	13.24
.085	13.03
.090	12.81
.095	12.60
.100	12.39
.110	11.85
.120	11.32
.130	10.61
.140	9.47
.150	8.75
.160	8.46
.170	7.94
.180	7.17
.190	6.51
.200	5.93
.300	3.26
.400	.25
.500	-1.08
.600	-1.68
.700	-2.29
.800	-3.44
.900	-5.30
1.000	-5.72
1.100	-5.41
1.173	-5.18

LOAD TRANSFER CURVE FOR DEPTH OF 60 INCHES

MOVEMENT INCHES	LOAD TRANSFER PSI
0.000	0.00
.005	1.77
.010	3.30
.015	4.12
.020	4.74
.025	5.27
.030	5.77
.035	6.19
.040	6.39
.045	6.60
.050	6.83
.055	7.00
.060	7.07
.065	7.15
.070	7.23
.075	7.27
.080	7.31
.085	7.35
.090	7.39
.095	7.41
.100	7.40
.110	7.40
.120	7.34
.130	6.80
.140	6.44
.150	6.39
.160	6.34
.170	6.29
.180	6.13
.190	5.86
.200	5.66
.300	5.49
.400	4.93
.500	4.87
.600	4.71
.700	4.82
.800	4.52
.900	3.88
1.000	4.12
1.100	4.57
1.158	4.84

LOAD TRANSFER CURVE FOR DEPTH OF 120 INCHES

MOVEMENT INCHES	LOAD TRANSFER PSI
0.000	0.00
.005	.88
.010	1.48
.015	1.89
.020	2.19
.025	2.49
.030	2.78
.035	3.07
.040	3.36
.045	3.66
.050	3.88
.055	4.03
.060	4.18
.065	4.33
.070	4.48
.075	4.63
.080	4.77
.085	4.92
.090	5.06
.095	5.20
.100	5.34
.110	5.62
.120	5.59
.130	5.55
.140	5.66
.150	5.82
.160	6.14
.170	6.30
.180	6.27
.190	6.26
.200	6.40
.300	7.33
.400	8.20
.500	8.70
.600	8.83
.700	9.31
.800	9.51
.900	9.57
1.000	10.05
1.100	10.55
1.144	10.77

Note: Remaining load-transfer data are omitted from Sample Output.

REGRESSION LINE FOR GAUGE LEVEL -- 1

CONSTANTS FOR REGRESSION LINE

A(0) = 0.
A(1) = 1.236E-03
A(2) = 5.149E-11
A(3) = 1.926E-16
A(4) =-2.342E-22
A(5) = 8.404E-29

APPLIED LOAD(LBS)	AVE GAUGE READINGS	COMPUTED READINGS	ERROR	SLOPE OF CURVE
0.0	0.0	0.0	-0.0	1.236E-03
95149.0	117.7	118.3	.6	1.251E-03
195129.4	242.3	244.3	2.1	1.272E-03
295553.5	372.9	373.3	.4	1.296E-03
392575.9	502.3	500.2	-2.0	1.319E-03
499409.0	641.7	642.4	.7	1.341E-03
600868.4	783.1	779.4	-3.8	1.359E-03
692566.4	903.9	904.5	.6	1.370E-03
795603.4	1050.0	1046.3	-3.7	1.381E-03
898640.4	1181.7	1189.0	7.3	1.390E-03
992310.4	1308.1	1319.7	11.6	1.400E-03
1039145.4	1388.6	1385.4	-3.2	1.406E-03
1078585.4	1443.8	1441.0	-2.8	1.413E-03
1122955.4	1499.9	1503.9	3.9	1.422E-03
1158944.4	1566.0	1555.2	-10.8	1.432E-03
1201342.4	1614.9	1616.2	1.3	1.445E-03
1234866.4	1677.8	1664.9	-12.9	1.458E-03
1287124.4	1741.4	1741.6	.2	1.482E-03
1328536.4	1792.6	1803.5	10.9	1.506E-03
1365511.4	1857.9	1859.6	1.8	1.530E-03
1405444.4	1924.0	1921.3	-2.7	1.562E-03
1444884.4	1989.0	1983.6	-5.4	1.597E-03
1494677.4	2054.0	2064.4	10.4	1.651E-03
1533131.4	2121.8	2128.8	7.0	1.698E-03
1575036.4	2192.0	2201.2	9.2	1.758E-03
1593770.4	2260.9	2234.4	-26.5	1.787E-03
1648000.4	2326.8	2333.8	7.0	1.882E-03

THE SQUARE OF THE COEFFICIENT OF CORRELATION IS EQUAL TO 9.999E-01

REGRESSION LINE FOR GAUGE LEVEL -- 2

CONSTANTS FOR REGRESSION LINE

A(0) = 0.
A(1) = 6.304E-04
A(2) = 2.044E-10
A(3) =-2.143E-17
A(4) = 4.785E-23
A(5) =-2.777E-29

APPLIED LOAD(LBS)	AVE GAUGE READINGS	COMPUTED READINGS	ERROR	SLOPE OF CURVE
0.0	0.0	0.0	-0.0	6.304E-04
95149.0	61.7	61.8	.1	6.688E-04
195129.4	128.6	130.7	2.1	7.089E-04
295553.5	203.5	203.9	.4	7.495E-04
392575.9	279.9	278.6	-1.4	7.892E-04
499409.0	365.6	365.2	-.3	8.337E-04
600868.4	454.7	452.0	-2.7	8.763E-04
692566.4	535.3	534.1	-1.2	9.143E-04
795603.4	629.9	630.4	.6	9.557E-04
898640.4	726.4	730.9	4.6	9.942E-04
992310.4	816.3	825.6	9.2	1.025E-03
1039145.4	877.1	873.9	-3.2	1.039E-03
1078585.4	916.8	915.1	-1.7	1.049E-03
1122955.4	960.8	961.8	1.0	1.059E-03
1158944.4	1006.6	1000.0	-6.6	1.065E-03
1201342.4	1045.2	1045.3	.1	1.071E-03
1234866.4	1090.2	1081.3	-8.9	1.075E-03
1287124.4	1137.7	1137.6	-.1	1.077E-03
1328536.4	1175.2	1182.2	7.0	1.076E-03
1365511.4	1222.9	1221.9	-1.0	1.073E-03
1405444.4	1262.8	1264.7	1.9	1.068E-03
1444884.4	1307.1	1306.6	-.5	1.059E-03
1494677.4	1354.0	1359.0	5.0	1.044E-03
1533131.4	1397.2	1398.9	1.6	1.029E-03
1575036.4	1436.3	1441.5	5.3	1.008E-03
1593770.4	1474.9	1460.3	-14.6	9.976E-04
1648000.4	1509.5	1513.5	4.0	9.620E-04

THE SQUARE OF THE COEFFICIENT OF CORRELATION IS EQUAL TO 9.999E-01

REGRESSION LINE FOR GAUGE LEVEL -- 3

CONSTANTS FOR REGRESSION LINE

A(0) = 0.
A(1) = 5.777E-04
A(2) = 3.824E-10
A(3) =-2.860E-16
A(4) = 1.957E-22
A(5) =-6.027E-29

APPLIED LOAD(LBS)	AVE GAUGE READINGS	COMPUTED READINGS	ERROR	SLOPE OF CURVE
0.0	0.0	0.0	-0.0	5.777E-04
95149.0	59.3	58.2	-1.1	6.433E-04
195129.4	125.0	125.4	.4	6.996E-04
295553.5	198.3	198.1	-.1	7.467E-04
392575.9	272.6	272.5	-.1	7.859E-04
499409.0	357.8	358.6	.8	8.244E-04
600868.4	444.2	443.9	-.3	8.580E-04
692566.4	523.6	523.9	.3	8.866E-04
795603.4	617.9	616.8	-1.1	9.166E-04
898640.4	712.0	712.7	.7	9.438E-04
992310.4	795.6	802.1	6.6	9.646E-04
1039145.4	852.2	847.5	-4.7	9.731E-04
1078585.4	889.4	886.0	-3.3	9.791E-04
1122955.4	926.4	929.6	3.2	9.841E-04
1158944.4	969.4	965.1	-4.4	9.868E-04
1201342.4	1006.6	1006.9	.3	9.881E-04
1234866.4	1044.9	1040.0	-4.8	9.874E-04
1287124.4	1090.8	1091.6	.7	9.832E-04
1328536.4	1126.5	1132.1	5.6	9.766E-04
1365511.4	1167.7	1168.1	.4	9.681E-04
1405444.4	1202.9	1206.5	3.6	9.557E-04
1444884.4	1241.9	1243.9	2.1	9.400E-04
1494677.4	1288.4	1290.1	1.7	9.145E-04
1533131.4	1327.8	1324.8	-3.0	8.902E-04
1575036.4	1360.2	1361.5	1.3	8.587E-04
1593770.4	1390.8	1377.4	-13.4	8.427E-04
1648000.4	1413.6	1421.7	8.1	7.896E-04

THE SQUARE OF THE COEFFICIENT OF CORRELATION IS EQUAL TO 9.999E-01

REGRESSION LINE FOR GAUGE LEVEL -- 4

CONSTANTS FOR REGRESSION LINE

A(0) = 0.
A(1) = 6.436E-04
A(2) =-1.541E-09
A(3) = 3.337E-15
A(4) =-2.392E-21
A(5) = 5.503E-28

APPLIED LOAD(LBS)	AVE GAUGE READINGS	COMPUTED READINGS	ERROR	SLOPE OF CURVE
0.0	0.0	0.0	-0.0	6.436E-04
95149.0	36.8	50.0	13.1	4.329E-04
195129.4	78.8	88.4	9.6	3.562E-04
295553.5	125.5	124.7	-.8	3.811E-04
392575.9	174.0	165.4	-8.7	4.630E-04
499409.0	233.0	221.0	-12.0	5.807E-04
600868.4	293.3	285.6	-7.8	6.892E-04
692566.4	352.8	352.5	-.3	7.657E-04
795603.4	427.0	434.2	7.2	8.126E-04
898640.4	503.1	518.2	15.1	8.097E-04
992310.4	574.5	592.2	17.6	7.624E-04
1039145.4	618.1	627.0	8.9	7.238E-04
1078585.4	651.1	654.8	3.7	6.846E-04
1122955.4	680.3	684.1	3.8	6.340E-04
1158944.4	713.1	706.1	-7.0	5.889E-04
1201342.4	742.6	729.9	-12.8	5.322E-04
1234866.4	773.6	746.9	-26.7	4.856E-04
1287124.4	797.7	770.4	-27.3	4.123E-04
1328536.4	822.2	786.3	-35.9	3.556E-04
1365511.4	768.6	798.5	29.9	3.079E-04
1405444.4	783.1	809.9	26.7	2.614E-04
1444884.4	799.7	819.4	19.7	2.225E-04
1494677.4	821.3	829.5	8.3	1.872E-04
1533131.4	835.0	836.4	1.4	1.732E-04
1575036.4	845.0	843.6	-1.4	1.742E-04
1593770.4	856.7	846.9	-9.7	1.810E-04
1648000.4	862.3	857.8	-4.5	2.263E-04

THE SQUARE OF THE COEFFICIENT OF CORRELATION IS EQUAL TO 9.971E-01

REGRESSION LINE FOR GAUGE LEVEL -- 5

CONSTANTS FOR REGRESSION LINE

A(0) = 0.
A(1) = 2.345E-04
A(2) = 3.939E-10
A(3) =-2.612E-16
A(4) = 1.992E-22
A(5) =-6.160E-29

APPLIED LOAD(LBS)	AVE GAUGE READINGS	COMPUTED READINGS	ERROR	SLOPE OF CURVE
0.0	0.0	0.0	-0.0	2.345E-04
95149.0	27.1	25.7	-1.4	3.030E-04
195129.4	61.7	59.1	-2.6	3.638E-04
295553.5	100.0	98.3	-1.7	4.171E-04
392575.9	139.6	141.1	1.6	4.639E-04
499409.0	190.1	193.3	3.2	5.126E-04
600868.4	244.2	247.6	3.4	5.577E-04
692566.4	297.5	300.6	3.1	5.981E-04
795603.4	367.5	364.5	-2.9	6.432E-04
898640.4	440.2	433.1	-7.1	6.871E-04
992310.4	503.4	499.2	-4.1	7.247E-04
1039145.4	536.4	533.6	-2.8	7.421E-04
1078585.4	564.6	563.1	-1.5	7.557E-04
1122955.4	593.5	597.0	3.5	7.697E-04
1158944.4	623.0	624.9	1.9	7.798E-04
1201342.4	653.6	658.2	4.5	7.901E-04
1234866.4	683.1	684.8	1.6	7.968E-04
1287124.4	723.3	726.6	3.3	8.042E-04
1328536.4	756.8	760.0	3.2	8.071E-04
1365511.4	789.2	789.8	.6	8.072E-04
1405444.4	823.3	822.0	-1.3	8.044E-04
1444884.4	855.2	853.6	-1.6	7.982E-04
1494677.4	895.6	893.1	-2.5	7.850E-04
1533131.4	923.3	923.0	-.3	7.704E-04
1575036.4	953.5	954.9	1.4	7.495E-04
1593770.4	981.1	968.8	-12.3	7.383E-04
1648000.4	998.6	1007.8	9.2	6.993E-04

THE SQUARE OF THE COEFFICIENT OF CORRELATION IS EQUAL TO 9.998E-01

REGRESSION LINE FOR GAUGE LEVEL -- 6

CONSTANTS FOR REGRESSION LINE

A(0) = 0.
A(1) = 1.954E-04
A(2) = 2.258E-10
A(3) =-4.202E-16
A(4) = 2.804E-22
A(5) =-5.372E-29

APPLIED LOAD(LBS)	AVE GAUGE READINGS	COMPUTED READINGS	ERROR	SLOPE OF CURVE
0.0	0.0	0.0	-0.0	1.954E-04
95149.0	21.5	20.3	-1.2	2.279E-04
195129.4	45.3	44.0	-1.3	2.434E-04
295553.5	70.7	68.6	-2.0	2.456E-04
392575.9	91.7	92.2	.5	2.398E-04
499409.0	114.4	117.3	3.0	2.295E-04
600868.4	137.0	140.1	3.1	2.199E-04
692566.4	155.8	160.0	4.1	2.142E-04
795603.4	185.8	182.0	-3.9	2.139E-04
898640.4	211.2	204.3	-6.8	2.219E-04
992310.4	230.0	225.8	-4.2	2.376E-04
1039145.4	238.6	237.2	-1.4	2.487E-04
1078585.4	246.7	247.2	.4	2.597E-04
1122955.4	256.3	259.0	2.7	2.739E-04
1158944.4	267.5	269.1	1.6	2.868E-04
1201342.4	279.1	281.6	2.5	3.036E-04
1234866.4	288.2	292.0	3.8	3.181E-04
1287124.4	307.2	309.3	2.1	3.426E-04
1328536.4	323.3	323.9	.6	3.635E-04
1365511.4	337.7	337.7	.0	3.833E-04
1405444.4	354.9	353.5	-1.4	4.056E-04
1444884.4	370.2	369.9	-.3	4.286E-04
1494677.4	394.1	392.0	-2.1	4.586E-04
1533131.4	409.4	410.1	.6	4.824E-04
1575036.4	429.4	430.8	1.5	5.087E-04
1593770.4	451.2	440.5	-10.7	5.205E-04
1648000.4	462.2	469.6	7.4	5.546E-04

THE SQUARE OF THE COEFFICIENT OF CORRELATION IS EQUAL TO 9.993E-01

REGRESSION LINE FOR GAUGE LEVEL -- 7

CONSTANTS FOR REGRESSION LINE

A(0) = 0.
A(1) = 7.519E-05
A(2) = 2.028E-10
A(3) =-5.904E-16
A(4) = 6.946E-22
A(5) =-2.099E-28

APPLIED LOAD(LBS)	AVE GAUGE READINGS	COMPUTED READINGS	ERROR	SLOPE OF CURVE
0.0	0.0	0.0	-0.0	7.519E-05
95149.0	7.8	8.5	.7	1.000E-04
195129.4	18.3	19.0	.6	1.060E-04
295553.5	28.6	29.5	1.0	1.040E-04
392575.9	40.4	39.6	-.8	1.046E-04
499409.0	52.2	51.3	-.9	1.167E-04
600868.4	66.7	64.4	-2.3	1.453E-04
692566.4	79.4	79.6	.1	1.879E-04
795603.4	101.1	102.2	1.1	2.553E-04
898640.4	131.6	132.8	1.2	3.410E-04
992310.4	166.7	168.9	2.2	4.305E-04
1039145.4	188.2	190.1	1.9	4.776E-04
1078585.4	210.4	209.8	-.6	5.177E-04
1122955.4	231.9	233.7	1.8	5.622E-04
1158944.4	257.1	254.6	-2.5	5.974E-04
1201342.4	281.2	280.8	-.4	6.369E-04
1234866.4	306.7	302.6	-4.1	6.660E-04
1287124.4	339.4	338.5	-.9	7.064E-04
1328536.4	368.3	368.3	.0	7.327E-04
1365511.4	395.7	395.8	.0	7.510E-04
1405444.4	427.5	426.0	-1.4	7.641E-04
1444884.4	455.9	456.3	.5	7.693E-04
1494677.4	492.4	494.5	2.1	7.629E-04
1533131.4	517.9	523.6	5.7	7.466E-04
1575036.4	548.0	554.3	6.2	7.161E-04
1593770.4	579.1	567.5	-11.6	6.976E-04
1648000.4	602.4	603.5	1.1	6.260E-04

THE SQUARE OF THE COEFFICIENT OF CORRELATION IS EQUAL TO 9.997E-01

REGRESSION LINE FOR GAUGE LEVEL -- 8

CONSTANTS FOR REGRESSION LINE

A(0) = 0.
A(1) = 3.318E-05
A(2) = 9.586E-11
A(3) =-3.019E-16
A(4) = 3.518E-22
A(5) =-1.048E-28

APPLIED LOAD(LBS)	AVE GAUGE READINGS	COMPUTED READINGS	ERROR	SLOPE OF CURVE
0.0	0.0	0.0	-0.0	3.318E-05
95149.0	5.1	3.8	-1.3	4.440E-05
195129.4	8.3	8.4	.1	4.581E-05
295553.5	12.0	12.8	.9	4.307E-05
392575.9	16.4	16.9	.5	4.158E-05
499409.0	21.4	21.5	.1	4.576E-05
600868.4	27.9	26.7	-1.2	5.843E-05
692566.4	33.2	32.9	-.2	7.856E-05
795603.4	42.6	42.6	.0	1.113E-04
898640.4	56.1	56.2	.1	1.538E-04
992310.4	71.9	72.7	.8	1.989E-04
1039145.4	81.3	82.6	1.2	2.229E-04
1078585.4	92.4	91.8	-.6	2.434E-04
1122055.4	102.2	103.1	.8	2.664E-04
1158944.4	114.2	113.0	-1.2	2.847E-04
1201342.4	125.5	125.5	-.0	3.054E-04
1234866.4	137.5	136.0	-1.5	3.210E-04
1287124.4	153.6	153.4	-.2	3.429E-04
1328536.4	167.5	167.9	.4	3.576E-04
1365511.4	180.6	181.3	.7	3.694E-04
1405444.4	196.3	196.2	-.2	3.769E-04
1444884.4	211.0	211.2	.1	3.816E-04
1494677.4	229.7	230.2	.5	3.815E-04
1533131.4	243.1	244.8	1.7	3.759E-04
1575036.4	258.4	260.3	1.9	3.637E-04
1593770.4	272.9	267.0	-5.9	3.559E-04
1648000.4	283.6	285.5	2.0	3.247E-04

THE SQUARE OF THE COEFFICIENT OF CORRELATION IS EQUAL TO 9.997E-01

REGRESSION LINE FOR GAUGE LEVEL -- 9

CONSTANTS FOR REGRESSION LINE

A(0) = 0.
A(1) = 3.813E-05
A(2) = 8.696E-11
A(3) =-2.970E-16
A(4) = 3.657E-22
A(5) =-1.120E-28

APPLIED LOAD(LBS)	AVE GAUGE READINGS	COMPUTED READINGS	ERROR	SLOPE OF CURVE
0.0	0.0	0.0	-0.0	3.813E-05
95149.0	4.3	4.2	-.1	4.783E-05
195129.4	8.5	9.0	.6	4.820E-05
295553.5	13.4	13.7	.3	4.519E-05
392575.9	18.0	18.0	.0	4.428E-05
499409.0	23.9	23.0	-.9	5.012E-05
600868.4	29.5	28.8	-.7	6.527E-05
692566.4	35.9	35.7	-.1	8.830E-05
795603.4	45.9	46.6	.7	1.248E-04
898640.4	61.4	61.8	.4	1.713E-04
992310.4	79.1	80.1	1.0	2.198E-04
1039145.4	89.5	91.0	1.5	2.452E-04
1078585.4	101.1	101.1	-.0	2.669E-04
1122955.4	112.9	113.4	.5	2.909E-04
1158944.4	125.7	124.3	-1.4	3.099E-04
1201342.4	138.4	137.9	-.6	3.311E-04
1234866.4	152.0	149.2	-2.8	3.468E-04
1287124.4	168.4	167.9	-.5	3.684E-04
1328536.4	183.1	183.5	.4	3.824E-04
1365511.4	197.1	197.8	.7	3.921E-04
1405444.4	213.3	213.6	.4	3.990E-04
1444884.4	229.0	229.4	.4	4.015E-04
1494677.4	248.3	249.3	1.0	3.976E-04
1533131.4	262.4	264.5	2.1	3.885E-04
1575036.4	278.8	280.4	1.6	3.716E-04
1593770.4	292.7	287.3	-5.4	3.615E-04
1648000.4	304.6	305.9	1.3	3.222E-04

THE SQUARE OF THE COEFFICIENT OF CORRELATION IS EQUAL TO 9.998E-01

LOAD-DISTRIBUTION CURVE FOR APPLIED LOAD OF 50000

DATA FROM GAUGES BY DEPTH

LEVEL NO.	DEPTH INCHES	MEASURED LOAD(LBS)	COMPUTED LOAD(LBS)	ERROR (LBS
1	0	48557.3	50000.0	1442.7
2	162	33842.6	33842.6	.0
3	258	29568.4	29568.4	-.0
4	414	27799.2	17966.4	-9832.8
5	498	11073.2	11073.2	.0
6	642	5597.7	4113.7	-1484.0
7	678	3476.0	3476.0	-.0
8	713	2818.2	2989.0	170.8
9	713	3159.8	2989.0	-170.8

THE SQUARE OF THE COEFFICIENT OF CORRELATION IS EQUAL TO 9.556E-01

CONSTANTS FOR REGRESSION LINE

A(0) = 5.000E+04
A(1) =-2.275E+02
A(2) = 1.338E+00
A(3) =-4.238E-03
A(4) = 5.632E-06
A(5) =-2.630E-09

LOAD DISTRIBUTION, SHAFT MOVEMENT AND LOAD TRANSFER ALONG SHAFT

DEPTH INS.	LOAD POUNDS	MOVEMENT INCHES	LOAD PSI	TRANSFER TSF	PERCENT LOAD TO APPLIED	MAXIMUM
0	50000	.003	1.81	.130	100.0	3.0
30	44271	.003	1.26	.091	88.5	2.7
60	40326	.002	.86	.062	80.7	2.4
90	37633	.002	.59	.042	75.3	2.3
120	35756	.002	.42	.030	71.5	2.2
150	34342	.002	.34	.024	68.7	2.1
180	33119	.002	.32	.023	66.2	2.0
210	31886	.002	.34	.025	63.8	1.9
240	30505	.001	.39	.028	61.0	1.9
270	28893	.001	.46	.033	57.8	1.8
300	27017	.001	.53	.038	54.0	1.6
330	24884	.001	.60	.043	49.8	1.5
360	22532	.001	.65	.047	45.1	1.4
390	20027	.001	.68	.049	40.1	1.2
420	17449	.001	.69	.049	34.9	1.1
450	14892	.001	.67	.048	29.8	.9
480	12448	.001	.63	.045	24.9	.8
510	10206	.001	.56	.040	20.4	.6
540	8241	.001	.48	.034	16.5	.5
570	6607	.001	.39	.028	13.2	.4
600	5330	.001	.29	.021	10.7	.3
630	4399	.001	.20	.015	8.8	.3
660	3761	.001	.14	.010	7.5	.2
690	3308	.001	.11	.008	6.6	.2
720	2876	.001	.13	.009	5.8	.2

LOAD-DISTRIBUTION CURVE FOR APPLIED LOAD OF 200000

DATA FROM GAUGES BY DEPTH

LEVEL NO.	DEPTH INCHES	MEASURED LOAD(LBS)	COMPUTED LOAD(LBS)	ERROR (LBS
1	0	195731.8	200000.0	4268.2
2	162	141555.7	141555.7	.0
3	258	127642.2	127642.2	-.0
4	414	87131.9	82529.4	-4602.5
5	498	53130.3	53130.3	.0
6	642	24583.9	19809.3	-4774.6
7	678	16122.1	16122.1	-.0
8	713	12984.3	13507.9	523.6
9	713	14031.5	13507.9	-523.6

THE SQUARE OF THE COEFFICIENT OF CORRELATION IS EQUAL TO 9.983E-01

CONSTANTS FOR REGRESSION LINE

A(0) = 2.000E+05
A(1) =-8.773E+02
A(2) = 5.418E+00
A(3) =-1.710E-02
A(4) = 2.227E-05
A(5) =-1.016E-08

LOAD DISTRIBUTION, SHAFT MOVEMENT AND LOAD TRANSFER ALONG SHAFT

DEPTH INS.	LOAD POUNDS	MOVEMENT INCHES	LOAD TRANSFER PSI	TSF	PERCENT LOAD TO APPLIED	MAXIMUM
0	200000	.011	6.98	.503	100.0	12.1
30	178112	.011	4.74	.342	89.1	10.8
60	163451	.010	3.13	.225	81.7	9.9
90	153860	.009	2.04	.147	76.9	9.3
120	147552	.009	1.37	.099	73.8	9.0
150	143087	.008	1.05	.075	71.5	8.7
180	139340	.007	.98	.070	69.7	8.5
210	135470	.007	1.10	.079	67.7	8.2
240	130889	.006	1.35	.097	65.4	7.9
270	125239	.006	1.66	.119	62.6	7.6
300	118355	.005	1.99	.143	59.2	7.2
330	110238	.005	2.31	.166	55.1	6.7
360	101028	.004	2.57	.185	50.5	6.1
390	90970	.004	2.75	.198	45.5	5.5
420	80388	.003	2.84	.205	40.2	4.9
450	69654	.003	2.83	.204	34.8	4.2
480	59157	.003	2.72	.196	29.6	3.6
510	49274	.002	2.51	.181	24.6	3.0
540	40343	.002	2.22	.160	20.2	2.4
570	32631	.002	1.87	.134	16.3	2.0
600	26303	.002	1.49	.107	13.2	1.6
630	21396	.002	1.12	.081	10.7	1.3
660	17786	.002	.81	.058	8.9	1.1
690	15162	.002	.61	.044	7.6	.9
720	12991	.002	.58	.042	6.5	.8

LOAD-DISTRIBUTION CURVE FOR APPLIED LOAD OF 400000

DATA FROM GAUGES BY DEPTH

LEVEL NO.	DEPTH INCHES	MEASURED LOAD(LBS)	COMPUTED LOAD(LBS)	ERROR (LBS
1	0	396239.3	400000.0	3760.7
2	162	299375.8	299375.8	.0
3	258	275074.3	275074.3	-.0
4	414	163050.5	188243.8	25193.3
5	498	126059.4	126059.4	.0
6	642	51126.5	44066.4	-7060.1
7	678	33415.8	33415.8	-.0
8	713	26047.0	26914.3	867.3
9	713	27781.6	26914.3	-867.3

THE SQUARE OF THE COEFFICIENT OF CORRELATION IS EQUAL TO 9.954E-01

CONSTANTS FOR REGRESSION LINE

A(0) = 4.000E+05
A(1) =-1.517E+03
A(2) = 9.333E+00
A(3) =-2.890E-02
A(4) = 3.589E-05
A(5) =-1.540E-08

LOAD DISTRIBUTION, SHAFT MOVEMENT AND LOAD TRANSFER ALONG SHAFT

DEPTH INS.	LOAD POUNDS	MOVEMENT INCHES	LOAD PSI	TRANSFER TSF	PERCENT APPLIED	LOAD TO MAXIMUM
0	400000	.028	12.07	.869	100.0	24.3
30	362149	.027	8.20	.591	90.5	22.0
60	336812	.025	5.40	.389	84.2	20.4
90	320296	.024	3.50	.252	80.1	19.4
120	309520	.022	2.33	.168	77.4	18.8
150	301962	.021	1.77	.127	75.5	18.3
180	295622	.020	1.67	.120	73.9	17.9
210	288969	.018	1.91	.138	72.2	17.5
240	280904	.017	2.40	.173	70.2	17.0
270	270710	.016	3.03	.218	67.7	16.4
300	258008	.015	3.72	.268	64.5	15.7
330	242713	.014	4.39	.316	60.7	14.7
360	224990	.013	4.99	.360	56.2	13.7
390	205205	.012	5.48	.394	51.3	12.5
420	183887	.011	5.80	.418	46.0	11.2
450	161675	.010	5.95	.428	40.4	9.8
480	139279	.010	5.90	.425	34.8	8.5
510	117434	.009	5.66	.407	29.4	7.1
540	96853	.009	5.23	.377	24.2	5.9
570	78185	.008	4.65	.335	19.5	4.7
600	61966	.008	3.94	.284	15.5	3.8
630	48579	.008	3.15	.227	12.1	2.9
660	38207	.007	2.35	.169	9.6	2.3
690	30786	.007	1.60	.115	7.7	1.9
720	25963	.007	.99	.071	6.5	1.6

Note: Remaining load-distribution data are omitted from the Sample Output.

LOAD TRANSFER CURVE FOR DEPTH OF 0 INCHES

MOVEMENT INCHES	LOAD TRANSFER PSI
0.000	0.00
.005	3.14
.010	6.13
.015	8.06
.020	9.57
.025	11.07
.030	12.24
.035	12.75
.040	13.27
.045	13.78
.050	14.09
.055	13.92
.060	13.76
.065	13.60
.070	13.43
.075	13.27
.080	13.04
.085	12.73
.090	12.41
.095	12.09
.100	11.77
.110	11.14
.120	10.50
.130	9.87
.140	9.39
.150	8.91
.160	8.43
.170	7.95
.180	7.47
.190	6.99
.200	6.51
.300	3.25
.400	.52
.500	-.39
.600	-1.23
.700	-2.06
.800	-2.90
.900	-3.73
1.000	-4.44
1.100	-4.96
1.173	-5.18

LOAD TRANSFER CURVE FOR DEPTH OF 60 INCHES

MOVEMENT INCHES	LOAD TRANSFER PSI
0.000	0.00
.005	1.65
.010	3.15
.015	3.89
.020	4.64
.025	5.38
.030	5.75
.035	6.12
.040	6.48
.045	6.77
.050	6.85
.055	6.92
.060	7.00
.065	7.07
.070	7.15
.075	7.14
.080	7.10
.085	7.06
.090	7.03
.095	6.99
.100	6.95
.110	6.87
.120	6.79
.130	6.69
.140	6.59
.150	6.49
.160	6.39
.170	6.29
.180	6.20
.190	6.10
.200	6.00
.300	5.38
.400	4.86
.500	4.81
.600	4.75
.700	4.70
.800	4.64
.900	4.59
1.000	4.59
1.100	4.65
1.158	4.84

LOAD TRANSFER CURVE FOR DEPTH OF 120 INCHES

MOVEMENT INCHES	LOAD TRANSFER PSI
0.000	0.00
.005	.85
.010	1.47
.015	1.92
.020	2.17
.025	2.48
.030	2.77
.035	3.06
.040	3.33
.045	3.54
.050	3.74
.055	3.94
.060	4.15
.065	4.35
.070	4.48
.075	4.59
.080	4.70
.085	4.82
.090	4.93
.095	5.05
.100	5.16
.110	5.39
.120	5.55
.130	5.67
.140	5.79
.150	5.91
.160	6.03
.170	6.15
.180	6.27
.190	6.39
.200	6.51
.300	7.27
.400	7.93
.500	8.29
.600	8.66
.700	9.02
.800	9.38
.900	9.74
1.000	10.08
1.100	10.40
1.144	10.77

Note: Remaining load-transfer data are omitted from the Sample Output.